Aggregated understanding of characteristics of wheat straw node and internode with their interfacial bonding mechanisms

By

Seyed Hamidreza Ghaffar

Department of Mechanical, Aerospace and Civil Engineering
College of Engineering, Design and Physical Sciences

A thesis submitted for the degree of Doctor of Philosophy

May 2016

Abstract

The demand for the efficient utilisation of straw biomass requires detailed analyses of its fundamental chemical structures, morphological complexity, individual cell wall components and the correlation of physicochemical to mechanical properties. The study involved two main areas: understanding the details of microstructure and characterisation/differentiation of properties of various profiled wheat straw. Comprehensive and systematic experimental programmes were therefore designed in order to thoroughly investigate the node and internode of wheat straw with quantitative appraisals and qualitative interpretations. This could contribute towards its valorisation in bio-refinery pathways.

The sophisticated morphology of node and internode, inner and outer surface was investigated. It was found that the morphology across node area has a great variety when the longitudinal profile is investigated in the upwards direction to grain head. A 3D image of nodes illustrated the dense core with elliptical shaped rings organised in order to provide the mechanical strength to the overall stem. The variation of cell wall composition across wheat straw node and internode showed that node yielded slightly higher Klason lignin, extractives and ash content than internode, which could be related to their morphology, precisely the higher ash and extractives content in the node are explained by thicker epidermis tissue.

The physicochemical and mechanical properties of node and internode were differentiated and the effects of a combination of mild physical pre-treatment were monitored. The results indicated: i) the reduction of waxes from the outer surface, ii) significantly lower ($P < 0.05$) extractives and iii) the dissolution of silicon (Si weight %) on the outer surface of node and internode. The tensile strength of nodes and internodes after pre-treatments also resulted in a significant increase ($P < 0.05$).

The accumulated characteristic data enabled the investigation of interfacial properties and bonding mechanisms of the inner and outer surface of wheat straw with thermosetting resins. Different surface functionalities and anatomical sections, altered the bonding performance, i.e. waxes and silica concentrated on the outer surface inhibited the quality of the interface. Nevertheless, the treatment improved interface ($P < 0.05$) between resins and the micro-porous surface of wheat straw by causing the microcellular structure of straw to expand and hence inspire the mechanical entanglement on a micro level upon resin solidification.

Acknowledgements

It was the grace of God that gave me the strength to continue the work that culminated in this thesis. For this to take shape, no one is more deserving of recognition than my supervisor and motivator Professor Mizi Fan. I would like to express my sincere gratitude for his expert supervision and guidance throughout the course of this study. Not only was there a constant interest and close contact with the work as a supervisor, but also continuous inspiration and encouragement as a friend. It has been my great fortune and privilege to be working with him.

Dr Xiangming Zhou is also greatly acknowledged as the second supervisor for all his expert advice and support from the very beginning of the research.

I would like to acknowledge the industrial partner of this project, Stramit Ltd and in specific Mr Bruce McVicar, who has supported the research with critical discussions and questions throughout the project.

The Engineering and Physical Sciences Research (EPSRC) are acknowledged for their financial support through the course of this research.

My very grateful thanks are expressed to the academics in the civil engineering department. In particular: Dr Nuhu Braimah, Dr Philip Collins, and Dr Zhaohui Huang.

The technicians in engineering labs, including, Mr Simon Le Geyt, Mr Neil Macfadyen, Mr Paul Szadorski, Mr Gerald Edwardson, Mr Richard Parish, Mr Abdul Ghani and Mr Malcolm Austin are also acknowledged for their continuous help throughout the experimental stages.

I would also like to give profound thanks and gratitude to my parents, Mr Seyed Mehdi Ghaffar and Mrs Simin Alizadeh for their moral support. Special appreciation also goes to my brothers, Ali and Amin.

Last but not least, I thank all my friends and colleagues.

Declaration

The work in this thesis is based on research carried out at Brunel University London, United Kingdom. I hereby declare that the research presented in this thesis is my own work except where otherwise stated, and has not been submitted for any other degree.

Table of Contents

Abstract i

Acknowledgements ii

Declaration iii

List of Figures viii

List of Tables xi

List of abbreviations xii

1 Introduction 1

1.1 Overview 2

1.2 The challenges to be addressed 3

1.3 Objectives of the project 5

1.4 Research strategy 6

1.5 Outline of thesis 8

1.6 Novel research contributions 10

1.7 Some of the outcomes of this PhD research 10

2 Literature review 12

2.1 Utilisation and bioconversion of straw biomass 13

2.1.1 Introduction 13

2.1.2 Biological pre-treatments for straw biomass 14

2.1.2.1 Combination of biological with chemical and/or physical pre-treatments 14

2.1.2.2 Roles of microorganisms in biological pre-treatments 17

2.1.2.3 White-rot fungi functions 17

2.1.2.4 Brown-rot fungi functions 18

2.1.3 Straw lignin biodegradation 19

2.1.3.1 Role of laccase in lignin biodegradation 21

2.1.4 Bioconversion of straw biomass 23

2.1.4.1 Bio-energy 24

2.1.4.2 Bio-composites 26

2.2 Structural analysis for lignin characteristics in biomass straw 29

2.2.1 Introduction 29

2.2.2 Composition and morphology of straw 30

2.2.3 Analytical techniques for structural analysis of straw lignin 31

2.2.3.1 Quantitative analysis 32

2.2.3.2 Qualitative analysis 40
2.2.4 Structure of straw lignin 42
2.2.4.1 LCC linkages 43
2.2.4.2 Physical properties 44
2.2.4.3 Lignin distribution and concentration 45
2.2.4.4 Lignin functional groups and their characteristics 46
2.3 Lignin in straw and its applications 48
2.3.1 Introduction 48
2.3.2 Straw biomass lignin for emerging applications 49
2.3.3 Types and variations of straw lignin 50
2.3.4 Lignin as adhesive 52
2.3.4.1 Lignin as phenol-formaldehyde resin 54
2.3.4.2 Lignin as epoxy resin 56
2.4 Interim conclusions and outlook 57
3 Materials and methodologies 59
3.1 Materials 60
3.1.1 Wheat straw 60
3.1.2 Chemicals and thermosetting resins 61
3.2 Analytical techniques 61
3.2.1 ATR-FTIR 61
3.2.2 XRD 62
3.2.3 FEG-SEM 62
3.2.4 SEM-EDAX 63
3.2.5 OM 63
3.2.6 TGA 64
3.3 Testing procedures 64
3.3.1 Tensile testing 64
3.3.2 Contact angle 66
3.3.3 Extractives content 67
3.3.4 Acid insoluble lignin/Klason lignin 67
3.3.5 Ash content 68
3.3.6 Weight lost calculation 69
3.3.7 Single lap joint tensile test specimen 69
3.4 Statistical data analysis 72

3.5 Interim conclusions 72
4 Revealing the morphology and chemical distribution of nodes and internodes in wheat straw 73
4.1 Introduction 74
4.2 Experimental plan 74
4.3 Results and discussion 75
4.3.1 Wheat straw stem 75
4.3.2 Node morphology 76
4.3.3 Internode morphology 81
4.4 Chemical distribution of wheat straw 84
4.4.1 Elemental composition 84
4.4.2 Functional groups of wheat straw 85
4.5 Crystallinity of wheat straw 89
4.6 Interim conclusions 92
5 Differential behaviour of nodes and internodes of wheat straw 93
5.1 Introduction 94
5.2 Experimental plan 95
5.3 Pre-treatment methods 95
5.3.1 Combinational pre-treatment (H+S) 95
5.3.2 Hot water and steam pre-treatment (0.5H and 0.5S) 96
5.3.3 Mild alkaline pre-treatment (0.5NaOH) 96
5.4 Results and discussion 98
5.4.1 Surface chemical functional groups analysis 98
5.4.2 Wettability of outer surface of wheat straw 102
5.4.3 Tensile test analysis 103
5.4.4 Thermal characterisation and ash content 107
5.5 Interim conclusions 109
6 Physicochemical properties and surface functionalities of wheat straw node and internode 111
6.1 Introduction 112
6.2 Experimental methods 112
6.2.1 Analysis of cell wall components and various profiles of node and internode 112
6.2.2 Pre-treatment 113
6.3 Results and discussion 115
6.3.1 Surface chemical distribution of node and internode 115
6.3.2 Cell wall composition of node and internode 119

6.3.2.1 Extractives 119
6.3.2.2 Klason lignin 120
6.3.2.3 Ash content 120
6.3.3 Effects of treatment on cell wall compositions of node and internode 121
6.3.3.1 Extractives 121
6.3.3.2 Klason lignin 122
6.3.3.3 Ash content 123
6.3.4 Surface elemental composition of node and internode 124
6.3.5 Morphological characteristics of node and internode 125
6.4 Interim conclusions 128
7 Interfacial properties and bonding mechanisms of wheat straw bio-composites 130
7.1 Introduction 131
7.2 Experimental plan 132
7.2.1 Single lap joint tensile test 132
7.2.3 Surface chemistry of different profiles 132
7.2.4 Surface modification 133
7.3 Results and discussion 133
7.3.1 Surface Functionalities of various straw profiles 133
7.3.2 Interfacial bonding mechanisms 136
7.3.3 Bonding scenario and interface qualification 139
7.3.4 Failure mechanisms 142
7.4 Interim conclusions 146
8 Concluding remarks and future prospectives 147
8.1 Introduction 148
8.2 Concluding remarks 149
8.3 Future prospectives 152
References 154

List of Figures

Figure 1.1 Schematic objective chart of research project.....7

Figure 2.1 Schematic of the role of biological pre-treatment in biomass lignin degradation.....19

Figure 2.2 Enzymatic oxidation of phenol compounds.....22

Figure 2.3 a) Surface of a wood fibre made for bio-composite production. b) Surface of a wood fibre incubated for 12hours with laccase.....23

Figure 2.4 schematic process flow diagram for ligni recovey and bioenergy.....24

Figure 2.5 Three primary lignin monomers: (a) monolignols *p*-coumaryl alcohol M_H, (b) coniferyl alcohol M_G and (c) sinapyl alcohols M_S.....29

Figure 2.6 Cellulose strands surrounded by hemicellulose and lignin.....30

Figure 2.7 i) wheat straw internode SEM (a) epidermis, (b) parenchyma, (c) lumen, (d) vascular bundles; (ii) rice straw internode SEM.....31

Figure 2.8 Droplets on surface of pre-treated biomass due to the isolation and migration of lignin (a: untreated biomass; b: pre-treated at 120˚C; c: pre-treated at 130˚C; d: pre-treated at 140˚C).....40

Figure 2.9 TEM micrograph of an ultrathin transverse section of the cell wall of Forsythia suspensa fibre: S1= outer secondary wall, S2= middle secondary wall and S3= inner secondary wall.....41

Figure 2.10 Light micrograph of cross section of grass stem, showing four basic parts.....41

Figure 2.11 A tentative chemical structure of wheat straw lignin.....42

Figure 2.12 Lignin phenolic carbohydrate complexes in wheat straw.....43

Figure 2.13 Phenolic compounds in flax and wheat straw.....51

Figure 3.1 a) the separation of leave from stem of wheat straw, b) the straw stems cleaned, c) the internodes separated from the d) nodes.....60

Figure 3.2 The XRD machine during testing of samples.....62

Figure 3.3 SEM-EDAX integrated analysis machine.....63

Figure 3.4 OM for morphological analysis.....64

Figure 3.5 - The tensile testing grips a) the upper part, b) the lower part.....65

Figure 3.6 Contact angle machine for surface wettability analysis.....66

Figure 3.7 Soxhlet extractor set up.....67

Figure 3.8 Klason lignin determination.....68

Figure 3.9 The furnace and the residue after the duration of the test.....69

Figure 3.10 Schematic test specimens for the single lap joint tensile test.....71

Figure 4.1 Sample fabrication for FEG-SEM and EDX-SEM.....75

Figure 4.2 Schematic diagram of wheat straw with nodes (N) and internodes (IN).....76

Figure 4.3 The schematic image of the node outer (a) and inner (b) surface longitudinal view and the OM images corresponding to the position in the node shown by the arrows……77
Figure 4.4 a) Node cross-section b) node transverse inner surface view……79
Figure 4.5 Cross-section profiles of the connection between grain head and internode……79
Figure 4.6 a) Node cross-section view showing the elliptical shaped rings in the outer circular ring, b) node core cross-section view showing tightly packed elliptical rings……..80
Figure 4.7 OM image of internode cross-section……..82
Figure 4.8 An example of internode cross-section showing the epidermis and distance between spiral vessels in vascular bundles……83
Figure 4.9 ATR-FTIR spectra of wheat straw internode and node outer and inner surface……86
Figure 4.10 X-ray diffractogram of wheat straw node and internode……91
Figure 5.1 Flow diagram showing the combinational treatment strategy……97
Figure 5.2 ATR-FTIR spectra of a) internode outer surface (IO) and b) internode inner surface (II) subjected to different pre-treatments (H+S, 0.5H, 0.5S and 0.5NaOH) and compared to untreated (UN) samples……100
Figure 5.3 ATR-FTIR spectra of a) node outer surface (NO), and b) node inner surface (NI) subjected to different pre-treatments (H+S, 0.5H, 0.5S and 0.5NaOH) and compared to untreated (UN) samples……101
Figure 5.4 Optical micrograph of wheat straw internode cross-section……102
Figure 5.5 a) Initial contact angle θi b) equilibrium contact angle θe……103
Figure 5.6 (1) Typical failure in the gauge length in node (2) a) node cross-section (b) node transverse inner surface view……105
Figure 5.7 (1) Typical failure in the gauge length in internode (2) surface of internode longitudinal direction showing a) the defects b) longitudinal fibres……106
Figure 5.8 TGA of untreated (UN) node (N) and internode (IN) and H+S (N-IN) with onset degradation temperature……109
Figure 6.1 ATR-FTIR spectra of a) Internode and b) node of UN and H+S inner and outer surface…118
Figure 6.2 The cross section of internode showing the epidermis size……126
Figure 6.3 Node cross-section view……127
Figure 6.4 SEM images, cross section of a) H+S treated internode, showing the expanded structure b) UN internode……128
Figure 7.1 ATR-FTIR spectra of a) internode and b) node, (I) inner and outer (O) surface untreated (UN) and treated (H+S)……135
Figure 7.2 Schematic illustrations of wheat straw surface modification and mechanism (a) for

better interfaces after the modifications (b)……137
Figure 7.3 SEM images, cross section of a) H+S treated internode, showing the expanded microstructure and b) UN internode……..138
Figure 7.4 Contact angle of distilled water and outer surface internode change as a function of time……138
Figure 7.5 Comparison of different bonding scenarios in node and internode of UN and H+S samples (average for all 7 thermoset resins)……141
Figure 7.6 Comparison of bonding performance between the a) internode and b) node, UN and H+S samples with thermosetting resins……141
Figure 7.7 Cross section view interface of (a) UN samples showing the nucleation of micro crack leading to delamination, and b) showing strong bonded interface in H+S sample……144
Figure 7.8 Failure modes observed during experiments - a) adhesive failure-poor bonding, b) cohesive failure, c) mixed adhesive and cohesive failure, d) substrate failure-strong bonding……144
Figure 7.9 Failure morphology in (a) good bonding scenario of H+S treated samples; SEM images of (b) and (c) with OM (d) and (e) for cross section view, and longitudinal surface view in (f) and (g)……145

List of Tables

Table 2.1 The key enzymes essential for biodegradation of lignocellulose to monomers……13
Table 2.2 Combination of biological and physical/chemical pre-treatment for straw biomass……16
Table 2.3 Biological bioconversion of straw biomass to oils……25
Table 2.4 Fibreboard produced from enzymatic activation of agricultural/forest biomass fibres……28
Table 2.5 The thickness and PVF of wheat straw……31
Table 2.6 Assignments of FT-IR absorption bands (cm^{-1})……34
Table 2.7 H/S/G ratios for types of biomass resources……39
Table 2.8 Molecular weight and functional groups of lignin……44
Table 2.9 Lignin concentration and distribution in wheat straw……46
Table 2.10 Chemical composition of agricultural residues (% dry matter)……48
Table 3.1 Viscosity of the resins used……61
Table 4.1 Wheat straw node and internode elemental composition……85
Table 4.2 Band characteristics of ATR-FTIR spectra……88
Table 4.3 Crystallinity index calculation of wheat straw node and internode……91
Table 5.1 Experimental tensile strength results……104
Table 6.1 Parameters analysed with their relative methodologies and purpose of investigation……114
Table 6.2 Surface characteristics bands of node and internode……116
Table 6.3 Chemical analysis of untreated (UN) and pre-treated (H+S) wheat straw (% dry straw)….124
Table 6.4 Node and internode profile elemental composition based on EDX-SEM analysis……125
Table 7.1 Distilled water and wheat straw contact angle properties……138

List of abbreviations

FAO	Food and agricultural organisation
HAVC	Heating, ventilation and air conditioning
DMSO	Dimethyl sulfoxide
NMI	*N*-methylimidazole
GC-MS	Gas chromatography-mass spectrometry
^{13}C-NMR	Carbon nuclear magnetic resounance
^{1}H-NMR	Proton nuclear magnetic resounance
^{31}P-NMR	Phosphorus nuclear magnetic resounance
Lip	Lignin peroxide
MnP	Manganese peroxide
ML	Middle lamella
P	Primary wall
S	Secondary wall
PVF	Percentage volume fraction
CC	Cell corner
CML	Compound middle lamella
HSQC	Heteronuclear single quantum coherence
LCC	Lignin carbohydrate complexes
MWL	Milled wood lignin
SSL	Sulphite spent liquors
CH_4	Methane
COOH	Carboxyl acid
M_n	Molar mass
H_2SO_4	Sulforic acid
$K_2\ Cr_2\ O_7$	Potassium dichromate

pH	Potentia hydrogenii
NaOH	Sodium hydroxide
rpm	revolution per minute
w/v	weight per volume
$H_2 O_2$	Hydrogen peroxide
V (redox potential unit)	Volts
PF	Phenol formaldehyde
LPF	Lignin phenol formaldehyde
NREL	National renewable energy laboratory
HW	Hot-water extractives
ET	Ethanol extractives
KL	Klason lignin
OM	Optical microscopy
UN	Untreated
TGA	Thermogravimetric analysis
FTIR	Fourier transform infrared spectroscopy
ATR-FTIR	Attenuated total reflectance-FTIR
θ_i	Initial contact angle
θ_e	Equilibrium contact angle
VE	Vinylester
EP	Epoxy
PU	Polyurethane
UPE	Unsaturated polyester
Si-O	Silicon oxide
Si-C	Silicon carbide
CI	Crystallinity index
LOI	Lower order index

Chapter 1 Introduction

Highlights:

- Straw biomass background information;
- Wheat straw utilisation requires detailed understanding and the behaviour tracking of the material characteristics following pre-treatments and/or pre-processing;
- Sustainable development and recycling the agricultural waste with the bio-conversion purpose to value added products.

This chapter provides a general background on the research field and states the overall goals of the project. It also discusses the challenges to be addressed combined with the strategies adopted for tackling these issues. In the process of achieving the aims and objectives of the project, several novel contributions have been made which are listed in this chapter.

Key words: Wheat straw (*Triticum aestivum* L.); Straw biomass; Bio-refinery.

1.1 Overview

Tailoring new bio-products within the perspective of sustainable development is a philosophy which should be applied to progressively more material-based technologies in different industrial sectors. Ecological concerns drive the increasing interest in renewable and bio-based resources as the basis of novel products which could be considered as environmentally friendly substitutes for petroleum-based products.

Wheat straw, as a by-product of wheat production, is an annually renewable, low-cost and abundant source of natural fibres in the UK, where wheat is the most widely grown arable crops (around 2 million hectares), producing about 12-15 million tonnes each year (data from FAO) [1]. The European countries (27 countries) produce 137.5 million tonnes of wheat collectively which is 16.6% higher than that produced in China [2]. The global wheat production in 2014 was 716 million tonnes [3]. Assuming a residue/crop ratio of 1.3 [2], around 931 million tonnes of total wheat residue is annually produced. If 60% is used for ground cover to prevent soil erosion, 559 million tonnes of wheat straw is available as waste [3].

Utilisation of these inexpensive raw materials leads to socio-economic and environmental benefits by making additional income to the farmers, generating cost-effective high performing bio-products, and minimising the burning of the straw in the field [4]. Straw can be utilised as alternatives to wood flour or other bast fibre composites with comparable density, and could reduce the cost of bio-composite products.

Wheat straw is also an attractive feedstock for the production of bio-energy [4]. However, a successful utilisation of wheat straw requires comprehensive understanding of its structure, chemistry, morphology and how these characteristics are affected by a given production procedure, i.e. pre-treatment and processing. The bridging between the research-based adaptation of efficient pre-treatments on the extraction, separation and fractionation of waste crops components, has unique potential to yield innovative added value green chemicals. The direct extraction of specifically engineered or naturally occurring chemicals from the complex molecular components of different parts of straw biomass is also a possibility which requires the detailed investigations of anatomical parts. It must be recognised that not all parts of the crop residue are equally valuable [5]. For efficient utilisations of straw biomass, the undesirable parts must be removed by highly selective separation technologies. For

instance, biofuel and chemical processors only require the high yielding cellulose and hemicellulose biomass. A strategy for identifying and subsequently reducing the amount of undesirable parts of feedstocks is, therefore, vital.

Wheat straw is anatomically composed on a mass basis of internodes (57 ± 10%), nodes (10 ± 2%), leaves (18 ± 3%), chaffs (9 ± 4%) and rachis (6 ± 2%) [4,5]. The composition of the main chemical substances changes between and within different anatomical parts of the wheat plant.

Wheat straw is a polymeric composite with cell walls made up of mainly cellulose, hemicellulose and lignin. The cellulose and hemicellulose are fibrous materials and the lignin is the binder holding the fibres together providing rigidity to the fibres. The amounts of cellulose and lignin are in general lower in straws than in wood. Consequently, the amount of hemicellulose is higher [6,7] and a more hydrophilic characteristic of the refined straw fibres is expected compared with wood-based fibres. In addition to three main groups of organic mixtures (cellulose, hemicellulose and lignin), straw also contains various other organic compounds including protein and extractives (wax, which protect the epidermis of the straw), sugars, salts and insoluble ash including silica.

1.2 The challenges to be addressed

This project is set to tackle the issues associated with the lack of effective utilisation of wheat straw for further bio-refinery and bio-conversion to value added products. The term bio-refinery is widely used as it covers a variety of industrial sectors, but is defined differently by different stakeholders. Several descriptions have been developed over the recent years according to the context, where the core concept is the conversion of straw biomass with the integration of various technologies and processes, in a sustainable way, into several product streams i.e. chemicals, materials, energy, food and feed. In the context of bio-refinery the straw biomass recalcitrance, (i.e. the chemical and structural features) influences the liquid penetration and/or enzyme accessibility and activity, therefore, bio-conversion costs [8].

The complex chemical and structural features of straw biomass have mechanisms for resisting attacks on their structural sugars from microorganisms, the factors which contribute to the recalcitrance of straw biomass to chemicals or enzymes include: 1) the epidermal tissue, particularly the cuticle and waxes, 2) the arrangement and density of the vascular bundles, 3)

the relative amount of sclerenchymatous (thick wall) tissue, 4) the degree of lignification, 5) the heterogeneity of cell wall constituent, which makes the crystalline cellulose cores of micro-fibrils less accessible by an amorphous coating of hemicellulose and lignin [8]. To overcome the biomass recalcitrance and to reach the goal of producing cost-competitive bio-products from straw biomass, the new findings and/or understandings of the fundamental properties of straw material sciences must be translated and integrated into the conversion processes.

In construction industry worldwide for instance, buildings are responsible for more than 40% of global energy consumption and as much as 33% of carbon dioxide equivalent emissions (CO_2e), which sums to about 8.1 gigatonnes (Gt) annually [9]. Therefore, strategies to reduce the environmental impact of construction by using bio-based renewable materials should be the main goal. Various plans have been developed to reduce carbon emissions, including: 1) improved thermal insulation for both new build and retrofit, 2) better building design (e.g. PassivHaus), 3) enhanced efficiency of heating, 4) reduction in the carbon emissions of energy production through the use of nuclear energy ventilation and air conditioning (HVAC) systems and 5) renewable energy sources (e.g. biomass, hydro, wind, tidal, photovoltaic) [9].

However, not much emphasis is on reducing the embodied energy within buildings. Collaboration between different sectors within the construction industry, from farmers to policy makers is vital for success in the utilisation of renewable local resources. An intensive R&D work should be focused on the transition from an oil based economy towards a bio-based economy. Specific focus should be put on the integration of local, sustainable cultivation of straw biomass.

The challenges with bio-based products must be tackled through the whole product chain (production and supply), as well as in the marketing of these products so that this bio-economical business could develop in a sustainable and profitable way for every stakeholder in the product chain.

The challenges are within different fronts, including but not limited to i) the need for technical development and product innovation, ii) increasing the bio-based product market demand and iii) gathering sufficient and accurate/robust information about specific variations in straw biomass properties, which is not straight forward. The lack of a comprehensive and detailed database on the fundamental properties of wheat straw node and internode is the

main reason behind the underutilisation of this biomass. Information about the properties of straw biomass is either limited or differs significantly according to different sources and measurement techniques. There is also a lack of differentiation between the node and internode characteristics, the straw is characterised as a whole without detailing the anatomical parts.

This project is therefore designed in a way to better understand wheat straw (i.e. identify the associated problems of wheat straw for specific application) and overcome the issues with an environmental friendly strategy. This requires a comprehensive and harmonised characterisation of every single parameter and detailed science of straw biomass. It is envisaged that the success of this project will make the developed approach as a significant contribution in research of renewable material science, (i.e. for other types and variations of straw biomass and natural plants). A robust framework could be emerged in which bio-based resources/feedstocks can come to a sustainable and efficient establishment/existence for bio-refinery processes.

1.3 Objectives of the project

This PhD project is aimed at developing a good and thorough understanding of wheat straw, including:

- The morphology and chemical distribution of node and internode;
- Surface chemistry, mechanical and thermal properties of wheat straw;
- Physicochemical properties, cell wall composition and surface functionalities of wheat straw;
- The different behaviour of nodes and internodes with various pre-treatments;
- The effects of pre-treatment on the composition of node and internode;
- Interfacial properties with the bonding and failure mechanisms of straw composites with thermosetting resins.

The schematic objective chart in Fig. 1.1 illustrates the connections between each sub objective. The completion and conclusion of each specific objective will serve as the foundations for the subsequent stage of the project. To build up on outcomes for successfully achieving the goals of the project, it is necessary to establish robust links between the sub objectives. The detailed objective of each chapter is explained in its introduction.

1.4 Research strategy

The strategy for effective completion of the project is to draw together the different themes concerning wheat straw utilisation and its thorough characterisation. This will help realise the full potential of straw biomass, guide their smart utilisation, exploit the potential commercial market and promote the further development of bio-based products.

The investigation work is organised after the extensive review of the state of art research based on the important material sciences of wheat straw. Fundamental aspects of material characterisation are examined and interpreted to understand the microstructure of node and internode, inner and outer surface. Detailed characterisation of various properties are carried out to enable the differentiation between node and internode, leading to their smart utilisation based on their characteristics.

Specific work programme can be summarised as follows:

1) Extensive review of literature as the initial step, to determine critical information regarding straw biomass material scinces and its bio-refinery.

2) Examination of morphological details of node and internode with their chemical distribution and structure. This is a systematic approach to achieve an understanding of the microstructure and chemical distribution of wheat straw.

3) Investigation of surface, chemical structure, mechanical and thermal properties of node and internode with the determination and quantification of changes induced with various pre-treatments.

4) Determination of physicochemical properties with their correlation to surface functionalities and cell wall components of node and internode. To reveal how the characteristics of node differs from that of internode the comprehensive investigation and interpretation of different parameters is required.

5) Investigation of interfacial bonding mechanisms and failure modes of node and internode bio-composites. Based on the observations and outcomes of previous tasks, specifically the surface chemistry, different bonding scenarios of surface contacts are carried out to interpret the bonding quality and failure mechanisms.

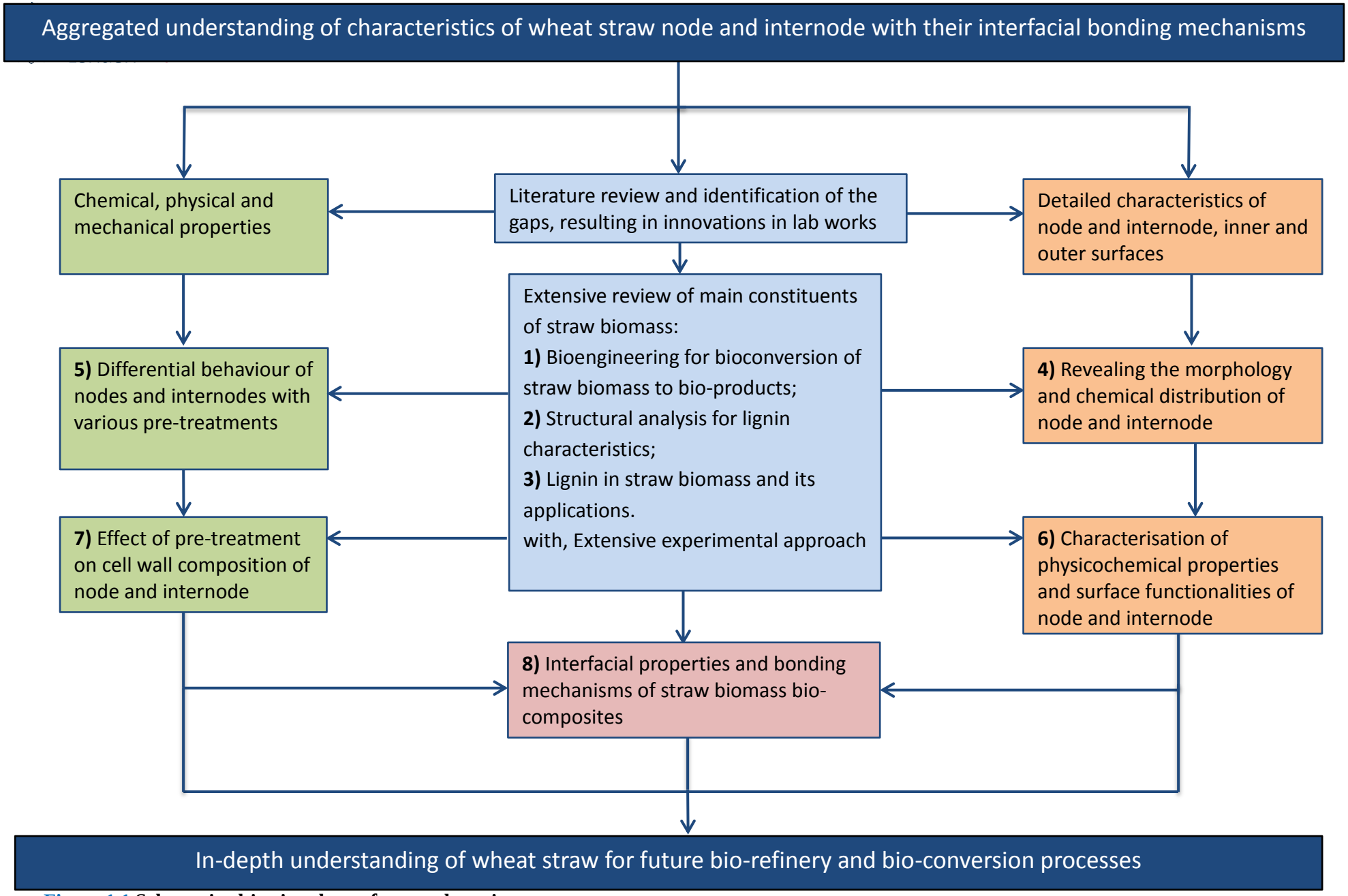

Figure 1.1 **Schematic objective chart of research project**

1.5 Outline of thesis

This thesis consists of nine chapters. The structure and the brief overview of the chapters are outlined below:

Chapter 1 Introduction

This chapter introduces the topic generally and states the problems and challenges to be addressed. The research motivation along with the strategies to achieve the goals is also explained.

Chapter 2 Literature review

This review aims to compile a database of broad information in existing literature regarding the material science and the main constituents of straw biomass, i.e. cellulose, hemicellulose and lignin. Comprehensive analyses of lignin and its fundamental chemical structures with developments of analysing technologies have been compiled where quantitative and qualitative structural analyses techniques have been differentiated. The applications of lignin in straw biomass as an adhesive and its various modifications for facilitating the compatibility with phenol are reviewed. While biotechnology for utilisation and bioconversion of straw biomass into bio-products, e.g. bioethanol, biogas and bio-composites are also discussed extensively in this chapter.

Chapter 3 Materials and methodologies

This chapter describes the materials used throughout the project, as well as a detailed description of the analytical methodologies and testing procedures carried out. It highlights the important parameters of each test and sample preparations prior to testing.

Chapter 4 Revealing the morphology and chemical distribution of nodes and internodes in wheat straw

In chapter 4 a systematic experimental study is carried out in order to build the fundamental wheat straw knowledge which will then contribute to the following chapters. Specifically, however, it focuses on the morphological properties, chemical functional groups, surface elemental composition and crystallinity of node and internode. A 3D model of the node morphology is revealed in this chapter.

Chapter 5 Differential behaviour of nodes and internodes of wheat straw

A scientific in-depth analysis is accomplished in this chapter, focusing on the differences between the node and internode and the impact of pre-treatments on their properties, i.e. surface chemistry, mechanical and thermal properties. A combinational environmentally friendly pre-treatment is designed and its effectiveness is quantitatively measured in improvements on tensile property and thermal stability. Each stage of the combination pre-treatment is also assessed as an individual pre-treatment to monitor the details and contributions from different stages of pre-treatment. In addition a well-known traditional chemical pre-treatment is also carried out for comparative purposes.

Chapter 6 Physicochemical properties and surface functionalities of wheat straw node and internode

Chapter 6 explores the physicochemical characteristics of node and internode with their relative surface profiles, i.e. inner and outer surface. This chapter carries on the investigations from Chapter 5, with the addition of the wet chemistry properties of wheat straw node and internode, including, extractives content, acid insoluble lignin and ash content. Surface elemental compositions are also assessed. The differences in untreated and pre-treated wheat straw in aforementioned properties constitute the second part of this chapter with the emphasis on the effects of the pre-treatment on the cell wall composition.

Chapter 7 Interfacial properties and bonding mechanisms of wheat straw bio-composites

This chapter utilises the outcomes of all the detailed studies in previous Chapters 4, 5 and 6 to scientifically investigate the mechanisms of interfacial bonding and its link to the failure behaviour in the straw composite interface. The same combinational pre-treatment designed in Chapter 5 is used to assess the effectiveness of surface modification and the possible interfacial bonding improvement. Failure mechanisms were modelled into four main groups.

Chapter 8 Concluding remarks and future prospective

Chapter 8 contains the concise summary and conclusive statements established within this project. On this platform, future prospective and recommendations are also listed. Particular emphasis is given on the valorisation of wheat straw for bio-refinery pathways.

1.6 Novel research contributions

This research contributes to the comprehensive understanding of wheat straw (*Triticum aestivum* L.), where novel methodologies/strategies were exploited leading to the specific contributions as follows:

1) Critical reviews which identify the gaps and future prospective in research fields of i) lignin in straw and its optimisation as an adhesive, i.e. thermosetting resins, ii) structural analysis techniques for lignin characterisation with differentiation of quantitative and qualitative analyses, and iii) bioengineering concept for straw biomass bio-conversion to bio-energy/bio-composite with specific functions of microorganisms, i.e. fungi and enzymes (refers to Chapter 2).
2) Revealing the morphology of node and internode in wheat straw with a 3D model of node and its core, investigated from the root to the grain head direction in stem (refers to Chapter 4).
3) In-depth scientific identification of differential physicochemical properties of node and internode with relative surface profile functionalisation (refers to Chapters 5 and 6).
4) Environmentally friendly pre-treatment strategy with effective surface modification of wheat straw for the optimisation of interfacial bonding (refers to Chapter 7).
5) Interfacial bonding and physical model of failure mechanisms in straw composite (refers to Chapter 7).

1.7 Some of the outcomes of this PhD research

The following scientific publications and presentations have been produced to disseminate the findings of the research results:

Journal articles

1) **S.H. Ghaffar**, M. Fan, Structural analysis for lignin characteristics in biomass straw, Biomass Bioenergy 57 (2013 July) 264-279. http://dx.doi.org/10.1016/j.biombioe.2013.07.015
2) **S.H. Ghaffar**, M. Fan, Lignin in straw and its applications as an adhesive, Int. J. Adhes. Adhes. 48 (2014 May) 92-101. http://dx.doi.org/10.1016/j.biombioe.2013.07.015
3) **S.H. Ghaffar**, M. Fan, B. McVicar, Bioengineering for utilisation and bioconversion of straw biomass into bio-products, Ind. Crops Prod. 77 (2015 December) 262-274. http://dx.doi.org/10.1016/j.indcrop.2015.08.060

4) **S.H. Ghaffar**, M. Fan, Revealing the morphology and chemical distribution of nodes in wheat straw, Biomass Bioenergy 77 (2015 March) 123-134. http://dx.doi.org/10.1016/j.biombioe.2015.03.032
5) **S.H. Ghaffar**, M. Fan, Differential behaviour of nodes and internodes of wheat straw with various pre-treatments, Biomass Bioenergy 83 (2015 December) 373-382. http://dx.doi.org/10.1016/j.biombioe.2015.03.032
6) **S.H. Ghaffar**, M. Fan, An aggregated understanding of physicochemical properties and surface functionalities of wheat straw node and internode, Ind. Crops Prod. 95 (January 2017) 207-215. http://dx.doi.org/10.1016/j.indcrop.2016.10.045
7) **S.H. Ghaffar**, M. Fan, B. McVicar, Interfacial properties with bonding and failure mechanisms of wheat straw node and internode, Compos. Part A. (under review).

Book chapter

1) **S.H. Ghaffar**, Chapter 11 - Straw fibre-based construction materials. In: M, Fan and F, Fu, editors. Advanced high strength natural fibre composites in construction: Woodhead Publishing, 2017. http://dx.doi.org/10.1016/B978-0-08-100411-1.00011-X

Oral presentations at conferences

1) Conference on Future Emerging Materials for Green buildings: 30th of October 2015. *European Centre of Excellence, London, UK.*
2) Workshop/conference on Bioconversion of waste materials to bio-products: 20th of June 2015. *European Centre of Excellence, London, UK.*
3) European conference of Grow2build Innovation Tour Seminar: 2nd of September 2015. *Namur, Belgium.*
4) International conference on Biocomposites and Sustainable Developments in construction: 9th and 10th of September 2015. *European Centre of Excellence, London, UK.*

Poster presentations at conferences

1) ResCON13 Straw-based Eco building materials and systems: 22nd of June 2013. *Brunel University, London, UK.*
2) International conference of Renewable chemicals from Lignin: 18th of November 2014. *Royal Society of Chemistry, London, UK.*

Chapter 2 Literature review

Highlights:

- Straw biomass main components;
- Bioengineering and the use of biotechnology for utilisation of straw biomass;
  - Biological pre-treatment offers a sustainable and energy efficient strategy;
  - The microorganisms role in straw biomass modification;
  - The role of enzymes, i.e. laccase in lignin biodegradation;
  - Bio-products, i.e. bioenergy, bio-fuel and bio-composites.
- Analytical techniques for structural analysis of straw;
  - Quantitative and qualitative techniques;
  - The potential of straw biomass for further bio-refinery pathways;
  - Structure of lignin with its distribution and concentration in straw;
  - Lignin and its use as an adhesive;
  - Types and variations of straw with their chemical structure;
  - Optimisation of straw lignin through phenolation, ultrafiltration and reactivity improvement.

This chapter consists of three sections to understand the material science and identify the gaps in the research field for subsequent bio-refinery and/or bioconversion process. The key to a successful research is an extensive review, providing the foundations of knowledge by covering vast but detailed aspects of the research field.

Keywords: Straw biomass; Bioengineering; Biological pre-treatment; Biotechnology; Lignin biodegradation; Enzymes; Lignin; Quantitative and qualitative analysis; Structural characteristics; Thermal analyses; Lignin as adhesive; Lignin-based products.

2.1 Utilisation and bioconversion of straw biomass

2.1.1 Introduction

The exciting combination of biology and engineering called biotechnology is becoming an emerging solution for improving sustainability issues faced by industries. Many researchers have been working on these concepts, e.g. [10-24]. Straw biomass residues are predominantly ample in nature which have a great prospects for bioconversion. It was calculated that 73.9 teragram (Tg) of dry wasted crops (e.g. agricultural residues) could possibly yield 49.1 gigaliter (GL) of bioethanol in the world [25]. Asia could be the major potential producer of bioethanol from straw biomass, estimated to be up to 291 GL/year of bioethanol. Europe could be the second largest producer with a potential of 69.2 GL/year of bioethanol, mostly from wheat straw. In North America main feedstock is corn stover, which has a potential of producing 38.4 GL/year of bioethanol [25].

Biological microorganisms degrade and use cellulose and carbohydrates as sources of energy and carbon. Other collections of filamentous fungi possess the capability of breaking lignin. Microorganisms which are able to completely and efficiently biodegrade lignin to CO_2 and breakdown the lignin carbohydrate complexes are categorised as white-rot fungi. Further categories of fungi are brown-rot fungi that depolymerise and modify the lignin in biomass [26]. The fungi's ability to biodegrade straw biomass efficiently and selectively is because of their effective enzymatic system and the mycelial growth routine that permits the fungus to carry nutrients, for instance nitrogen and iron into the less nutrient lignocellulose substrate that creates its carbon source. A variety of enzymes that have different functions are important in biodegradation of the constituents of biomass [27,28]. Table 2.1 summarises the enzymes which are essential for biodegradation of lignocellulose components [24].

Table 2.1 The key enzymes essential for biodegradation of lignocellulose to monomers [24]

Component	Type of enzyme
Lignin	Laccase, manganese peroxidase, lignin peroxidase
Pectin	Pectin methyl esterase, pectate lyase, polygalacturonase, rhamnogalacturonan lyase
Hemicellulose	Endo-xylanase, acetyl xylan esterase, β-xylosidase, endomannanase, β-mannosidase, α-L-arabinofuranosidase, α- glucuronidase, ferulic acid esterase, α-galactosidase, *p*-coumaric acid esterase
Cellulose	Cellobiohydrolase, endoglucanase, β-glucosidase

The key step for bioengineering of straw biomass to bio-products is an efficient pre-treatment. Several uses have been suggested for bioengineering of straw biomass. Amongst them the production of bioethanol [20,25,29-31], biogas [32-35] and bio-products [36] (e.g. organic acids, amino acids and vitamins [26]) have received much attention with sufficient success in the process. The exploration which is required for future agricultural biomass technology is of a comprehensive nature linking contributions from biochemistry, microbiology and biotechnology. The main emphasis of this section is on biological pre-treatments and the use of various enzymes for lignin biodegradation leading to optimisation of straw biomass. Scientific insights and concepts of biotechnology are discussed with feasible strategies to overcome the problems associated with the bioconversion of straw biomass.

2.1.2 Biological pre-treatments for straw biomass

In comparison to chemical pre-treatment, biological pre-treatment weakens the heterogeneous straw biomass with lignin biodegrading microorganisms. Fungi have potential for degradation of aromatic compounds. A biological process removes a substantial quantity of lignin, hence increases the enzymatic hydrolysis efficiency. When straw biomass is fermented by fungi, the biological pre-treatment can achieve a greater sugar yield (20–65%) and lignin biodegradation (>15%) [15,37]. While the key benefits of biological pre-treatments are small energy input, no chemical obligation, environmentally friendly working style and minor environmental conditions, the drawbacks are the slow pre-treatment rate which requires a careful monitoring of the growth parameters [38]. The fact that some of the carbohydrates segments of biomass would deplete by microorganisms could also be a disadvantage. Biological pre-treatment is therefore not as striking on an industrial scale, and the introduction of some kind of catalyst is necessary that can speed up the process and also improve the efficiency [24]. One way of improving the efficiency of biological pre-treatment is that it could be exploited as an initial stage default pre-treatment in combination with one or more pre-treatment methods [29].

2.1.2.1 Combination of biological with chemical and/or physical pre-treatments

Biological pre-treatment combined with mild physical/chemical or mechanical pre-treatments presents an efficient solution for straw biomass bioconversion to bio-products. It is important for biological pre-treatment to be industrially efficient (i.e. in terms of duration). Hence the mild chemical or physical pre-treatment prior to biological pre-treatment can help reduce the pre-treatment time, therefore enhance the industrial feasibility [29]. Combined pre-treatments

can also potentially reduce the issues related to physical and chemical pre-treatments, e.g. severe energy contribution for mechanical treatments and intense chemical loading for chemical treatments.

Combined pre-treatment should lead to a synergistic effect, enhancing the yields of final products, as summarised in Table 2.2. Two un-catalysed hydrothermal methods, hot water extraction and liquid hot water pre-treatments, were compared in an investigation of the synergistic effects of hydrothermal-fungal pre-treatment [39]. Hydrothermal pre-treatment enhanced the fungal biodegradation for soybean and wheat straw that seemed to be resistant to *C.subvermispora* degradation. The hot water extraction (85˚C for 10 min) enabled fungal pre-treatment of wheat straw by eliminating water soluble extractives [39]. Pressurised hot water pre-treatment (170˚C for 3 min at 0.75MPa) helped fungal biodegradation of soybean straw [39], where the glucose yield of the collective liquid hot water and fungal pre-treatment was 65%. Yu et al. [40] showed that pre-treatment of corn stalks with *Irpex lacteus* could modify the lignin structure and facilitate lignin biodegradation and xylan elimination under mild alkaline environment (1.5% NaOH, 30–75˚C for 15–120 min). The synergic result mainly rest on the harshness of alkaline pre-treatment. The less the harshness of the alkaline pre-treatment, the further the cellulose digestibility was enhanced by fungal pre-treatment. A fungal screening of basidiomycetes was implemented, combined with mild alkali washing (0.1% NaOH (5% w/v), at 50˚C and 165 rpm for 60 min), for second generation bioethanol from wheat straw [41]. Arrangement of a biological pre-treatment by *I. lacteus* or *P. subvermispora* with mild alkali pre-treatment did not yield inhibitors for downstream processes, improving ethanol production [41].

Mild alkali treatment (NaOH (25% w/v) per gram of wheat straw, 165 rpm and 50˚C for 60 min) was performed prior to enzymatic hydrolysis, as the fraction of the lignin that remains after pre-treatment is removed, the enzymatic hydrolysis are improved. The digestibility of untreated wheat straw was 16% for cellulose and 12% for hemicellulose which improved to 21 and 17%, respectively, as a result of alkaline treatment, this further improved to 27 and 23%, respectively, when the autoclave sterilisation (120˚C, 20 min without overpressure) of wheat straw was also carried out before alkaline treatment [19]. In another study, by combining biological pre-treatment, using same fungus (*I. lacteus*), with an alkaline wash, improved enzymatic hydrolysis of corn stalk were achieved, the results also showed that the time of biological process could be shortened as a result of this combination [42].

Improvement of the digestibility from biological pre-treatment was also achieved by optimising the operational settings of the mechanical and thermal pre-treatments for substrate conditioning. Mechanical particle size reduction is essential to homogenise the substrate and thermal process is needed to reduce the presence of unwanted microorganisms. In these conditions, the rate of substrate consumption increased as the fungal accessibility of the substrate was increased [19].

Table 2.2 Combination of biological and physical/chemical pre-treatment for straw biomass.*

Substrate	Fungi	Physical/chemical treatment	Effectiveness	Ref.
Wheat straw	19 white-rot fungi tested**	Alkaline (NaOH)	Strong alkaline pre-treatment masked the synergistic result of fungal pre-treatment for the combined procedure	[43]
	C.subvermispora	Hot water extraction	Hot water extraction enhanced delignification and the subsequent sugar produced	[39]
	I. lacteus or P.subvermispora	Alkaline (NaOH)	No significant inhibitors of yeast growth improving significantly ethanol production.	[41]
Soybean straw	*C.subvermispora*	Liquid hot water	Liquid hot water pre-treatment enhanced delignification and the subsequent sugar yield	[39]
Corn stalk	*Irpex lacteus****	Alkaline (NaOH)	Fungal pre-treatment enhanced delignification and xylan elimination through mild alkaline pre-treatment	[40]
Rice hull	*Pleurotus ostreatus*	Ultrasound	Ultrasound enhanced fungal delignification and improved cellulose and hemicellulose loss, leading to higher sugar yield in comparison to fungal pre-treatment on its own.	[44]
	Pleurotus ostreatus	H_2O_2	H_2O_2 enhanced fungal delignification, leading to sugar yield that is similar to that achieved from long term fungal pre-treatment.	[44]

*Fungal pre-treatment is the following step of combined pre-treatment for all the rest of table.
**of 19 white-rot fungi tested, *Pleurotus ostreatus*, *Pleurotus* sp. 535, *Pycnoporus cinnabarinus* 115 and *Ischnoderma benzoinum* 108 increased the vulnerability of straw to enzymatic saccharification
*** fungal pre-treatment is the first step of combined pre-treatment.

2.1.2.2 Roles of microorganisms in biological pre-treatments

White-rot and brown-rot fungi are responsible for lignocellulose degradation. Brown-rots, unlike white-rots, mostly attack cellulose and hemicellulose while white-rots attack cellulose and lignin.

Due to the insolubility of the main constituents of straw biomass the fungal biodegradation happens exocellularly, either in association with the outer cell envelope layer or extracellularly. Fungi possess two categories of extracellular enzymatic processes, the hydrolytic and oxidative ligninolytic. The former process yields hydrolases that are responsible for polysaccharide biodegradation, the latter system biodegrades lignin and opens phenyl rings [26]. Fungal performance on biodegradation and the subsequent digestibility differs with i) feedstocks, ii) fungi species and iii) pre-treatment times. A summary of previous studies of solid state fungal pre-treatment has been provided [45] where critical pre-treatment factors influencing the efficiency of fungal pre-treatment, with enzymes involved in biodegradation of biomass feedstock have been discussed.

2.1.2.3 White-rot fungi functions

White-rot fungi have a high tolerance to toxic surroundings and they can endure elevated temperatures and an extensive range of pH. Lignin degradation is needed to increase the contact to cellulose and hemicellulose. White-rot basidiomycetes efficiently mineralise lignin, however different species cause different gross morphological patterns of decay [46-48]. Robust oxidative action and small substrate specificity of the ligninolytic enzymes in white-rot fungi make lignin degradation efficient through the action of secreted enzymes. The 3 main oxidative enzymes (ligninolytic enzyme) secreted by white rot fungi are phenol oxidase (laccase), lignin peroxide (LiP), and manganese peroxide (MnP) [49].

LiP and MnP were revealed in 1980s in *P. chrysosporium*, labelled as lignases due of their great potential redox value [50]. LiP and MnP oxidise the substrate by two successive one-electron oxidation steps with intermediate action radical formation. They require hydrogen peroxide (H_2O_2) for their actions, although they could be deactivated by high concentration of H_2O_2. LiP is capable to oxidise phenolic and non-phenolic lignin substructures, while MnP and laccase only biodegrade phenolic lignin substructures [50]. Unsaturated fatty acid allows MnP to biodegrade non-phenolic lignin substructures.

Not all of ligninolytic enzymes are detected in fungal cultures. A study conducted by Guerra et al. [51] on *Pinus taeda* (loblolly pine) biodegraded by *Ceriporiopsis subvermispora* indicated no sign of a link between oxidative enzymes and lignin biodegradation. The mineralisation of lignin occurred after the lignin modification. This indicates a sequence of reactions which elaborate in lignin depolymerisation. The most extensively investigated white-rot fungus is *P. chrysosporium,* which possesses a high cell growth rate and good efficiency for lignin degradation [37]. *P. chrysosporium* strains at the same time biodegrade cellulose, hemicellulose and lignin, while *Ceriporiopsis subvermispora* tend to eliminate lignin first. *P. chrysosporium* yields multiple isoenzymes of LiP and MnP, however, it does not yield laccase. Several additional white-rot fungi produce laccase as well as LiP and MnP in varying arrangements [52]. The white-rot fungus *Pleurotus ostreatus* assert several laccase genes encoding isoenzymes with different characteristics [53]. Biodegradation of wheat straw by *P. chrysosporium* was studied [17] to discover the consequences of the lignin biodegradation process. The result showed about 30% loss of total lignin in 3 weeks of pre-treatment. The analysis of lignin confirmed the important decrease of guaiacyl (G) units. The lignin from pre-treated wheat straw also varied in its aromatic composition [17].

2.1.2.4 Brown-rot fungi functions

Brown-rot fungi successfully depolymerise and partially eliminate cellulose and hemicelluloses from straw biomass, but also oxidise lignin. They are in the category of basidiomycetous microorganisms [54-56]. Demethylation of methoxyl groups of phenolic lignin, along with aromatic hydroxylation is caused by brown-rot fungi. Therefore phenolic hydroxyl groups and the carboxyl content are high in brown-rotted lignin due to the oxidation of originally made catechol groups along with side-chain oxidation [54,57]. When brown-rotted lignin is pre-treated with a phenol-oxidising enzyme it becomes suitable as adhesive for bio-composites. The increased phenolic hydroxyl content promotes radical development in lignin and would subsequently have a positive effect on adhesion. Brown-rot fungi also produce laccase in some species [58]. This modifies the lignin in the brown-rotted biomass. Hence it is interesting to investigate the brown-rot fungi as a possible method to produce reactive lignin from biomass to be used for adhesive.

The activities of brown-rot fungi on lignin are not limited to minor oxidative modifications [59]. A new technique (one-bond ^{1}H-^{13}C nuclear magnetic resonance spectroscopy) was applied for the complete solubilisation of lignocellulose to show that brown-rot of spruce

wood by *Gloeophyllum trabeum*, resulted in a depletion of all inter-monomer side chain linkages of lignin. In another study the structural modifications which occurred in brown-rotted lignin were determined with the solubilisation method [60]. It was illustrated that polysaccharide signals diminished compared to aromatic ones in the brown-rotted specimen. Numerical comparison of the NMR signals for C_α in arylglycerol-b-aryl ether structures indicated, on a methoxyl basis, this major structure of lignin was diminished to 29% of its original amount after the brown-rot process.

2.1.3 Straw lignin biodegradation

The comprehensive understanding of biological lignin degradation is useful for an efficient pre-treatment procedure, to break straw biomass to achieve sugars (see Fig 2.1). The significance of biological delignification has been established in many grounds of biotechnology. Therefore, in this section lignin biodegradation is examined in detail.

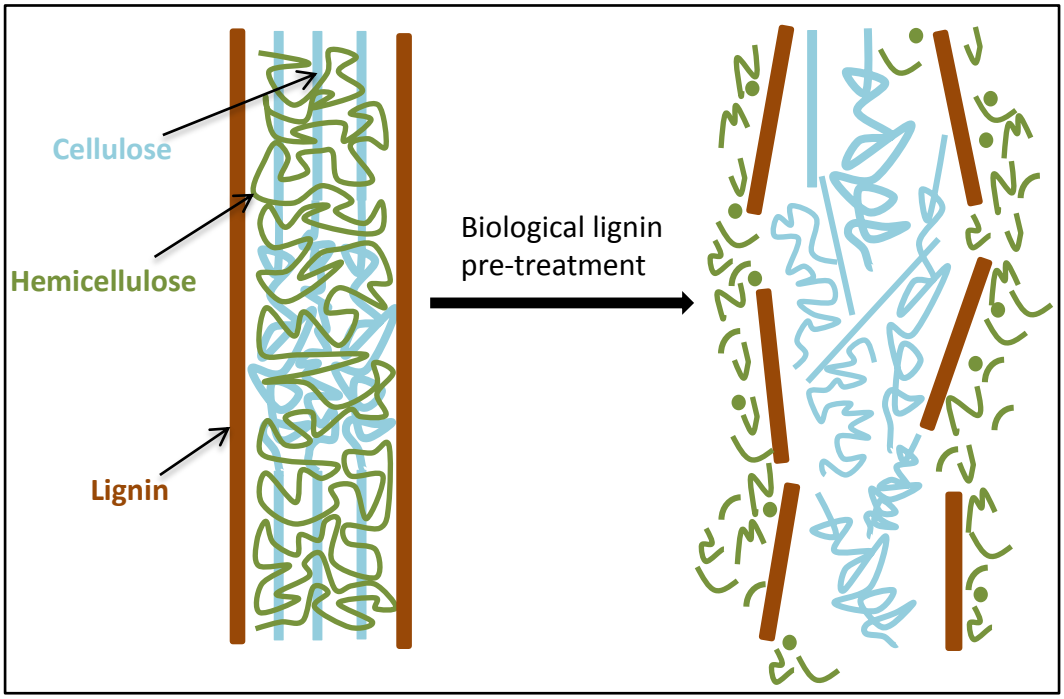

Figure 2.1 Schematic of the role of biological pre-treatment in biomass lignin degradation

Delignification of straw biomass improves their digestibility and also advances their nutritive value. Breaking down the arylglycerol-β-aryl ether bond through biological pre-treatment represents a significant commercial interest. The initial step of lignin biodegradation is when the oxidative enzymes induce new functional groups into lignin's macromolecular structure, making lignin vulnerable to consequent degradation by other enzymes. The natural structure of lignin has numerous different functional groups that could be specifically functionalised

via oxidation [61]. Technologies pointing at the oxidative advancement of lignin via radical paths have been reviewed [62] with the focus on enzymatic catalyses, i.e. laccase and peroxidase where important systematic aspects and possibilities to further improve the industrial exploitation of these enzymes are highlighted.

The available values in terms of biodegradation of lignin through white-rot fungi are rather variable dependent on the strain, fermentation type and incubation period. Jalč [63] in a review paper examining the results from numerous researchers presented the values of wheat straw lignin biodegradation ranging from 2 to 65%. The results from a study on the enzyme complexes of white-rot fungi under solid state fermentation of wheat straw showed significant lignin degradation after an increase in the laccase activities [64]. Enzymatic complexes yielded by white-rot fungi changes extensively the cell wall structure of wheat straw as a result of an intensive action between various groups of enzymes. When it comes to the biodegradation of recalcitrant cell wall components in straw biomass, fungal feruloyl and *p*-coumaroyl esterases which release feruloyl and *p*-coumaroyl units play a significant part [65]. These enzymes perform synergistically with xylanases to break the hemicellulose and lignin link, without mineralisation of lignin [66]. Thus, hemicellulose biodegradation is essential before efficient lignin elimination. A detailed report on ligninolytic enzymes of several fungi and their lignin biodegradation capabilities, using wheat straw as a substrate, was reported [11]. It was clear that either LiP or MnP production in combination with laccase causes high lignin degradation, as observed in *Phlebia spp.* and *P. chrysosporium* in the previous studies [11,67]. Therefore, no single ligninolytic enzyme could be responsible for lignin biodegradation, as the distribution of LiP, MnP and laccase varies considerably in different fungi. The capability of white-rot, brown-rot and soft-rot fungi separately and in combination with each other through semi solid biodegradation, showed that *Deadaleaflavida* plus *P. chrysosporium* was the best combination for a lignin loss of 36% in wheat straw [12]. Selective biodegradation of lignin in rice straw was reported by white-rot fungi (*Pleurotus ostreatus*), where the overall weight loss and the degree of klason lignin diminished, were 25% and 41%, respectively [13].

The primary moisture content of the lignocellulosic substrate is important for the fungal growth, as it influences secondary metabolism in fungal pre-treatment, which impacts the quantity of lignin biodegradation [68]. Earlier investigations showed that primary moisture between 70 to 80% was ideal for lignin biodegradation and ligninolytic activities of most

white rot fungi. Shi et al. [14] noticed that after 14 days cultivation of cotton stalks by *P. chrysosporium*, lignin biodegradation of 27% was achieved at 75% moisture content, which was about 7% more than that at 65% moisture content.

Apart from the use of fungi for biodegradation of lignin, other mediums have also been investigated. Hou et al. [69] carried out selective delignification of biomass using Cholinium amino acids ionic liquids ([Ch][AA] ILs), a novel type of bio-ILs that can be made from biomaterials, showing a great potential for pre-treatment of biomass. The capability of bacteria to break down lignin was also investigated [70,71], with potential for the usage of bacterial gene products for lignin biodegradation. The applications of bacteria in lignin bioconversion to aromatic chemicals have been illustrated [72,73]. Recent scientific publications indicate aromatic degrading soil bacteria, are capable of biodegrading lignin with extracellular peroxidase and laccase enzymes involved [71,74,75]. A lignin degrading bacterial consortium, "LDC", was separated from the sludge of a reedy pond which is capable of biodegrading 61% lignin in reeds at 30˚C in the conditions of static culture in 15 days [75]. Additionally, organosolv approaches treat biomass with a mixture of water and organic solvents, such as ethanol or methanol, along with the addition of a catalyst at 140-200˚C, which results in more than 50% lignin removal through cleavage of lignin-carbohydrate bonds and subsequent solubilisation in the organic solvent [76].

2.1.3.1 Role of laccase in lignin biodegradation

Fungal laccases play a key part in lignin degradation and modification processes. Laccase extensive substrate specificity leads to oxidation of different organic compounds that opens up opportunities of their utilisation in biotechnological applications. Laccases are versatile, phenol-oxidising enzymes found in white-rot fungi. They could show ligninolytic and polymerising (cross-linking) capabilities on lignin. Biotechnological applications of laccase have been widely provided in numerous review papers [77-80].

For industrial delignification applications laccase is the greatest ligninolytic enzyme, as it is more available and simpler to manipulate than LiP and MnP. Laccase has relatively low redox potential (≤ 0.5-0.8 V) and therefore its direct use for lignin biodegradation could be restricted to the oxidation of the phenolic lignin moiety as the non-phenolic structures possess a redox potential of >1.3 V. However laccase on its own is not enough for lignin biodegradation since there are only a minor fraction of the phenolic groups in lignin structure, thus the capacity of the bulk laccase molecule to enter the cell wall is restricted. These

boundaries are conquered through simulating the nature by means of redox mediators, which are able of realising the oxidation of non-phenolic lignin [81].

Smaller mediator molecules are initially oxidised or activated by the laccase, and then the mediator breaches the dense lignocellulosic structure easier and consequently starts the oxidation of lignin. The key features for an efficient laccase mediator system for delignification are: i) efficient oxidations of the mediator, ii) higher redox potential of the activated mediator for efficiently oxidising non-phenolic lignin, and, iii) ability to stop the laccase from being deactivated by the free radical form of the mediator [82,83].

The role of laccase mediator 1-hydroxybenzotriazol (HBT) in laccase oxidation, is to enable radical mediated reactions, which include the oxidation of side chains and oxygen addition in lignin [84]. Laccase in the presence of the mediators oxidises lignin via hydrogen atom transfer that differs from the electron transfer mechanism in direct laccase oxidation [85]. Lignin is not degraded under anaerobic conditions. The carbon-carbon and ether bonds joining subunits together should be separated with an oxidative mechanism. Laccase biodegrades *β*-1 and *β*-*O*-4 diminishes via C_α-C_β cleavage, C_α oxidation, and alkyl-aryl cleavage. Aromatic ring cleavage could be identified after the action of lactase [86]. The laccase enzyme could be utilised for bonding biomass materials by oxidation of phenol compounds (Fig. 2.2). Laccase activates the phenolic substrates by catalysing oxidation of their phenolic hydroxyl group to phenoxy radical while dioxygen (O_2) is condensed to H_2O [87,88].

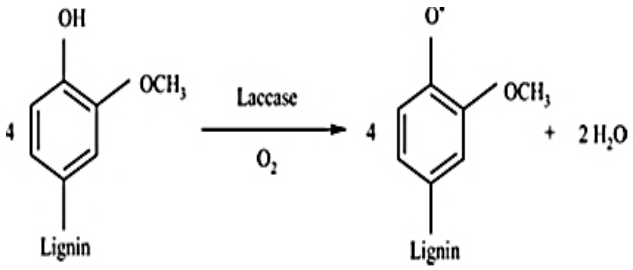

Figure 2.2 Enzymatic oxidation of phenol compounds [89]

Laccase and laccase-mediator pre-treatments using common redox mediators, like 2,2'-azinobis-(3-ethylbenzenthiazoline-6-sulfonic acid) (ABTS), lead to fibre modifications, which were investigated by spectroscopic methods [90,91]. The lignin in middle lamella is plasticised through the refining process which creates a coating on the surface of the fibre. Examination of the pre-treated fibres showed the initially existing crust of lignin (see Fig. 2.3a) has been eliminated entirely by the enzyme pre-treatment, shown in Fig. 2.3b. Indicating that lignin on the surface of fibre is vulnerable to reaction with laccase [92].

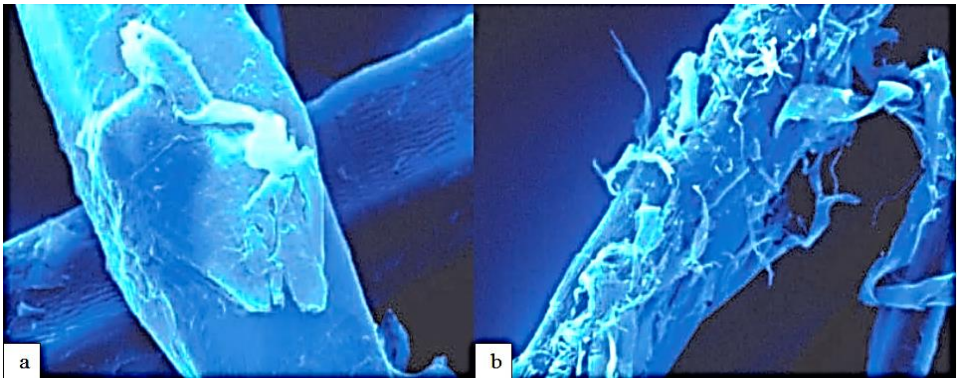

Figure 2.3 a) Surface of a wood fibre made for bio-composite production. b) Surface of a wood fibre incubated for 12hours with laccase [92]

It was revealed that laccase from *trametes hirsute* could activate and polymerise different technical lignins [85]. The reactivity of laccase with different lignin was examined by the extent of oxygen consumption and clear oxidation of lignin by laccase was observed in 3 hours of treatment on the basis of the oxygen consumption results. The factors which determine the activity of laccase include the pH of the medium, dosage of enzyme, substrate, temperature, and incubation time which should be long enough to activate the lignin. The pH level determines the structure of the enzyme and its active centre. The highest enzymatic activity is always observed at ideal pH level. Kharazipour et al. [93] found that relatively short incubations of wood fibres with laccase are sufficient to activate lignin. The fibres were incubated for 3 hours, and pH 5 was identified as the ideal pH of laccase.

2.1.4 Bioconversion of straw biomass

Bioconversion of main constituents of straw biomass has great value as one of the emerging trends. Operative pre-treatment strategies, as discussed earlier, are necessary which lead to efficient energy processing or even further leads to the biodegradation of the main components of straw biomass. For bioconversion of straw biomass, retting process has effectively been utilised for the preparation of wheat straw fibres that could be used as reinforcements in composites. Sain and Panthapulakkal [94] isolated fungus from the bark of an elm tree for retting of wheat straw, fungal retting was followed by mechanical defibrillation. The retted fibres were mechanically superior to the un-retted ones, and also chemical distribution analysis showed the elimination of hemicellulose and lignin from the retted fibres.

The bioconversion of biomass using enzymatic hydrolysis usually takes two methodologies, single enzyme or combinations of commercial mixtures. The use of single enzymes leads to

better evaluation of synergy and collaboration amongst enzymes to biodegrade a compound substrate such as lignin, while the usage of commercial enzymes could be a faster way to industrialisation. It is crucial to optimise factors such as, enzyme ratios, substrate loadings, enzyme loadings, inhibitors, adsorption and surfactants for the successful bioconversion of biomass [24]. The processes and technologies available for bioconversion of lignocelluloses are reviewed [95] with the discussion of their limitations. Despite progress in the field of bioengineering, the large scale conversion of biomass by biological fermentation to bio-products is still a problem as the rate of biological pre-treatment is slow for industrialisation [96]. The main struggle in effective biomass utilisation is its crystalline un-reactivity and in specific its resistance to hydrolysis.

2.1.4.1 Bio-energy

Although widespread, cost-competitive biofuels production at the industrial scale must overcome multiple technical and economic challenges, several commercial cellulosic ethanol plants have been commissioned, and the first plant now generates 75 million per year of cellulosic ethanol in Italy [76]. Currently, most integrated biologically based bio-refinery concepts comprise three main sections, 1) pre-treatment, 2) enzymatic hydrolysis, and 3) sugar fermentation to ethanol or other fuels (see Fig 2.4).

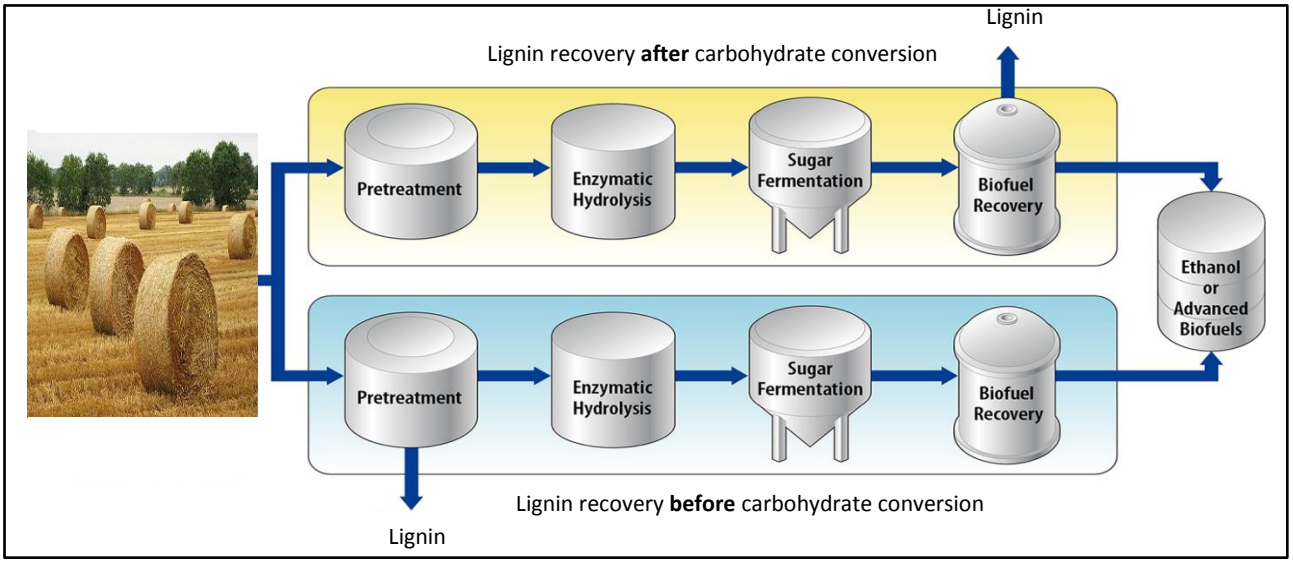

Figure 2.4 Schematic process flow diagram for lignin recovery and bio-energy

Technologies for bioethanol production from lignocellulose are reviewed [30] where numerous parameters that must be considered for low cost and efficient pre-treatment, are discussed with recent advances for bioethanol production. Biofuels have become more important as potential alternative energy sources due to climate change and oil prices. In the hydrolysis of any biomass a mixture of hexose and pentose sugars are generated [96]. The

efficient use of these sugars is crucial for the economical bioethanol production. Varieties of oleaginous microorganisms typically yeast or fungi, have the ability of applying hydrolyses of wheat straw, rice straw and corn stover for lipids accumulation [97]. Liquid biofuels, such as ethanol, could be made from straw biomass through fermentation of sugars extracted from cellulose and carbohydrates [16].

Another way could be to gasify straw biomass and utilise the generated gas as a feedstock for the synthesis of ethanol [98]. Biogas could be achieved in an anaerobic environment from straw, human wastes, animal dung and organic wastes. A key constituent of biogas is CH_4 (60–70%), which has a heat value of about 2.5×10^4 kJ/m^3, which is equal to 1 kg raw coal or 0.76 kg standard coal [99].

Hydrothermal pre-treatment (200˚C for 10 minutes) was the initial stage in the procedure of turning wheat straw into second generation bioethanol [22], where the enzymes were added to the fibre mass (mostly of cellulose and lignin), for bioconversion of cellulose to lower carbohydrates, enabling the fermentation of ethanol in the following stage. Pre-treatment of straw for the production of bioethanol is estimated to account for 33% of the summed cost of bioethanol production [100]. Developing an economically suitable processing is therefore the key for bioconversion of straw biomass into bioethanol. The ideal pre-treatment in terms of technical aspects would be to i) expose the cell wall constituents for enzymatic attack, ii) increase the porosity and surface area of the substrate, iii) diminish the cellulose crystallinity and disturb the heterogeneous structure of lignocellulosic biomass [29].

Dilute acid, lime and alkaline peroxide pre-treatments and enzymatic saccharification processes were assessed for the bioconversion of barley straw to monomeric sugars for bioethanol production [101], where alkaline peroxide pre-treatment performed best followed by lime and dilute acid pre-treatments in terms of sugars released. The yield of bioethanol by the mixed sugar using recombinant *Escherichia coli* strain FBR5 in 17 hours was 11.9 g/L from 26.2 g sugars/L obtained from alkaline peroxide pre-treated barley straw [101]. However the pre-treatments are not environmentally friendly and feasible for an industrial scale.

Sustainable carbon sources, including straw biomass have been used for microbial oil production [102]. Straw biomass is interesting as a carbon source for the production of [25]microbial oils. Some examples of straw biomass used for production of microbial oils are

given in Table 2.3 [97]. The overall economic processing feasibility needs to be assessed in more details. With the advances in biotechnology, microbial oil from straw biomass will emerge as one of the feedstocks for production of biodiesel in the near future.

Table 2.3 Biological bioconversion of straw biomass to oils.

Carbon source	Microorganisms	Biomass conc. (gL^{-1})	Lipid cont. (%)	Ref.
Wheat straw	*Cryptococcus curvatus*	17.2	33.5	[103]
Wheat straw	*Aspergillus oryzae*	NA	36.6 mg/g dry substrate	[104]
Rice straw	*Trichosporon fermentans*	28.6	40.1	[105]
Rice hulls	*Mortierella isabellina*	5.6	64.3	[106]
Corn stover	*Trichosporon cutaneum*	15.44	23.5	[107]

Pyrolysis of straw biomass on the other hand, is a procedure leading to the generation of charcoal, asphalt and other gaseous and organic products. These products are considerable alternative sources of energy. Nonetheless the pyrolysis reaction of biomass is complicated due to the formation of many intermediate products [108].

Technologies for the lignocellulosic production of bio-hydrogen, from pre-treatments to fermentations have also been reviewed [32]. The integrated bio-hydrogen processes have the features of high chemical oxygen demand reduction, low CO_2 emission and high hydrogen yield. When biogas is largely derivative of agricultural waste and residues, it is categorised as second generation biofuel. Although the first generation biofuels have the benefit of higher sugar content, this makes them easier for bioconversion to biofuel [109]. The biogas production is popular in some countries, and last few years it has been strongly implemented in Europe for generation of electricity or as transportation biofuel (upgrading to bio-methane).

2.1.4.2 Bio-composites

Producers of medium density fibreboard (MDF), particleboard (PB), plywood and oriented strand board (OSB) must reduce dangerous formaldehyde emissions from the petroleum derived adhesives, and to recover product recyclability. Novel method to reduce the quantity of adhesive whilst ensuring product superiority could serve as an important strategy, i.e. optimisation of lignin to be used as natural adhesive.The lignin enzymatic activation for biomass bio-composite, could contribute to the self-bonding characteristics by oxidation of the surface lignin [110]. The in situ cross-reaction of lignin via laccase were used to produce bio-composites, addition of hot pressing to this process further increased the crosslinking

[111-113]. The bonding mechanism of fibreboards produced from laccase pre-treated fibres could be related to phenoxy radicals on biomass surfaces that cross-link when the biomass is pressed into boards [111,112,114-116]. The condensation of hemicellulose degradation products, hydrogen bonding and molecular entanglement are also other contributions to the enhanced bonding quality [112,116]. In small scale trials by Felby et al. [114] and Kharazipour et al. [93,115], fibres were incubated with laccase [114,115] or peroxidase [93] at low consistency in H_2O medium at an appropriate pH or laccase solution was sprayed on fibres [115]. According to European standard [117], none of enzymatically bonded MDF obeys with the standards for mechanical strength and dimensional stability [110]. Nevertheless some bio-composite with higher densities, of good mechanical strength and adequate dimensional stability were developed on pilot-scale which passed the European specifications ([118]) [119,120].

The physical and mechanical properties along with the processing parameters of bio-composites made through biological pre-treatment from forest and agricultural biomass are presented in Table 2.4. Particleboards using flax and hemp, treated by laccase enzyme and its mediators (ABTS, 1-hydroxybenzotriazole (HBT), 3'-Hydroxyacetanilide (NHA)) were processed by Batog et al. [89]. The particleboards treated by laccase had better strength, and the laccase mediators and processing medium (by using buffer and an organic solvent, dioxane solution) improved the enzymatic oxidation of lignin, as it improved the laccase activity. In another study, Halvarsson et al. [121] used wheat straw for fibreboard production without synthetic resin. The bonding was triggered by activation of fibre surface by oxidative pre-treatment, where Fentons reagent (ferrous chloride and hydrogen peroxide) was used during the defibration process.

To summarise, it is clear that the surface has an important influence in the bonding mechanisms of enzymatically activated fibres. The surface (fibre/particle) entanglement on a macro-scale and the level of contact which is induced by changes in surface morphology is vital in enhancing the bonding quality. The enzyme catalysis initiates stable lignin radicals, which face thermal decay by cross-linking across biomass fibres or particles during the hot press procedure. These robust covalent bonds increase interfacial adhesion and are resistant to moisture, leading to bio-composites with a relative strength improvement [112]. The enzyme pre-treatment could also produce radical decay products leading to improved levels of carbonyl groups that enables Lewis acid–base bonding (hydrogen bonding) links.

Table 2.4 Fibreboard produced from enzymatic activation of agricultural/forest biomass fibres

Enzyme	Fibre	Incubation parameters				Pressing parameters					Fibreboard properties				Ref.
		T, ˚C	t, h	pH	Enzyme dosage U/g	Mat water content %	T, ˚C	t, min	P, MPa	ρ, g/cm^3	Thickness, mm	IB, MPa	MOR, MPa	MOE, GPa	24 h TS %	
Laccase SP504 (*Tramates versicolor*)	80% spruce/pine mixture with 20% beech	35	12	5	26,900	Dry fibres	190	5	1	0.78	5.4	0.95	-	-	23	[122]
Laccase SP504 (*Tramates versicolor*)	Beech	20	1	4.5	-	12	200	5	n/a	0.90	3	1.57	44.6	3.36	19	[114]
Peroxidase SP502	80% spruce/pine mixture with 20% beech	RT	4	7	4200	Dry fibres	190	5	1	0.8	5	0.63	41.7	4.02	28	[93]
Tramates versicolor medium	Rape straw	-	-	-	-	Dry fibres	-	-	-	0.8	-	0.35	20	-	50	[123]
Laccase (*Myceliophtora thermophila*)	Beech	50	0.5	7	24	11-13	200	5	n/a	0.85	8	0.93	46	3.95	46	[111]
Laccase (*Trametes villosa*)	Beech	20	1	4.5	3	Dry fibres	200	5	n/a	0.85	3	-	40.3	4.08	-	[112]
Laccase (*Myceliophtora thermophila*)	Beech (TMP)	RT	6	6.7	500	40	190	7	0.3	0.92	4-45	1.4	53	4.8	26	[124]
Peroxide (4%H_2O_2 + 1% Ferrous sulphate) based on dry wheat straw	Wheat straw	-	-	-	-	Wet fibres	200	1.3	0.5	1.0	6	0.67	23	3.5	85	[121]

2.2 Structural analysis for lignin characteristics in biomass straw

2.2.1 Introduction

The word lignin was put forward in 1865 by Schulze to describe the dissolved part of wood when treated with nitric acid [125,126]. The structure of lignin is probably the single most important parameter for understanding and hence utilising straw [127-129].

A number of chemical and physical methods used for characterising lignin's structure are destructive. However, there are non-destructive methods too (i.e. non degratative, consists of various microscopic and spectroscopic methods), such as 1) fourier transform infrared spectroscopy (FT-IR) which is believed to be one of the most informative methods of lignin investigation, 2) ultraviolet (UV), 3) carbon-13 nuclear magnetic resonance spectroscopies (^{13}C-NMR) and 4) gas permeation chromatography (GPC) [130].

Lignin is an extremely complex three-dimensional polymer formed by radical coupling polymerisation of *p*-hydroxycinnamyl, coniferyl and sinapyl alcohols. These three lignin precursors monolignols give rise to the so-called *p*-hydroxyphenyl (H), guaiacyl (G) and syringyl (S) phenylpropanoid units (see Fig.2.5) [131]. The definition of lignin has never been as clear as that of other natural polymers such as cellulose and protein, the reason being the extremely complicated isolation, compositional analysis and structural characterisation [132].

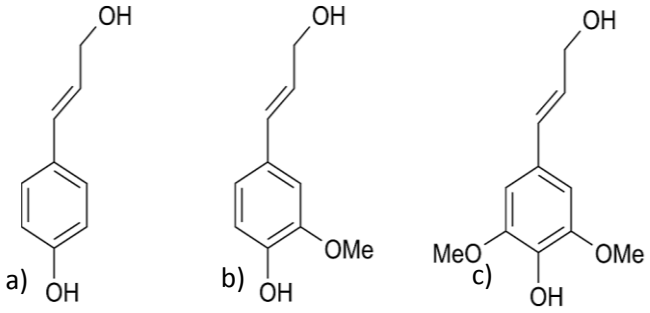

Figure 2.5 Three primary lignin monomers: (a) monolignols *p*-coumaryl alcohol M_H, (b) coniferyl alcohol M_G and (c) sinapyl alcohols M_S [133]

These aromatic building units are linked to a variety of ether and carbon-carbon bonds. The predominant linkage is the so called *β-O*-4 linkage. About 40–60% of all inter-unit linkages in lignin are via this ether bond. Different types of linkage between phenyl propane units form three dimensional net structures which make it difficult to completely degrade non-regular lignin macromolecules. Lignin is primarily a structural material to add strength and rigidity to cell walls and constitutes between 15 and 40 weight% of the dry matter of plants,

whether wood, straw or other natural woody plants [134-136]. Lignin acts as a matrix together with hemicelluloses for the cellulose microfibrials which are formed by ordered polymer chains that contain tightly packed, crystalline regions, represented in Fig. 2.6.

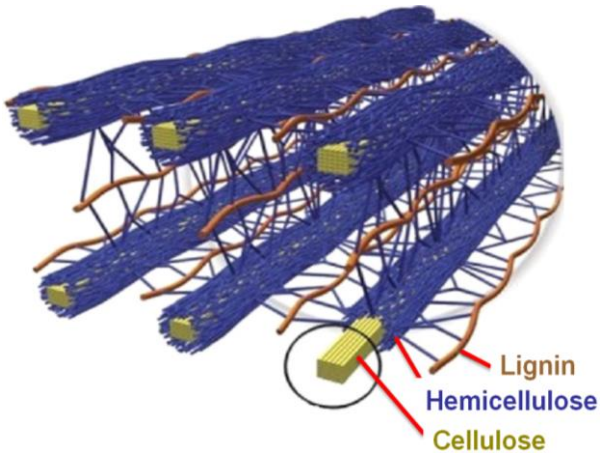

Figure 2.6 Cellulose strands surrounded by hemicellulose and lignin [137]

Covalent bonds between lignin and the carbohydrates have been suggested to consist of benzyl esters, benzyl ethers and phenyl glycosides [132,138,139]. Despite lignin's unique characteristics as a natural product with multiple chemical and physical functionalities, it is largely underutilised. The current work of researchers has focused on expanding the frontiers of application of NMR to straw lignin analysis in order to explore lignin's potential [128,140,141]. The main goal of this section is to study in details the structure of straw lignin and to review the analytical techniques up to date. This will then contribute to a better understanding of lignin and hence could lead to the optimisation of straw biomass for specific and value added industrial utilisations.

2.2.2 Composition and morphology of straw

Straw is considered a natural composite material because of its composition of polysaccharides (cellulose and hemicelluloses) and lignin. The former two components are hydrophilic and the latter is hydrophobic. However, they are practically insoluble in water due to hydrogen bonding and covalent bonding with lignin [130]. The ultrastructure of wheat straw fibres, like wood tracheids, consists of the middle lamella (ML), primary wall (P) and secondary wall (S3, S1, S2). The percentage volume fraction (PVF) and thickness of various morphological layers of wheat straw can be different from those of wood (e.g. spruce), as shown in Table 2.5 [142], especially the S1 layer of wheat straw fibre is thicker than that of the spruce tracheid. Additionally PVF of ML and cell corner (CC) in wheat straw fibre is greater than that of spruce tracheid.

Table 2.5 The thickness and PVF of wheat straw [142]

Morphological layers	Wheat straw				Spruce tracheid	
	Thick fibre		Thin fibre			
	Thickness (μm)	PVF (%)	Thickness (μm)	PVF (%)	Thickness (μm)	PVF (%)
ML+P	0.1-0.2	9.3	0.06-0.12	12.3	0.05-0.1	10.2*
S1	0.1-0.3		0.2-0.3		0.15-0.2	9.9
S2	1.8-2.5	83.5	0.5-0.8	80.7	0.7-2.0	75.9
S3	0.15-0.3		0.1-0.2		0.1	4.0
CC	-	5.4	-	7.0	-	-

*containing the CC region

When it comes to the morphology of straw, normally the sclerenchyma cells in the bundle itself have a small diameter and a thick fibre wall while the extra vascular fibres often have a much larger diameter and a very variable wall thickness. In wheat straw these fibres occur as coarse bast fibres just inside the epidermal layer shown in Fig. 2.7i [143]. Unlike wheat, the cross-section of rice straw reveals a different type of ultrastructure, beside the tubular concentric ring structure, the centre of the rice straw internodes contains a core, Fig. 2.7ii. Moreover, rice is an aquatic plant and has a different type of protecting layer, including substances composed of lignin, amorphous silica, and other inorganic substances.

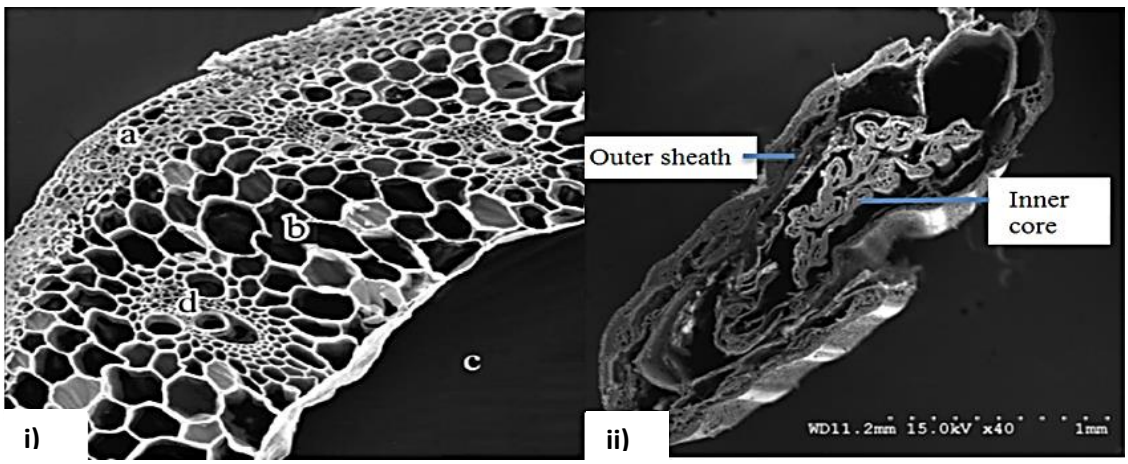

Figure 2.7 i) Wheat straw internode SEM (a) epidermis, (b) parenchyma, (c) lumen, (d) vascular bundles[143]**; (ii) rice straw internode SEM** [144]

2.2.3 Analytical techniques for structural analysis of straw lignin

There is a need of properly characterising and classifying lignin for the promotion of the new applications. At the product development level, appropriate analysis will facilitate the

definition of specifications for commercial purposes. This also allows the reliable monitoring of physical and chemical modifications which eventually will lead to understanding the relationship between properties and performance. The structure of lignin has been traditionally revealed by a series of chemical analysis, such as thioacidolysis (TA) [145], nitrobenzene oxidation (NBO) [146] and derivatization followed by reductive cleavage (DFRC) [147]. Nevertheless, recent developments in nuclear magnetic resonance (NMR) technology have made this technique the most widely used technique in the structural characterisation of lignin, the reason being its versatility in indicating structural features, and structural changes of lignin.

The studies on lignin are divided into two different sections: qualitative and quantitative analyses. Some researchers (e.g. Wen et al. [127] divided the analytical methods of lignin characterisation into two groups of destructive and non-destructive methods. TA [145], NBO [146] and DFRC [147] are amongst the destructive methods used. The non-destructive methods include various spectroscopic methods (e.g. UV, FT-IR and near infrared spectroscopy [148,149]) and NMR techniques. Other techniques to analyse lignin in the cell wall are based on mercurization which was firstly used in the early history of lignin chemistry to characterise its structure [150]. Mercurization is a reaction occurring under mild conditions. It is less sensitive to the substitution pattern of the aromatic ring.

2.2.3.1 Quantitative analysis

Quantitative measurement of lignin structures is an important aspect when it comes to investigating lignin. The measurement of various structures of lignin is possible when appropriate standards or pulse sequences are applied [151-153]. Quantitative analysis is based on gravimetry or UV-absorption [154] either to estimate lignin as an insoluble residue after strong sulfuric acid treatment (Klason lignin) [155] or to oxidise away the lignin from a holocellulose preparation (acidic chlorite lignin or permanganate lignin) [156]. The spectroscopic techniques, such as infrared (IR) and ^{13}C-NMR spectroscopy, are complementary to the above procedures since they provide information on the whole structure of the polymer and avoid the possibility of degradation artefacts [157].

1) FT-IR

Among all the quantitative analysis techniques, FT-IR spectroscopy shows interesting characteristics, including high sensitivity and selectivity, high signal-to-noise ratio, accuracy,

data handling facility, mechanical simplicity and short time with small amount of sample required for the analysis [158]. In addition, the spectrum of a lignin sample gives an overall view of its chemical structure [159].

FT-IR opens perspective to find structural discrepancies in lignin isolated by different methods. Infrared radiation covers the wavenumbers between 13300 cm^{-1} and 3.3 cm^{-1}. The infrared region is usually divided into 3 regions: near infrared (13300 - 4000 cm^{-1}), mid infrared (4000 – 200 cm^{-1}) and far infrared (200 – 3.3 cm^{-1}) regions. Organic compounds have fundamental vibration bands in the mid infrared region, which is why the region is widely used in infrared spectroscopy.

An infrared spectrum is unique to each substance and can therefore, in principle, be used as an impartial characteristic to identify the sample. Every lignin IR spectrum has a strong wide band between 3500 – 3100 cm^{-1} assigned to OH stretching vibrations. This band is caused by the presence of alcoholic and phenolic hydroxyl groups involved in hydrogen bonds. The intensity of the band increases during demethylation and decreases during methylation since during demethylation the O-CH_3 bonds in methoxyl groups bonded to 3^{rd} or 5^{th} carbon atom of the aromatic ring are split and CH_3 is replaced by a hydrogen atom producing a new -OH group. During methylation the O-H bonds are split and H is replaced by CH_3 group and the amount of -OH group decreases hence the intensity of the band decreases [160]. Acetylation of the lignin causes a partial or full band loss since almost all of -OH groups is replaced by CH_3COO [161].

The assignments of FT-IR absorption bands for the lignin normally include the aromatic skeleton vibrations at 1606, 1507 and 1434 cm^{-1}, in which the aromatic semicircle vibration (a vibration involving both C-C stretching and a change of the H–C–C bond angle) is assigned at 1507 cm^{-1} [162], the carbonyl and unconjugated ketone and carboxyl group stretching at 1732 cm^{-1} and the small band of the conjugated carbonyl stretching such as detected in organosolv lignin at 1653 cm^{-1}. More detailed assignment are summarised in Table 2.6 [131,163,164].

Table 2.6 Assignments of FT-IR absorption bands (cm^{-1}) [131]

Absorption bands	Assignment
3429	-OH stretching
2945	CH stretching of methyl, methylene or methane group
1732, 1726	C=O stretch in unconjugated ketone and carboxyl group
1660, 1653	C=O stretch in conjugated ketone
1606	Aromatic skeletal vibration
1507	Aromatic skeletal vibration
1460	Aromatic methyl group vibrations
1434	Aromatic skeletal vibration
1374	Aliphatic C-H stretch in CH_3
1328	Syringyl ring breathing with C-O stretching
1242	Aromatic C-O stretching
1165	C-O stretch in ester groups
1135	Aromatic C-H in-plane deformation for syringyl type
1043	Aromatic C-H in-plane deformation for guaiacyl type
855, 844	Aromatic C-H out of plane bending

2) Thermal analysis

Thermal analysis is a set of techniques used to describe the physical or chemical changes associated with substances as a function of temperature. The thermal stability of the isolated hemicellulose, cellulose and lignin is determined by thermogravimetric analysis (TGA) and differential scanning calorimetry (DSC). TGA can be used to monitor the weight loss of the lignin as it is heated, cooled or held isothermally, while DSC is performed to determine the melting temperature and enthalpy of the lignin. DSC is also the most widely accepted method for determining glass transition temperatures (Tg) of lignin [165]. Thermo-analytical techniques, in particular TGA and derivative thermogravimetric (DTG), allow the information about the chemical composition of straw to be obtained in a simple and quantitative manner. For TGA and DSC the heating rate is usually between 5-10˚C. The tests are undertaken in both nitrogen and air atmosphere between room temperature of 25-30˚C up to 730-800˚C [166]. Pyrolysis–gas chromatography/mass spectrometry (Py–GC/MS) has also been applied to examine reaction products of thermal degradation [167] and an effective tool to investigate fast pyrolysis of biomass and on-line analysis of the pyrolysis vapours [168,169]. Py–GC/MS provides a rapid and easy alternative to tedious chemical degradation

procedures for analysing the monolignol composition of lignin samples [170]. It requires only a small amount of lignin (<1 mg) and samples do not have to be isolated from the associated plant polysaccharides to be effective. Compounds separated on a GC column can easily be identified from their mass spectra as being derived from *p*-hydroxyphenyl (H), syringyl (S), or guaiacyl (G) propane units. Integration of the chromatograph peaks can determine if the sample in question comes from a G, S/G, or H/S/G type lignin. Thermal degradation of lignin is reviewed by Brebu and Vasile [171] where the information on the temperature range, kinetics and mechanism of thermal degradation are presented.

Müller-Hagedorn and Bockhorn [172] obtained kinetic parameters for straw lignin in a TGA based on the Levenberg–Marquardt and improved Runge–Kutta laws. The activation energies and frequency factor for barley straw lignin varied from 92 to 102 $kJmol^{-1}$ and from $10^{7.3}$ to $10^{7.9}$ min^{-1} respectively. Ghaly et al. [173] used TGA and differential thermal analysis (DTA) to study the behaviour of oat straw in an oxidising atmosphere (15% oxygen and 85% nitrogen). Two distinct reaction zones were observed on the TGA and DTA curves. Higher thermal degradation rates were observed in the first reaction zone due to the rapid release of volatiles as compared to those in the second reaction zone. The activation energies were in the range of 83-102 and 58-75 $kJmol^{-1}$ for the first and the second reaction zones, respectively. The thermogravimetric dynamics parameters of wheat straw enzymatic acidolysis lignin were calculated by two methods of Kissinger and Ozawa, where the activation energy was 103.92 and 107.69 $kJmol^{-1}$ respectively [174].

Carrier et al. [175] have also investigated the suitability of TGA as a new method to obtain lignin, hemicellulose and α-cellulose content in biomass. The study indicated comparable results to common methods used for α-cellulose content. However, this method cannot be extended to the lignin content due to important deviations in the correlation curves. This alternative method it's suitable for determining the hemicelluloses and α-cellulose contents of biomass samples. Is faster, easier to implement and less cost effective than the existing wet chemical techniques.

3) NMR

NMR has been shown to be reliable and comprehensive among the various methods for the characterisation of lignin. It could provide both quantitative and qualitative information. An inclusive review on NMR application for structural analysis of lignin was published in 1971 [176]. Lundquist [177-179] has also published works about the NMR characterisation of

lignin. In the past, proton NMR (^{1}H-NMR) was mainly used for lignin characterisation and the ^{1}H-NMR spectrum of acetylated lignin was used to determine the quantity of different hydroxyl groups. With the development of NMR techniques, ^{13}C-NMR became popular in lignin characterisation as it is powerful and capable of revealing a large amount of lignin structural information, including the presence of aryl ethers, condensed and uncondensed aromatic and aliphatic carbons. Since the 1980s, many studies on ^{13}C-NMR spectra of lignin have been conducted [180-183]. Attempts have been made to increase the sensitivity and signal-to-noise ratios of the quantitative ^{13}C-NMR spectra [127].

The most recent practices in the use of quantitative ^{13}C-NMR spectroscopy for the characterisation of lignin are confined to using the aromatic and methoxyl signals as internal standards in expressing the various functional groups per C_9 [184]. Such a practice is applicable to native lignin, but not for industrial lignin or modified lignin [185]. To overcome the above defects, Xia et al. [185] suggested a novel protocol for acquiring quantitative ^{13}C-NMR spectra of lignin by using the internal reference compounds 1,3,5-trioxane and pentafluorobenzene. Trioxane offers a convenient internal standard for collecting inverse gated proton decoupled ^{13}C-NMR spectra for lignin. The internal reference compounds provide single and un-overlapped sharp signals in the middle of the spectral region, permitting superficial integration.

Detailed approaches for the quantification of different lignin structures in milled wood lignin (MWL) have also been reported by using quantitative ^{13}C-NMR techniques [186,187], including the amount of different linkages, various phenolic/etherified non-condensed/condensed guaiacyl and syringyl moieties. This approach is comparable to that reported from other wet chemistry techniques, but takes shorter experimental times.

Both solid-state and solution-state ^{13}C-NMR have been used for structural characterisation of lignin [188,189]. However the solution-state NMR is more informative because of its better resolution, although soluble lignin preparations may not be representative of the whole lignin fraction in straw biomass [190,191]. It is worth mentioning that structural characterisation of lignin could be directly investigated by NMR techniques via non derivatization solvent systems, such as DMSO-d_6/NMI-d_6 [192], DMSO-d_6 [193] and DMSO-d_6/pyridine-d_5 (as gelling solvent) [194]. The rapid NMR characterisation method provides what appears to be the best tool for the detailed structural study of the complex cell wall polymers. Based on

these non-acetylated solvent systems, lignin composition (notably, the syringyl: guaiacyl: *p*-hydroxyphenyl ratio) could be quantified without the need for lignin isolation [127].

For the ^{13}C-NMR, there still remain some issues to be overcome, such as precise signal assignments and true quantification based on ^{13}C-NMR spectra of lignin, which are difficult due to signal overlap. Fortunately, most of the NMR techniques are adequate when the researchers want to monitor changes in structure of straw biomass during a particular treatment.

4) Two-dimensional HSQC NMR

The interest to study lignin has created the demand to employ high magnetic field NMR spectrometers to improve resolution and sensitivity. Proton–carbon correlated two-dimensional (2D) NMR can exploit the wide chemical shift range of carbon, thus offering a significantly improved resolution [195]. 2D NMR of both homo- and heteronuclear became popular with much powerful tools for lignin characterisation [196-198]. The most used and valuable 2D NMR is heteronuclear-single-quantum-coherence (HSQC) that provides the correlation between directly bonded protons and carbons in two dimensions [186,199]. Overlapping protons that are attached to carbons with different shifts are separated by their carbon shift difference. While overlapping carbons may be separated by their attachment to protons with differing chemical shifts. The apparent resolution of 2D spectra is, therefore, much better than anything that can be achieved in 1D spectrum [132]. Quantitative measurement of various structures of lignin is possible when appropriate standards or pulse sequences are applied [152,186]. The assignment for lignin correlations comes from the extensive database of lignin model compounds along with data from a long history of NMR of both isolated and synthetic lignin [151,200-205]. The 2D-HSQC experiments of non-acetylated lignin samples have been valuable in assigning major structures (*β*-O-4, *β*-*β*, *β*-5, etc.) in the lignin samples from different origins, such as some non-woody plants [151], Jute fibres [200], bamboo [202,203,205], Triploid poplar [206-208] and wheat straw [201]. HSQC spectra have been crucial in recognising new, but also minor lignin structural units. The clear identification of dibenzodioxocins (5-5 linkages) as major new structures in lignin has been a significant finding [209,210].

Evidence provided by 2D NMR is far more diagnostic than 1D data purely because of the simultaneous constraints that are revealed in the data. Consequently, the observation that there is a proton at 4.9 part per million (ppm) directly attached to a carbon at 84.4 ppm and a

proton at 4.1 ppm attached to a carbon at 82.5 ppm is more revealing than just observing two new carbons at 84.4 and 82.5 ppm in the 1D spectrum [210]. Zhang and Gellerstedt [152] presented a new analytical method based on the 2D-HSQC NMR sequence and quantitative ^{13}C-NMR, which can be applied for quantitative structural determination of complicated polymers, such as lignin and cellulose derivatives. This method is a combination of HSQC and quantitative ^{13}C-NMR techniques, which gives more reliable data about the lignin linkages. The 2D-HSQC NMR technique is also useful in the determination of the structural characteristic features of the oxygenated aliphatic region of lignin polymeric framework [151,211]. A recent study showed that 2D-HSQC NMR spectra of enzymatic hydrolysis residue (EHR) delivered very well resolved spectra that can be compared to that of MWL [212]. Based on the results obtained, it was found that in situ characterisation of pre-treated biomass by HSQC NMR analysis is a beneficial structural analysis method in the emerging field for the characterisation of EHR. Heteronuclear multiple quantum coherence (HMQC) or HSQC spectra of lignins have been reviewed [198] and well reported by previous researchers [60,213-216]. The assignments in HMQC/HSQC spectra should be made with comprehensive knowledge of both carbon and proton chemical shifts for each structural type.

5) DFRC method

The derivatisation followed by reductive cleavage method (DFRC) was developed by Lu and Ralph in 1997 as an alternative to thioacidolysis [147,217]. Because of the mild conditions used and its unique selectivity, the DFRC method has become widely used for characterising lignin from various origins [218-220]. DFRC is a flexible method due to its distinctly separated steps, which allow the quantification of different monomeric units and structures. On the basis of this flexibility, Tohmura and Argyropoulos [221] proposed the combination of DFRC with quantitative ^{31}P-NMR data. The DFRC procedure, as a basic component, has been modified or combined with other techniques to provide more precise and specific quantitative data about lignin structures. The combination of DFRC with quantitative ^{31}P-NMR was shown to have significant potential for the determination of arylglycerol-α-aryl ether and other linkages [222]. Coupled with the spread of advanced NMR techniques, lignin structural inquiries have been greatly facilitated by the development of various degradative protocols, i.e. DFRC which efficiently cleaves the β-aryl ethers in lignin.

One unique feature of the DFRC method is that esters on lignin remain fully intact during the DFRC procedure [223]. Therefore, *p*-coumarates on lignin from straw biomass can be detected and measured [224]. With a few modifications to the standard DFRC procedure by

replacing the acetyl-containing reagents (acetic acid and acetyl bromide) with the propionyl analogs, the modified DFRC method was applied to detect and quantify the naturally occurring acetates on lignin from kenaf, aspen and other non-woody plants [225].

6) H/S/G ratio

Qualitative or semi-qualitative indication of H/S/G (*p*-hydroxyphenyl/syringyl/guaiacyl) ratio units are not too informative and on the other hand, they are very laborious, lengthy and also prone to errors. The quantification of lignin H/S/G ratio has been reported by ^{13}C NMR and HSQC NMR analysis [226,227]. Table 2.7 shows the *p*-hydroxyphenyl–syringyl–guaiacyl (H/S/G) ratio for different types of biomass which vary considerably amongst each other. Thioacidolysis is the most used analytical method for lignin analysis to obtain information about uncondensed structures (H/S/G ratios) [132]. Thioacidolysis was developed by Lapierre, as an extension of acidolysis, to cleave β-aryl ethers in lignin so that the basic units linked by β-aryl ethers are released as monomers to be quantified by gas chromatography [145]. Therefore, the yields of monomers released by thioacidolysis reflect the proportion of uncondensed units in lignin. When thioacidolysis is used for straw lignin, esters on straw lignin may decrease the efficiency of β-ether cleavage by thioacidolysis [228,229]. This should be taken into consideration when interpreting thioacidolysis results for straw biomass. Permanganate oxidation, nitrobenzene oxidation, GC-MS pyrolysis, thioacidolysis and DFRC are degradative methods that reveal the H/S/G composition of the lignin polymer. All these methods release only a fraction of the lignin for analysis. They are based on the cleavage of lignin backbone and provide partial data due to the specificity of the treatment.

Table 2.7 H/S/G ratios for types of biomass resources

Type	Lignin %	H	S	G	Reference
Wheat straw	16-21	9	46	45	[230]
Rice straw	6	15	40	45	[230]
Rye straw	18	1	53	43	[231]
Hemp	8-13	9	40	51	[170]
Jute	15-26	2	62	36	[232]
Flax	21-34	4	29	67	[230]

2.2.3.2 Qualitative analysis

The qualitative lignin analysis relies rather much on studies of lignin concentration and distribution. These methods only provide preliminary information which could then be useful for the quantification of lignin in the straw.

1) SEM-EDX

Scanning electron microscopy (SEM) is used to examine the microstructure, morphology and crystalline structure of the straw. The microscope could be equipped with energy-dispersive X-ray (EDX) analyser, which provides useful element compositions and information about the chemical composition of the straw and its surface. SEM analysis also provides information on the particle and/or cell size. When the straw is being treated by means of chemical or mechanical methods, the particle sizes and morphology might change (i.e. surface of straw might become smoother or rougher) depending on the type of treatment [233]. This could be monitored by qualitative comparison.

The distribution of lignin could also be qualitatively analysed, for instance, field emission scanning electron microscopy (FE-SEM) was used by Koo et al. [233] in order to observe the change in lignin distribution during pre-treatment, see, Fig. 2.8.

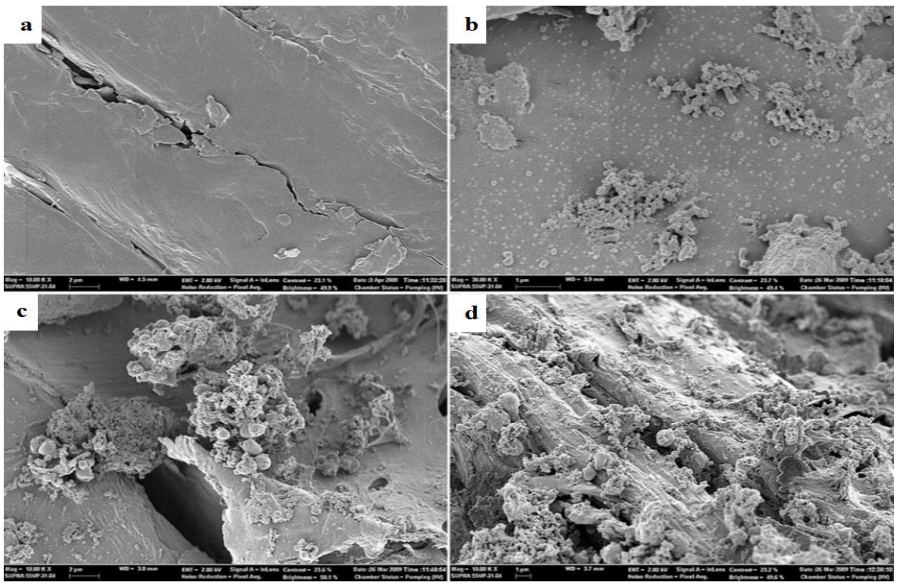

Figure 2.8 Droplets on surface of pre-treated biomass due to the isolation and migration of lignin (a: untreated biomass; b: pre-treated at 120˚C; c: pre-treated at 130˚C; d: pre-treated at 140˚C) [233]

2) TEM and optical microscopy

Transmission electron microscopy (TEM) has been proved to be an effective tool for determining cell wall ultrastructure. TEM observations deliver further details of lignification

and the distribution of lignin. Based on the intensity of the staining, the concentration of lignin in different morphological regions of straw could be qualitatively examined by TEM micrograph. For example, Fig. 2.9 shows the distribution and concentration of lignin under TEM. The dark staining of the cell corner middle lamella (CCML) and compound middle lamella (CML) indicates that both of them are strongly lignified.

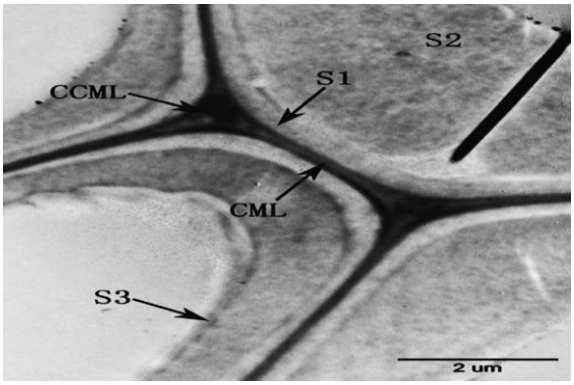

Figure 2.9 TEM micrograph of an ultrathin transverse section of the cell wall of Forsythia suspensa fibre: S1= outer secondary wall, S2= middle secondary wall and S3= inner secondary wall [234]

Optical microscopy (OM) is unable to provide the detailed features of the straw, but is a good tool to observe the lignin distribution within the straw. It is also a quick and easy method to observe the overall structure of straw and to observe the changes that may occur after any treatment. The evaluation of straw morphology for preliminary research can usually be carried out using OM or light microscopy. Basic parts, including epidermis, cortex, vascular bundle and pith of the straw, can be observed. The epidermis cells are arranged in parallel rows and packed closely to protect the internal parts of the plant, the cortex is the zone between epidermis and the vascular bundles and contains collenchyma and parenchyma cells. The pith is the central part of the stem which is composed of thin walled parenchyma cells, and the vascular bundles in the stem of the grass are also observed, which vary in number and size, as shown in Fig. 2.10.

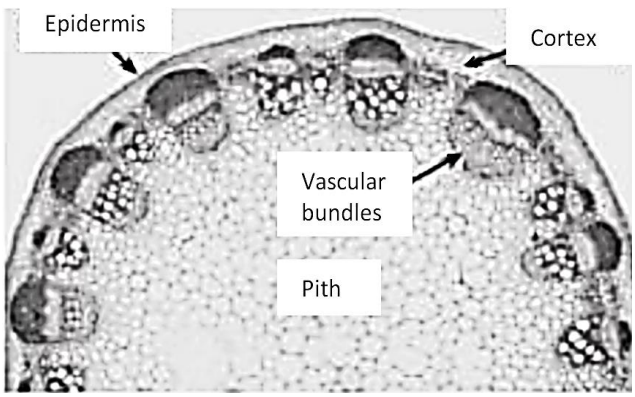

Figure 2.10 Light micrograph of a cross section of grass stem, showing four basic parts [235]

2.2.4 Structure of straw lignin

Plants have lignin containing significant levels of other unusual components and it is likely that no plant contains lignin that is solely derived from the three main precursors, hence lignin is viewed not as a constitutionally defined compound, but as a composite of physical and chemically heterogeneous materials, whose structure may be represented by models such as those proposed for wheat straw [236], shown in Fig. 2.11. This should not be regarded as depicting the structural formulas for lignin in the usual sense, but as a medium for illustrating the types and linkage modes of structural elements and the proportions in which they are believed to occur in lignin [235]. Lignin monolignols are polymerised by a radical coupling process that links them by carbon-carbon or ether bonds. A linkage may occur at any of several different locations on each phenolic unit, causing many different linkage types to be possible. The most common linkage types found in a lignin molecule are *β*-O-4, α-O-4, *β*-5, 5-5, 4-O-5, *β*-1 and *β*-*β* [237,238].

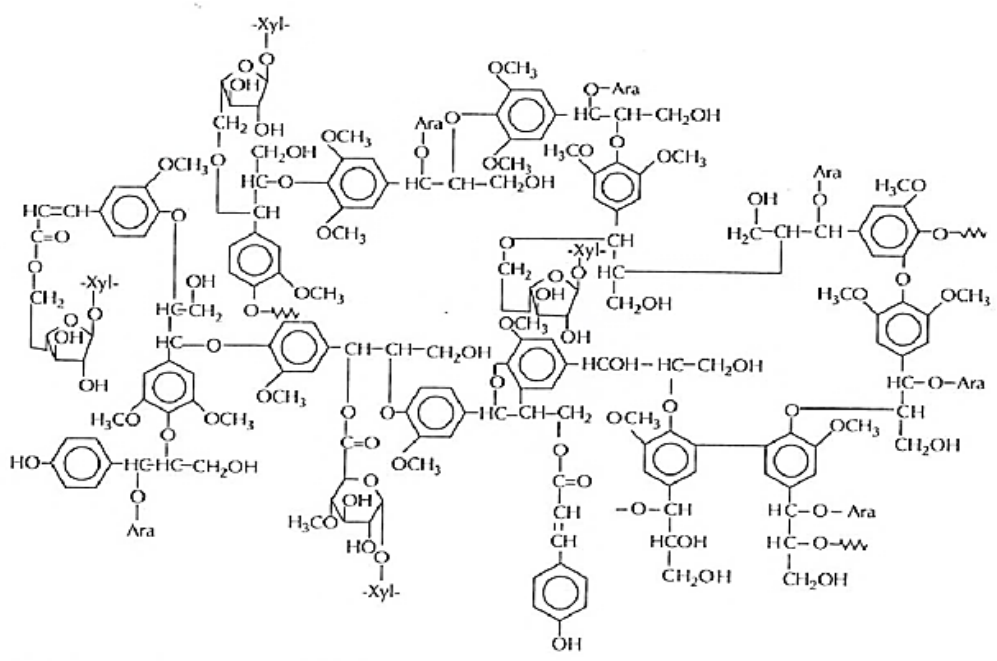

Figure 2.11 A tentative chemical structure of wheat straw lignin [236]

The composition and structure of lignin varies considerably within and amongst plants. Lignin has been classified into three groups: Gymnosperm (softwood), Angiosperm (hardwood) and Grass lignin. However, it was recently found that these categories are inadequate because of ignoring most of the herbaceous angiosperm lignin and some conifer families containing guaiacyl and syringyl types of lignin. It was suggested by Gibbes that lignin should be categorised into two groups: guaiacyl lignin and guaiacyl-syringyl lignin according to their overall chemical constitutions [132]. Each type also generally contains a

small proportion of *p*-coumaryl units, though grass lignin generally contains a higher amount of *p*-coumaryl units than woody lignins [239]. Other phenolic compounds (alcohols, aldehydes, acids, esters and amides) have been reported to act as lignin precursors and illustrate the structural ‘‘plasticity” of the polymer and the adaptability of the lignification mechanisms [240,241]. Several of these compounds (such as p-hydroxycinnamaldehydes, ferulic acid or 5-hydroxyconiferyl alcohol) only provide a significant contribution to lignin in transgenic plants with modified monolignol biosynthesis [241] and are minor lignin precursors in normal plants [242]. On the other hand, some phenolic compounds with saturated or no side-chains, e.g. dihydrocinnamyl alcohol, sporadically incorporate to the lignin polymer as terminal units, confirmed by 2D NMR [243,244]. Early attempts at establishing the acylation regiochemistry (the site on lignin where the acylation occurs) utilised UV and concluded that *p*-coumarates were mainly at the γ-position of lignin side chains [245]. NMR work on wheat straw lignin [128] showed that the acylation was exclusively at the γ-position, implicating enzymatic processes in the formation of the ester. The DFRC method, which leaves such γ-esters intact, further established the γ-acylation and, as for acetates, indicated that *p*-coumarates were predominantly on syringyl units [224].

2.2.4.1 LCC linkages

Lignin is always associated with carbohydrates (in particular with hemicelluloses) via covalent bonds at two sites: α-carbon and C-4 in the benzene ring, and this association is called lignin carbohydrate complexes (LCC). The major inter-unit linkages within the lignin monomer (H, S, and G) are *β*-O-4, *β*-*β*, *β*-5, *β*-1 arrangements. The chemical linkages limit the efficient separation of lignin from plant cell walls. Thus, it is important to understand the LCC linkages of lignin samples. The LCC from straw are structurally different from those in the woods. They contain ferulic bridges between lignin and carbohydrates (arabionxylans) through ester-linked ferulic acids [246]. Therefore, they are often referred to as “lignin/phenolics–carbohydrate” complexes as shown in Fig. 2.12 [236].

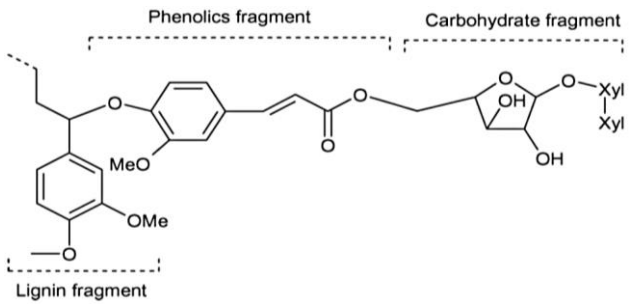

Figure 2.12 Lignin phenolic carbohydrate complexes in wheat straw [236]

The association of lignin and carbohydrates in straw cell walls is largely through free radical coupling of ferulates or diferulates with monolignols or growing lignin oligomers. Due to the complexity of LCCs, the isolation of homogeneous preparations is the most important step for the compositional analysis and structural characterisation. Many isolation methods for LCC have been tried, however, the finely divided plant meal [247,248] and MWL [249] were preferred sources for LCC isolation due to the fact that any chemical or biochemical treatment before LCC isolation would break linkages between lignin and carbohydrates.

The cross-linking of carbohydrates and lignin by ferulates presents the greatest barrier to efficient utilisation of straw cell wall [228].

2.2.4.2 Physical properties

The physicochemical state of lignin determines how and where it could be used in the synthesis of different products. The source of lignin and the method of extraction have a strong influence on its physical properties [250]. The reactivity and physicochemical properties of lignin are dependent to a certain extent on their molecular weight distribution, see Table 2.8. The reactivity of lignin will impact on the qualities of the end products. For instance, Muller et al. [251] found that kraft lignin-based phenol formaldehyde resins have superior properties to steam exploded lignin-based phenol formaldehyde resins. Methods for lignin molecular weight determinations are developed and described by previous researchers [252,253], i.e. size-exclusion chromatography which measures the molecular weight distribution of lignin.

Another important factor is the glass transition temperature, T_g, which is an indirect measure of crystallinity and degree of crosslinking and directly indicates the rubbery region of the material [254]. Lignin cross-linking degree will depend on the quantity of water and polysaccharides, as well as molecular weight and chemical functionalisation. It generally increases with increasing molecular weight.

Table 2.8 Molecular weight and functional groups of lignin [1]

Lignin type	M_n (g mol^{-1})	COOH (%)	OH phenolic (%)	Methoxy (%)
Soda (bagasse)	2160	13.6	5.1	10.0
Organosolv (bagasse)	2000	7.7	3.4	15.1
Soda (wheat straw)	1700	7.2	2.6	16
Organosolv (hardwood)	800	3.6	3.7	19
Kraft (softwood)	3000	4.1	2.6	14

2.2.4.3 Lignin distribution and concentration

Lignin's properties are significantly different with carbohydrates such as their activity and solubility, according to which the distribution of lignin in plant cell wall can be analysed. Many techniques have been applied to the study of distribution of lignin. Some of the old procedures are selective staining which is followed by the study under light microscope or electron microscopy [255]. The studies that focused on quantitative data on the lignin distribution in the secondary wall and CML have been carried out by UV microscopy [256]. UV absorption is a tool used for lignin identification as lignin absorption occurs at 280 nm. The weight concentration of lignin was estimated to be 16% and 73% for the secondary wall and CML of Norway spruce tracheids respectively [257]. Lange and Kjaer [258] proposed interference microscopy based on the pathways of rays which is another method for quantitative analyses of lignin distribution within the cell wall layers. The lignin distribution in wood and straw was determined with interference microscopy combined with electron dispersive X-ray analysis (EDXA), in differentiating xylem and in chips during pulping [259,260]. The technique is fully quantitative and precise. Donaldson [261] used confocal laser scanning microscopy (CLSM) to study lignin distribution in agricultural fibres. Although many chemical studies of grass lignin have been carried out, there are still little quantitative data on lignin distribution in grass species.

Zhai and Lee [142] used SEM-EDXA technique to determine the Br-L X-ray counts of the different brominated wheat straw cells which are presented in Table 2.9. In fibre and non-fibre cells of wheat straw, the lignin concentration is the highest in the cell corners (CC) and the lowest in the secondary wall. In the morphological regions of all cells, the lignin concentration is the highest in parenchyma cells followed by fibres, and is the lowest in epidermis cell [142]. Interference microscopy [259] and CLSM [262] were also used by researchers to examine the lignin concentration of wheat straw in the ML and in the secondary wall.

Table 2.9 Lignin concentration and distribution in wheat straw [22]

Cells	S	CML	CC
Br-L X-ray counts			
Thick wall fibre	1620	2156	2992
Thin wall fibre	1340	2004	3336
Parenchyma cell	2005	2599	-
Epidermis cell	1022	1690	1743
Lignin concentration (g/g)			
Thick wall fibre	0.168	0.412	0.571
Thin wall fibre	0.154	0.339	0.664
Lignin distribution (%)			
Thick wall fibre	67.5	18.0	14.5
Thin wall fibre	57.5	20.3	22.22

2.2.4.4 Lignin functional groups and their characteristics

The key chemical functional groups in lignin are the hydroxyl, methoxyl, carbonyl and carboxylic groups. The quantity of these groups depends on the genetic origin and isolation processes adapted. Functional groups characterisation can be used to determine the lignin structure. Various analytical methods for determining functional groups in technical lignin have been studied, while the statistical comparison of the different analytical methods for hydroxyl groups has been found not fully comparable [263]. The aminolysis and non-aqueous potentiometry are assumed to be the most reliable for phenolic hydroxyl groups, whereas the oximating method was found the most reliable method for determining the total carbonyl which was first described by Faix et al. [264]. The phenolic hydroxyl group is a significant functionality which influences the physical and chemical properties of lignin polymer. Lai described a procedure to determine free phenolic hydroxyl groups in lignin [265]. The Common physical method used to estimate the phenolic hydroxyl content of lignin is UV spectroscopy, which is based on differences in absorption of phenolic units in neutral and alkaline solutions [266].

Methoxyl groups (-OCH_3) are found in lignin from all plants. The amount of the methoxyl groups is often used as a measure of the purity of lignin, since the isolated lignin sometimes is contaminated with hydrocarbons. The classical method for methoxyl determination of lignin uses hydroiodic acid to promote demethylation and gas chromatography to determine

the percentage methoxyl. Alternative method, which is less tedious, involves the use of proton nuclear magnetic resonance (^{1}H NMR) [267]. On the other hand, when it comes to hydroxyl groups of lignin, there are the primary aliphatic hydroxyl groups bonded to the γ-C-atom, secondary aliphatic hydroxyl groups bonded to the α-C-atom and phenolic hydroxyl groups bonded to the 4-C-atom of the aromatic ring in lignin. The accurate determination of these types is difficult since they have similar chemical properties and reactivity. Although the total amount of hydroxyl groups in lignin could be determined by potentiometry [268].

Natural lignin contains a low concentration of COOH-groups. However, when lignin is subjected to chemical or biological treatments, carboxyl groups are frequently detected in significant quantities, hence quantitative measurements of carboxyl groups may provide information regarding the degree to which the lignin has been degraded or modified as a result of treatments. Further carboxyl groups are produced during delignification as a result of oxidation of hydroxyl and carbonyl groups. Oxidation of the lignin structure will result in an increase of carboxyl absorption in the FT-IR spectra [131]. FT-IR analysis on lignin characterisation could provide the differences in the bonding pattern and the functional groups [269].

2.3 Lignin in straw and its applications

2.3.1 Introduction

The chemical content of straw varies according to the stage of maturity, soil type and fertiliser treatment, as shown in Table 2.10 [270]. The lignin content for those main straw species ranges from 12 to 21%, although it varies from one to another species. The research on lignin has proceeded at a fast pace since the 1960s when powerful modern analytical tools of biochemistry and organic chemistry were applied and therefore interesting information was gathered. Lignin has also attracted much attention because of the dominant pulping industries [271].

The creative design and wise application of innovative technology for the optimisation of renewable resources is one of the novel research topics. Using a system-based approach to design technologies for the sustainable development, management and conservation of natural resources is what researchers are keen to develop. Potential high-value products from isolated lignin include low-cost carbon fibre, plastics/thermoplastic elastomers, polymeric foams/membranes, and a variety of fuels and chemicals, which are all sourced from petroleum [76]. These lignin based products must be low-cost and perform as well as petroleum-derived counterparts [76].

Table 2.10 Chemical composition of agricultural residues (% dry matter) [270]

Type	Lignin	Cellulose	Hemicellulose	Water-soluble	Wax	Ash	Others
Wheat straw	14.1	38.6	32.6	4.7	1.7	5.9	2.4
Rice straw	12.3	36.5	27.7	6.1	3.8	13.3	0.3
Rye straw	17.6	37.9	32.8	4.1	2.0	3.0	2.6
Barley straw	14.6	34.8	27.9	6.8	1.9	5.7	8.3
Oat straw	16.8	38.5	31.7	4.6	2.2	3.1	3.1
Rape straw	21.3	37.6	31.4	-	3.8	6.0	0
Corn cobs	14.6	43.2	31.8	4.2	3.9	2.2	0.1
Bagasse	19.4	39.2	28.7	4.0	1.6	5.1	2

2.3.2 Straw biomass lignin for emerging applications

The history of lignin utilisation traces back to the late 19th century, when lingosulfonates produced from the bisulfite pulping process were claimed to be effective leather-tanning agents and dye-bath additives [272]. Most lignin waste is burned to generate energy for the pulp mills. The water solubility and reactivity of lignin could increase due to the introduction of hydrophilic groups and cleavage of linkages between structural units in the pulping process. This makes the further chemical modification possible. Hence many kinds of useful chemicals can be manufactured from the technical lignins [273]. It has always been and still is a challenging task to use technical lignins (i.e kraft lignin, lignosulfonate, soda lignin, organosolv and ethanol process lignin) efficiently and cost effectively. These lignin types not only lack sulfur groups, but possess interesting properties for different applications. Several technical purposes for lignins have been investigated based on their properties, e.g. where the modified lignin has been used in cross-linked phenolic resin [274], and conventional kraft and sulphite lignin were used as dispersants and binders [132]. Lignosulfonate has excellent dispersing properties and has been used as a superplasticiser in concrete or gypsum to improve their fluidity. However, the most interesting new applications are related to sulfur-free lignin [275], the reason being for their versatility and processed without odour release, which on the other hand, is commonly observed with commercial kraft lignin. Among lignin chemical products, lignosulfonate obtained from spent sulfite pulping liquors are the most available. Various value added products such as vanillin, ferulic acid, coumaric acid, syringol acid, guaiacol, catechol, HPHTM (hydroxyphenyl-(hydroxytolyl) - methane) [276-280] have been produced from lignin.

Lignin can also be converted into a transportation fuel by dehydroxygenation or zeolite upgrading [281]. One-step process to convert lignin into non-viscous organic liquid and oil has been developed in 2008 [282]. Shabtai et al. [283] described a two-stage process in their work for conversion of lignin into high quality reformulated gasoline compositions. Biomass-derived fuels share many of the same characteristics as their fossil fuel counterparts [284-286]. Once formed, they can be substituted in whole or in part for petroleum-derived products. Biofuels such as bioethanol may be easier to commercialise than other fuels due to their acceptable performance. However the pre-treatment process which aims to separate the carbohydrates from the lignin matrix, while minimising chemical destruction of fermentation sugars for ethanol production needs careful evaluation [286]. Success with innovative

production and technology is critical to expanding financial and governmental support for this concept. The intensity of research and the magnitude of capital investment on straw biomass commercialisation should increase once commercial feasibility seems probable.

2.3.3 Types and variations of straw lignin

Lignin is found as a cell wall component in all vascular plants [125]. Lignin acts as water sealant in the stems and plays an important role in controlling the water transport through the cell wall. It also acts as permanent glue, bonding cells together in the plant stems and thus giving the stems their rigidity and impact resistance [287].

Straw lignin comprises all three H, G and S subunits. On the other hand, wood lignin contains mainly G and S subunits (except for compression wood which contains H and G units) [230]. The lignified plant cell walls are developed by successive deposition of cellulose, hemicellulose and lignin to form a composite in which these components are physically and chemically connected to each other [132]. The existence of covalent bonds between lignin and carbohydrates are reported and four types of linkages between lignin and carbohydrates are listed as: 1) glycosidic linkages; 2) ester linkages; 3) benzyl ether linkages and 4) hemiacetal or acetal linkages [132].

1) Lignin in wheat straw

When compared to corn stover, wheat straw comprises lower amounts of lignin and higher cellulose and hemicellulose [230]. The analysis of degradation products following cleavage of ether linkages by thioacidolysis indicated the respective proportions of H, G and S units in wheat straw lignin to be 5, 49 and 46% [288,289]. A specific feature of wheat straw cell walls is the presence of a non-core lignin which is simply soluble in alkali and represents up to 20% of total lignin. The removal of this particular lignin increases the digestibility of the material and improves further microbial or enzymatic bioconversion [290]. The solubility of the straw lignin in alkali has been attributed mainly to the presence of significant amounts of *p*-hydroxyphenyl (H) residues, which are bound to lignin as *p*-coumarate units [291,292].

Tapin et al. [276] compared phenolic compounds found in oilseed flax straw with those in wheat straw, shown in Fig. 2.13, the total content of phenolic compounds is higher in wheat straw than flax straw. Except the vanillin content, ferulic acid and coumaric acid content for wheat straw are much higher than flax straw, the reason being related to the lignin/phenolics-

carbohydrate complexes which have phenolic bridges between lignin and carbohydrates. This shows that there are no such phenolic bridges between lignin and carbohydrates in flax straw.

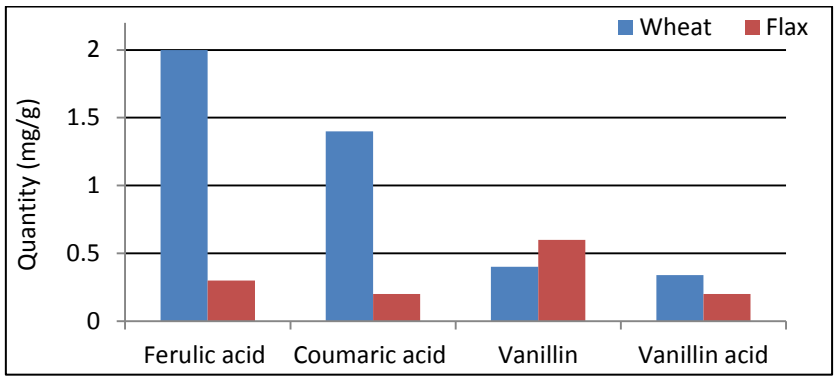

Figure 2.13 Phenolic compounds in flax and wheat straw [276]

2) Lignin in rice straw

World production of rice straw is 525 million tons per year, 90% of this rice straw is produced in Asia [25]. Rice straw is unique relative to other cereal straws as it contains lower lignin but higher silica (ash) [230]. Rice straw lignin is also called p-hydroxyphenyl–guaiacyl– syringyl (H–G–S) lignin and contains all three monolignol units in significant amounts. The analysis of degradation products following cleavage of ether linkages by thioacidolysis indicated the respective proportions of H, G and S units in rice straw lignins to be 15, 45 and 40% respectively. The *p*-hydroxyphenyl content in rice straw is significantly higher than that of corn and wheat straw [288,289]. Azuma and Koshimjima [293] describe the methods of isolation, purification and fractionation of LCC from rice straw in their work. The LCC was removed from extractive free and depectinated plant meal with 10 L of 80% aqueous dioxane for 48 hours. The analysis of LCC from rice straw showed that it contains 63.9% carbohydrates (xylose, 80.1%; arabinose, 13%; glucose, 4.3%; galactose, 2.3; mannose, 0.4%), 2.8% of uronic acid, 27.7% klason lignin, 5.6% acid-soluble lignin, 4.2% acetyl group, 4% trans-*p*-coumaric acid (4%) and 0.8% trans-ferulic acid [230].

3) Lignin in corn stover

Corn stover is the surface material remaining after the grain is removed. About 520 million tons per year of dry corn is produced annually in the world. The main production regions are North America (42%), Asia (26%), Europe (12%) and South America (9%) [25]. Lignin content of corn stover is 15–21%, depending on the location. This is relatively low compared to other herbaceous crops [230]. The analysis of degradation products following cleavage of ether linkages by thioacidolysis indicated the respective proportions of H, G and S units in

lignins in corn stover to be 4, 35 and 61% respectively [288,289]. In contrast to wheat straw, the monomeric composition of corn lignin does not change significantly during nitrobenzene oxidation at high temperature and reaction time [294]. The fractionation of corn stover has been extensively studied for the production of biofuels and biochemicals due to its lower lignin content and large amount of annual production. The availability of significant amounts of ester bonds in lignin/phenolic–carbohydrate complexes of corn stover requires the use of alkali for the fractionation process. The fractionation technologies used for corn stover are based on different alkalis in various physical processes.

2.3.4 Lignin as adhesive

A primary objective of lignin utilisation research has been to use industrial lignin as adhesives. Most of the research for this specific property has focused on the incorporation of lignin with phenolic wood adhesives for panel products [295]. The thermosetting adhesives used in MDF and PB are mainly urea formaldehyde (UF), melamin-urea-formaldehyde (MUF) and phenol-formaldehyde (PF). Apart from being expensive, a further problem is that the cured adhesives within the panel products limit the reuse options of the discarded boards [296]. Formaldehyde resin was classified by the World Health Organization (WHO) as toxic to humans. The use of formaldehyde-based adhesives also contaminates the environment and causes health problems for workers and consumers [297]. Both economical and health benefits could thus be obtained from binder-less (synthetic resin-free) production processes or developing non-toxic adhesives from lignin [298-300]. One of the most traditional applications of using lignin as the binder is fibreboard production, where fibreboard thermo-mechanical pulping (TMP) converts wood chips to largely lignin-covered fibres by shearing wood fibres along the lignin-rich middle lamellae [114,122,301,302].

Industrial soda bagasse lignin was shown to have high reactivity toward formaldehyde, due to a lower degree of condensation and more phenyl-propanoid units from *p*-coumarate [303]. There is the dilemma that the water-soluble technical lignin reduces the dimensional stability of the composites, while water-insoluble lignin may not be reactive enough to provide sufficient cross-linking. The creation of the same environment in the lignocellulosic materials, in order for lignin to function as it does with hemicellulose, is what could lead to the development of lignin based adhesives with enhanced properties. A great deal of research work has been carried out to modify/optimise lignin materials. In the following sections some of them are reviewed.

1) Reactivity improvement

The approaches of optimising the strength properties of lignin-based adhesives are to increase the reactivity of technical lignins toward formaldehyde with demethylation [304], hydroxyalkylation [305] and phenolation [306]. Olivares et al. [307] tested particleboards mechanical and physical properties, prepared from 19% ultrafiltrated high molecular weight kraft lignin, 23% phenol and 58% formaldehyde which was identified as the best combination to have comparable properties with commercial PF resins. Yang and Liu [308] reported that hydroxylmethylation produces resins with enhanced properties in comparison to original lignin. The increase in lignin reactivity by reaction with $K_2Cr_2O_7$, and subsequent formation of catechol groups through demethylation has been reported previously [309]. Dichromate in the presence of acetic acid was used [310], decreasing the concentration of methoxyl groups from 12 to 3%, and increasing the phenolic hydroxyl groups from 2 to 11%.

Alternative chemical modification of lignin is methylolation which is a simple way for increasing lignin reactivity by introducing methylol groups by reacting lignin with formaldehyde [311]. Lignin in alcoholic solution was treated with formaldehyde (lignin: formaldehyde = 1:1) for 12 hours at 40˚C, pH=8 with constant agitation. These conditions were reported as most favourable where the kinetics and mechanism of the reaction of lignin with formaldehyde were studied [310].

None of the chemical modification methods can be used commercially for the production of lignin based products due to the environmental concerns (i.e. toxic environment/agents, health and safety issues) and costs. Although, there is a commercial chemical method of lignin degradation based on alkaline reactions of lignin, which is used in the alkaline pulping process of woods, NaOH serves as the hydrolytic reagent for the degradation of the lignosulfonates [230].

2) Phenolation

Phenolation treatment under alkaline conditions is conducted to enhance the reactivity of the technical lignins, so it could be utilised in the synthesis process of lignin phenol formaldehyde (LPF). To improve the reactivity position of rice hull acid-insoluble lignin after hydrolysis, phenolation was used to facilitate the lignin molecules to be incorporated into the resin through the polymerisation [268]. Ysbrandy et al. [303] modified auto hydrolysis bagasse lignin through phenolation and used the phenolated bagasse lignin to make lignin-based PF resin [303]. Physical properties of impregnated paper laminates were then evaluated

and the effect of substitution levels of different phenolic components with lignin was studied, where it was found that with 33% phenolated bagasse lignin, the produced laminates had better physical properties [303].

Phenolated soda bagasse lignin was also used to prepare lignin-based PF resin [312,313]. Liu et al. [313] phenolated wheat straw soda lignin and used it to substitute up to 70% of the phenol in formulating PF resin, which had comparable performance to the original PF resin. In another study the phenolation of rice hull lignin was carried out [314] in combination with three step polymerisation of the resin to improve the reactivity of rice hull acid-insoluble lignin, it was found that the good properties of the product, such as morphology, temperature stability, yields, water and ultraviolet resistance are due to the increase of the covalent interaction between the resin and lignin.

3) Ultrafiltration

The other approach used for lignin optimisation is ultrafiltration. Ultrafiltration is used when lignin of a specific molecular weight is required for a product. In a kraft mill, CO_2 and H_2SO_4 precipitation are the most appropriate methods [315]. Technical lignins purified by ultrafiltration process were found to be promising materials for making lignin-based PF adhesives, Forss and Fuhrman [315] claimed that adhesives made with phenolic resin and high molecular weight kraft lignin fractions illustrate improved adhesive strength. The removal of high molecular weight lignin by ultrafiltration was also found to be feasible and economically attractive in simulation studies [316]. However the adhesive made from ultrafiltration-fractionated ammonium-based sulfite spent liquors were found to produce high quality wafer-boards with low molecular weight (<5000) lignosulfonates, and poor mechanical properties wafer-boards with high molecular weight (>5000) lignosulfonates [317]. The two main advantages of using ultrafiltration for lignin recovery are that no adjustment of the pH or temperature is needed and the concentration of the liquor to be treated is not crucial [318].

2.3.4.1 Lignin as phenol-formaldehyde resin

The phenolic nature of lignin makes it prone to replace phenol with lignin derivatives in PF resins. The method of extraction and the source of lignin have a strong influence on the properties of the PF resin [319]. There are different methods used to derive lignin for formation of PF resins as follow: 1) the lignin reacts with phenol and the lignin–phenol

complex is then reacted with formaldehyde, 2) the lignin which reacts with phenol and formaldehyde, and the pre-polymer is then reacted with phenol, 3) phenol reacts with formaldehyde and the mixture is then reacted with lignin, and 4) the lignin reacts with formaldehyde and the hydroxymethylated lignin is then reacted with phenol.

A variety of different lignins, including organosolv lignin, soda lignin and lignosulfonates, have been used in PF resin preparation [320, 321], and black liquor has been applied directly [322]. Lignosulfonates are the most used technical lignins for making lignin-based adhesives [132], produced as by-products from sodium, calcium and ammonium-based sulphite spent liquors (SSL). These lignin derivatives in SSL can be used directly for formulating wood adhesives [295]. PF resins have been prepared from lignosulfonate from grasses such as bagasse and wheat straw [313,323]. Peng and Riedl [324] proved that the reactivity of lignosulfonate with formaldehyde increases when wheat starch is added as filler, which produced the lowest level of condensation resulting in the highest reactivity of the lignin-starch combinations to formaldehyde.

Khan, et al. [325] assessed the possibility of preparing adhesives from bagasse lignin. They optimised the parameters for the preparation of LPF, such as lignin concentration, catalyst concentration, reaction time, temperature, and formaldehyde to phenol molar ratio. The results indicated that up to 50% of phenol can be substituted by bagasse lignin to achieve comparable bonding strength to a commercial PF adhesive. The optimised condition for preparation of bagasse lignin-based resin was as follows: lignin to phenol ratio of 50%, formaldehyde to phenol molar ratio of 2, 10% catalyst concentration of phenol, reaction time of 4 hours and the reaction temperature of 80˚C. Other attempts to replace phenol with lignin for wood adhesive products have shown the resin properties to be similar to those of commercial resins up to 35 weight% partial replacement with lignin [326]. The use of acetosolv lignins in PF resin and the direct replacement of organosolv lignin for phenol in PF resins have both been investigated. Plywood made with the former showed better knife-test shear strength compared to those obtained with a commercial PF resin [327]. Organosolv lignin could replace 20–30% of the phenol in PF resins for particleboards production without adversely influencing the bonding properties [328,329].

Zhang et al. [330] used the ethanol residue (ER), which is the by-product of lignocellulosic ethanol production with rich activated lignin, to partially replace phenol in the range of 10-70% to prepare LPF adhesive. The results revealed that ER, with rich hydroxyl group and

less methoxyl group as well as lower molecular weight, was suitable for the synthesis of LPF. Liu et al. [331] also concluded that the best adhesive properties on incorporation into PF resins of wheat straw soda-lignin are for the lower molecular weight fractions.
Enzymatic hydrolysis lignin extracted from residues of cornstalk was partially substituted by the phenol component in PF resin by a one-step process [332]. Plywood using this resin was produced and the bonding strength met the Chinese National Standard (GB/T 14732-2006).

In general, it has been impractical to use LPF resin on a pilot/industrial scale, due to several reasons, one of which is related to the molecular size of the adhesive, the lignin molecules have generally been too large to penetrate the surface of the wood to get good adhesion. On the other hand the size of lignin molecules also prevents its condensation with phenol to any meaningful extent, hence when large amounts of lignin are employed in such resins, adhesive properties have been found to be deteriorating. Additionally LPF resins tend to have a high degree of variability in adhesion performance. Previous studies have shown that the presence of the plasticisers or contaminants (e.g. very low molecular weight lignin monomeric units) are partially responsible for the low bond strength [333]. There are always reports based on simple substitution of phenol in PF resin. However, this is an old technology and unfortunately not a successful one in industrial scales.

2.3.4.2 Lignin as epoxy resin

Lignin has also been used in epoxy resins where different formulation approaches have been explored [334-336]. With specific reference to phenol-epoxy resins, lignin could flourish as a crosslinking agent [337]. Epoxy resins are known to be one of the most important thermoset polymers. The synthesis of lignin-based epoxy resins can be divided into three categories as follows: 1) blending the epoxy resins with technical lignin obtained directly from the pulp and paper process [338-340], 2) direct modification of technical lignin by epoxides [335,341,342], and 3) modification of lignin by several chemical reactions in order to improve their reactivity prior to the epoxidation reaction [341,342]. Previous studies have shown that the epoxy modified lignin-based resins can be prepared in significant quantities with relative simple purification schemes involving the reduction of lignin with epichlorohydrin, subsequent recovery of the unused epichlorohydrin and filtration to purify the ultimate resin [343,344].

A very wide variety of comonomers and curing reagents have been applied to prepare lignin-derived epoxy resins. The effect of lignin blending with epoxy resins are strongly influenced

by the type of lignin used [345]. Ismail et al. [346] modified sodium lignosulfonate by reaction with anhydrides to form ester-carboxylic acid derivatives, which are used to crosslink glycerol diglycidyl ether and ethylene glycol diglycidyl ether to obtain the lignin-based epoxy resins.

Different methods create different products having diverse physicochemical properties which may be used in different applications. Soluble lignin has been formulated with epoxy resin and cross-linked by heat. The epoxy resins that contained 50% lignin were successfully prepared and applied to printed circuit board (PCB) production [347], which had physical and electrical properties similar to those of common laminate resins.

2.4 Interim conclusions and outlook

Agricultural by-products are the most promising feedstocks for the generation of renewable, carbon neutral substitutes for synthetic materials (e.g. biofuel, building materials). Agricultural biotechnology was discussed with references to success and limitations for the bioconversion of straw biomass to bio-energy and bio-composite. Biological pre-treatments have been linked with fungi capable of generating enzymes that biodegrade lignin, hemicellulose and polyphenols. Lignocellulolytic enzymes are considered as prospective biomass degraders, although lignin which is the most recalcitrant constituent of straw biomass, links to hemicellulose and cellulose, thus turns into a barrier for enzymes and stops their infiltration to biomass structure. It was found that biological pre-treatment in combination with mild chemical and or physical pre-treatments are the most critical process for the success of bioengineering. Pre-treatment is an essential step to increase the digestibility of biomass, by making cellulose and carbohydrates accessible for following bio-processes.

The detailed analyses of straw fundamental chemical structures using diverse analysing technologies are essential for more in depth microstructure and chemical interpretation of their characteristics. Amongst many techniques reviewed, the magnetic resonance techniques have proved to be efficient analytical tools for the structural elucidation of straw biomass main components, i.e. lignin. Although different analytical methods applied to same lignin samples could provide significantly different results that are not directly comparable. This problem, coupled with the extreme heterogeneity of lignin has made the quantitative structural characterisation of lignin an open debate. It is difficult to find a single technique to

analyse straw and its lignin structure, hence the most accurate way to study the straw lignin could be to use a combination of several techniques, each providing partial but complimentary information, which contributes to a comprehensive understanding.

The relevant information about the lignin in straw biomass and its applications revealed that 1) lignin as an abundant natural and renewable product has a great potential for many applications across various industrial sectors as a replacement for scarce and expensive petroleum based materials, including traditional products, e.g. resins, and composites, and emerging materials, e.g. biofuel and commodity chemicals. 2) The type of lignin differs not only from one to another species, but also depending on the isolation protocol. Lignin could function as a structural backbone in resin systems such as phenol formaldehyde and epoxy. However, the lack of optimising and/or processing technologies is significant when it comes to using technical lignin. Creation of the functionalities of lignin as it does with cellulose and hemicellulose, could lead to radical development of lignin-based products with superior quealities and performances.

Chapter 3 Materials and methodologies

Highlights:

- All the sample preparations;
- Experimental details for all the chapters;
- Instrumentation parameters for each analytical technique used in this project;
- Statistical data analysis.

This chapter describes the specifications of materials used in this project as well as experimental methodologies. The analytical techniques used throughout this project are described along with specific standards. The testing procedures and their standards are comprehensively explained.

Key words: Materials; Analytical techniques; Testing procedures.

3.1 Materials

3.1.1 Wheat straw

Wheat straw (*Triticum aestivum* L.) for this study was obtained from farms in Rickinghall, Norfolk, United Kingdom; Dixon Brothers Porters Farm, which was harvested in summer 2012. Wheat straw bales were prepared and dried directly on site. Bales were collected and homogenised carefully. They were stored in an ambient room temperature atmosphere to confirm air-dryness. The whole stem of wheat straw was selected, cleaned and grouped for characterisation.

Figure 3.1 a) the separation of leave from stem of wheat straw, b) the straw stems cleaned, c) the internodes separated from the d) nodes.

The material preparation and separation were important steps prior to testing characterisation and/or pre-treatments. As shown in Fig. 3.1, the leaves were separated from the stem, and then the stems were grouped and cleaned. The internodes were grouped and nodes were carefully cut and separated. The stem had to be examined carefully for nodes seperation, in order to separate the node, a sharp scissors was used to cut the exact node area without the inclusion of internodes.

3.1.2 Chemicals and thermosetting resins

Sodium hydroxide for the mild alkali pre-treatment (Chapter 5) was purchased from Sigma-Aldrich UK.

The following thermosetting resins are used for Chapter 7. Unsaturated polyester (UPE), vinylester (VE) and epoxy (EP) were all purchased from East Coast Fibreglass Supplies, UK. Phenol formaldehyde (PF) was purchased from John Winter & Co Limited, UK. Polyurethane (PU) was kindly donated from the Inwood Developments Limited, UK. Lignin-phenol-formaldehyde resin with 50% and 25% phenol replacement by lignin (LPF50 and LPF25) was kindly donated from Chimar Hellas S.A., Greece. Methyl ethyl ketone peroxide was used as initiator for VE and UPE, (1.5% by weight).
Table 3.1 compares the viscosities of thermosetting resins used based on the product information sheets.

Table 3.1 Viscosity of the resins used

Thermosetting resisn	Viscosity in Poise at 23˚C
UPE	5
VE	7.5
EP	8
PF	3.5
PU	3.6
LP50	3.2
LPF25	3.0

3.2 Analytical techniques

3.2.1 ATR-FTIR

Attenuated total reflectance-fourier transform infrared spectroscopy (ATR-FTIR), spectra were recorded on PerkinElmer Spectrum one Spectrometer. This method was used for surface chemical functional groups examination. As it enables the analysis of surface to a penetrating depth of 0.5-3.0 μm. Samples were mounted on an ATR equipped with 3× bounce diamond crystal and an incident angle of 45˚ was used to make sure that the wave could penetrate into the surface of samples. The instrument was operated under the following conditions: 4000–650 cm^{-1} range; 4 cm^{-1} resolution; 16 scans which could reduce the testing time without negatively influencing the accuracy of spectra.

3.2.2 XRD

A powder X-ray diffraction method analysis (PXRD) was used to measure the crystallinity index of node and internode of wheat straw. This was carried out using a D8 advanced Bruker AXS diffractometer, Cu point focus source, graphite monochromator and 2D-area detector GADDS system. The diffracted intensity of CuKα radiation (wavelength of 0.1542 nm) was recorded between 5˚ and 40˚ (2θ angle range) at 40 kV and 40 mA. Samples were analysed in transmission mode. Fig. 3.2 illustrates the powdered straw samples being tested by the XRD machine.

The sample to be studied was finely ground and the powdered material was placed and levelled within a small round hole bevelled out of a sample holder.

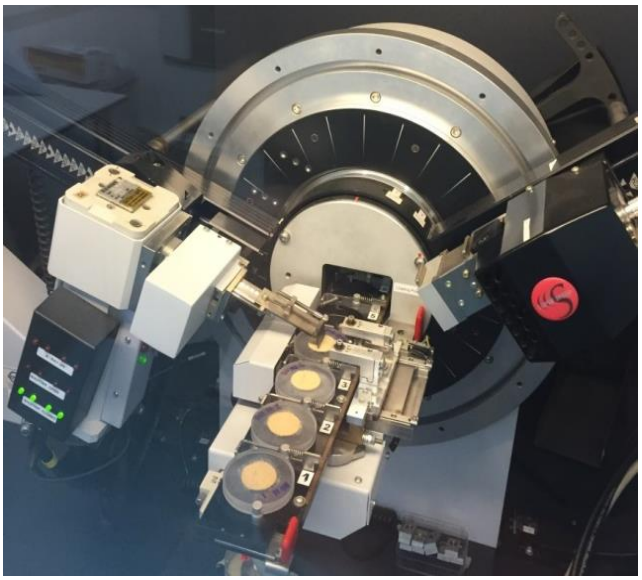

Figure 3.2 The XRD machine during testing of samples

3.2.3 FEG-SEM

Field emission gun-scanning electron microscopy, Zeiss Supra 35 VP FEG-SEM was used to examine the microstructure, surface profiles and failure morphology of wheat straw. All samples were platinum coated prior to tests using Edwards S150B sputter coater to provide electrical conductivity. The samples were carefully cut using sharp blades for the cross sectional view examination.

Alternatively they were finely polished in order to reveal the morphological details of the straw. In the first step, samples are casted into cylinders with Buhler acrylic resin. Then,

samples are polished with sand papers starting with 100 grit and ending on 2400 grit. Water is used as lubricant. Additionally, the surface is polished with a diamond paste. The sample is washed between steps with distilled water in an ultrasound cleaner in order to remove SiC particles and milling products. The cleaning prevents coarser grit particles from migrating. Between polishing stages, polishing progress is monitored with an optical microscope.

3.2.4 SEM-EDAX

The energy dispersive X-ray spectra were obtained using an INCA Energy 400 microanalysis system (Oxford instruments, England). The chemical elements detected were quantitatively analysed using the database of standard samples programmed in the software. The elemental ratio of all elements detected was automatically calculated from their normalised peak areas. SEM-EDAX samples were platinum coated prior to tests. For quantitative element analyses, the recorded EDAX results were analysed by using Oxford INCA Version 4.02. Fig. 3.3 illustrates the SEM machine used.

Figure 3.3 SEM-EDAX integrated analysis machine

3.2.5 OM

Olympus BX51 optical microscope was used in this project as an analytical technique to assess the morphology of samples and their surface profiles. Digital imaging solution Olympus analysis software was used on the images acquired for further morphological measurements and evaluations. The OM equipment is illustrated in Fig. 3.4.

Figure 3.4 OM for morphological analysis

3.2.6 TGA

Thermogravimetric analysis (TGA) was performed to compare the degradation characteristics of untreated and pre-treated wheat straw. Thermal stability of each sample was determined using a SDT Q600 V8.3 Build 101 (TA instrument) with a heating rate of 10˚C/min (20 to 600˚C) in a nitrogen environment.

3.3 Testing procedures

3.3.1 Tensile testing

For the tensile testing, three different batches of samples were selected from each pre-treatment along with untreated wheat straw and from each batch 20 individual samples were randomly selected and tested for their tensile strength. In total for each pre-treatment and untreated straw 60 samples were tested (i.e. 60 for UN, 60 for H+S, 60 for 0.5H, 60 for 0.5S, 60 for 0.5NaOH).

In order to reduce the variance of the result the following steps were implemented for testing: a) 60 mm of second internode and second node from the root in each stem of wheat straw was selected for the determination of tensile strength. They were carefully cut in half (using a sharp razorblade) longitudinally. b) All the samples prior to testing were oven dried for 24 hours at 100˚C. Different moisture content could change the mechanical strength of wheat

straw [348]. All the samples were checked carefully by eye for defects or small longitudinal or cross-sectional cuts within the gauge length prior to tensile testing.

The gripping of straw is problematic as the rigid nature of them will result in crushing at sample ends. Hence the grips were designed out of pieces of wood that had a strip of abrasive paper attached to them using super glue and then those pieces of wood grips were attached to the original Instron tensile grips using magnetic tape, see Fig. 3.5. This testing procedure ensured that breaking occurred between the gauge lengths (i.e. the failures in specimens tested occurred in the tension area).

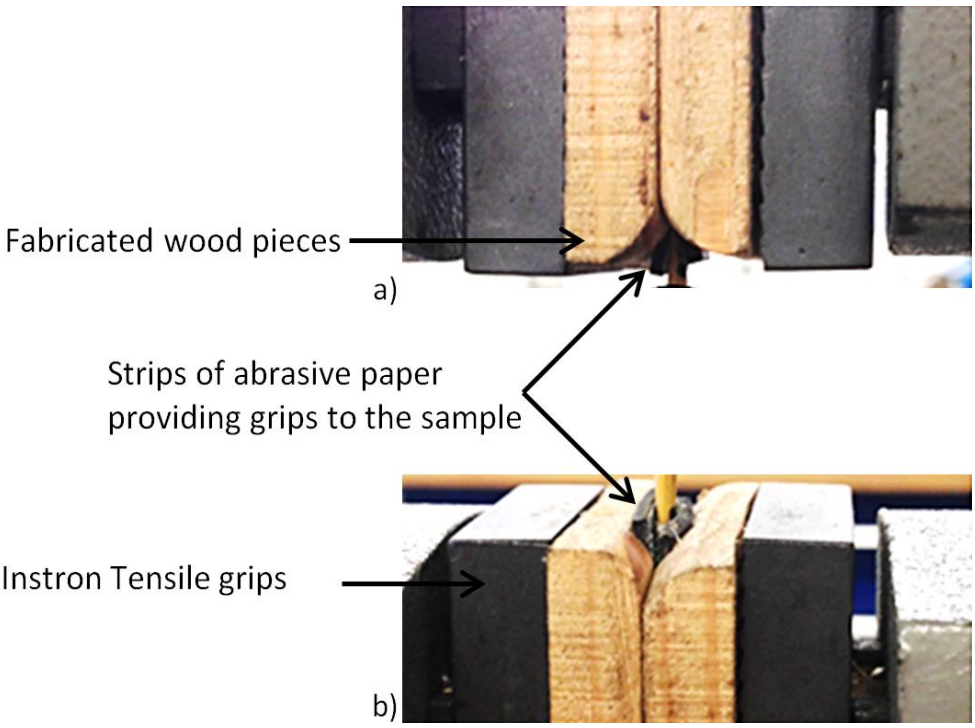

Figure 3.5 - The tensile testing grips a) the upper part, b) the lower part

The gauge length was 20 mm and grips held 20 mm on each end of the straw specimen (60 mm test specimens). The rate used was 5 mm/min using an Instron 2670 series testing machine. Cross sectional area of each sample was carefully measured using a digital micrometer.

The tensile failure stress σ, of each specimen was calculated using Equation 3.1.

$$\sigma = \frac{F_t}{A} \tag{3.1}$$

Where F_t is the tension force at failure and A is the wall area of the test specimen at the failure cross section.

3.3.2 Contact angle

The contact angle between water and the surface of wheat straw was measured using First Ten Angstroms FTA 1000 Analyzer System. The images of the drop shape on the specimens were captured by a camera connected to the computer, shown in Fig. 3.6. The outer surface of pre-treated and untreated wheat straw (10 mm × 5 mm) was tested for 10 different specimens. A drop of water (2μL) was placed on the outer surface of wheat straw using a micro syringe at 18±2˚C.

Wettability is expressed as the advancing contact angle of distilled water on the outer surface of the wheat straw. The spreading and penetration rate of the surface pre-treatment is also assessed through this test. Only internode outer surface is investigated as node's surface is not flat. The moment the contact angle of droplets fell the solid surface is the initial contact angle (θi) and after some time of penetrating and spreading the straw surface, it will reach the equilibrium value (θe).

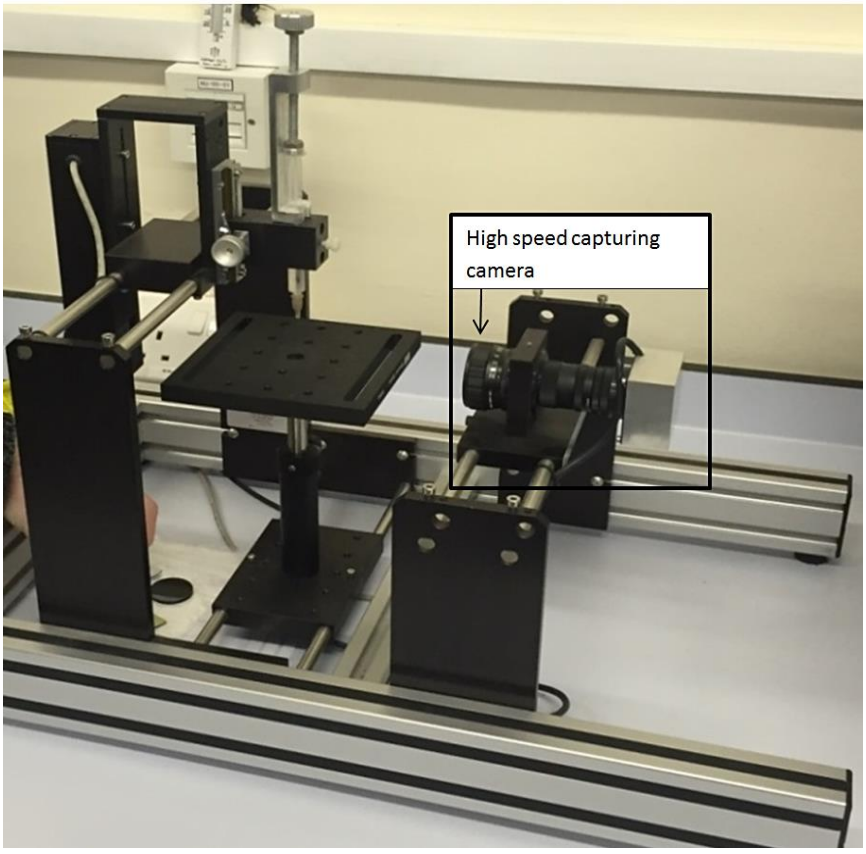

Figure 3.6 Contact angle machine for surface wettability analysis

3.3.3 Extractives content

The following method descriptions correspond to Chapter 6. Dried milled wheat straw (5g) was weighed into a cellulose Soxhlet thimble and placed in a standard Soxhlet extraction apparatus, shown in Fig. 3.7.

Extractives content was measured using two solvents, hot-water (HW) and ethanol (ET), with respective boiling point of 100 and 78˚C. Straw samples were extracted for 24 hours following National Renewable Energy Laboratory - NREL/TP-510-42619 standards (this procedure is optimised for the removal of extractives in biomass). The solid extracted samples were collected and oven dried prior to weighting and subsequent extractives content calculation. It is essential to remove non-structural material from biomass prior to analysis to prevent interference with later analytical steps. This procedure uses a two-step extraction process to remove water soluble and ethanol soluble material.

Figure 3.7 Soxhlet extractor set up

3.3.4 Acid insoluble lignin/Klason lignin

Klason lignin (KL) was determined according to NREL/TP-510-42618. Collection of insoluble residue was performed using a glass fibre filter (Whatman GF/A) on a glass frit

filter support and funnel vacuum filtration apparatus. KL determinations were corrected for their relative ash content.

This procedure is only suitable for samples that do not contain extractives. It uses a two-step acid hydrolysis to fractionate the biomass into forms that are more easily quantified. The lignin fractionates into acid insoluble and acid soluble material. The acid insoluble material may also include ash, which was accounted for during gravimetric analysis.

Fig. 3.8 illustrates some parts of the procedure for klason lignin investigations and the solid residue on the filter paper.

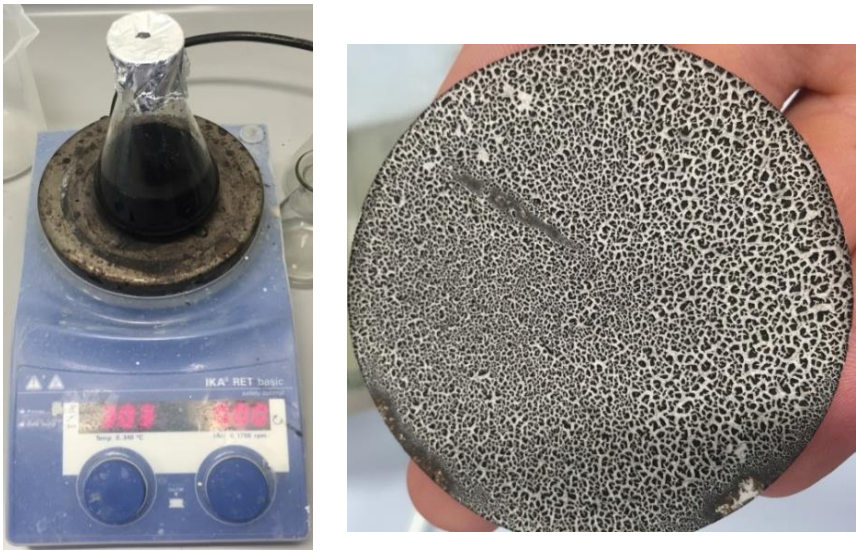

Figure 3.8 Klason lignin determination

3.3.5 Ash content

The residues after combustion of the organic matter of straw at a temperature of 525±25˚C is the ash content determined following NREL/TP-510-42622.

Milled wheat straw samples of node and internode were accurately weighted into a porcelain crucible and combusted in a Carbolite chamber furnace. The furnace was heated to the desired temperature and equilibrated for 5 minutes before the crucible was added and combustion occurred for a set period of time. The crucibles were removed and their weight were measured to obtain the ash content of the samples. Fig. 3.9 shows the furnace used for wheat straw samples combustion.

Figure 3.9 The furnace and the residue after the duration of the test

3.3.6 Weight lost calculation

The weight loss calculation was carried out in order to further assess the pre-treatment severity of wheat straw. One of the many ways to investigate the effectiveness of a pre-treatment strategy is to calculate the weight loss of substrate undergoing the pre-treatment. The weight loss was calculated following the Equation (3.2).

$$WL\% = \frac{W_{i-}W_f}{W_i} \times 100 \quad (3.2)$$

where weight loss percentage (WL%) is calculated based on dry weight of straws, (W_i) is the initial dry weight of the straws before pre-treatment and (W_f) is the final dry weight of the straws after the pre-treatment. The drying was done in an oven for 24 hours at 100˚C.

3.3.7 Single lap joint tensile test specimen

The interfacial bonding mechanisms and failure mechanisms were investigated via the single lap joint tensile test. Six different profiles in terms of alternation of surfaces (inner and outer) and stem sections (node and internode) were investigated. The test was categorised into two major groups, namely, internode and node and then each group had three scenarios of surface bonding, namely, inner to inner, inner to outer and outer to outer. Fig 3.10 illustrates the internode category, inner to inner profile for the single lap joint tensile test. Twelve replicates were made for each scenario. The length of straw sample was 60 $\pm$ 0.5 mm, the contact span

was 10 ± 0.5 mm, length of the test piece was 110 ± 0.5 and each grip seized a 20 mm of straw.

The samples were oven dried prior to the preparation, according to the BS ISO 6237:2003. The adhesive was uniformly spread in the contact area of straw surface using a small notched trowel.

The same volume of adhesive was applied for all the samples. After the preparation, the samples were conditioned in oven at 100˚C for two hours, and then kept in an environmental chamber with 25˚C and a 55% relative humidity for 24 hours prior to testing. Small clamps were used to apply the required pressure evenly over the contact area. Uniform crosshead speed of 1.0 mm/min was used for testing.

Tensile shear strength of lap joints was calculated using formula from EN 205:2003.

$$\sigma = \frac{F_t}{A} = \frac{F_t}{wl} \text{(MPa)} \quad (3.3)$$

where, σ is the tensile shear strength (MPa); F_t is the maximum load at failure (N), A is the bonding area (w is the width of bonded surface and l is the length of bonded surface) of the specimen (mm^2).

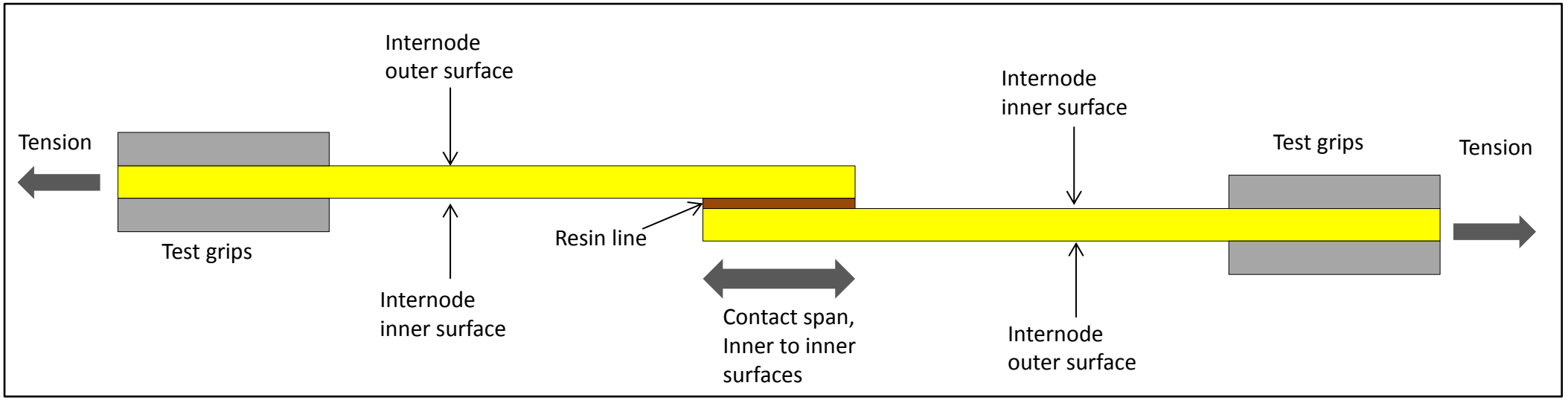

Figure 3.10 Schematic test specimen for the single lap joint tensile test

3.4 Statistical data analysis

For all the property experiments, including tensile testing, data analysis was conducted using Microsoft Excel 2010. For instance the improvement of tensile property of H+S treated straw samples over the UN straws was evaluated by one-way analysis of variance (ANOVA) and the F-test was used to test (σ = 0.05) for significant differences between the factors and levels. As a result of significance testing, the significance probability value (P value) was obtained.

Coefficient of variance (CV) also known as the relative standard deviation (RSD) is a standardised measure of dispersion of a probability distribution and in general is more appropriate method to evaluate the consistency and accuracy of the results. CV is simply calculated as the ratio of standard deviation to the mean.

3.5 Interim conclusions

All the details of the experiments and materials used in this project have been presented in this chapter. In the following experimental Chapters 4,5,6 and 7 the described methodologies were used to gather results, such that with detailed interpretation leads to achieving the goals of the project.

Chapter 4 Revealing the morphology and chemical distribution of nodes and internodes in wheat straw

Highlights:

- 3D model of node and internode morphology;
- Morphological analysis of node and internode;
- Chemical distribution of inner and outer surface profiles;
- Elemental composition analysis and their differences in node and internode;
- Crystallinity index of node is lower than internode.

This chapter serves as a fundamental for in-depth understanding of wheat straw, covering important aspects of morphological properties and surface chemical functionalities of node and internode. The morphology across the node area has great variety when the longitudinal profile was investigated in the upward direction to grain head. It was revealed that the outer surface of the wheat straw stem has a higher concentration of aliphatic fraction of waxes compared to the inner surface, with the highest being in the node area. The knowledge established in this chapter will then build the foundations for the Chapter 5, where the pre-treatment concept and its effects on the wheat straw will be carefully assessed.

Keywords: 3D model morphology; Wheat straw; Node; Internode; Chemical distribution.

4.1 Introduction

Most of the studies on straw biomass are comparative studies between different types of straws to establish the structural differences in the overall straw without specifics of anatomical details (e.g. [201,349-352]). This chapter, profiles wheat straw nodes and internodes, and in-depth analyses their chemical structure and morphology. Due to the complexity of the chemical composition and morphology, combined techniques, both qualitative and quantitative analyses such as ATR-FTIR (attenuated total reflectance-fourier transform infrared spectroscopy), XRD (X-ray diffraction), FEG-SEM (field emission gun-scanning electron microscopy), SEM-EDAX (energy dispersive X-ray) and OM (optical microscopy), are used to fully understand the chemical structure and morphology of wheat straw [350,352]. The morphological studies are linked directly to the chemical structure properties of anatomical sections investigated. The emphasis is on node together with the subdivision of the inner and outer surfaces. What is happening morphologically in the node area of wheat straw as it is investigated from down to up (root to grain head) is the question which is answered in this chapter for the first time. The results are also compared to internode for better understanding. This in-depth analysis could aid the better utilisation of the anatomical parts of wheat straw for different applications as a result of the detailed understanding of morphological and chemical properties.

4.2 Experimental plan

Nodes and internodes were randomly selected. They were carefully cut in half (using a sharp razor blade) longitudinally so that the inner and outer surface could both be examined quantitatively and qualitatively. The samples of node and internode were also cut transversely for the cross-section investigation (qualitative analysis, such as OM and FEG-SEM).

For the preparation of samples for FEG-SEM and SEM-EDAX wheat straw nodes and internodes (1-2 cm length) were carefully placed in a small mould in a way to have both inner and outer surface exposed vertically and horizontally, see Fig. 4.1, and then all samples were vacuum impregnated with epoxy resin mixture. After curing of the resin the bottom surface of the sample was first grinded using different level of grinding papers and finally they were polished before examinations. The grinding and subsequent polishing of the sample were carried out using EcoMet 250 Grinder-Polisher from Buehler.

Five representative samples of about 40g were selected for morphological characterisation. The samples were dried in the oven for 24 hours and stored for surface chemical characterisation.

The XRD samples of nodes and internodes were carefully extracted to ensure that all samples contained only the crystallinity of the node but without the internode. They were ground individually using a grinder and then the samples were sieved (between 250 to 125 μm) to get uniform particle size. The analytical techniques with relevant details of parameters are explained in Chapter 3.

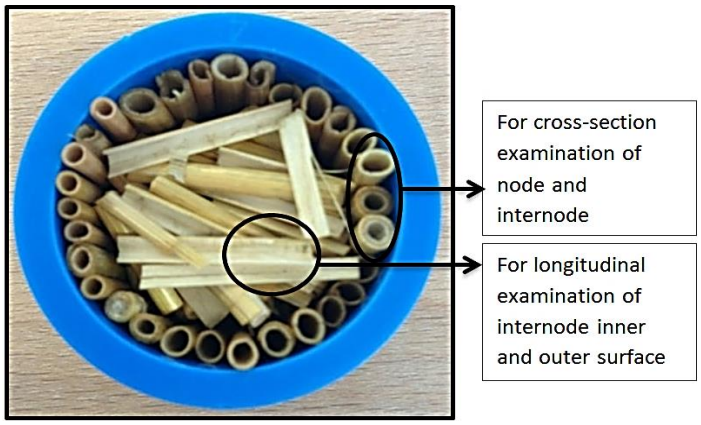

Figure 4.1 Sample fabrication for FEG-SEM and EDX-SEM

4.3 Results and discussion

4.3.1 Wheat straw stem

Wheat straw stem comprises internodes separated by nodes, at which leaves are attached to the stem, as shown in Fig. 4.2. The internodes are formed as concentric rings leaving a void or lumen in the centre. The outermost ring is a cellulose-rich dense layer (termed the epidermis), which has a concentration of silica on the surface. Beneath the epidermis is a loose layer containing parenchyma and vascular bundles [95, 349].

The length of the internodes increases from the ground to the top. Wheat straw is less homogenous than the perennial softwoods or hardwoods in the morphological structure and consists of solid nodes and hollow internodes. The stem of wheat straw is inherently formulated in a multi-layered structure. The top layer is a cuticle, which is defined as the continuous non-cellular membrane lying on the epidermal walls. The estimated cuticle thickness is generally 1 mm and contains a wax layer in the form of a thin film or

characteristic wax crystals. The cuticular waxes are formidable barriers of the straw plants to control the exchange of water, solutes, and even gases and vapours [353].

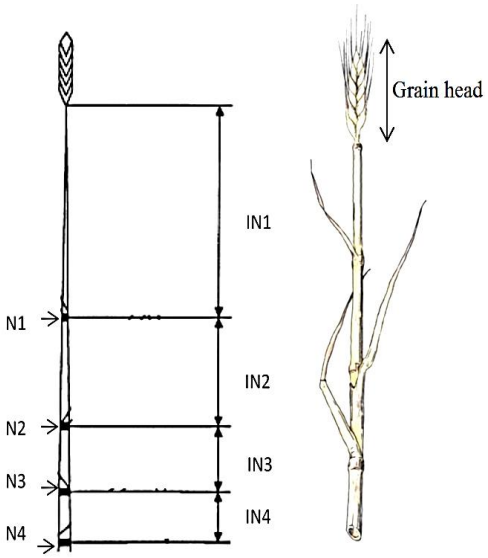

Figure 4.2 Schematic diagram of wheat straw with nodes (N) and internodes (IN)

4.3.2 Node morphology

The examination of the nodes compact architecture in wheat straw revealed a very different morphology from that of the internode. The node structure along the longitudinal direction was investigated by taking cross-section images after carefully grinding layer by layer with smooth abrasive paper (grit size: SiC Abrasive paper, P180, Buehler) moving towards the wheat grain, shown in Fig. 4.3. This would then enable the 3D model of the node morphology.

The investigation starts from the internode immediately before the node and then enters the node core zone and continues forward to where the brown elliptical rings get smaller and the beginning of the upper internode reveals. Those brown elliptical rings start to get smaller and smaller until they disappear, i.e. the start of the hollow upper internode. The same morphology repeats until the grain head is reached and the connection of the internode to grain head is investigated in Fig. 4.5.

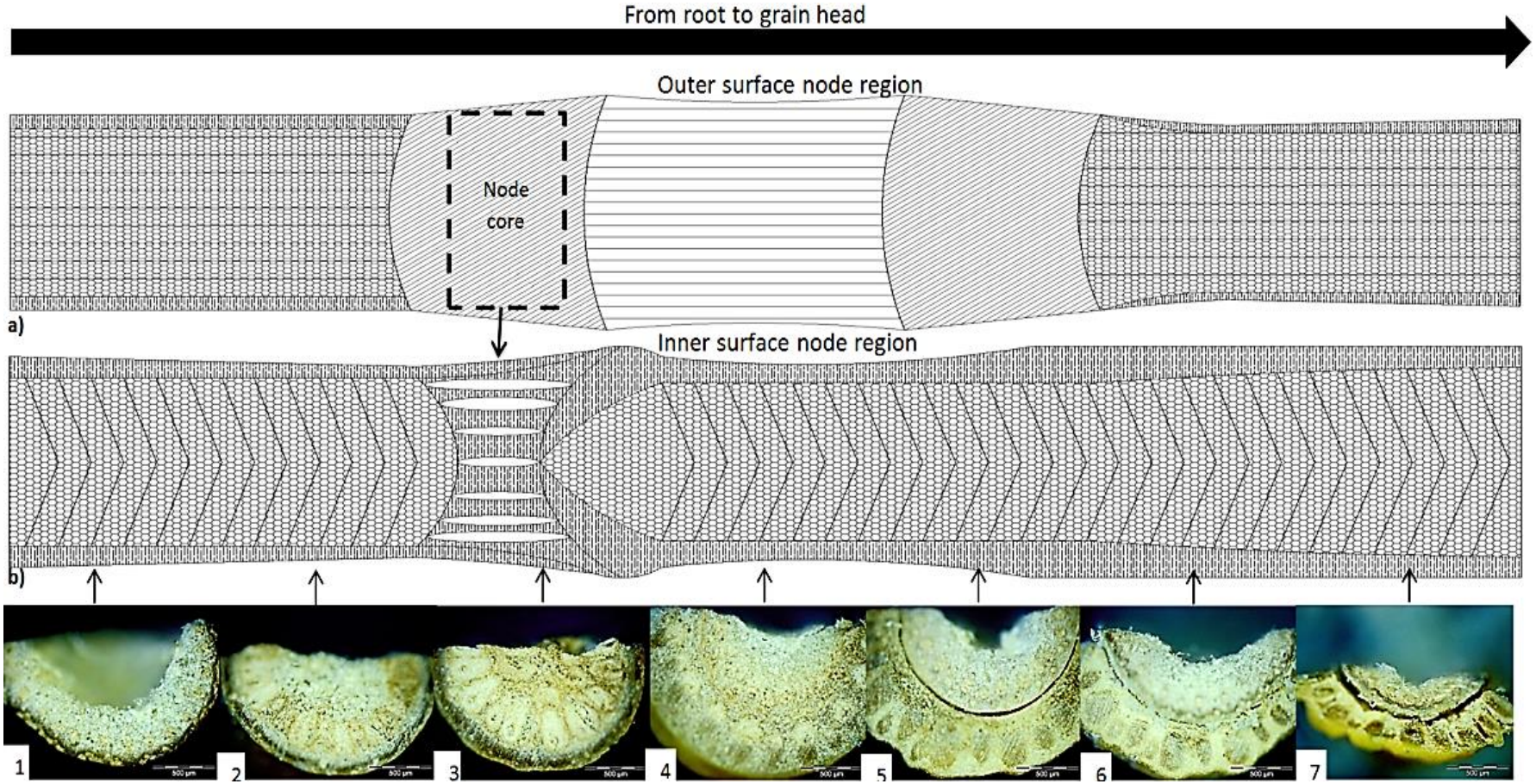

Figure 4.3 The schematic image of the node outer (a) and inner (b) surface longitudinal view and the OM images corresponding to the position in the node shown by the arrows

Fig. 4.3 shows the outer and inner surfaces of node region, and their corresponding OM images are shown by the arrows indicating their positions in the node region. It is apparent that the structure of the node is not symmetrical along the length direction and the morphology changes clearly from left to right (moving upwards to the grain head). The outer ring of the node is revealed after the dense area of node core in image number 4. There are significant different characteristics between the first OM image, which is the end of lower internode and just the beginning of node core, with the seventh OM image, which is the end of node region and the start of the upper internode. In image number 1, the elliptical rings associated with the node region are absent whereas in number 7 the elliptical rings are apparent and the cut between the upper (new) internode is quite clear.

The second and third OM images are quite similar in morphology, but the detailed differences are in the size and the occurrence of the elliptical rings which become more prominent in the third image, hence it is labelled as the node core. In image number 4 the cut between the outer elliptical rings and the internode is not visible, whereas in number 4 the internode becomes distinguishable from the outer elliptical rings. Therefore, it is gathered that in the initial stage of the internode, the morphology is not hollow and is filled with small white and circular or bubbled shaped cells.

Image number 6 is morphologically quite similar to number 5 except that the internode is slowly becoming hollow. All in all it can be concluded that after the node core zone the internode starts to appear from the centre and the elliptical rings become smaller and smaller until the upper internode becomes hollow and hence the outer elliptical rings disappear. This detailed morphological investigation of node region reveals why it is the hardest anatomical part of stem.

The investigation of node region profile across the diameter of the node was performed along a 1.8 cm distance as shown in Fig. 4.4. The cross-section of the node core, as the node region was cut in transverse direction, shows the very dense core, with tightly packed bubbled shaped cells in the centre (Fig. 4.4a). There are brownish colour elliptical shaped rings which are ordered in a circle occupying the overall node core. The centre of these elliptical shaped rings is white, and are constituted with small circular cells, which are soft, i.e. some cuts are visible within the brown elliptical shaped rings (Fig. 4.4a), due to handling prior to

examination. Fig. 4.4b shows the morphology of the brown elliptical rings in the longitudinal direction with the white cells occupying the centre of these rings.

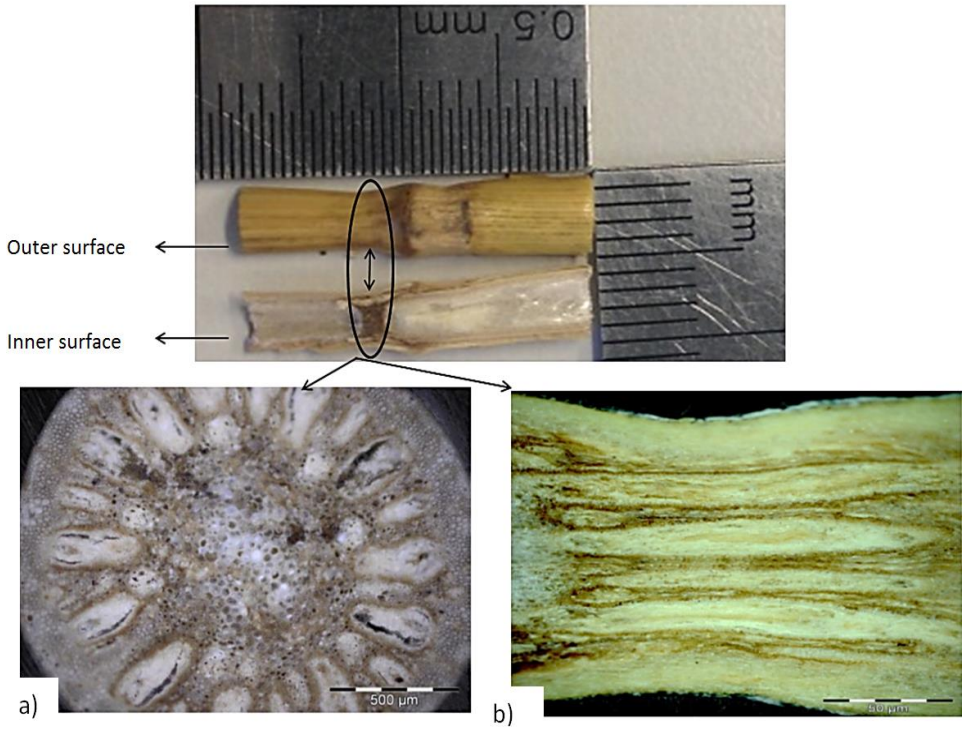

Figure 4.4 a) Node cross-section b) node transverse inner surface view

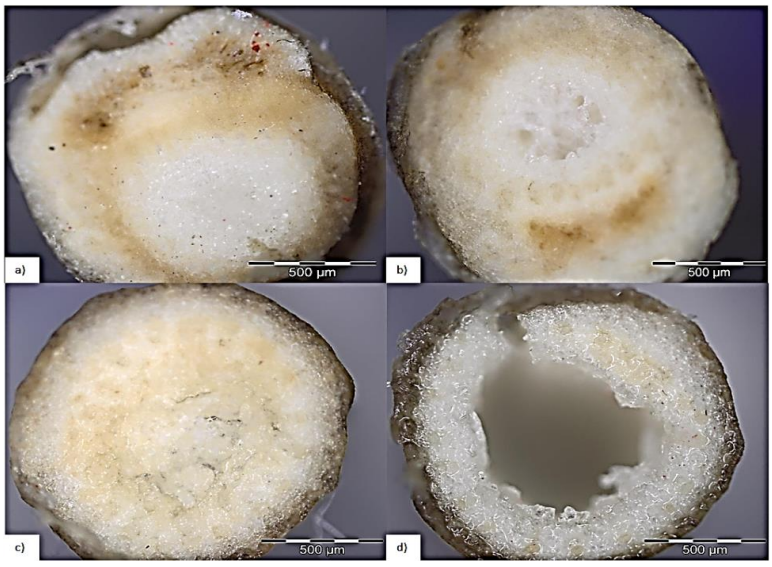

Figure 4.5 Cross-section profiles of the connection between grain head and internode

Fig. 4.5 shows the full cross-section view of the connection of the grain head to the internode. Fig. 4.5a is the cross-section immediately below the grain head and the subsequent images Fig. 4.5b-d are the ones ground towards the internode (i.e. from the grain head to the root direction). The grinding stopped as the hollow section of internode was revealed (Fig. 4.5d).

Cross-section view of a node in FEG-SEM is shown in Fig. 4.6a which corresponds to the image number 5 in Fig. 4.3. The image is magnified on the elliptical rings. This position is just after the node core and it shows the very dense population of the elliptical rings full of small polygonal cells tightly packed in order to provide the rigidity and strength of the node.

The brownish zone of the node core section as observed in Fig. 4.4a was investigated by FEG-SEM in Fig. 4.6b. The elliptical rings are longer and occupy a larger area of node core section whereas in Fig. 4.6a these elliptical rings are shorter and in good order with more consistent shape. In the centre, the new internode starts to appear, which, however, is not immediately hollow as shown in Fig. 4.6a(1).

One important observation in Fig. 4.6b is the size of epidermis which is approximately 200-230 µm. It is also pointed out that there are further bubbled shaped cells in between each elliptical ring. Although the size of the cells is much smaller and tightly packed next to each other within the elliptical shaped rings than in between the rings Fig. 4.6 (2-3).

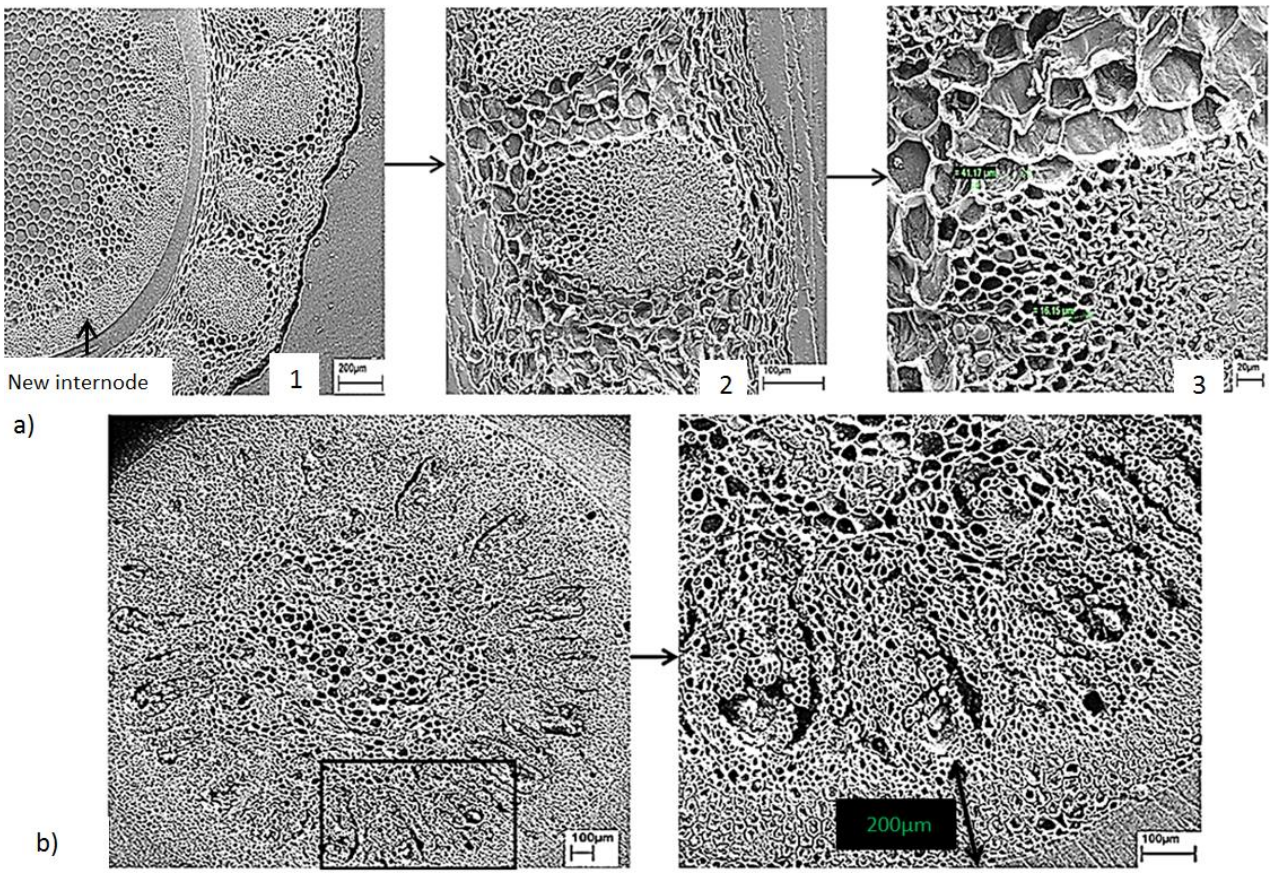

Figure 4.6 (a) Node cross-section view showing the elliptical shaped rings in the outer circular ring (b) node core cross-section view showing tightly packed elliptical rings

4.3.3 Internode morphology

The internode morphology is examined in order to complete the morphological studies of wheat straw stem and compare their changes to the node. Unlike node the morphological longitudinal profile of internode was found to be consistent. The only morphological difference exists in the beginning stages and termination of the same internode from the lower node to upper node. This difference is simply in the partial occupation of small cellular cells that exist in the termination of internode, which is absent in the beginning stages, that is immediately hollow.

The outer part of the straw internode contains wax and inorganic substances on the surface, and then follows a region with fibre bundles (vascular bundles) integrated in a region of parenchyma and vessel elements. The lignin material forms a thin layer around the parenchyma, and although it contains vascular bundles, its main function is considered to stiffen the stem structure.

The epidermis is a complex tissue with bubble-shaped polygonal short and long cell types, see Fig. 4.7. Wheat straw epidermis is thin, but has dense and thick-walled cells with an outer wall coated with a waxy film of cutin cuticle [352]. The function of the epidermis is to control gas exchange and water balance. The vascular system has xylem tissue with dense lignified structures in the secondary wall, surrounded by a strong sheath of sclerenchyma cells, which have elongated thick lignified cell walls resistant to microbial degradation [352]. The observations are in agreement with the earlier report [354]. In wheat straw the protoxylem vessels are developed with a very strong lignified cell wall. These cells have an extreme length and honeycomb shape, as shown in Fig. 4.7. The dense layers of epidermal cells may give additional mechanical strength to the stem. Apart from the two rings of vascular bundles there are considerable amounts of extra vascular fibres (Fig. 4.7). Fibres on the phloem side of the vascular bundles represent the most valuable fibrous material in the stem strongly bonded to the epidermis.

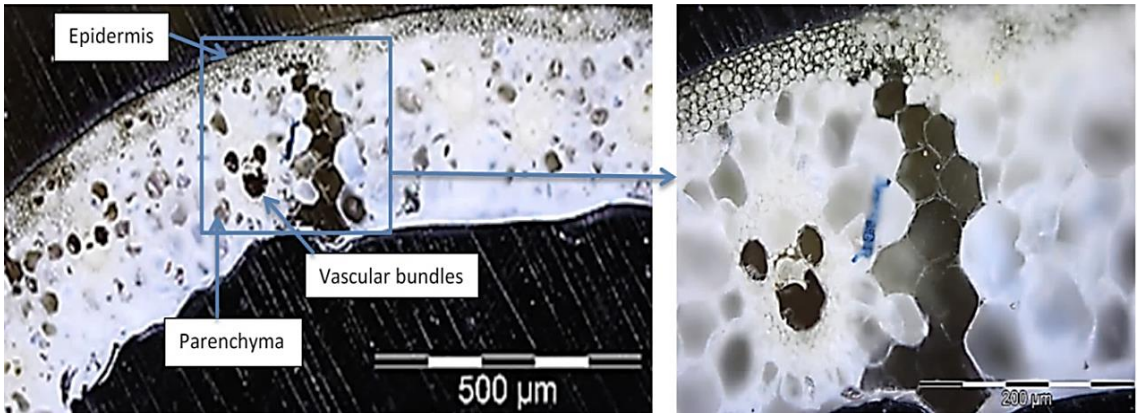

Figure 4.7 OM image of internode cross-section

The longitudinal section of vascular bundles has some parts of densely lignified thickenings in the secondary wall, arranging as annular rings or spiral structure to form vessels which are capable of stretching. It has been reported that the protoxylem vessels are formed early in the season, then during growth they are partially broken down and form an internodal cavity called lacuna [355]. Strengthening tissue of sclerenchyma fibres surrounds the vascular cells.

The spiral structure is in the lignified thickening secondary wall, which mainly consists of cellulose surrounded by the primary wall. The annular and spiral vessels arise at the earlier growth stage during which the plant growth is very fast, and a higher stress exists during the formation process of the two types of structure. This leads to a higher orientation order of cellulose chains in the biosynthesis process of cellulose [356]. The distance between the spiral vessels in vascular bundle is measured to be roughly 200 µm, see Fig. 4.8 where, FEG-SEM was used to further examine the microstructure of internodes. Fig. 4.8 shows that the internode cross-section of wheat straw and the observations are similar to those of the OM images. A scrutiny of images shows that there is an inconsistency in terms of sizes and distances in different parts (Fig. 4.8).

The morphology of cellulose in vascular protoxylem consists of annular rings or spiral form backbones with thin cellulose film around them. The parenchyma consists of vascular bundles embedded in a soft cellular material composed mainly of cellulose. The cellulose rich epidermis forms a hard, rigid outer layer which protects the living cells and stiffens the stem. Cellulose microfibrils are very important in wheat straw tissues and make the major contribution to the mechanical strength and act as the framework of cell walls in the vascular bundles.

The size of epidermis in Fig. 4.8 is 145 µm which is an important observation as the epidermis size in the node core was around 200-230 µm in Fig 4.6b. It should be mentioned that the internode and the node investigated for the size of epidermis are from the same stem, hence it is gathered that the epidermis size in the node core is greater than the internode.

Specialised epidermal cells are developed to physically "lock" the fibres to the tangent to the surrounding layer (Fig. 4.7). As shown in Fig. 4.8 the chlorenchyma cells are irregular in shape and arrangements, situated close to the vascular bundles. The parenchyma cells gradually increase by a small margin in size towards the centre of the stem, whereas the wall thickness of the cells is decreasing. The non-fibrous materials in wheat straw internode are more heterogeneous. The reinforcement elements in a plant stem are fibres which give the stem strength, whereas rigidity is provided by the solid nodes in the stems.

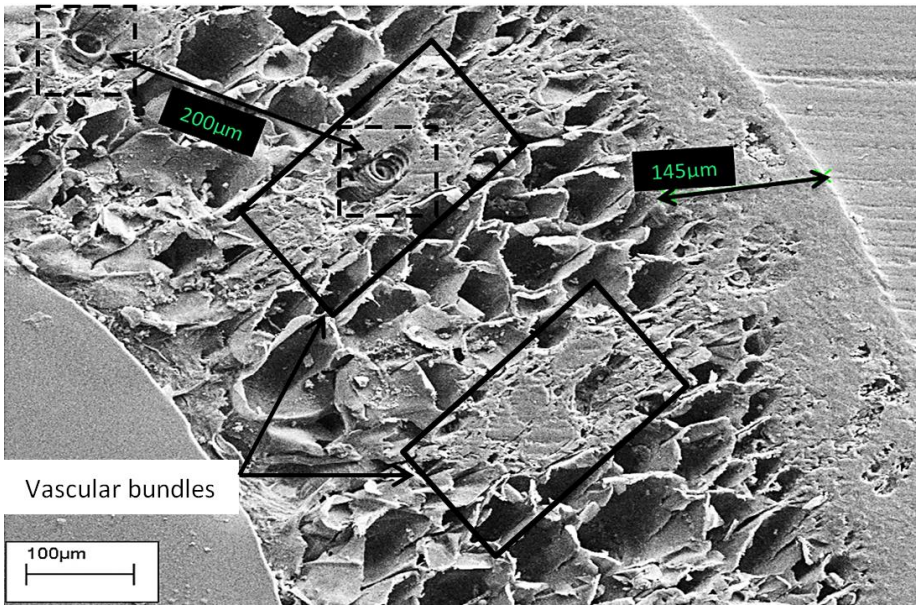

Figure 4.8 An example of internode cross-section showing the epidermis and distance between spiral vessels in vascular bundles

4.4 Chemical distribution of wheat straw

The results illustrate that the chemical distribution of wheat straw is not consistent throughout the anatomical parts. Although it might have similarities in general terms, but the differences may not be negligible. Understanding these differences could be very useful for the pre-treatment and processing design, for example, the chemical properties of wheat straw surfaces are vital for establishing the interfacial bonding properties in composites, hence effective modification to improve interfacial adhesion requires relevant quantitative analyses of the surface.

4.4.1 Elemental composition

The elemental composition of the node and internode inner and outer surface was gathered using SEM-EDAX in order to get the chemical information of the localised surface. The results are average of the 10 measurements taken in different areas for each section, shown in Table 4.1. It is apparent that the bulk structure of the wheat straw consisted of carbohydrates and lignin with significant amount of carbon (C) and oxygen (O), and small amount of silicon (Si) (weight %). The outer surface of the internodes had considerably higher Si weight percentage than the inner surface. In comparison, the Si weight percentage of the outer surface of nodes is about 2 times that of the inner surface. It is well known that Si prevents the binder from spreading on the surface of wheat straw. It is most surprising that the Si weight percentage of the nodes are much lower than that of internodes, only about one fourth. In previous research the stem of wheat straw outer surface was found to have the highest Si weight percentage [166].

The slightly higher ratio of oxygen to carbon in the node inner surface indicated a more carbohydrate-rich area than the rest of wheat straw. The lower O/C ratio in internode inner surface indicates a higher proportion of aliphatic and aromatic carbons close to the surface which is due to the lignin presence with higher concentrations in the inner surface. The theoretical O/C ratio of cellulose was reported as 0.83 and that of lignin as 0.33 [357,358]. The O/C ratio for wheat straw in all areas is similar to cellulose indicating the presence of carbohydrate-rich surface (Table 4.1).

Comparatively higher proportion of carbon atoms in the internode inner surface may be attributed to the predominance of lignin [94]. It is worth mentioning that higher content of C on the node outer surface is an indication of high quantity of wax [358].

Table 4.1 Wheat straw node and internode elemental composition

	Elemental Content (weight %)			
	C	O	Si	O/C
Node inner surface	51.0 (2)	48.7 (1)	0.3 (7)	0.95
Node outer surface	52. 2 (6)	47.1 (3)	0.7 (4)	0.90
Internode inner surface	54.5 (2)	44.7 (2)	0.8 (8)	0.82
Internode outer surface	51.2 (9)	45.1 (6)	3.6 (9)	0.88
Average node (inner and outer)	51.6	47.9	0.5	0.92
Average internode (inner and outer)	52.9	44.9	2.2	0.85
Average inner surface (node and internode)	52.8	46.7	0.6	0.88
Average outer surface (node and internode)	51.7	46.1	2.2	0.89

*values in () are coefficient of variance percentages

4.4.2 Functional groups of wheat straw

ATR-FTIR was used for this study to investigate the surface of wheat straw to get useful data in terms of functional groups. This technique was selected because it permits analysis of the surfaces to a penetrating depth of 0.5-3.0 μm.

The spectra were normalised at around 650 cm^{-1} where the spectra are free of distinct IR bands and then offset was used for better comparison. Results are the average of 10 tests for each section. ATR-FTIR spectrum of the node and internode outer and inner surface is shown in Fig. 4.9.

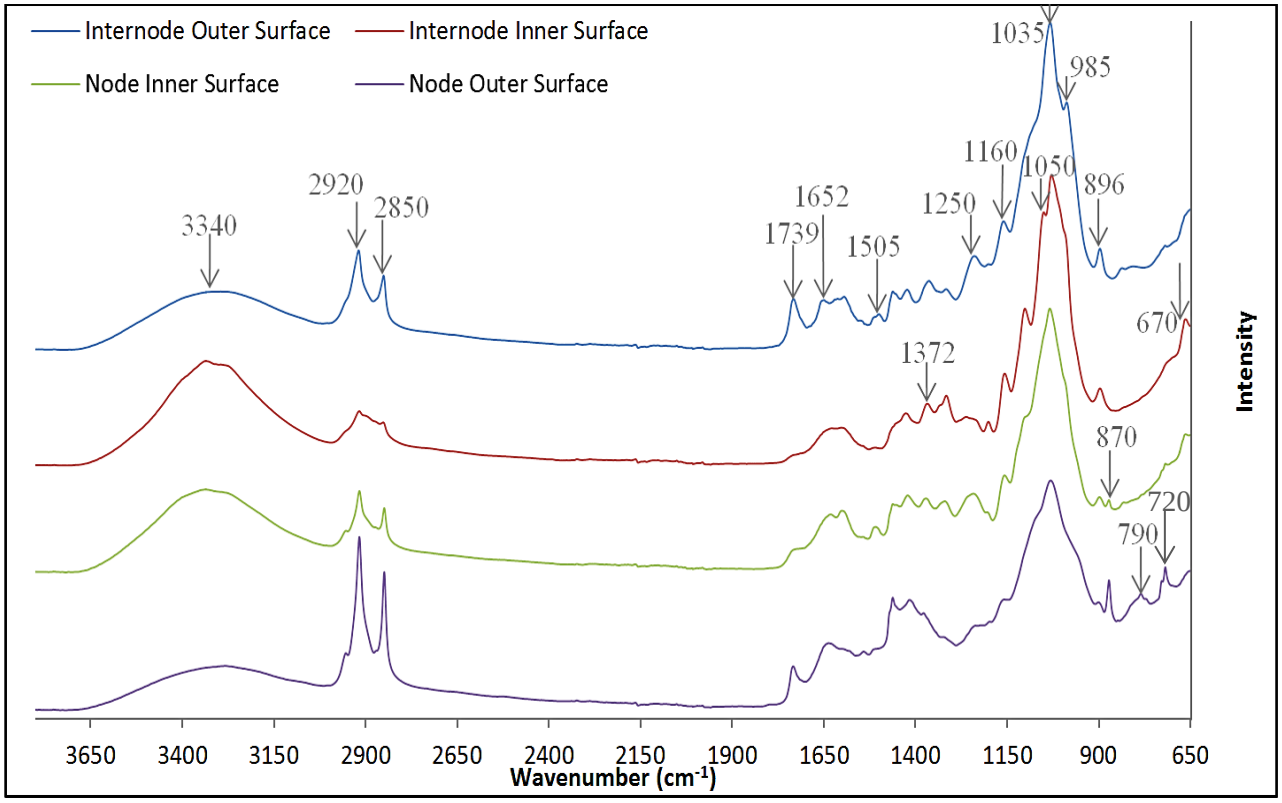

Figure 4.9 ATR-FTIR spectra of wheat straw internode and node outer and inner surface

The spectra of wheat straw are dominated by the peaks at 3340 and 1035 cm^{-1} corresponding to the stretching vibrations of -OH and CO respectively [130]. Starting the assignment from the lower bands, it is found that the small sharp band at 720 cm^{-1}, being characteristic of the methylene (CH_2) in-plane deformations rocking, was only observed in node outer surface with the highest intensity compared to other sections.

This observation indicated that sufficient lipophilic extractives were present on the wheat straw outer surface to protect the plant cell from environmental damage and pathogenic invasion during growth and development [359]. The two peaks of 790 and 985 cm^{-1} were observed in the spectrum of the outer surface of wheat straw, and absent in the spectrum of the inner surface. The two bands were attributed to the Si–C (silicon carbide) stretching vibration and Si–O (silicon oxide) vibration respectively [360,361].

This shows that the components containing silicon were mainly present on the outer surface and not detectable on the inner surface. The peak at 1160 cm^{-1} is assigned to C–O–C antisymmetric bridge in hemicellulose, cellulose and aromatic C–H deformation of the syringyl and guaiacyl units in lignin [362,363]. This band had a prominent intensity in internode inner and outer surface. The peak at 1372 cm^{-1} reflects CH asymmetric

deformations [364] with polysaccharides source [365]. The C=C stretch of aromatic rings of lignin is presented at peaks 1435 and 1510 cm^{-1} [94,130,364,366]. The intensity of these peaks was highest in node outer surface followed by internode outer surface hence the outer surface has higher concentration of aromatic rings of lignin.

The aromatic skeletal vibration coupled with C–H in plane deformations is at 1600 cm^{-1} peak [359]. Peak at 1739 cm^{-1} is assigned to the acetyl and uronic ester groups of the hemicellulose or the ester linkage of carboxylic group of the ferulic and *p*-coumeric acids of lignin and/or hemicellulose [94,365-368]. Two strong and sharp peaks at 2850 and 2920 cm^{-1} are assigned to the asymmetric and symmetric stretching of the CH_2-group comprising the majority of the aliphatic fractions of waxes, respectively [369,370].

The outer part of the straw surface (epidermis) contains wax and inorganic substances and hence the intensity of the bands associated with aliphatic fractions of waxes is much higher on the outer surface of node and internode. Additionally the intensity of these bands in node outer surface is higher than internode outer surface. This could be due to the epidermis size in node being larger than internode (Fig. 4.5 b and 4.7).

By looking at the spectra in Fig. 4.9 it appears that inner and outer surface in both node and internode have a rather very similar structure. However the intensities of bands differ. Comparatively, in terms of concentration of bands based on their intensity it was observed that 1425, 1465 and 1510 cm^{-1} had the highest intensity in node outer surface, suggestive of C-H deformations and aromatic ring vibrations [371]. The rest of the semi-quantitative comparative analysis of ATR-FTIR bands in different anatomical sections are shown in Table 4.2.

Table 4.2 Band characteristics of ATR-FTIR spectra.

Wave-number (cm^{-1})	Assignment	Observations	Ref.
670	Characteristic for cellulose, -OH torsional vibration band	Highest peaks observed in internode and node inner surface	[372,373]
870	Aromatic C–H out of bending of cellulose	Observed in node inner and outer surface with higher intensity in outer surface	[371]
896	A characteristic peak of cellulose, β-glucosidic linkages between the sugar units	High intensities in internode	[304,374]
1035	Aromatic C-H in-plane deformation from guaiacyl type lignin and C-O-C glycosidic linkage from hemicellulose and cellulose	High intensities in internode outer surface	[375]
1050	C-O-C pyranose ring skeletal vibration	Peaks observed in inner surface of node and internode with higher intensity in internode	[374]
1160	Presence of C-O from *p*-coumaric ester group, typical for *p*-hydroxyphenyl, guaiacyl and syringal lignin	Highest intensities in internode inner and outer surface	[376,377]
1372	CH deformation in cellulose and hemicellulose	Highest intensities in internode outer and inner surface	[378]
1600	Aromatic skeleton vibrations in the lignin	No peak observed in node outer surface; highest peak in internode outer surface	[371]
1652	correspond to the bending vibration of absorbed water in cellulose	Only peak observed in internode outer surface	[374]
1739	C=O stretching vibration, esterified, with the sources of pectin, waxes and hemicellulose	high intensities in outer surface with highest in internode	[379-381]
3340	attributed to aliphatic and phenolic O-H stretching bands, respectively from cellulose, hemicellulose and lignin	high intensities in internode with highest in inner surface	[382]

Using FTIR technique could also allow the investigation of lignin units. Lignin is composed of three basic units (discussed in Chapter 2), namely *p*-hydroxyphenyl (H), guaiacyl (G) and syringyl (S) [133]. Guaiacyl (G) and syringyl (S) are the main units of lignin, but the ratio of S/G varies in straw biomass [349]. It was reported by del Río et al. [170] that S/G values calculated upon FTIR were in agreement with those calculated upon Py-GC/MS (Pyrolysis Gas Chromatography Mass Spectrometry) at the bands of 1250 cm^{-1} and 1325 cm^{-1} assigned as G ring stretching and S ring stretching respectively. The results of S/G ratio based on the intensities of these bands were calculated for node inner and outer surface to be 1.02 and 1.05 respectively, and for internode inner and outer surface were 1.28 and 0.92 respectively. These seem to be in agreement with the previous work on wheat straw, which report the ratio of S/G as about 1.02 [230]. According to the investigation carried out on barley straw by Love et al. [383], syringyl-rich areas (i.e. higher S/G ratio) of the lignin network are more rigid than guaiacyl-rich areas. It could therefore be concluded that the lignin network in the internode inner surface would be more rigid than the rest of the regions investigated.

Interestingly, on the other hand, internode outer surface is a guaiacyl-rich area with the lowest S/G ratio of 0.92. Akin et al. [384] reported that syringy lignin is tightly embedded within the ordered, close-packed structure of the secondary walls of sclerenchyma cells, whereas the guaiacyl lignin is preferentially located in the less ordered middle lamella and primary walls. On the cellular scale, the guaiacyl-rich lignin of the middle lamella, which is not reinforced by cellulose, is probably the weakest point in the whole structure of the tissue and can be liberated mechanically to separate the cells during pulping [385].

4.5 Crystallinity of wheat straw

The crystallinity index (CI) was evaluated by using Segal et al. [386] empirical method as follow:

$$CI\% = \frac{I_{0\,0\,2} - I_{amorph}}{I_{0\,0\,2}} \times 100 \qquad (1)$$

where $I_{0\,0\,2}$ is the maximum intensity of diffraction of the (0 0 2) lattice peak at a 2θ angle between 21˚ and 23˚, which represents both crystalline and amorphous materials. I_{amorph} is the intensity of the diffraction of the amorphous material, which is taken at a 2θ angle between 18˚ and 20˚ where the intensity is at a minimum. Five replicates were used. It should be mentioned that the crystallinity index is valuable only on a comparative basis as it is used to

specify the order of crystallinity rather than the crystallinity of crystalline regions (i.e. cellulose).

Crystalline microfibrils of cellulose are surrounded by amorphous hemicellulose where they are embedded in the matrix of lignin. Crystalline structure of cellulose and hemicellulose exhibits variability in both structure and constitution. Lignin and hemicellulose are fundamentally amorphous polymers, while cellulose has both amorphous and crystalline regions. X-ray powder diffraction spectra from wheat straw node and internode are presented in Fig. 4.10. The XRD patterns of wheat straws node and internode showed spectra typical of cellulosic materials, having the major peak at a diffraction angle (2θ) of 21˚-22˚ and a broader, secondary peak at 18˚, which indicates that the cellulose is in its cellulose I crystal form.

Crystallinity index analysis is summarised in Table 4.3. It is shown that the major crystalline peak of the wheat straw occurs from 21.49˚ to 21.71˚, which represents the cellulose crystallographic plane (0 0 2, Bragg reflection). The minimum intensity between 0 0 2 and 1 0 1 peaks (I_{amorph}) is from 18.32˚ to 18.51˚. The crystallinity index for wheat straw node and internode is 34.73% and 45.00%, respectively, which indicated that node has more amorphous regions than internode.

The result thus could also reflect that there is more concentration of lignin and hemicellulose in the node area or that the cellulose in the node has more amorphous region when compared to internode. The increasing of crystalline regions increases the rigidity of cellulose, but decreases the elasticity of polymeric substances. In addition, the ratio of the crystalline region to the amorphous region in a cellulose structure influences the accessibility of cellulose molecules. When it comes to crystallinity of straw biomass most of the pre-treatments are designed in a way to increase the crystallinity which is achieved by removal of lignin and hemicellulose. It is important to know the untreated crystallinity of anatomical parts (i.e. node, internode) before designing any type of pre-treatment that focuses on the changes in crystallinity.

Table 4.3 Crystallinity index calculation of wheat straw node and internode

	2θ (˚)		Intensity (a.u.)		Crystallinity
	I_{amorph}	$I_{0\,0\,2}$	I_{amorph}	$I_{0\,0\,2}$	index (%)
Node	18.32	21.49	2913	4463	34.73 (6)
Internode	18.51	21.71	2950	5364	45.00 (4)

*values in () are coefficient of variance percentage

The crystallinities of wheat straw in different anatomical parts are different and fairly low, about 40% on average of node and internode, as shown in Table 4.3. This means that the cellulose from wheat straw is a suitable parent polymer for the preparation of cellulose derivatives [387].

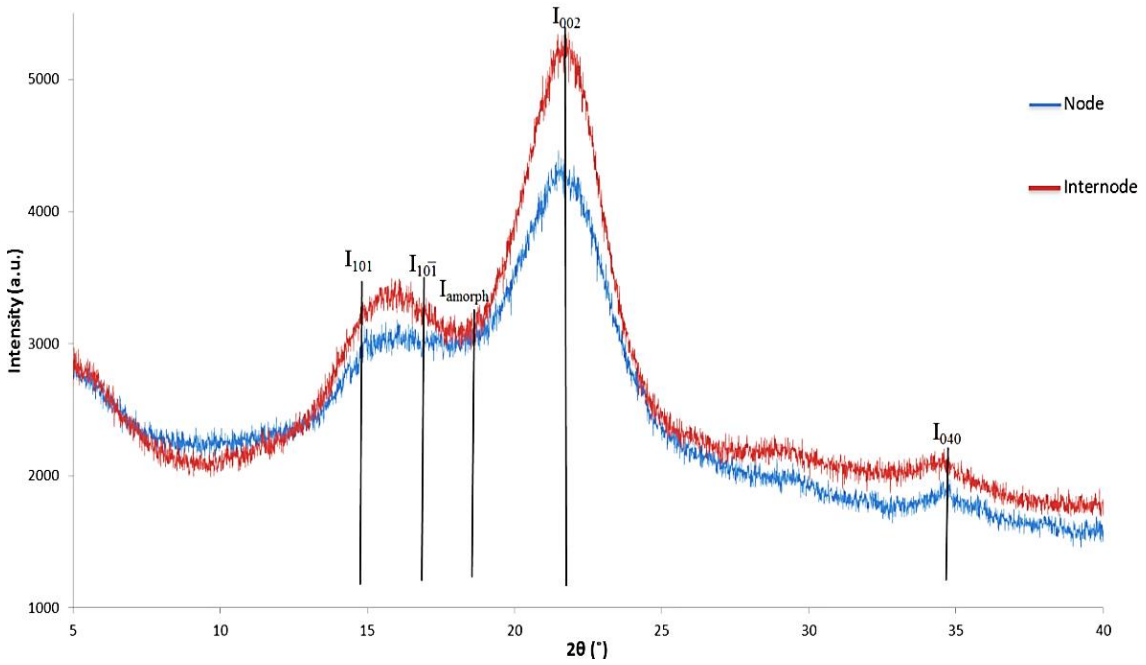

Figure 4.10 X-ray diffractogram of wheat straw node and internode

4.6 Interim conclusions

A systematic approach was developed to thoroughly examine the morphology and chemical distribution of wheat straw node in comparison with those of internode. This also establishes a detailed database on the featured information of wheat straw.

Firstly the morphology was investigated and revealed by OM and FEG-SEM and then the chemical structure with the aid of SEM-EDAX, ATR-FTIR and XRD. The morphology of node was very different from that of internode and there were considerable morphological changes within the node itself as profiled and investigated along and/or across the node region. However, the sophisticated morphology of node region was found to be consistent in all the nodes throughout the stem. Although their outer diameters differed, hence the features within the node region also differed in size only.

Chemical functional groups of straw nodes and internodes were (semi) quantified, showing the difference between inner and outer surfaces and between node and internode. ATR-FTIR results for the chemical functional groups showed differences in terms of concentration of functional groups present in different sections. It was found that the outer surface of wheat straw had considerable higher silicon contents than the inner surface, as confirmed from SEM-EDAX. Higher content of carbon in the node outer surface is also an indication of high quantity of wax which was in agreement with ATR-FTIR results.

The crystallinity of the node and internode was investigated using XRD. It was found that node is more amorphous than internode with the crystallinity index of 35% compared to 45% of internode.

These are important parameters for optimising the yield and economics of various bioconversion pathways. Unfortunately, despite wheat straw's potential for bio-refinery to value added products, it still remains underutilised due to the lack of understanding the complexity of its constituents. The detailed information from this study shall serve as valuable and fundamental basis/database for researchers and industries in the sector of bio-refinery of straw biomass.

Chapter 5 Differential behaviour of nodes and internodes of wheat straw

Highlights:

- Node and internode are characterised in terms of chemical, surface, thermal and mechanical properties;
- The relation of pre-treatments to the structural integrity of wheat straw node and internode;
- Improvement ($P<0.05$) of tensile strength of pre-treated straws;
- Higher thermal stability of straws achieved through pre-treatment.

This chapter aims at further differentiating characteristics of the node and internode by investigating important properties for further processing and production of bio-composites and bio-fuels. A combination of mild physical treatments and the synergistic effect of each physical treatment were investigated in terms of chemical surface distribution, thermal and mechanical properties. Essentially the changes were tracked based on the microstructure characteristic variations induced by pre-treatments. This chapter serves as one of the important sub objectives depicted in Chapter 1 (Fig. 1.1), in terms of identification of an efficient and effective pre-treatment to overcome the issues with wheat straw leading to the optimisation of bio-refinery process.

Keywords: Node; Internode; Pre-treatments; Surface chemistry; Mechanical properties; Thermal analysis.

5.1 Introduction

Finding the limitations with the straw biomass for the targeted bio-product (i.e. bio-composite) is the key to an outstanding research and development. The detailed study of straw is required to finding the limitations associated with it in different applications.

In this chapter wheat straw stem is investigated as a whole, rather than particles or fibres and is pre-treated in order to optimise its surface chemical distribution and mechanical properties so it could be utilised in bio-composite. Research on the bio-composites from wheat straw has been on utilising straws in particle form with very short lengths (i.e. [121,388-392]), whereas the mechanical properties could potentially be increased by using longer straws and also the energy consumption of the processing of raw materials could be lowered. Limited research has been done to characterise the surfaces of wheat straw and specifically on the differences between node and internode.

The waxy layer on the outer surface of wheat straw is the main inhibiting factor for the reduction of bonding quality in bio-composites and on the other hand it makes the straw less accessible to the main components such as cellulose and hemicellulose which could be utilised as bio-energy source. Waxes appear primarily in the cuticular and epidermal tissues along with micro-sized silica particles (phytoliths) that are unique to each plant species [121].

Wax particles of 1-2μm across and 2-3μm high cover the stem [393]. They are made up of a mixture of primarily long chain fatty acids and fatty alcohols, sterols and alkanes [394]. The bio-composites from straw biomass will experience lower quality without any pre-treatments to address the associated issues raised from the waxy layer on the surface (i.e. interfacial bonding). On the other hand the pre-treatments should be environmentally sustainable and should not deteriorate the mechanical integrity and rigidity of each individual straw.

Traditionally wax layer was extracted by the organic solvents like ethanol/benzene. Han et al. [395] reported that the wettability of wheat straw surface was enhanced through ethanol/benzene extraction and the bond-ability of particleboards made from extracted wheat straw was improved due to the removal of wax-like substances and other nonpolar extractives from the straw surface. Other approaches have been used to increase interfacial adhesion between straw surface and resin system, such as steam explosion [396,397], acid or alkali treatment [398,399], coupling agents modification [400], and enzyme treatment [7,401].

Combinatorial pre-treatment strategies are identified as an emerging pre-treatment technology in enhancing the biomass digestibility and overcoming the relative bottlenecks in the utilisation and optimisation of biomass.

This chapter evaluates whether a combination of mild pre-treatments are sufficient for an economically feasible and environmentally sustainable system for the optimised utilisation of biomass for bio-products. The objective of this study is to investigate in detail the differences in node and internode of wheat straw when subjected to various pre-treatments. This would enable smart selection of the best possible anatomical section of the wheat straw stem after the pre-treatments, for the application of bio-composites. The reason for the very detailed investigation of surface of node and internode (inner and outer surface) is that when it comes to bio-composite production, inevitably various scenarios of interfacial connection between different anatomical sections is going to occur. Hence it is useful to assess whether these properties play any important role in interfacial bonding quality. Bonding quality determines the consequent physical and mechanical properties of the overall composite.

5.2 Experimental plan

The stems of wheat straw with the best condition were selected, cleaned and grouped for pre-treatment. To separate the nodes and internodes the stems were cut carefully above and below the nodes. For analysis of the surface, the stem was cut longitudinally in half using a razor blade. All the samples were oven dried for 24 hours at 100˚C prior to testing and pre-treatments. The analytical techniques and testing procedures used in this chapter are explained in Chapter 3.

5.3 Pre-treatment methods

5.3.1 Combinational pre-treatment (H+S)

The combinational pre-treatment was carried out as follows: the straws were firstly introduced to the pressure cooker with water at an initial temperature of 100˚C. The cooker was then sealed to maintain a pressure of about 0.1 MPa. The internal temperature was monitored for the duration of the pre-treatment (30 min) and meanwhile increased to a maximum of 106 ± 1˚C with advancing of time and pressure. The solid to liquid ratio of 1:20 (by weight) was used for this pre-treatment. Wheat straws were then removed from the hot

water and placed in a mesh basket positioned above hot water inside the pressure cooker, and such steam at 100 ˚C passes through the wheat straw for another 30 min in order to complete hot water and steam pre-treatment, H+S Fig. 5.1.

Hot water and steam pre-treatments, which actually use acetic acid liberated from cell wall hemicellulose, represent the lowest degree of severity in pre-treatment severity scale.

5.3.2 Hot water and steam pre-treatment (0.5H and 0.5S)

The hot water and steam pre-treatments were carried out exactly as the combinational pre-treatment procedure. In 0.5H the untreated wheat straw was pre-treated for 30 min in hot water in a pressure cooker and for 0.5S the untreated wheat straw was pre-treated for 30 min in a mesh basket placed above boiling water. These treatments were used individually for the characterisation purposes in order to understand the synergistic effect and to evaluate where the most contribution to each characteristic arises from.

5.3.3 Mild alkaline pre-treatment (0.5NaOH)

A mild alkali pre-treatment was also carried out on wheat straw in order to compare and evaluate the designed physical pre-treatment. Sodium hydroxide (NaOH) solution concentration of 10 g kg^{-1} was used for pre-treatment of wheat straw for 30 min of incubation. The samples in this solution were kept in an environmental chamber with 25˚C and a 55% relative humidity. After the pre-treatment the samples were washed with distilled water several times.

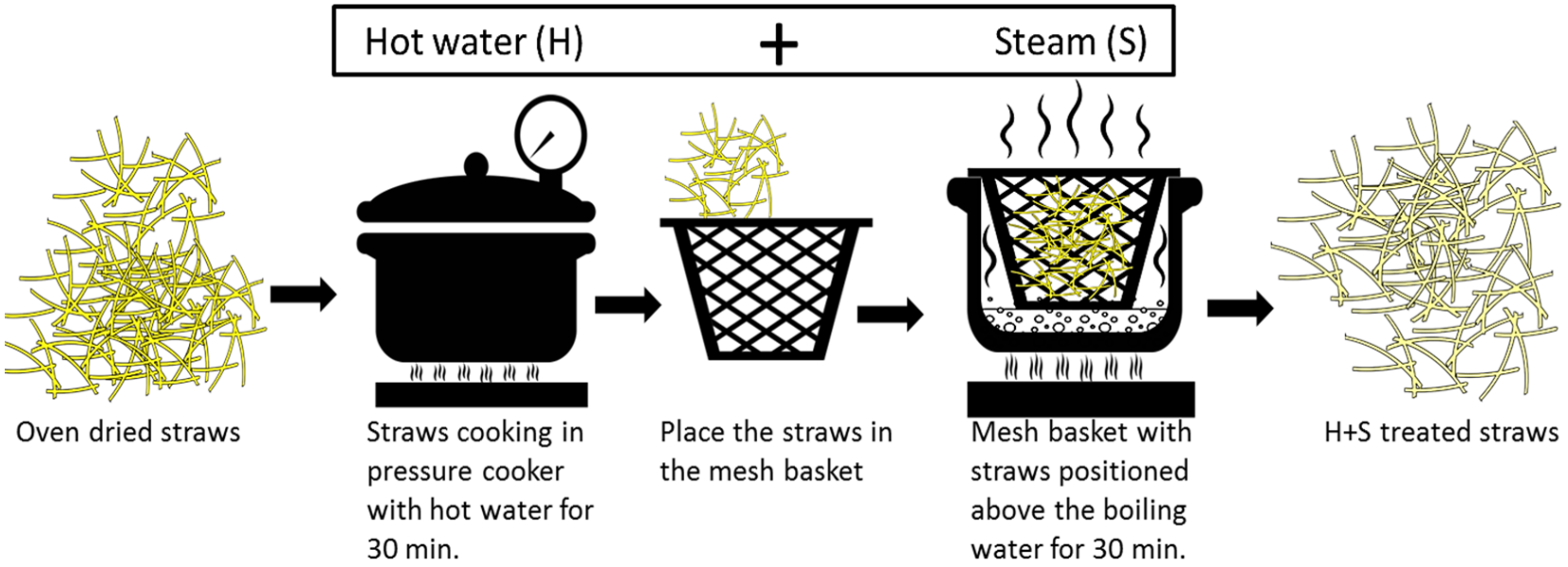

Figure 5.1 Flow diagram showing the combinational treatment strategy

5.4 Results and discussion

5.4.1 Surface chemical functional groups analysis

The surface chemical distribution was analysed using ATR-FTIR spectroscopy. The results of the wheat straw node and internode, inner and outer surface with different pre-treatments are shown in Fig. 5.2 and Fig. 5.3.

The intensity of 790 cm^{-1} in internode and 985 cm^{-1} in node has diminished in all the pre-treatments, with the most intensity reduction in 0.5NaOH and H+S pre-treatments. These two bands are more likely attributed to the silicon carbide (Si–C) stretching vibration, and silicon oxide (Si–O) vibration, respectively [361]. This suggested that silicon present on the outer surface is diminished through the pre-treatments.

Bands observed between 1000 and 1500 cm^{-1} wavenumber show the presence of hemicellulose [402] and cellulose [403] in wheat straw. The sharp band at 1250 cm^{-1} in untreated (UN) sample (Fig. 5.2) decreased in intensity and broadened after all the pre-treatments in the internode outer surface which indicates the partial removal of hemicelluloses. The most reduction in internode outer surface was observed in 0.5H and 0.5NaOH pre-treatment.

The intensity of the bands at 1160 and 1435 cm^{-1} are stronger at the inner surface on internode and node than outer surface. This was expected, as the outer surface was more visibly glossy than inner surface, which indicated that the outer surface had more lipophilic extractives and less polysaccharides and lignin than the inner surface [359].

The cellulose assigned bands at 897 cm^{-1} (asymmetric out-of-phase ring stretch in the C1–O–C4 glycosidic linkage), 1372 cm^{-1} (C–H bending), 1429 cm^{-1} (C–H wagging), and 2900 cm^{-1} (C–H stretching) are used for quantitative indices evaluation of the overall crystallinity of cellulose [404], the lower order index (LOI) and total crystallinity index (TCI) were calculated based on FTIR spectra [403,405]. Higher values of TCI (H1372/H2900) and LOI (H1429/H897) indicate higher crystallinity and more ordered structure of cellulose in the material [406,407].

H1429/H897 (LOI) increased by 14% (0.74 for UN to 0.85 for H+S) in internode and by 11% (0.9 for UN to 1.0 for H+S) in node. On the other hand H1372/H2900 (TCI) also increased by 24% (1.1 for UN to 1.4 for H+S) in internode and by 9% (1.1 for UN to 1.2 for H+S) in

the node. It is apparent that change in the crystalline structure of cellulose varies in different regions, and improvement in the crystallinity of cellulose in H+S straw may provide a great stability to the cellulose chain [408].

Lignin bands at approximately 1595 and particularly at 1510 cm^{-1} (aromatic ring stretch) [130] are strongly enhanced in the H+S and 0.5H pre-treated sample compared with untreated and 0.5NaOH samples. The intensity of these bands is reduced for 0.5NaOH, shown in Fig.5.2 a. The reason for the enhanced lignin bands is that the lignin is released and re-deposited on the surface as a result of H+S and 0.5H treatment. This is also previously observed by other researchers [366,409] for hydrothermal pre-treatment of wheat straw and for aspen wood by steam explosion pre-treatment [410].

As discussed in Chapter 4 a sharp band at 1739 cm^{-1} in the untreated wheat straw outer surface is assigned to the carboxyl groups in the acids and esters of acetic, *p*-coumeric, ferulic, and uronic acids, which are the main constituents of the extractives and hemicellulose [368]. The intensity of this band diminishes in the samples pre-treated by H+S and 0.5NaOH, although 0.5NaOH shows greater reduction compared to H+S (see, Fig. 5.2 and 5.3). Alkaline solubilisation of hemicelluloses is due to the disruption and breaking of hydrogen bonds.

The two strong bands at 2920 and 2850 cm^{-1}, corresponding to asymmetric and symmetric CH_2 stretching respectively [370] decrease in intensity in the pre-treated samples in all the cases of internode and node, inner and outer surface in comparison to the untreated. These two bands showed the biggest difference in terms of reduction of intensity after the H+S and 0.5NaOH pre-treatments. The reduction in the intensity of these bands in H+S and 0.5NaOH pre-treatment leads to a conclusion that the extractives in particular waxes have been partially removed.

The spectrum of 0.5H and H+S are very similar in the intensity reduction of aliphatic fraction of waxes which shows most of the contribution for this phenomena comes from the 0.5H and not the following 0.5S pre-treatment. It has been reported that pre-treatment of wheat straw with hot water at 80–95˚C for 30 minutes released 41–53% of the original lipophilic extractives [411]. Wax is an important group of the lipophilic extractives.

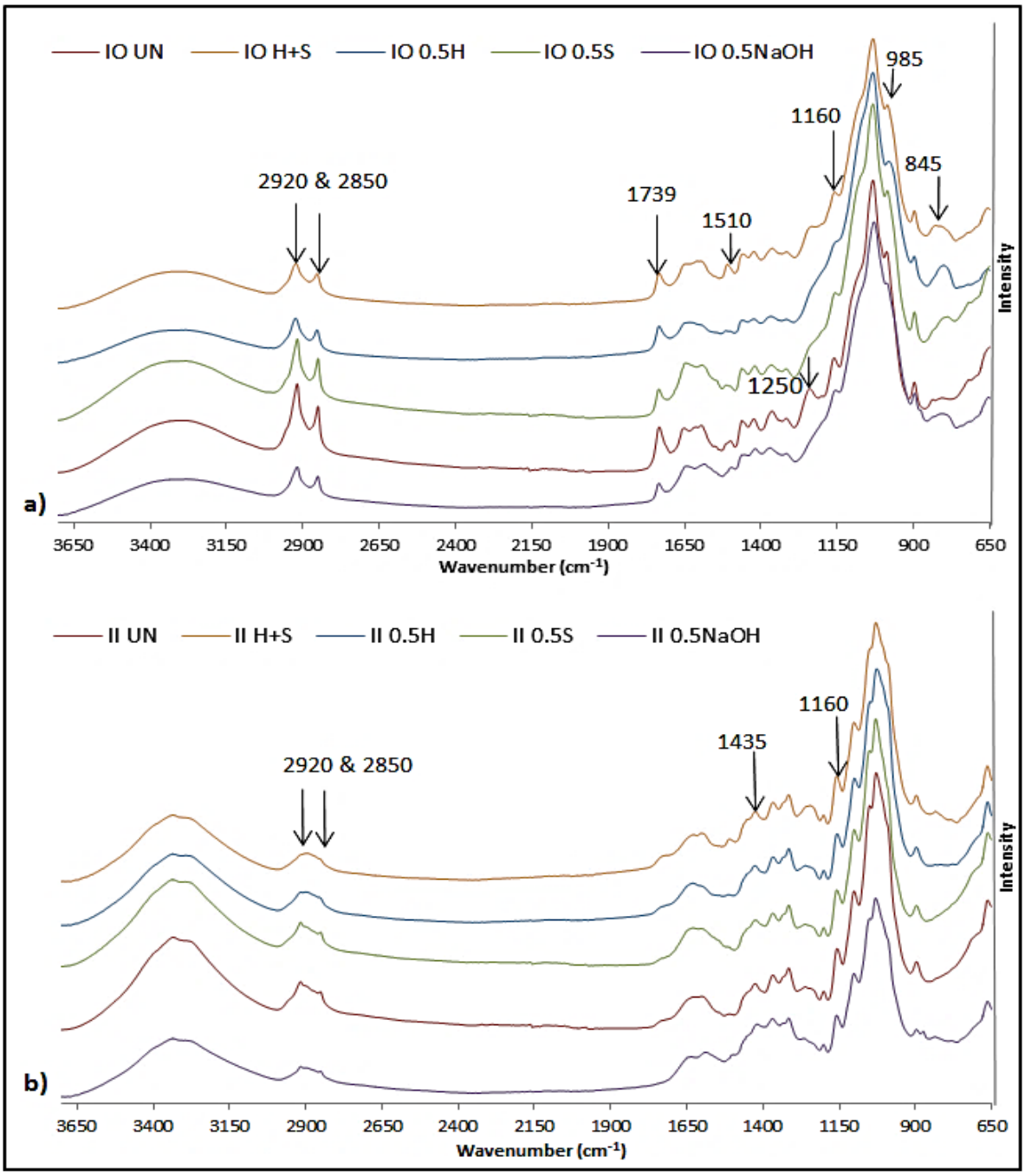

Figure 5.2 ATR-FTIR spectra of a) internode outer surface (IO) and b) internode inner surface (II) subjected to different pre-treatments (H+S, 0.5H, 0.5S and 0.5NaOH) and compared to untreated (UN) samples

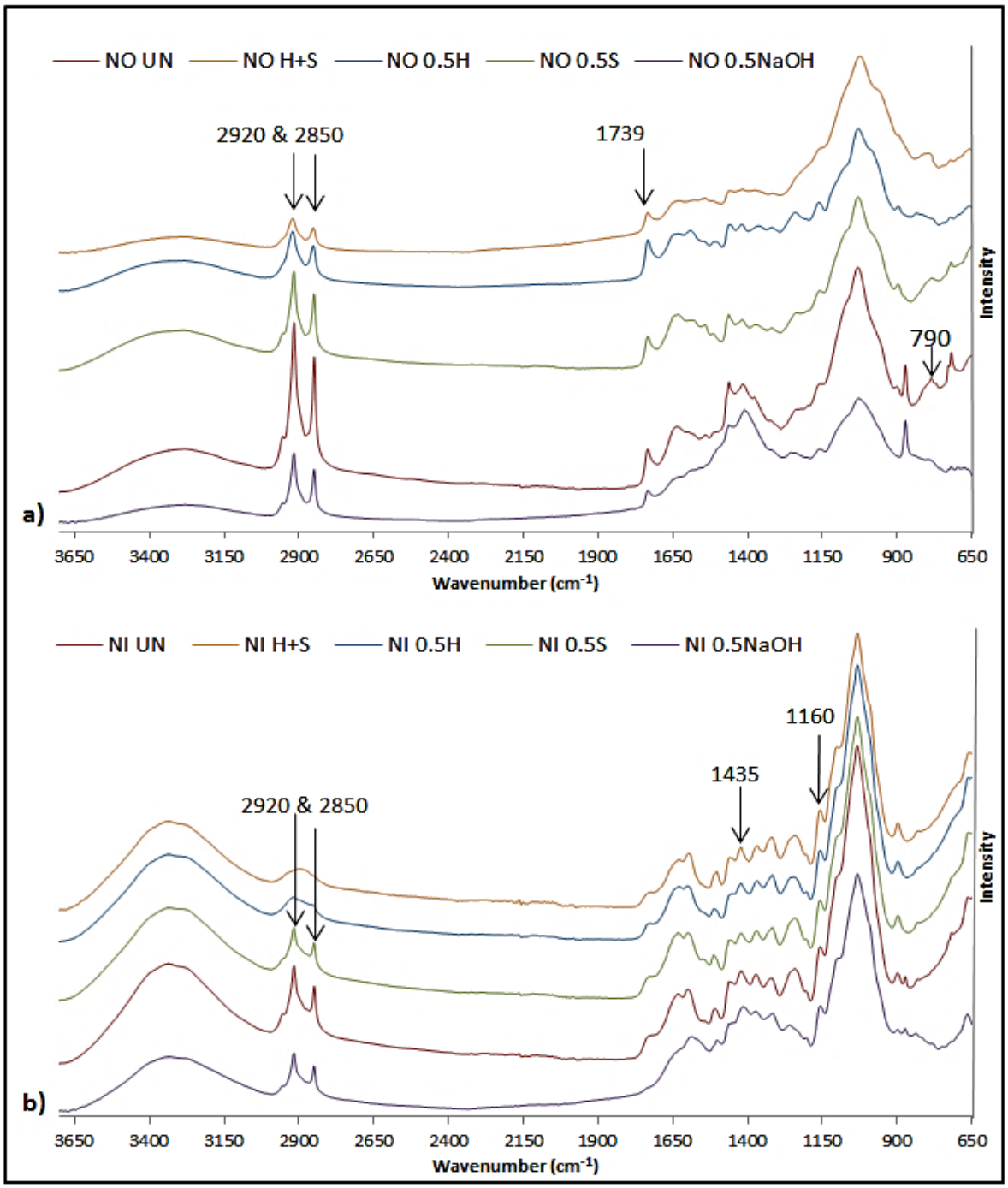

Figure 5.3 ATR-FTIR spectra of a) node outer surface (NO), and b) node inner surface (NI) subjected to different pre-treatments (H+S, 0.5H, 0.5S and 0.5NaOH) and compared to untreated (UN) samples

5.4.2 Wettability of outer surface of wheat straw

The contact angle has been used as an indicator of surface wettability which is a direct measure for the penetration of resin system in the cells. Wheat straw outer surface has a great number of cell elements as detailed in Chapter 4. It includes fibres, parenchyma cells, vessel elements, and epidermis cells, shown in Fig. 5.4. The outermost surface cell (epidermis) is thin, but has dense and thick-walled cell with an outer wall coated with a waxy film of cutin cuticle. Wetting is only influenced within a depth of 5 to 10 nm, only the outermost layer.

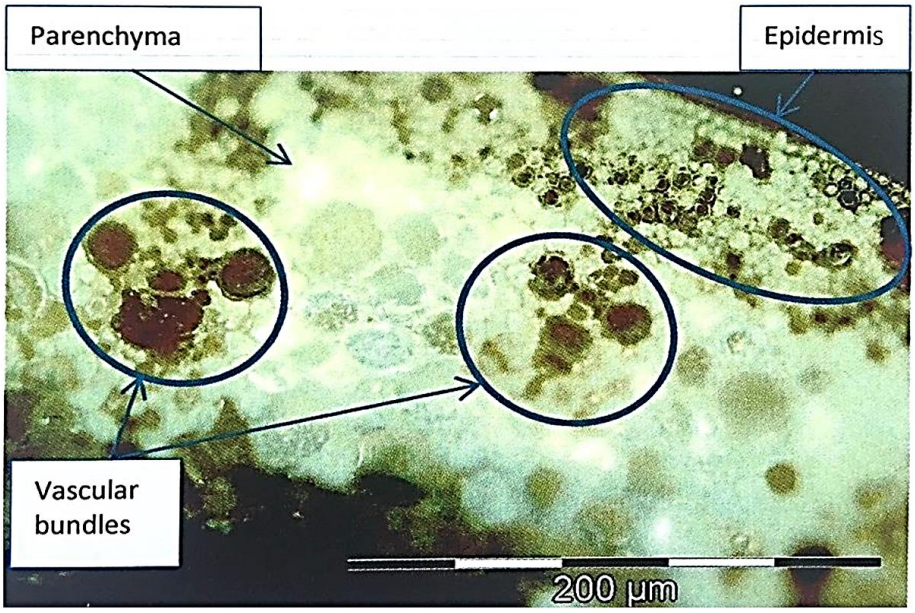

Figure 5.4 Optical micrograph of wheat straw internode cross-section

The results of the contact angle measurements are represented in Fig. 5.5. The 0.5NaOH and H+S pre-treatments illustrate that their influence on the outer surface is more significant for improving the wettability and penetration. After the H+S pre-treatment the θi (initial conact angle) and θe (equilibrium contact angle) were reduced by 32.6˚ and 41.5˚, respectively. On the other hand the same corresponding values for 0.5NaOH pre-treatments are 35.5˚ and 43.9˚.

The partial removal of surface wax and impurities is clearly the reason for improved wettability after the H+S pre-treatment which is encouraging as it is very much comparable to the 0.5NaOH pre-treatment. Chemical pre-treatment is used traditionally to remove lignin, pectin, waxy substances, and natural oils covering the outer surface of the stem [402]. The

ester-linked substituents of the hemicellulose and other cell wall components can be cleaved by alkali treatment which tends to decrease hydrophobicity [412].

The improved wettability of H+S pre-treated wheat straw surface could also be attributed to the increased porosity due to first partial removal of extractives (0.5H) but also the steam (0.5S) in the following stage of treatment which opens up the pores on the outer surface, developing sites for the penetration of liquid. The synergy positive effect of two steps in H+S pre-treatment is evident. H+S treatment partially removes hemicellulose and influences the structure and distribution of lignin in wheat straw. The depletion of hemicellulose, that is physically associated with cellulose, could lead in an increase in pore volume [409,413,414].

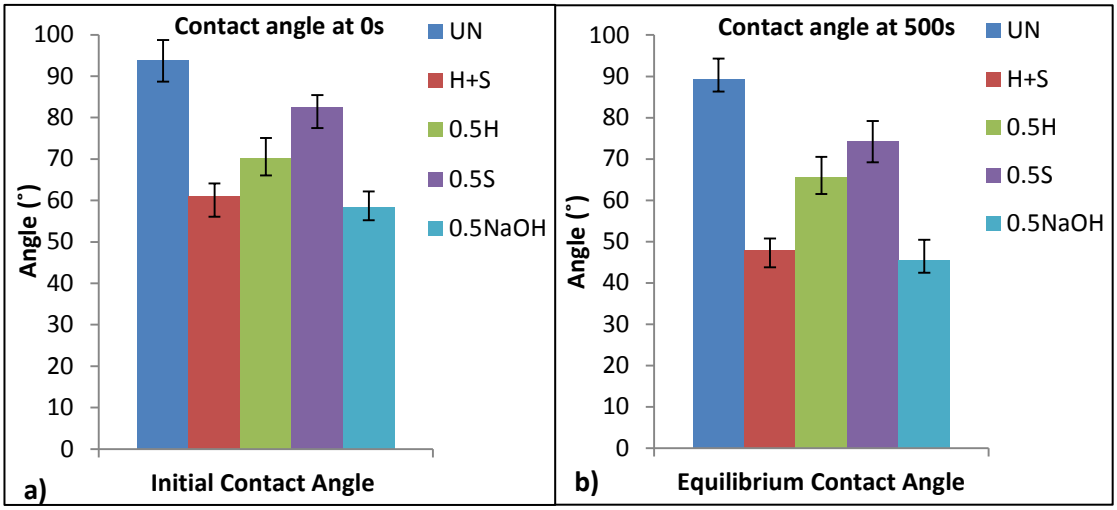

Figure 5.5 a) Initial contact angle θi b) equilibrium contact angle θe

The better wettability of treated straw surface could result in improvement of the bonding quality between straw and water-soluble resins, i.e. better interface bonding.

5.4.3 Tensile test analysis

One of the important properties governing the mechanical behaviour of straw biomass is the tensile strength. A comparative investigation is conducted to evaluate the influence of the pre-treatments on the internode and the node of wheat straw. The results are illustrated in Table 5.1. After the pre-treatment, it is important that the fibre structure within straw is not deteriorated. Otherwise the mechanical performance of the resulting straw composite will not be adequate.

Table 5.1 Experimental tensile strength results

Sample ID	Internode		Node	
	Tensile strength (MPa)	CV (%)	Tensile strength (MPa)	CV (%)
UN	66.0	10.0	12.4	4.2
H+S	88.9	9.4	20.1	7.4
0.5H	76.8	7.2	19.4	9.6
0.5S	69.6	5.1	15.8	7.2
0.5NaOH	57.9	6.3	12.0	3.8

The test results are very reliable with coefficient of variation (CV %) of 60 samples ranging from 3.8 to 10%. The H+S pre-treatment showed significant increase in tensile strength (35%) in the internode ($P < 0.05$) and (62%) in the node ($P < 0.05$), on the other hand the 0.5NaOH pre-treatment led to a significant reduction in tensile strength of (12%) in internode ($P < 0.05$) and (4%) in node ($P < 0.05$).

The tensile strength of untreated wheat straw (moisture content of 10-14% wet basis) is reported to vary from 9 to 32 MPa [348]. Kronbergs [415] reported much higher numbers for wheat stem (119 MPa). These values are based on the wall area of the whole stem specimen at the failure cross-sections. The tensile strength is likely to be underestimated in the literature where the whole straw stem is used for the test [348,415]. This is due to the straw stem not breaking consistently throughout the sample. Hence, the cross section area of the whole straw stem is larger than the actual area where the failure happens, which leads to an underestimated tensile strength.

Shang et al. [373] found the untreated wheat straw tensile strength to be around 50-53 MPa (oven dried). This value in this study, for untreated oven dry wheat straw internode is 66 MPa. The difference could be due to the position selected for the test or other factors which are related to the origin of straw.

Nevertheless, the comparisons between two different research studies are not appropriate when it comes to straw biomass, as the origin of straws could effect their characteristics. In this study, however the comparison between tensile strength helps the evaluation of the pre-treatments. It is also worth mentioning that there are no data available in literature on the tensile strength of wheat straw node.

One important observation in tensile strength testing was the significant difference in the strength of node and internode. This is due to the morphology of the node. The node in the stem of wheat straw acts as a joint, it connects the internodes together and hence it does not have the long stretched longitudinal fibres which are the main reasons for higher tensile strength of internode. The cross-section of the node core shows the very dense area as explained in Chapter 4, see Fig. 5.6 (2a and b). Fig 5.6 (1) shows the typical failure of a node which is exactly from the node core area which joins the two internodes and is the weakest link in tension.

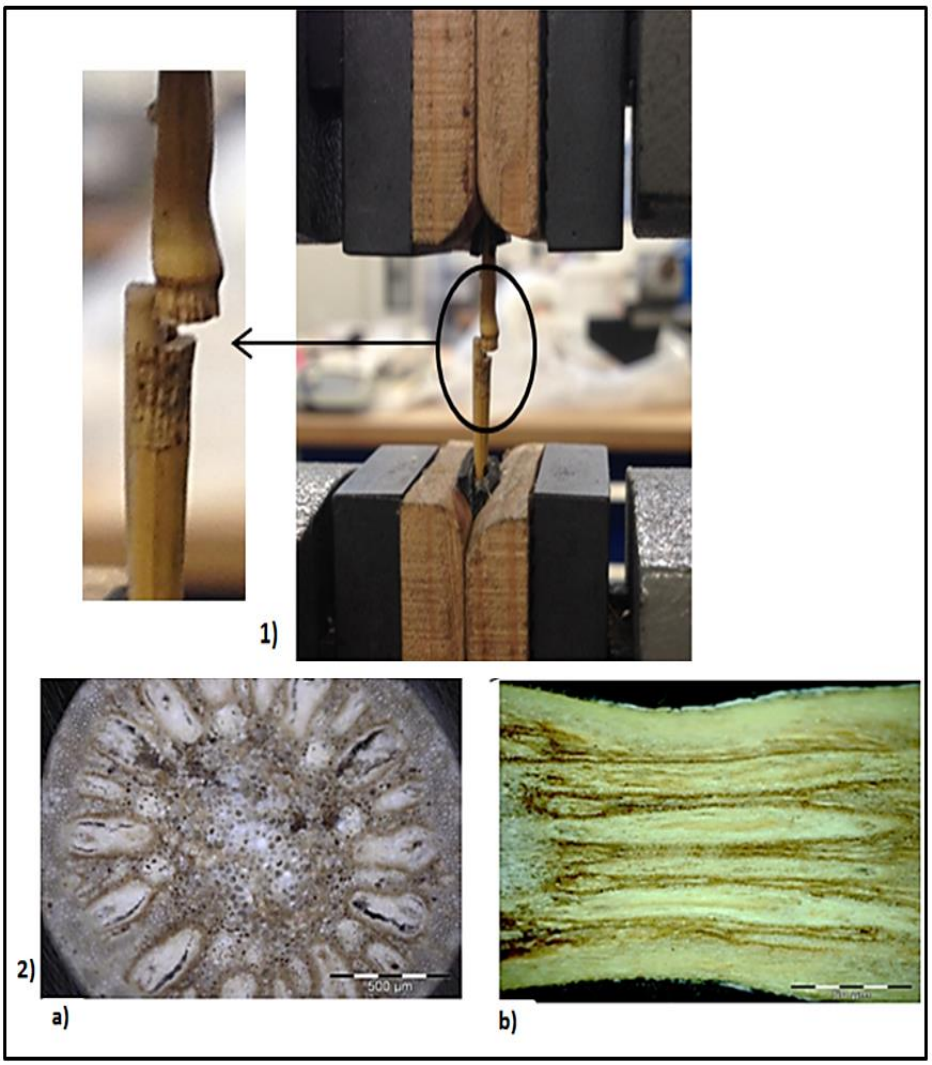

Figure 5.6 (1) Typical failure in the gauge length in node (2) a) node cross-section (b) node transverse inner surface view

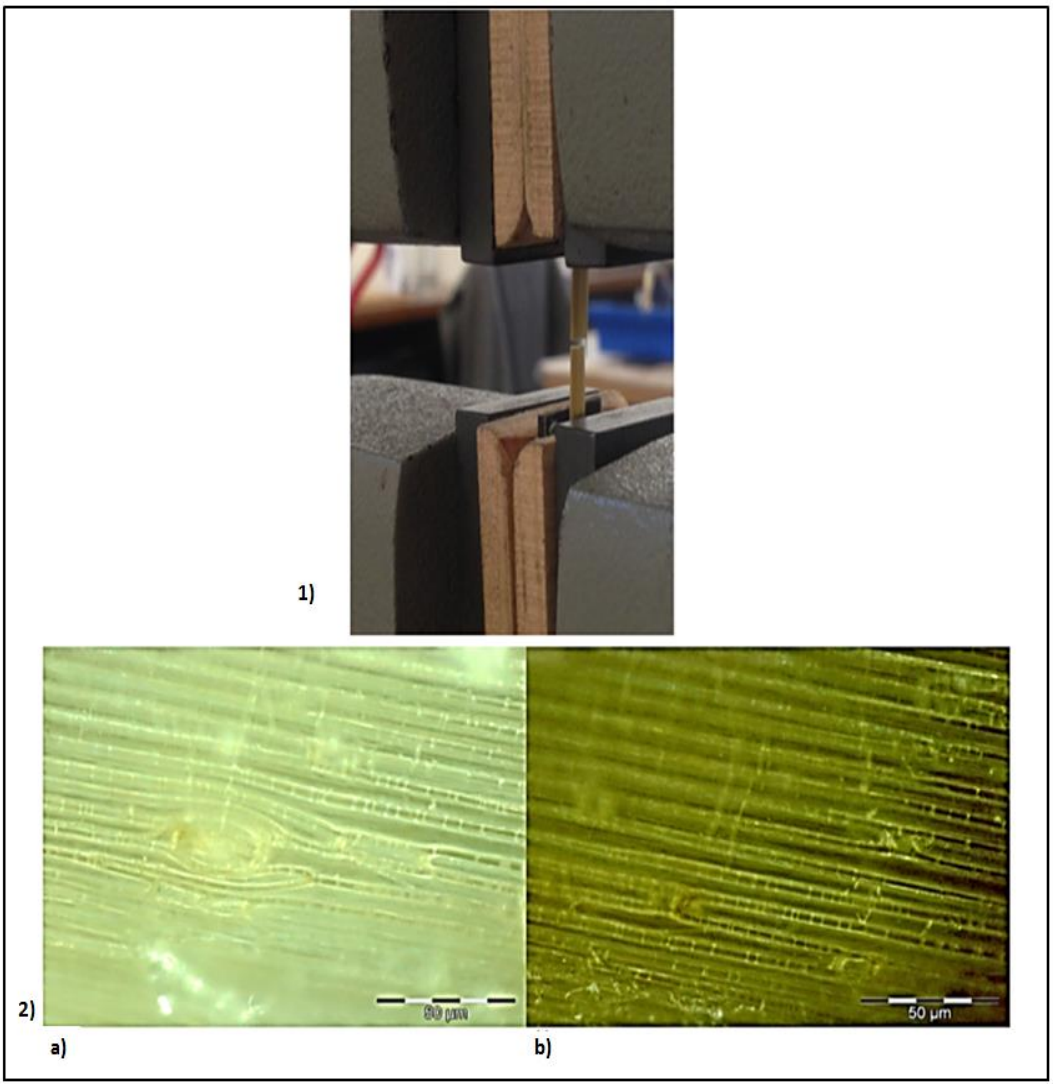

Figure 5.7 (1) Typical failure in the gauge length in internode (2) surface of internode longitudinal direction showing a) the defects b) longitudinal fibres

Fig. 5.7 (1) shows the typical failure of wheat straw internode in tension and Fig. 5.7 (2) is the inner surface morphology showing the long fibres in longitudinal direction. Although, the presence of defects, see Fig. 5.7 (2a), could negatively influence the tensile properties of internode.

The alkaline treatment degrades the wheat straws with increasing incubation time. It reduces the fibre structure stiffness and thus negatively influences the tensile strength [413]. Improved tensile strength of H+S pre-treated samples is due to the swelling of cell walls (but not disruption) which results from the steam pre-treatment in the second stage of H+S pre-treatment strategy.

The cellulose crystallinity increase in H+S treated straws, shown by the ratio of peak heights in FTIR, also contributes to the increase tensile strength. 0.5S pre-treatment on its own increased the tensile strength by 5% for internode ($P<0.05$), and 27% for node ($P<0.05$). In order for the steam to be effective in increasing the volume of cell walls, the 0.5H pre-treatment is critical as it cleans the surface from impurities and diminishes the surface wax. The 0.5H pre-treatment on its own contributes the most to the synergistic effect of H+S pre-treatment.

Although comparison to other studies are not appropriate as mentioned earlier, however, wheat straw fibres modified via pressurised steam treatment (1MPa for 10 mins) [416] had a tensile strength of 74 MPa which is lower compared to the H+S pre-treated straws (89 MPa) in this study. This could be due to the higher pressure used which might disrupt the integrity of fibres to some degree.

5.4.4 Thermal characterisation and ash content

Investigating the thermal properties of wheat straw is essential in order to assess their suitability for bio-composite production. Low thermal stability of most straw biomass is a hurdle in production of bio-composites. Fig. 5.8 shows the TGA results obtained from wheat straw node and internode for untreated and H+S pre-treated samples.

Generally there are three stages of degradation in the TGA curves in all cases. The first stage is the initial weight loss of straw (100–150˚C) which is because of the evaporation of the adsorbed moisture. This stage (loss) is dependent on the initial moisture content of the straw. The second stage is the severe weight loss (250–350˚C), degradation of cellulose and hemicellulose, and third stage is due to decomposition of the non-cellulosic components of the straw (lignin).

The higher onset of degradation temperatures indicates the improved thermal stability of the wheat straw samples. The relatively higher onset of degradation temperature of the H+S treated straws (291˚C and 315˚C for node and internode respectively) than the untreated straw (279˚C and 296˚C for node and internode) is due to the partial removal of hemicelluloses and waxy substances from the straw during this treatment (Fig. 5.8). This could also show a relationship between structure and the thermal degradation of cellulose. A greater crystalline structure requires a higher degradation temperature [417].

The respective residual weight before (UN) and after the treatment (H+S) was different, accounting for 11% and 4%, correspondingly in the case of internode and 8% and 5% in the case of node. This data concludes that some sources of ash are also removed from the wheat straw after H+S, resulting in a relatively low residual content [418].

The ash content (NREL/TP-510-42622) of UN wheat straw reduced from 2.7% to 1.3% in H+S treated internode, and from 4.9 to 2.9% for the node. More than 90% of the ash in wheat straw is silica [419], the data indicates significant reduction in the ash content of H+S treated wheat straw which is beneficial for the bio-composite application as silica inhibits the interfacial bonding [420,421].

In summary, due to the partial removal of hemicellulose, wax and ash, H+S treated wheat straw has higher thermal stability and lower ignition residue. The previous study has shown that some biomass fibres at certain NaOH concentration have reduced thermal resistance [402]. The influence of chemical pulping (NaOH solution) processes on the TGA of the wheat straw fibres was studied [389] and the onset of degradation was found to be 242˚C; also in other study, an onset decomposition temperature of 276˚C for chemically treated (NaOH solution) wheat straw is reported [422], these values are both lower than the values found in this study for H+S treated wheat straw (291 and 315˚C for node and internode respectively).

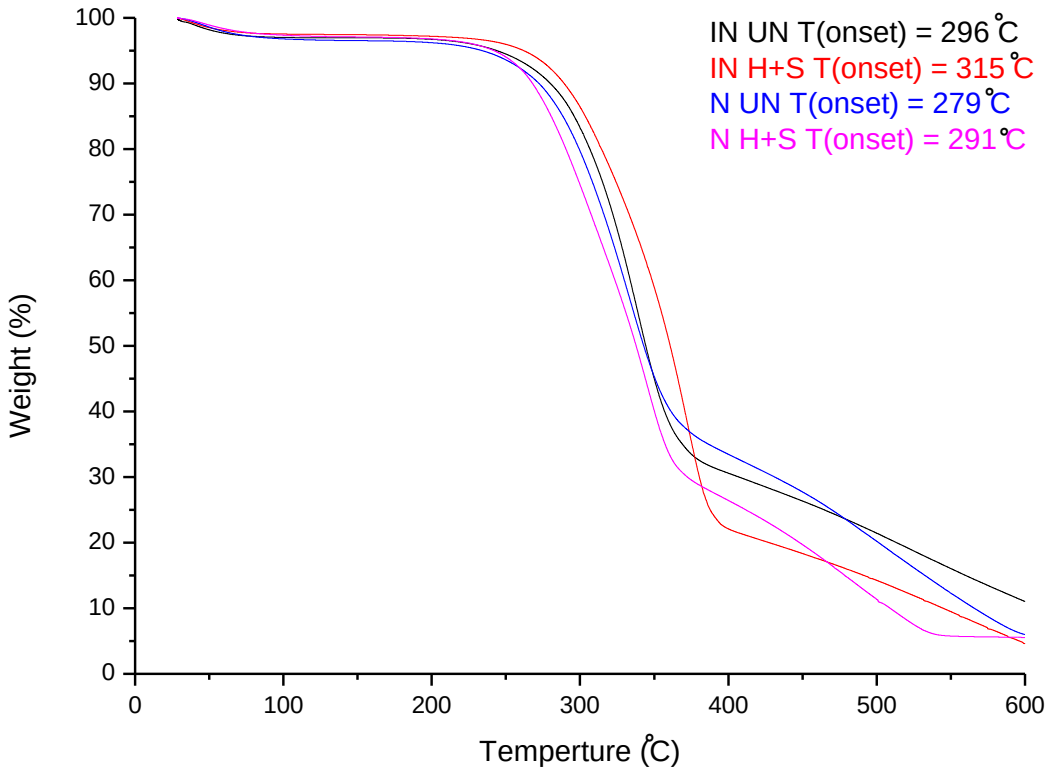

Figure 5.8 TGA of untreated (UN) node (N) and internode (IN) and H+S (N-IN) with onset degradation temperature

5.5 Interim conclusions

The differential behaviour of node and internode in wheat straw stem was investigated thoroughly under various pre-treatments. Combinational pre-treatment technologies achieve a synergistic effect (i.e. benefiting from different aspects of each stage, and reducing the disadvantages of each pre-treatment type).

Functional group changes were monitored in node and internode of wheat straw stem inner and outer surface, where the results showed a reduction in the intensities assigned to aliphatic fractions of waxes and silica after each stage of pre-treatments when compared to the untreated samples. The dissolution and/or removal of silica and wax on the outer surface led to reduced hydrophobicity (by 35%), therefore increasing the wettability. Improved wettability is advantageous for water-based adhesives used in bio-composite production. The thermogravimetric analysis also illustrated that the thermal stability of the wheat straw increased after the pre-treatment which is advantageous for the bio-composite application.

FTIR analysis of cellulose crystallinity showed a great stability of the cellulose chain in H+S treated samples. This resulted in significant ($P < 0.05$) improvement of tensile strength of single straw strands, where the tensile strength increased by 62 and 35% for node and internode.

According to the results of tensile and surface properties it is concluded that node could be a potential defect in straw bio-composite, as it has low tensile property and higher levels of surface wax.

The 0.5H stage of H+S pre-treatment contributed the most to the overall improved properties when compared to the subsequent 0.5S. Nonetheless 0.5S stage of H+S pre-treatment proved to be necessary, especially for the wettability improvement of outer surface.

Chapter 6 Physicochemical properties and surface functionalities of wheat straw node and internode

Highlights:

- Towards valorisation of wheat straw through identification of physicochemical properties;
- The node has higher extractives, klason lignin and ash content than internode;
- The outer surface is more hydrophobic and the inner surface is hydrophilic;
- Efficient and environmentally friendly pre-treatment reduced significantly ($P<0.05$) extractive and ash content along with the Si (weight %) of node and internode.

This chapter is towards the valorisation of wheat straw as improved feedstocks for bio-refinery processes. The effects of each physicochemical property in correlation with the surface functionalities on the intended bio-refinery pathway is studied. Selective fractionation of wheat straw proved to be essential for an efficient utilisation/bio-conversion. This chapter, builds on the outcomes of previous chapters, and completes two important sub objectives of the objective chart of this project (Fig. 1.1): i) the physicochemical properties are differentiated between node and internode and ii) the effects of an efficient, environmentally friendly pre-treatment on cell wall composition of node and internode is investigated.

Keywords: Node and internode; Klason lignin; Extractives; Ash content; Elemental composition.

6.1 Introduction

Agricultural crop residues have the potential of being a valuable renewable resource for bio-refinery feedstocks. Extensive studies in the past 10 years have been carried out to extend the uses of wheat straw and increase its additional value [4,19,22,33,121,349,350,368,423-426]. The smart extraction, separation and fractionation of waste crops components, presents a unique potential to develop innovative added value products.

As emphasised in Chapter 1, straw biomass efficient utilisation requires the detailed understanding of material sciences, as well as recognition that not all parts of the crop residue are equally valuable. For instance biofuel and chemical processors only require the high yielding cellulose and hemicellulose biomass parts delivered. This signifies a strategy for identifying and subsequently reducing the number of undesirable residue parts for feedstock. Additionally the heterogeneous nature of straw, where their chemical composition varies with species, location, storage time, harvest, stage of maturity, environmental conditions and anatomical parts, i.e. node and internode, makes their comprehensive characterisation essential prior to bioconversion process [423,424,427,428].

It is almost impossible to control the compositional variability of straw biomass, but it is feasible to monitor the variability and accordingly select the processing technologies for the specific bio-refinery. Hence, this chapter thoroughly investigates internode and node and monitors the changes in 1) surface chemistry, 2) elemental composition, 3) extractives yield, 4) klason lignin and 5) ash content, to deliver an aggregate understanding of material science leading to valorisation of wheat straw for bio-refinery pathways.

6.2 Experimental methods

6.2.1 Analysis of cell wall components and various profiles of node and internode

All samples for chemical compositional analysis were prepared according to NREL/TP-510-42620 [429]. In order to investigate the surface profiles, the node and internode were carefully cut in half longitudinally so that the outer and inner surface could be exposed to testing. Samples were oven dried (100˚C for 24hrs) prior to testing. Surface functionalities and elemental composition of straw profiles were also investigated.

Five replicates were taken for the wet chemistry (i.e. klason lignin and extractives content), ten replicates for surface analysis (i.e. surface functional groups and elemental composition) and ash content. Table 6.1 summarises the methodologies and drives for each analytical technique used. The results from each parameter analysed are interpreted to establish the correlation between various characteristics which will contribute to the understanding of wheat straw node and internode of various surface profiles.

All the procedures (i.e. extraction, klason lignin), were made separately for each sample (i.e. node and internode, treated and untreated) and for each extraction medium (i.e. hot-water and ethanol).

6.2.2 Pre-treatment

Apart from the untreated samples, a group of node and internode samples was also pre-treated to further understand the difference of node and internode. Efficient combination of physical pre-treatment (H+S) was the method used in this chapter. The details of this pre-treatment are previously mentioned in Chapter 5.

Table 6.1 Parameters analysed with their relative methodologies and purpose of investigation

Parameters investigated	Methods	Purpose
Extractives content	Extracted using two solvents, hot-water (HW) and ethanol (ET), in a soxhlet method for 24 hours following *NREL/TP-510-42619* [430].	1. Examine the different extractives between node and internode, 2. Identify efficient extraction solvent.
Acid insoluble lignin/Klason lignin (KL)	Determined according to *NREL/TP-510-42618* [431]. KL determinations were corrected for their relative ash content.	1. Inspect the KL yield in node and internode, 2. The effects of pre-treatment on KL content.
Ash content	According to *NREL/TP-510-42622* [432], the residue after combustion of the organic matter at a temperature of 525±25˚C.	1. Classify the ash content of node and internode, 2. The effects of pre-treatment on ash content, 3. Quantify both structural (non-extracted) and extractable ash content.
Surface chemistry	ATR-FTIR spectra were recorded on a PerkinElmer Spectrum one Spectrometer, operated under the following conditions: 4000–650 cm^{-1} range; 4 cm^{-1} resolution; 16 scans.	1. Interpret different surface functionalities in node and internode, 2. Track the changes to the surface chemical distribution after pre-treatment.
Surface elemental composition	The EDX-SEM spectra were obtained using an INCA Energy 350 microanalysis system.	1. Check the consistency of surface elemental components, 2. Evaluate the efficiency of pre-treatment in surface modification.
Profile morphology	Investigated using optical microscopy (OM) and field emission gun-scanning electron microscopy (FEG-SEM, Zeiss Supra 35 VP).	1. Differentiation of node and internode, 2. The correlation of morphology and surface chemical characteristics, 3. Changes to morphology induced by pre-treatment.

6.3 Results and discussion

The wheat straw was composed (on a mass basis) of 60-62% internodes, 14-17% leaves, 10-13% nodes, 7-9% chaffs and 3-5% rachis. In this project the focus is on the stem, 70-75% (node and internode) of wheat straw biomass.

6.3.1 Surface chemical distribution of node and internode

The surface chemical distributions of wheat straw node and internode, inner and outer surfaces are shown in Fig. 6.1. The most relevant bands have been summarised in Table 6.2 where the characteristics of surface profiles are qualitatively compared in node and internode (i.e. similar to Table 4.2). As observed in Chapter 4 the intensity of 2850 and 2920 cm^{-1} is much higher in a node (Fig. 6.1), which may be attributed to the higher intensity of waxes on the surface.

On the other hand, comparing inner to outer surface, it is recognised (Fig. 6.1a and b) that the hydrophilic tendency of the inner surface of both node and internode is reflected by the broad and more intense band in the 3200-3600 cm^{-1} region, which may be due to the -OH groups present in their main components. Interestingly, some bands were present in node, but absent in internode and vice versa, i.e. 2955, 720 and 790 cm^{-1} in node and 985 cm^{-1} in internode, these observations are interpreted later in the Chapter in correlation with wet chemistry analysis.

Table 6.2 Surface characteristics bands of node and internode

Wavenumber (cm^{-1})	Bands assignment	Observations	Ref.
720	Methylene CH_2 in-plane deformation rocking	Only detectable in node outer surface	[359]
790	Si-C stretching vibration		
985	Si-O stretching vibration	Only detectable in outer surface of internode	
1160	C-O-C antisymmetric bridge in hemicellulose and cellulose	Sharper in internode than node	
1435	C=O methoxyl group in lignin	Sharper in internode inner surface than outer surface	
1510	C=C lignin aromatic ring stretch	Sharper in internode of treated straws	[130]
1739	Carboxyl groups	High intensities in internode and node outer surfaces.	[368]
2850 & 2920	Symmetric & asymmetric stretching of CH_2 in aliphatic fraction of waxes	Sharper in node than internode and outer than inner surface	[370]
2955	Asymmetric stretching of CH_3 in fatty acids	Only detectable in node untreated	[433]
3200-3600	OH stretching vibration of hydroxyl groups	Higher intensity for the inner surface compared to outer surface, both in node and internode	[434]

The cellulose crystallinity index for node and internode was estimated with the lower order index (LOI) as proposed in the literature [4,435] according to the Equation 6.1.

$$\text{Crystallinity index of cellulose} = \frac{\text{LOI}}{1+\text{LOI}} \quad (6.1)$$

Motte et al. [4], using the same Equation 6.1 for crystallinity index calculation of cellulose, found values of $49 \pm 1\%$ for the internodes and $52 \pm 4\%$ for the nodes. In this study for untreated samples the crystallinity index (% of cellulose) is calculated to be 43% for the internodes and 47% for the nodes.

The LOI is calculated based on FTIR spectra [405] (intensity heights, H1429/H897). Higher values of LOI indicate higher crystallinity of cellulose in the material [406,407]. As presented in Chapter 5, the LOI increased by 15% in internode and by 11% in node for H+S straws. This improvement in the crystallinity of cellulose could provide great stability to the cellulose chain [408] and therefore increase the mechanical performance of straws (Chapter 5) [424], where the tensile strength of the H+S treated samples increased significantly ($P < 0.05$) by 35% in internode and 62% in node.

On the other hand the degradability of cellulose is correlated to its crystallinity. Crystallinity index of cellulose based on Equation 6.1 suggests that around 47 to 50% of the cellulose of nodes is crystalline and hence less degradable by anaerobic digestion processes. Internodes are, however, only 43 to 46% of crystalline cellulose, showing more amorphous cellulose content that could be favourable for anaerobic digestion. In anaerobic digestion, degradation is inhibited by the straw biomass recalcitrance (i.e. highly complex structures).

Hence there are various pre-treatments of straw biomass for increasing the cellulose accessibility, solubilising the hemicellulose and deconstructing lignin. These pre-treatments, however, require high energy and/or chemical compounds that impair the industrial scale-up. Feedstock management and selection, with the identification of features that would contribute to maximising process performance yields, are therefore, fundamental. These trends would suggest improved feedstock qualities for the intended bio-refinery pathway, thus a potential for upgrading the raw material by fractionating out the less desirable properties of the feedstock.

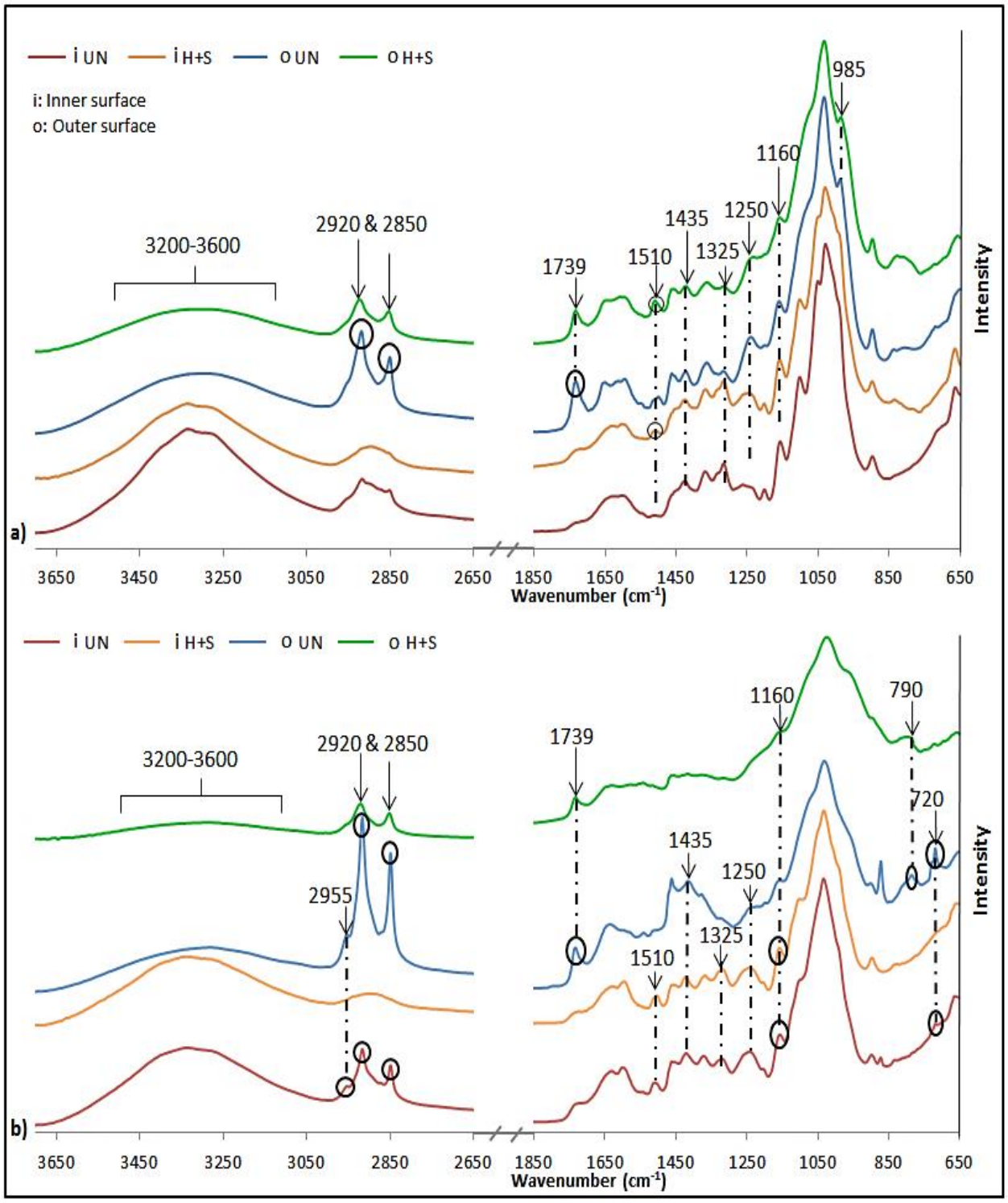

Figure 6.1 ATR-FTIR spectra of a) Internode and b) node of UN and H+S inner and outer surface

6.3.2 Cell wall composition of node and internode

The assessment of cell wall composition in straw biomass is traditionally carried out on milled samples of the whole stem, without accurate determination of node and internode separately. However, the cell wall composition of the internode may be rather different from that of the node.

6.3.2.1 Extractives

The extractives are a heterogeneous group of substances in straw biomass. The main extractives are resin acids, sterol esters, waxes, triglycerides, fatty acids, sterols, fatty alcohols and a selection of phenolic compounds [393]. Generally, the extractives are low molecular weight compounds and their chemical behaviour varies for different classes of extractives. Lipophilic extractives are materials extracted from lignocellulosic biomass with organic solvents such as ethanol and acetone [436].

It is evident that the extractives in nodes are higher than in internodes, as shown Table 6.3 as observed in all the cases investigated, for instance in (hot-water) HW extraction, the node has 10 to 15% higher extractives than internode. The sharp band at 720 cm^{-1} (Fig. 6.1b), being characteristic of the methylene (CH_2) in-plane deformations rocking [359], which is only observed in node outer surface and is absent in internode, also indicates the presence of lipophilic extractives. Therefore, the results of surface chemical distribution are in agreement with the wet chemistry analysis in terms of the difference between the extractives of node and internode. This identification would be constructive for the selection and process of straw for intended end application i.e. bio-composites as the higher extractives content of the nodes could lead to the inhibition of optimal interfacial bonding between the straw particles.

Interestingly a comparison of the extractive yields shows that HW is a stronger medium of extracting extractives from wheat straw than (ethanol) ET, 10 and 13% higher yields were observed for internode and node respectively. Moreover, the yield of extractives with HW medium increases dramatically in H+S pre-treated straws by 32 and 27% for internode and node respectively, compared to ET extraction. Clearly the extractives yield of wheat straw is dependent on the solvent used for extraction and the response is different between node and internode.

6.3.2.2 Klason lignin

It can be seen that there is no significant difference of KL content between the extracted samples, although lignin contents of HW were slightly lower than that of ET extracted samples. The KL ranged from 22 to 28%. The lowest KL is from HW extracted internode of (untreated) UN and the highest from ET extracted node of H+S pre-treated straws. Overall, the node has higher KL than internode, in both untreated and H+S pre-treated straws by 15 and 5% respectively, with HW extraction and by 13 and 5% for ET extraction.

The higher KL in node could also be explained by the crystallinity index calculation through X-ray diffraction, in Chapter 4, node and internode crystallinity index were calculated to be 35% and 45% respectively [423] for same wheat straws, this indicated that node has much more amorphous regions than internode. The result thus could also reflect that there is more concentration of amorphous lignin and hemicellulose in the node.

6.3.2.3 Ash content

Ash content is investigated in two forms, structural ash and extractable ash. Structural ash is inorganic material that is bound in the physical structure of the biomass while extractable ash is inorganic material that can be removed by washing or extraction [437].

It is observed in Table 6.3 that the node of wheat straw contains more ash, in both treated and untreated non-extracted samples (structural ash). The ash content in node is higher than internode by 40 and 52% in UN and H+S straws respectively (Table 6.3). This phenomenon is observed throughout, for both ET and HW extracted ash contents.

On the other hand, the extracted ash content of HW and ET samples are reduced abruptly compared to the non-extracted (structural ash) samples in both node and internode of H+S and UN. Compared to ET extracted samples, HW extracted ash contents are lower by 40 and 32% in UN, and by 13 and 33% in H+S for internode and node respectively. Therefore, HW extracted samples have less ash remaining.

The higher ash content of the node would be problematic for the pulping. Hence removal of nodes prior to pulping will upgrade straw quality as a feedstock. Separation of nodes during collection and storage steps would require modifications of harvesting equipment, or digital image processing [438] (i.e. pixel colour variation along the length was used as the principle

of identifying the nodes and internodes) or alternatively focus should be on pulping systems [439].

6.3.3 Effects of treatment on cell wall compositions of node and internode

The effect of pre-treatment could be described as a disruption of the cell wall matrix, the connection between carbohydrates, hemicelluloses and lignin. Depolymerisation of soluble hemicellulose polymers could also be amongst the effects of the treatment. The weight lost due to H+S pre-treatment was calculated based on oven dry weight of straw before and after the treatment (calculated based on the Equation 3.2 in Chapter 3).

The weight loss percentage averaged to 5.1% (coefficient of variance, CV% = 4). This loss is identified as the main effect of pre-treatment on cell wall composition and surface chemistry which is investigated in the following sections.

6.3.3.1 Extractives

Hot water pre-treatment has shown to release some materials from the cell structure of wheat straw, including condensed tannins and phenolics [440]. Extractives are difficult to remove and can lead to pitch problems during pulping and papermaking. Sterols and some waxes cannot form soluble soap under alkaline conditions (such as kraft pulping) and hence have a tendency to deposit and cause pitch problems.

The accumulation of these extractives leads to technical (i.e. reduce the paper strength by interfering with hydrogen bonding during sheet formation) and economic issues (i.e. reduce paper machine efficiency and increase energy consumptions) for pulp and paper manufacturers [437]. Diminishing the extractives prior to pulping through a treatment is, therefore, advantageous. Table 6.3 shows the significantly lower content of extractives in H+S pre-treated straws in both extraction mediums. HW extractives in H+S straws are reduced by 55 and 52% and ET extractives by 66 and 60% in internode and node respectively.

The effect of the pre-treatment on partial removal of extractives is also confirmed in the surface chemical distribution results (Fig. 6.1). A sharp band at 1739 cm^{-1} in the outer surface of internode and node of UN straws is assigned to the carboxyl groups in the acids and esters of acetic, *p*-coumeric, ferulic and uronic acids, which have been identified as the main constituents of extractives [368]. The intensity of this band is reduced after the H+S treatment (Fig. 6.1). Similarly, the strong bands at 2850 and 2920 cm^{-1} decrease in intensity in the H+S pre-treated straws (Fig. 6.1). They correspond to the symmetric and asymmetric stretching of

the CH_2-group respectively, which comprise the majority of the aliphatic fractions of waxes [370,441]. This leads to a conclusion that the extractives in particular waxes have been partially removed.

As aforementioned in Chapter 5, wax is an important group of the lipophilic extractives in wheat straw. Removing the wax adds value to the lignocellulosic fraction as it facilitates the penetration of pulping chemicals into straw.

In summary, the H+S pre-treatment is a convenient method for effective dissolution of the lipophilic extractives from wheat straw. The removal of nonpolar hydrophobic extractives from straw could i) improve the wettability which is beneficiary for bio-composite applications and ii) facilitate the papermaking by reducing the pitch problems and improving paper strength.

6.3.3.2 Klason lignin

There is a slight increase in the KL content in H+S straws compared to UN. In HW extracted samples the H+S pre-treatment increase the KL yield by 18 and 7.5% for internode and node respectively. The same increase is observed in ET extracted H+S straws, by 12 and 5% in internode and node respectively. A relative increase in the amount of KL in H+S straws could be due to the partial removal of hemicellulose prior to KL measurement. High temperature treatments have shown to remove hemicellulose [414], and disturb the structure and distribution of lignin in biomass [442].

In relation to the surface chemical distribution, as discussed in Chapter 5, the lignin bands, particularly at 1510 cm^{-1} (aromatic ring stretch) are intensified in the H+S straws (Fig.6.1a). The lignin could also be released and re-deposited on the surface as a result of treatment.

Similar to Chapter 4, the investigation of lignin units was carried out using the FTIR results. Guaiacyl (G) and syringyl (S) are the main units of lignin. The bands at 1250 cm^{-1} and 1325 cm^{-1} are assigned to G and S ring stretching respectively [170]. The results of S/G ratio for UN and H+S straws did not show significant difference. However, it was found that the internode inner surface of UN had the highest S/G ratio of 1.2 (compared to 1.0 of internode inner surface of H+S). It is therefore concluded that the lignin network in the internode inner surface of UN would be more rigid than the rest of the profiles investigated. The S/G ratios of node were very similar for both surfaces in UN and H+S.

It is reported that the structure of lignin influences the enzymatic digestibility of biomass. For instance, lignin with high S/G ratio is negative for biomass enzymatic digestibility in *Miscanthus* [443,444], whereas a high *p*-hydroxyphenyl H/G could positively affect lignocellulose saccharification in rice and wheat [445]. There are parameters beyond lignin and S/G ratio that influence recalcitrance to sugar release and point to a serious necessity for a deeper understanding of cell-wall structure before straw biomass can be engineered for reduced recalcitrance and efficient bio-product (i.e.biofuels) production [446].

6.3.3.3 Ash content

More than 90% of the ash in the wheat straw is silica [396], the data in Table 6.3 indicates a significant reduction in the ash content of H+S treated wheat straw, which is interesting for the bio-composite application as silica may inhibit the interfacial bonding [420,421]. In non-extracted H+S straws, the ash content has been reduced by 50% in internode and 38% in node, from 3.2% (UN) to 1.6% (H+S) and from 5.3% (UN) to 3.3% (H+S) respectively. This means that ash was volatilised and partially removed by H+S treatment.

The respective residual weight calculated based on TGA in Chapter 5 on the same wheat straws for UN and H+S was 11 and 4% for the case of internode and 8 and 5% for the case of node. This data further confirms the removal of some sources of ash after H+S treatment, resulting in a relatively low residual content [418]. As concluded in Chapter 5, due to the partial removal of hemicellulose and extractives, the H+S pre-treated straw has higher thermal stability and lower ignition residue.

Table 6.3 Chemical analysis of untreated (UN) and pre-treated (H+S) wheat straw (% dry straw)

Sample ID		Hot-water extraction (HW)			Ethanol extraction (ET)			Non-extracted samples
		Extractives (%)	Ash content (%)	Klason lignin (%)	Extractives (%)	Ash content (%)	Klason lignin (%)	Ash content (%)
UN	Internode	4.2 (4)	0.9 (8)	22.0 (2)	3.8 (9)	1.5 (2)	23 .7 (5)	3.2 (2)
	Node	4.6 (5)	1.3 (7)	26.0 (3)	4.0 (7)	1.9 (3)	27.1 (9)	5.3 (4)
H+S	Internode	1.9 (3)	0.7 (2)	26.8 (5)	1.3 (5)	0.8 (4)	27.0 (8)	1.6 (4)
	Node	2.2 (9)	1.0 (6)	28.1 (1)	1.6 (3)	1.5 (5)	28.4 (8)	3.3 (2)

*values in () are coefficient of variance %

6.3.4 Surface elemental composition of node and internode

Elemental composition of wheat straw profiles is shown in Table 6.4 obtained using SEM-EDAX. The structure of the wheat straw consisted of carbohydrates and lignin with a considerable amount of carbon (C) and oxygen (O), and a trace amount of silicon (Si) weight percentage, similar to Chapter 4, Table 4.1. The outer surface of internode had higher Si weight percentage than the inner surface, in UN straws the former is 5.8% and the latter is 0.8%. By contrast, the Si weight percentage in H+S internode compared to UN straws is reduced significantly ($P < 0.05$) by 83 and 100% in outer and inner surface respectively. A similar reduction of Si content (weight %) is observed in nodes of H+S straws compared to the UN, from 0.7 to 0% in the inner surface and 2.8 to 0.8% in the outer surface. This effect of treatment on Si weight percentage is supported by the significant reduction of the ash content in H+S compared to UN straws as discussed in the previous section.

Comparing the nodes and internodes, outer to inner surface, it could be concluded that more silicon (in the form of silica) is located mainly on the outer surface (epidermis) of wheat straw, the FTIR results (Fig.6.1a and b) also supports this finding, with the bands of 985 cm^{-1}

(Si–O stretching vibration [361]) and 790 cm^{-1} (Si–C stretching vibration [361]) being only present on the outer surface of internode and node respectively.

Table 6.4 Node and internode profile elemental composition based on EDX-SEM analysis

Profile Surface	Sample	ID	Percentage %			O/C
			C	O	Si	
Inner	Internode	UN	54.1 (2)	45 (1)	0.8 (4)	0.83
		H+S	53.5 (3)	46.4 (7)	0 (1)	0.87
	Node	UN	54.1 (9)	45.6 (7)	0.7 (6)	0.84
		H+S	53.5 (5)	46.2 (4)	0 (1)	0.86
Outer	Internode	UN	51.3 (2)	43.4 (5)	5.8 (2)	0.84
		H+S	54.4 (7)	44.5 (3)	1.0 (3)	0.82
	Node	UN	53.7 (3)	43.5 (8)	2.8 (2)	0.81
		H+S	54.5 (2)	44.6 (1)	0.8 (4)	0.82

*values in () are Coefficient of Variance %

6.3.5 Morphological characteristics of node and internode

The morphology of node and internode has been investigated in details in Chapter 4. Some of the outcomes are illustrated here in Fig. 6.2 and 6.3. When considering the node for bio-refinery, two important issues arise based on its morphology.

The node is a very dense area with tightly packed bubbled shaped cells in the centre and elliptical shaped rings ordered in a circle. This morphological discrepancy could signify the more recalcitrance structure in comparison to internode. This further translates to different physicochemical response to pre-treatments and subsequent enzymatic digestibility [447]. Heterogeneous morphology is one of the substrate properties which influence the enzyme

action and/or activity. Additionally, it has been previously shown that the morphology of node is responsible for a significantly lower tensile strength than internode (Chapter 5). This morphological characteristic is a defect for when it comes to bio-composites production from wheat straw.

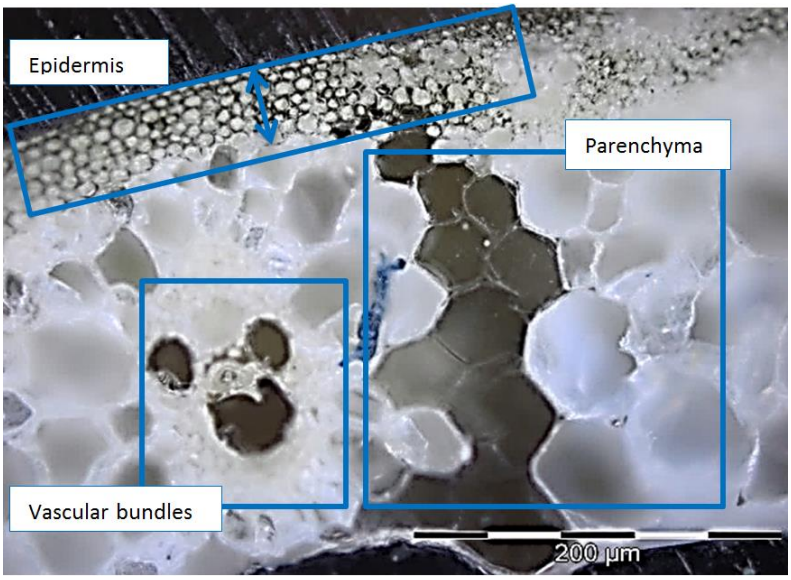

Figure 6.2 The cross section of internode showing the epidermis size

The higher content of extractives and ash in nodes than internode, as observed in Table 6.3, could be linked to their morphologies. The thicker epidermis in nodes, which results in the higher content of epidermal cells, is mainly composed by the suberized cells and silica cells [448], hence, the extractives and ash contents in nodes are comparatively higher than internodes. The epidermis tissue thickness is around 170-200 µm in node, see Fig 6.3, and around 45-47 µm, shown in Fig. 6.2 for internode.

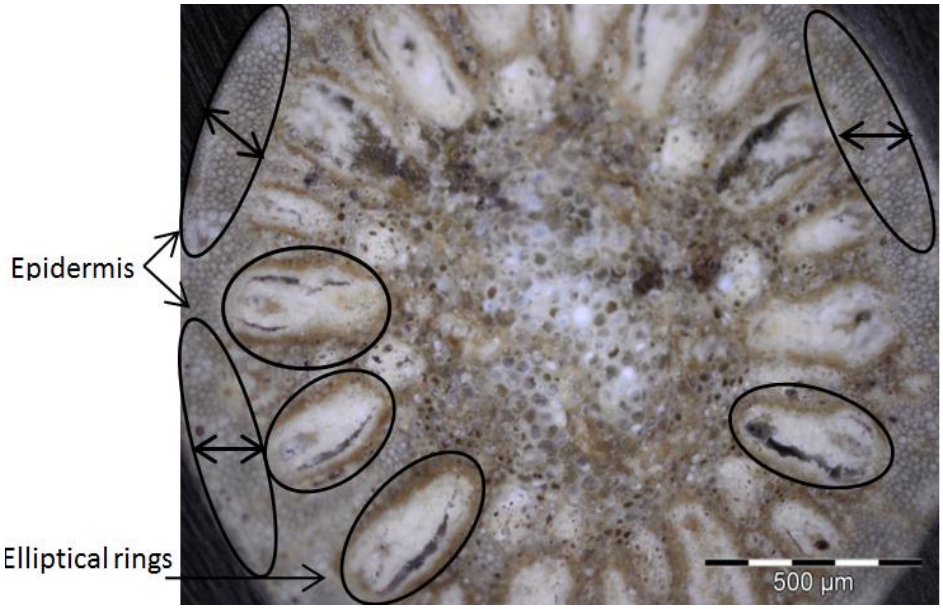

Figure 6.3 Node cross-section view

The most apparent effect of the H+S pre-treatment, apart from a colour change from bright yellow into lighter shade yellow, is the changes to the microstructure of wheat straw, as investigated in Fig. 6.4. The node morphology did not change substantially after the treatment.

However, there is a clear expansion of parenchyma in pre-treated internode straw that appears larger and deeper compared to the UN straw, shown in Fig. 6.4b, which on the other hand illustrates a relatively compact zone, arranged tightly with smaller circumferences of ellipsoidal honeycomb cells (Fig. 6.4a). The expansion of cells could be beneficial when i) it comes to bio-composites production where the resin overflows into the expanded cells, creating efficient entanglement upon solidification between the straw particles; and ii) bio-refinery process, as the expanded structure would facilitate the access of agents and hence fibrillation of straw for further ethanol process or other utilisation of the constituents of straw cells.

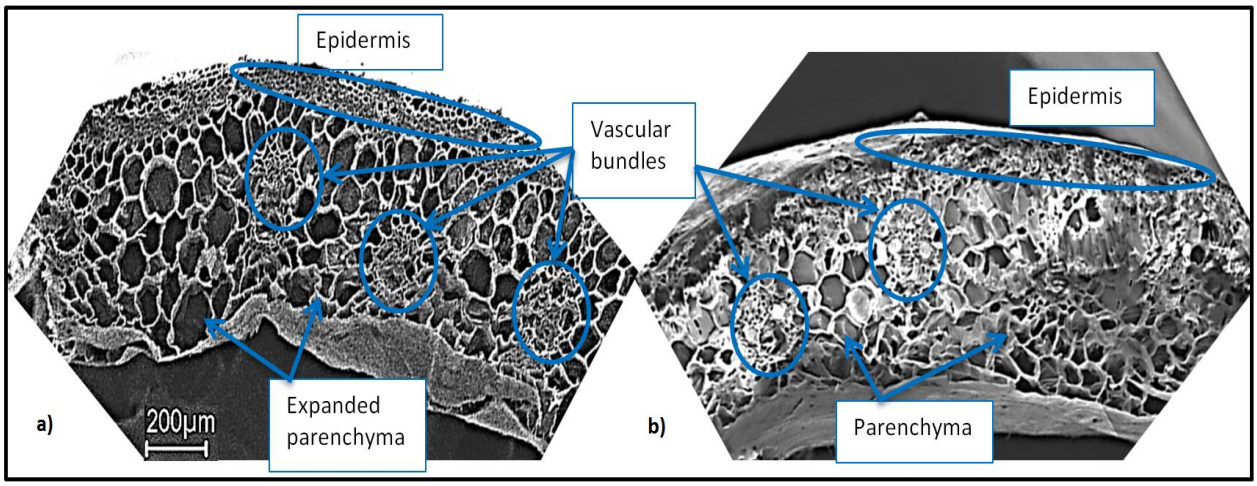

Figure 6.4 SEM images, cross section of a) H+S treated internode, showing the expanded structure b) UN internode.

6.4 Interim conclusions

Differential characteristics of wheat straw node and internode have been examined qualitatively or quantitatively, where distinct variations were found amongst them. The identification of specific features of each part of wheat straw signified essential prior to the pre-treatment selection and subsequent bio-refinery. Separation of node and internode, possessing different attributes, and utilising them in segregated processing could lead to enhanced processing efficiency, higher value-added products and better handling.

Node yielded slightly higher klason lignin and higher content of extractives and ash than internode. which could be related to their morphology, specifically the higher ash and extractives content in the node are explained by thicker epidermis tissue, as observed in optical microscopy images. These properties make nodes defects in bio-composite and bio-energy production, while internodes could be more favourable for aerobic digestion for biogas production.

Solvent extractions had an influence on subsequent extractives yields and ash content of straw biomass, but in the case of klason lignin, it did not make a difference as the yields were similar between hot-water and ethanol extraction.

The effects of the pre-treatment were identified as the partial removal of wax and extractives from the outer surface along with the depolymerisation of hemicellulose. This was further confirmed from the extractives yield in H+S straws which were significantly lower ($P < 0.05$)

than UN straws. The significant dissolution of Si (weight %) on the outer surface of both node and internode, was found and could be beneficial for possible bio-composite and bio-energy production. On the other hand the hydrophilic tendency of inner surface was reflected by the broad and more intense band in the 3200-3600 cm^{-1} region, due to –OH stretching vibration of hydroxyl groups. This could translate into better interface when water-based resins are used for wheat straw bio-composites.

Chapter 7 Interfacial properties and bonding mechanisms of wheat straw bio-composites

Highlights:

- Interface properties of internode are superior to the node;
- The bonding mechanisms could also be investigated through failure morphology;
- Four models of failure mechanisms are identified;
- Different bonding scenarios (i.e. inner to inner, and/or inner to outer surface contacts) results in different bonding performance/quality.

This chapter seeks to fully understand the bonding and failure mechanisms of wheat straw node and internode with inner and outer surface profiles. The surface modifications through the pre-treatment studied in previous chapters 5 and 6, have contributions in investigating the bonding quality and failure mechanisms of straw composites in this chapter. It is revealed that the H+S treatment could effectively ($P < 0.05$) i) modify the surface of the straw with the partial removal of waxes and silica, which made it more hydrophilic and more compatible with water based adhesives and ii) cause the microcellular structure of straw to expand and hence inspire the mechanical entanglement on a micro level.

Keywords: Straw composite interface; Bonding mechanisms; Failure mechanisms; Failure morphology.

7.1 Introduction

There is a rising interest in utilising straw biomass in novel hybrid bio-composite with competitive mechanical and physical properties in the face of climate change and demands for sustainable economic growth. Wheat straw could represent a great alternative to wood in manufacturing bio-composites.

The chemical composition of wheat straw is similar to wood but its structure is looser and its strength is lower. It contains less lignocellulose cells and more ash and extractives with lower molecular weights than wood. The hydrophobic extractives such as waxes on wheat straw surfaces inhibit interfacial bonding as aforementioned in Chapter 5.

One of the main drawbacks with straw stems for the production of bio-composite as building components is the bonding quality which is a major unsolved technical problem and this has impeded straw stems composite commercialisation. This issue needs to be tackled by better understanding of interface and bonding mechanism; which could be achieved by detailing and differentiating straw stem anatomical sections: node and internode, with their relative inner and outer surfaces. The interface properties can be studied by using 'model composites' [449,450], and investigating adhesion theories requires an understanding of straw characteristics, surface science, thermosetting polymer characteristics and the interactions between polymers and surfaces. The adhesion mechanisms can be categorised into seven theories: mechanical interlocking; electronic or electrostatic theory; adsorption (thermodynamic) or wetting theory; diffusion theory; chemical (covalent) bonding theory; acid-base theory; and theory of weak boundary layers [451,452]. These mechanisms may occur at the same time in a given adhesive and substrate, depending on their characteristics.

It is important to distinguish the surface properties between the anatomical sections within the straw stem when it comes to interfacial bonding in bio-composites. Previous Chapter 4-6 indicated that different profiles of node and internode of straw have different surface chemistry and morphological properties. The focus in this chapter is on the challenge of different interface profiles when exposed to resin, through the evaluation of interfacial bonding.

This will lead to a comprehensive understanding of interface and bonding mechanism. The efficient and environmentally friendly combinational pre-treatment designed in Chapter 5, H+S is used. Different responses of various surface profiles of straw to the treatment are

analysed, this is different from many of the previous studies that monitor the effect of treatments on straw stem as particles or fibres without paying attention to the anatomical sections and their surfaces.

7.2 Experimental plan

The materials (resins) with their sources and the testing procedures for this chapter are fully explained in Chapter 3. The resins used were: Unsaturated polyester (UPE), vinylester (VE), epoxy (EP), phenol formaldehyde (PF), polyurethane (PU) and lignin-phenol-formaldehyde resin with 50% and 25% (weight %) phenol replacement by lignin (LPF50 and LPF25).

7.2.1 Single lap joint tensile test

Single lap joint tensile test is a convenient method adapted for the evaluation of adherence between straw surfaces and the resin. The straw sections of internode and node were very carefully cut in half longitudinally so that the outer and inner surface could be exposed for testing. The preparation was according to the BS ISO 6237:2003. The same volume of adhesive was applied for all the samples. Tensile shear strength of lap joints was calculated using formula from EN 205:2003, Equation 3.3 in Chapter 3.

7.2.3 Surface chemistry of different profiles

The interface and bonding mechanisms cannot only be determined from the mechanical testing and hence supplementary analyses are necessary. Additional information about the chemical distribution of the surface and its wetting behaviour are complementary techniques which are used to investigate the comprehensive bonding mechanism. Therefore ATR-FTIR and contact angle techniques were used (details explained in Chapter 3).

For surface wettability, the wetting model equation developed previously was used [453]. The penetration and spreading constant (K) values were obtained using the Equation 7.1 where the contact angle θ changes as a function of time (t). To obtain a K value, a nonlinear curve fitting method is used to fit the empirical data in Equation 7.1 using ORIGIN software.

$$\theta = \frac{\theta_i\,\theta_e}{\theta_i + (\theta_e - \theta_i)\exp\left[K\left(\frac{\theta_e}{\theta_e - \theta_i}\right)t\right]} \tag{7.1}$$

The physical meaning of the K value illustrates how fast the liquid penetrates and spreads into the porous surface structure of straw.

7.2.4 Surface modification

It is necessary to enhance the surface morphology at the interfaces to maximise the load bearing capacity of bonded joints, and to improve their deformational characteristics. The use properties of the adhesive joints depend on the quality of the interface that is formed between the substrates. Surface preparation is crucial for optimum adhesion and pre-treatment serves as an important preparation step for the modification of surfaces. As mentioned in the introduction, H+S pre-treatment was the strategy designed to modify the surface of straws. The details of this pre-treatment are previously mentioned in Chapter 5.

7.3 Results and discussion

7.3.1 Surface Functionalities of various straw profiles

The surface chemical distributions of wheat straw node and internode, inner and outer surface are shown in Fig.7.1. As the wettability and then the penetration of liquid into the solid surface is related to the surface porosity and chemistry [370], the partial removal of wax and pectin from the surface could result in the improvement of the wettability, see Fig. 7.4 and Table 7.1. Strong bands at 2850 and 2920 cm^{-1} comprising the majority of the aliphatic fractions of waxes [370] are much intense for outer surface than inner surfaces, these two bands decrease in intensity in the H+S pre-treated samples (Fig. 7.1a-b). This is in agreement with previous chapters, which led to a conclusion that the extractives in particular waxes were partially removed.

The -OH stretching vibration region at 3200-3600 cm^{-1} is indicative of the amount of hydroxyl groups and as such potential bonding sites for water [434]. The spectra shows that the intensity of the -OH stretching vibration for the inner surface is much significant than that of outer surface, both in node and internode of UN and H+S straws, showing the hydrophilic tendency. On the other hand the hydrophobic components are only observed in the outer surfaces. The band of 985 cm^{-1}, that is most likely attributed to the Si–O stretching vibration [361], was observed in the spectrum of outer surface, but absent in the inner surface of internode (Fig. 7.1a). It is interesting that for the outer surface node, this is represented as the

band of 790 cm^{-1} being attributed to the Si–C stretching vibration (Fig.7.1b) [361] and again it is absent in the inner surface of node.

As established in previous chapter the components containing silicon are primarily on the outer surface and the finding is most important for the pre-treatment of the biomass either for composite development due to the inhibiting of interfacial bonding or bio-energy production as silica could affect the efficiency of processes.

A sharp band at 1739 cm^{-1} in the outer surfaces of UN internode and node is assigned to the main constituents of extractives and hemicellulose (Fig.7.1a-b) [368] (i.e. carboxyl groups in the acids and esters of acetic, *p*-coumeric, ferulic and uronic acids). These are the most influential parameters for compatibility and access of moisture. The intensity of this band is reduced after the H+S pre-treatment, indicating the effectiveness of the treatment in partial removal of extractives and hemicelluloses.

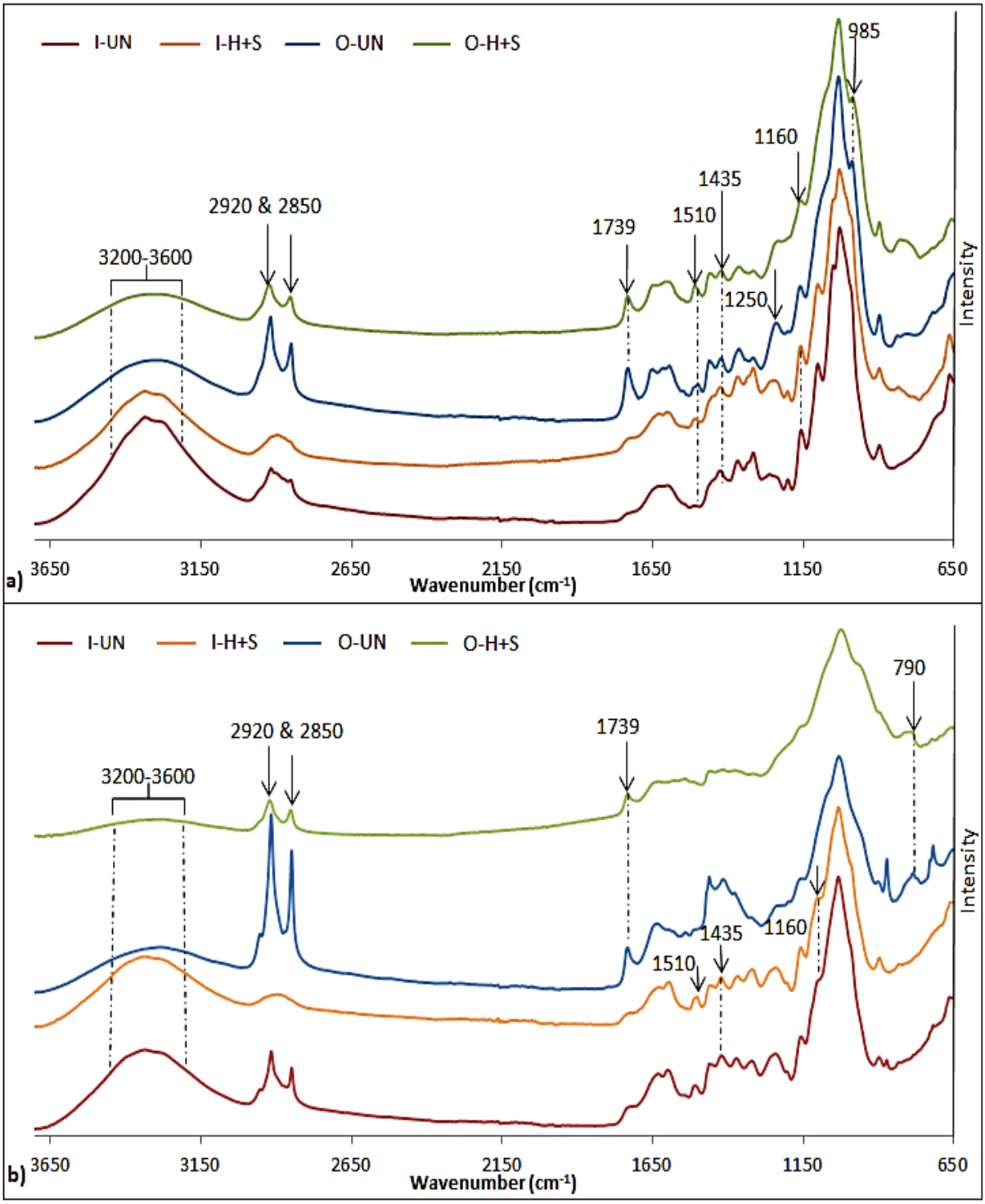

Figure 7.1 ATR-FTIR spectra of a) internode and b) node, (I) inner and outer (O) surface untreated (UN) and treated (H+S)

7.3.2 Interfacial bonding mechanisms

Interfaces play a crucial role in the physical and mechanical properties of composites [454]. The mechanisms for the improvement of interface could be reflected by the schematic diagram in Fig. 7.2.

Wheat straw has well ordered microfibrils which may be covered by impurities and aliphatic fraction of waxes (Fig. 7.1 and Fig. 7.2a). Waxes on the straw surface have a lubricating effect that reduces the friction and mechanical interlocking. High concentrations of hydrophobic extractives on wheat straw surface with weak boundary layers limit the adhesion mechanism by van der Waals forces [455].

Due to the microcellular characteristics of straw, as shown in Fig. 7.3, the mechanical interlocking theory may be the dominating mechanism in the bonding quality determination. Mechanical interlocking takes place through an adhesive that penetrates the porous surface of straw while it is in liquid form, then anchors itself through solidification. Mechanical interlocking happens on a millimetre and micron length scale, and diffusion entanglement within the cell wall pores could occur on a nanoscale.

The better bonding system of straw composite may be achieved by the enhanced chemical bonding, such as covalent and hydrogen bonding between the hydroxyl groups of straw surface, in conjunction with the mechanical interlocking of the adhesives which are able to penetrate deeper inside the straw micro porous structure.

Removing natural fats and waxes from the surface, such as in carrying out the hot water treatment to diminish the surface waxes (Fig. 7.1) and the steam treatment to swollen the cell walls, may create micro and/or nano sites for efficient penetration of the resin into the cell walls (Fig. 7.2b) and increase the exposure of chemically reactive functional groups like –OH.

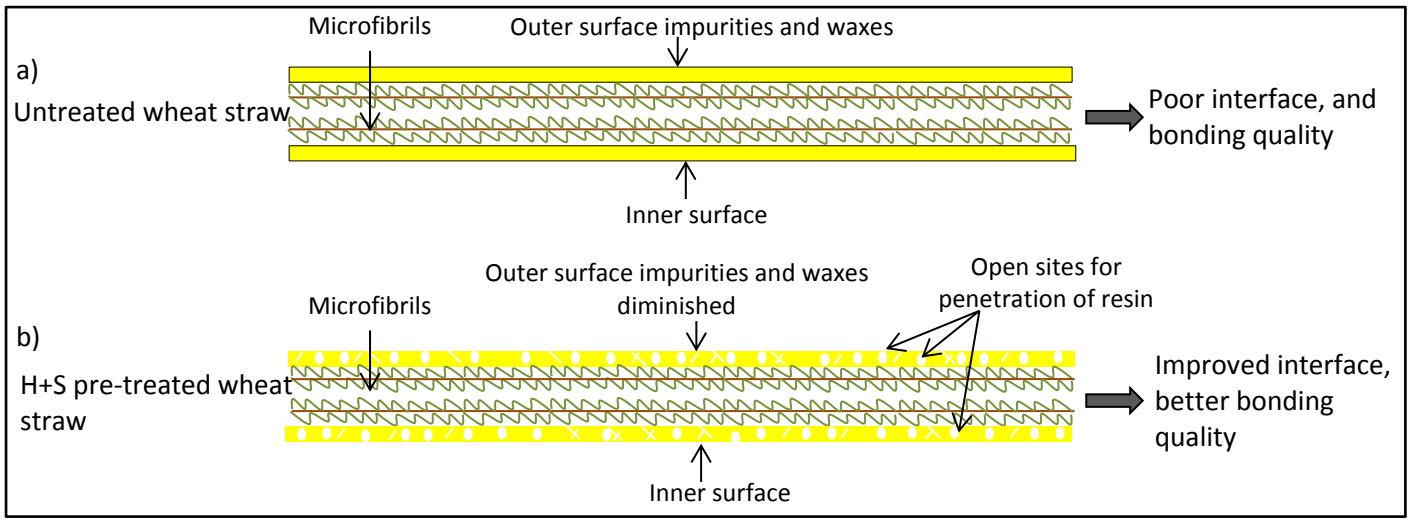

Figure 7.2 Schematic illustrations of wheat straw surface modification and mechanism (a) for better interfaces after the modifications (b)

The surface characteristics, wettability of the liquid over a solid surface e.g. roughness and polarity are also related to energy states on the solid surface structure, adsorption and wetting kinetics and hence the physical and chemical affinity between the straw surface and the adhesives. For instance the higher spreading/penetration (*K*) value in H+S samples means improved wettability (Fig. 7.4). As shown in Table 7.1, the treated wheat straw internode outer surface has much greater *K* value than UN sample which is clear indication of surface modification to a more hydrophilic surface. The treatment related microcellular structure could further facilitate resin overflow and penetration.

These may include expanded parenchyma (larger and deeper) in treated straw, shown in Fig. 7.3a compared to the UN straw, Fig. 7.3b, which on the other hand illustrates a relatively compact zone, arranged tightly with smaller circumferences of ellipsoidal honeycomb cells. The diminished level of aliphatic fraction of waxes (Fig. 7.1) and silica (Table 6.2 Chapter 6) on the epidermis of H+S straw may also increase the penetration of resin into the fine microstructure and hence also enhance the surface area of contact between the resin and straw.

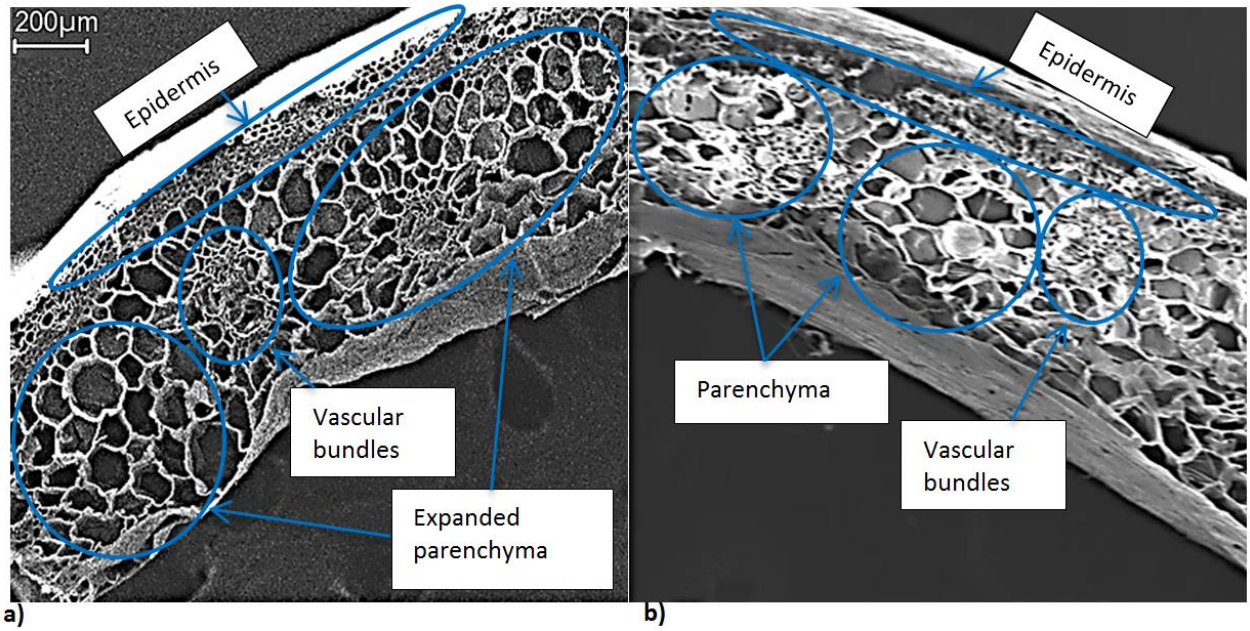

Figure 7.3 SEM images, cross section of a) H+S treated internode, showing the expanded microstructure and b) UN internode

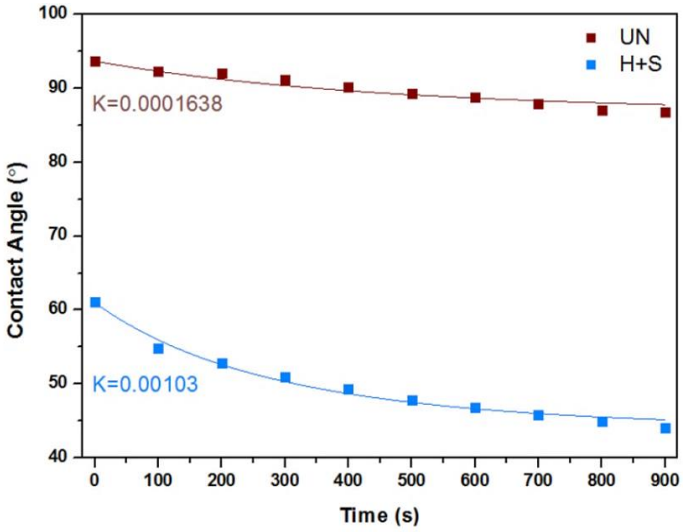

Figure 7.4 Contact angle of distilled water and outer surface internode change as a function of time

Table 7.1 Distilled water and wheat straw contact angle properties

Sample	$\theta_i(^\circ)$	$\theta_e(^\circ)$	Percent decrease (%)	K value ($\times 10^{-3}$)
UN	93.7 (4)	86.8 (5)	7.4	0.2
H+S	61.1 (5)	44.0 (6)	28.0	1.0

* The values in parentheses are coefficient of variance percentage (CV %)

7.3.3 Bonding scenario and interface qualification

The strongest and weakest bonding scenario for internode and node are identified in Fig. 7.5. The comparison is also on the performance of treated and untreated samples. Adhesive wetting behaviour or the level of penetration into the open pores of the surface differs in different scenarios of surfaces investigated.

It is clear as expected that inner to inner surface performed the best in terms of quality of bond. For instance in internode of H+S samples, inner to inner surface bond is 63 and 69% higher than the inner to outer and outer to outer respectively. The chemical functional distribution results have confirmed the lack of hydrophobic elements (extractives and waxes) on inner surface (Fig. 7.1a-b) and therefore when two inner surfaces are bonded together, they perform much better than inner to outer and outer to outer surfaces (Fig. 7.5).

On the other hand the inner surface is rougher in nature and outer surface has a much smoother surface, which also contributes to the better bonding performance of inner surface. Interestingly the outer surface seems to be the most dominant in determining the quality of bond as the inner to outer surface bond is not significantly higher compared to outer to outer (Fig. 7.5).

The outer to outer bonding quality in internode H+S samples is improved by 117% ($P < 0.05$) compared to internode UN. The same improvement is observed in node by 114% ($P < 0.05$). Inner to outer bonding quality in internode and node also improved by 93 and 100% respectively, while inner to inner bonding quality of internode and node improved by 91 and 55% respectively in H+S samples. It is evident that the highest percentage increase of bonding quality is for outer to outer bonding scenario.

The outer surface was identified to have the highest intensity of waxes and silica which prevents the effective wetting of surface, penetration and bonding of adhesives to the straw hydroxyl groups (Fig. 7.1 a-b). Hence this significant improvement in bonding quality induced by H+S treatment is promising.

Fig. 7.6 (a) and (b) illustrate the single lap joint tensile strength of the internode and node (all three surface scenarios) for UN and H+S samples with different thermosetting resins. The improvement in H+S sample bonding performance is clearly illustrated by comparing the

internodes (Fig.7.6a) and nodes (Fig.7.6b). The nodes show weaker bonding performance compared to internodes, however, nodes in H+S samples have higher values than the internode of UN samples. The reason for inferior bonding quality performance of node could be directly related to its morphology and surface which is not flat. Chapter 4 dealt with the morphology of node in wheat straw in detail.

Significant improvement is observed in water based adhesives (PF, PU, LPF25 and LPF50) after the H+S treatment, the surface reduced hydrophobicity induced by treatment is one potential reason for this improvement. In Fig.7.6 (a) and (b) it is observed that the UN values for single lap joint tensile strength of EP and UPE are lower than PF and LPF25, this could be due to the similarities between the chemical structural characteristics of phenolic resins and straw which lead to a higher affinity between them.

Important observation in Fig.7.6 (a) and (b) is the good bonding quality achieved by LPF25 which is similar to PF and higher than PU, this is encouraging as 25% (by weight) of phenol is replaced by a natural resource, lignin.

Molecular weight distribution, viscosity, solids content, and surface tension of the liquid phase of the adhesive influence the penetration into surface of straw. Additionally, additives could change these characteristics. These parameters all play important role in bonding performance, in this study, the focus is on surface modification where H+S treatment has shown to encourage all these parameters positively to increase the bonding performance compared to UN samples.

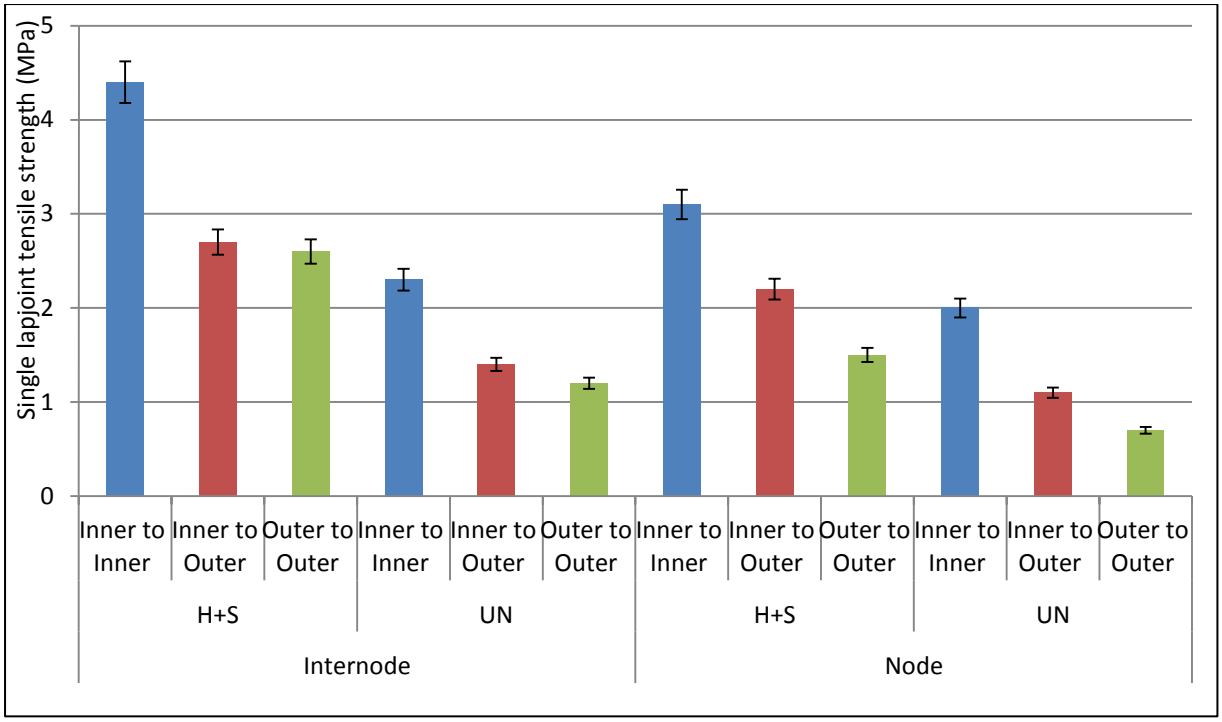

Figure 7.5 Comparison of different bonding scenarios in node and internode of UN and H+S samples (average for all 7 thermoset resins)

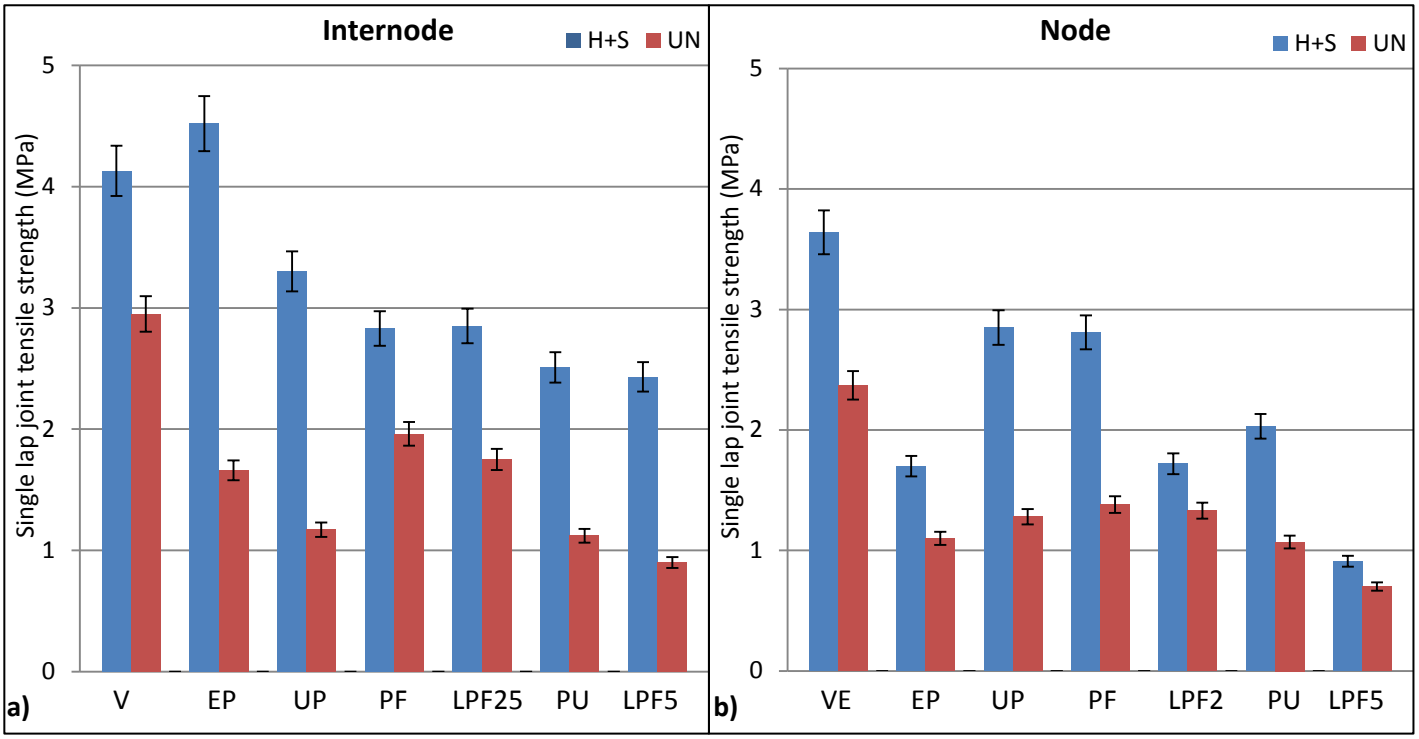

Figure 7.6 Comparison of bonding performance between the a) internode and b) node, UN and H+S samples with thermosetting resins

7.3.4 Failure mechanisms

The mechanisms of failure and its modelling are studied in depth for single lap bonded joints in composites [456-458], covering important aspects of inherent mechanisms at the very nanoscale and the evolution of the fatigue damage, where it was observed that a significant fraction of the fatigue life of the joint is spent in the nucleation of one or more cracks propagating up to the failure of the joint.

Investigation of the failure behaviour of the bonded joints indicated that the failure of straw composite interface initiates from a multiscale and hierarchical damage process, often represented by the nucleation of off-axis micro cracks in the resin, mainly resulting from the accumulation of damage at the micro scale in the form of i) resin micro cracking, ii) interface de-bonding/delamination (see Fig. 7.7 a) and iii) possible failure of straw fibres.

The initiation of off-axis micro cracks can influence the global behaviour of the composite, decreasing the stiffness and endorsing the formation of other failure behaviours. In Fig. 7.7 a, the position of failure initiation is identified in the cross-section view of fractured interface, where the failure path may have propagated by micro cracks up to a critical length leading to delamination at interface.

These failure mechanisms and domination/contributing levels could lead to several failure models of straw composite, depicted in Fig. 7.8. These failure models in association with experimental failure morphologies are as follows: a) the adhesive failure, which occurs between the adhesive and the substrate, representing weak bonding quality. This was mostly observed in outer to outer and inner to outer bonding scenario, b) the cohesive failure, which is the failure of the adhesive itself, i.e. the domination of resin micro crack (Fig. 7.7 a), this was common in outer to outer and scarce in inner to outer bonding scenario, c) mixed failure, including both adhesive and cohesive failure, i.e. combined effects of micro crack and straw defect failure, observable in inner to outer and outer to outer scenarios, and d) the substrate failure, presenting a strong interfacial bond, which is stronger than the substrate itself. This was achieved in inner to inner bonding scenario.

Intimate contact between the substrate and the adhesive reflects the strength of the straw and interface quality, e.g. the penetration of resin into the cell wall pores (interlocking). The failure behaviour could therefore be directly related to bonding mechanisms, where the mechanical interlocking between the straw surface and resin causes a perturbation of the

micro crack path, resulting in non-planar crack propagation and/or crack deflection. Consequently crack propagation involves higher energy absorption, which in turn, increases the overall toughness reflected by higher lap join tensile strength. The H+S treated straw (Fig. 7.7b) has strong interface properties and there is no delamination. These observations are consistent with the mechanical results, which altogether indicate improved interface due to H+S surface modification.

This can be further reflected in the optical microscopy (OM) and SEM observations (Fig. 7.9). It is evident that a quality interface bonding, e.g. aforementioned model "d" may be resulted from the filling of resin into cell lumens (Fig. 7.9b-g), where the flow of resin in liquid state has proceeded into the interconnected network of lumens and open pores. This is observable from both cross-sections (Fig. 7.9 b-e) and longitudinal section surfaces (Fig. 7.9 f, g).

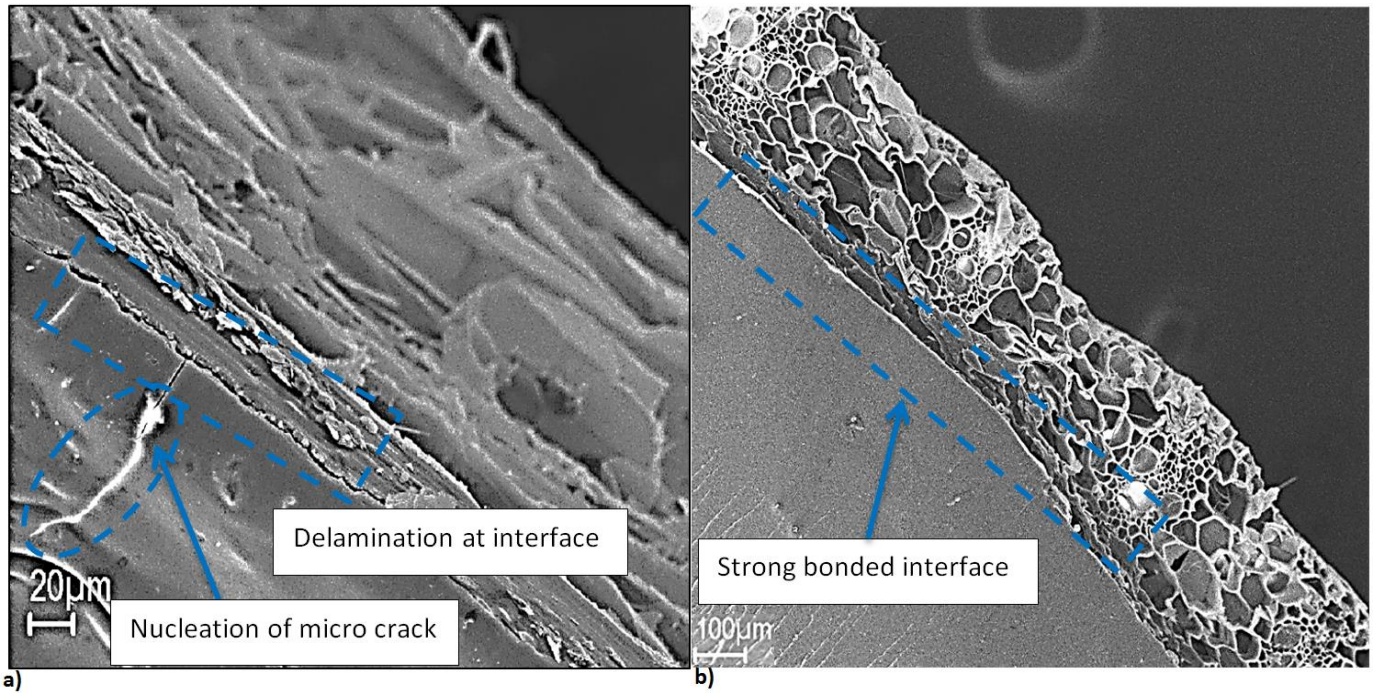

Figure 7.7 Cross section view interface of (a) UN samples showing the nucleation of micro crack leading to delamination, and b) showing strong bonded interface in H+S sample

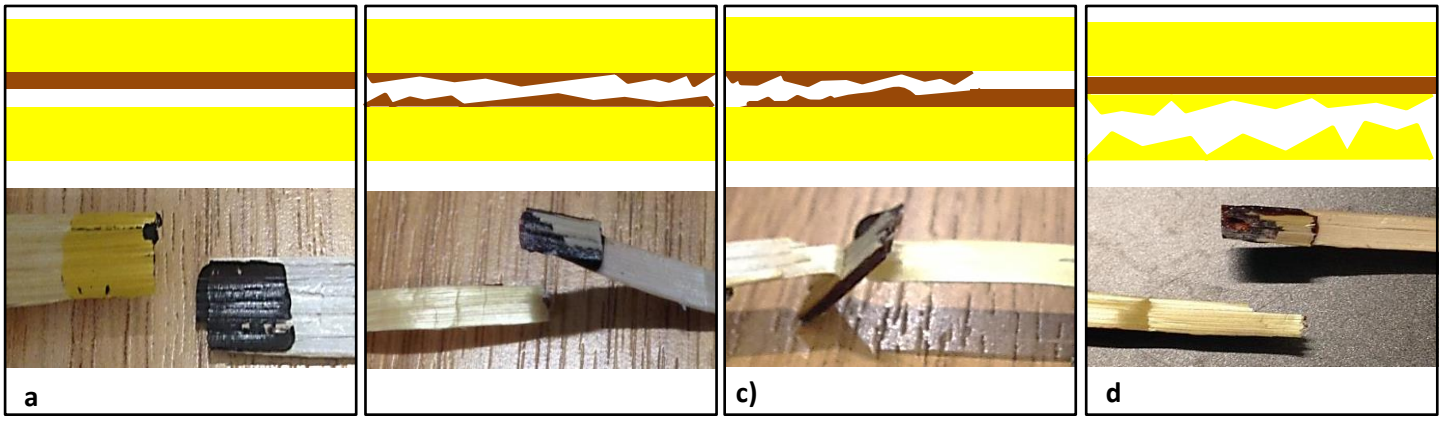

Figure 7.8 Failure modes observed during experiments - a) adhesive failure-poor bonding, b) cohesive failure, c) mixed adhesive and cohesive failure, d) substrate failure-strong bonding.

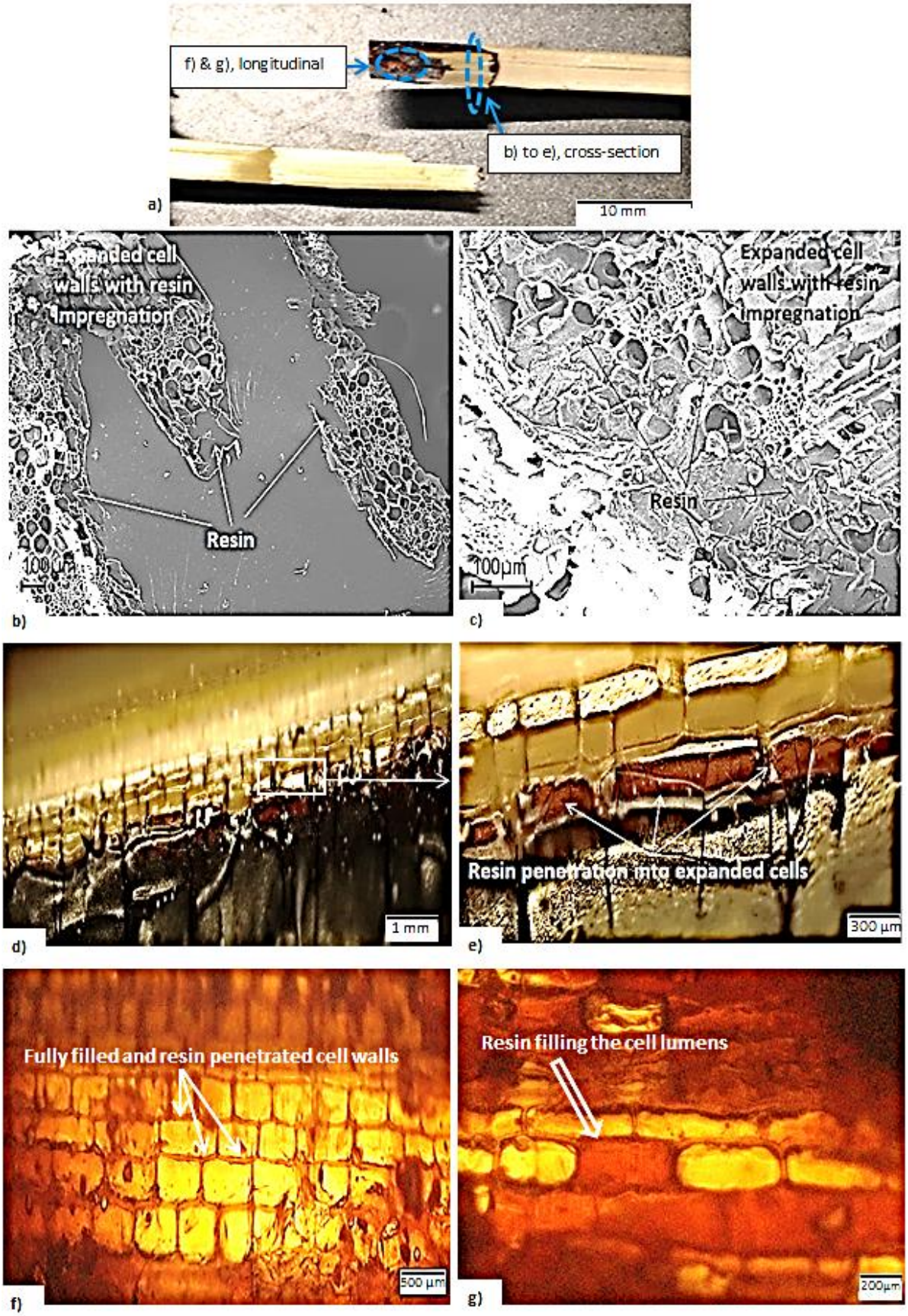

Figure 7.9 Failure morphology in (a) good bonding scenario of H+S treated samples; SEM images of (b) and (c) with OM (d) and (e) for cross section view, and longitudinal surface view in (f) and (g).

7.4 Interim conclusions

The bonding and interfaces of different profiles of node and internode, inner and outer surfaces of wheat straw were developed and analysed. The mechanical properties of composites depend not only on the fundamental characteristics of the substrate and of the resin, but also on the physicochemical properties of the interface between these components. Therefore, different surface chemical distributions and various bonding scenarios between various profiles, gave rise to different bonding performance and interface systems of straw-thermosetting resin composites. Especially the presence of aliphatic fraction of waxes and silica concentrated on the outer surface of node and internode inhibited the bonding and the establishment of good quality interface.

Efficient and environmentally friendly combinational pre-treatment (H+S) resulted in a significant increase in the bonding quality ($P < 0.05$) by modifying the surface characteristics and inspiring the mechanical interlocking through the change of surface chemistry or microstructure of straw.

The node and its bonding scenarios were identified weak points for possible bio-composite manufacture, due to its morphology and the chemical distribution of their surface. Extensive investigation on the failure mechanisms at microscopic scale enabled the physical modelling of failure behaviour where four categories of failure were matched with experimental results, from strong to weak.

Chapter 8 Concluding remarks and future prospectives

Highlights:

- Straw biomass conversion into value added products;
- Critical reviews;
- Towards valorisation of wheat straw;
- Characteristics of node and internode;
- Physicochemical properties in correlation to the cell wall components;
- Wheat straw efficient utilisation through selective fractionation based on the intended bio-refinery pathways;
- Efficient and environmentally friendly pre-treatment of wheat straw;
- Bonding and failure mechanisms of wheat straw composites with various thermosetting resins.

This chapter remarks in a concise summary, the conclusive statements from the outcomes of this project. The objective of this chapter is to give an ovrall appraisal to determine the success of the research work of the project. Based on the outcomes of the project, the future prospectives and directions have critically been establish for further research.

Key words: Bio-refinery; Climate change; Bio-based materials; Bio-conversion; Straw biomass.

8.1 Introduction

High global demands for energy, unstable/uncertain petroleum sources and concerns over climate change have led to the resurgence in the development of alternative energy and material sources. Straw biomass conversion processes are attractive because they are in practice today and extension to future scenarios is easy for the public to envision. Although fundamental research has historically focused on straw biomass conversion to fuels, chemicals, and materials, very limited amount of these efforts have been successfully translated into commercial practice.

Only biodegradable and bio-based materials can really provide a sustainable route to the bio-refinery and bio-conversion of agricultural wastes. In a fully green circular economy prospective, the renewability of sources is combined with biodegradability of end products.

A robust policy framework is needed to encourage the companies to invest in bio-based materials. The issues in the chain must be identified through systematic surveys of farmers, industrial actors, and stakeholders from the public sector. It would then be important to establish awareness by raising campaigns/organisations in order to promote bio-based products from renewable resources. This would consequently encourage contracting authorities to adopt products from renewable resources through procurement details. Governments can further stimulate bio-based materials by integrating them in their procurement policy.

An open central knowledge database with available biomass characterisation and/or bio-based materials specifications should be established. This could be a huge task which researchers are trying to contribute towards (i.e. this project) but it requires a greater international effort and collaborations. A mutual interest agreement amongst researchers and companies involved in bio-based materials should be introduced. Competition is good for innovation, but in the start-up phase, small companies should collaborate for R&D rather than compete with each other.

8.2 Concluding remarks

This research project has contributed to the science of straw biomass by improving the understanding of wheat straw through paying attention to the details of material science. The following seven key points highlight the conclusive statements gathered during this research.

The state of art study in the literature gave rise to the following three points:

1) The use of biotechnology for the bioconversion of straw biomass into bio-products has received some success. Research efforts are focused on bioengineering of straw biomass to modify and incorporate components that reduce the recalcitrance of the cell walls for bioconversion and facilitate recovery/processing. For upscaling of biotechnology, it is necessary to identify the optimal microorganisms based on their functionality and mechanisms, and carefully monitoring the parameters involved during fermentation, leading to optimised conditions and increasing the efficiency of the process.

2) The analytical techniques up to date for structural analysis of straw and its main components were also discussed. The resultant understandings of the structure of straw were then summarised based on quantitative and qualitative data. It was found that lignin's heterogeneous chemical and physical properties could be detailed using NMR and 2D HSQC techniques, which have greatly improved the knowledge on lignin and its products. However, the results from these analytical techniques could be further validated into improved force fields and high performance computational modelling to provide a predictive tool of lignin's properties.

3) Lignin in straw biomass is a potential source of valuable bio-products, specifically thermosetting resins. The lack of commercially viable production technology, variation in biomass types, and complexity of lignin's structure have hindered its utilisation. Lignin of superior quality and purity can lead to its valorisation which requires improving lignin processing in the bio-refinery. Refinement of biomass pre-treatment technologies could further facilitate lignin recovery. Functionality improvements (i.e. through genetic engineering and bioengineering) will then enable novel uses for this biopolymer, including low-cost carbon fibre, engineered plastics, thermoplastic elastomers, polymeric foams, fuels, and commodity chemicals.

The original studies designed in this project led to the following four conclusions:

4) A systematic approach was developed to examine the details of morphology and chemical distribution of node and internode inner and outer surface. The sophisticated morphology of the node was profiled as a 3D image investigated from root to grain head. The morphology of internode and its connection point to the node was also studied. Chemical functional groups were semi-quantitatively investigated where the results revealed the different characteristics of the inner and outer surface. It was evident from the surface chemical elemental composition and surface functionalities that outer surface has more i) hydrophobic aliphatic components, i.e. wax and extractives, and ii) silica, compared to the inner surface.

5) The differential behaviour of node and internode were further investigated under various pre-treatments. The pre-treatments included: 1) individual mild physical methods (i.e. steam and hot-water ptr-treatments on their own), 2) mild chemical methods (i.e. alkaline environment) and 3) combinational physical methods (i.e. hot-water followed by steam). The dissolution of silica and partial removal of wax on the outer surface of node and internode was evident from ATR-FTIR results, after all of the pre-treatments. This led to the reduced hydrophobicity of the outer surface, which is advantageous for water based adhesives, when it comes to bio-composites. This reduction in hydrophobicity will translate into improved wetting of surface with resin and therefore better interfacial bonding, leading to enhanced physical and mechanical properties of bio-composites. The hot-water followed by steam pre-treatment resulted in an increase in cellulose crystallinity of node and internode, which in turn increased the tensile strength significantly ($P < 0.05$) by 62 and 35% respectively.

6) In order to gain more aggregated understanding of node and internode, the physicochemical characteristics were examined in relation to their cell wall components. Distinct variations were found amongst the physicochemical characteristics and cell wall components of node and internode, making them suitable and/or defect for different specific bio-refinery pathways. Separation of node and internode, possessing different attributes, and utilising them in segregated processings could lead to higher value added products. For instance node had higher extractives and ash content which could be a

defect for bio-composites or bio-energy as these characteristics inhibit the performance of the intended end product.

7) The overall surface science understanding emerged from the previous chapters enabled the investigation of bonding and interface mechanisms of wheat straw composites with thermosetting resins. Surface modification was successfully carried out in order to significantly improve the interfacial bonding between the substrate (i.e. straw node and internode), and resins. A significant increase in the bonding quality was evident by modifying the surface characteristics and inspiring the mechanical interlocking through the change of surface chemistry and morphology. Extensive investigations in the failure morphology at microscopic scale enabled the physical modelling of failure mechanisms. Four different categories of failure models were developed based on comprehensive experimental observations. Strong to weak bonding qualities of straw composites were listed based on the failure models, after the single lap joint tensile tests.

8.3 Future prospectives

In this section, suggestions for extension of the work are listed based on the knowledge established through the completion of this project. The gaps are identified which should further add value to the research field.

1) The influence of the age of the straws on their characteristics. Although the ATR-FTIR results in experimental Chapters 4 to 7 have been carried out in different time scales on the same collected straws in 2012, no significant difference in the spectrums have been outlined. For instance Chapter 4 results were gathered in 2013 whereas Chapter 7 results were gathered in 2015. Nevertheless, SEM-EDAX results in chapter 4 and 7 show some differences in terms of chemical elemental composition quantities, but the general trends of the results are similar. It would therefore be a further research to focus on the scientific details of characteristic variations induced by age of straw (i.e. creep effect).

2) H+S scaling up, i.e. implementation for industrial production of bio-composites. The two simple steps of hot-water followed by steam treatment could represent a great pilot scale research opportunity. The efficiency and the environmental impacts of this treatment should also be considered in future research. This treatment on the other hand could be applied to other types of biomass, and it most certainly would be interesting to research the effects of H+S on rice straw, corn stover, wood chips and etc.

3) Industrially efficient separation technologies of nodes and internodes. Image processing/analysis for identification of nodes in the stem and subsequent mechanical cutting may be complicated, but would certainly be an interesting methodology to investigate. It will require the program to differentiate the node based on its morphology and then send the position coordinates on the conveyor belt to the cutting machine.

4) Lab scale production of bio-composites based on the following outcomes, i) removal of nodes from the stem, ii) H+S surface modification and iii) use of lignin phenol formaldehyde as thermosetting resin. It would be interesting to study the effects of bonding quality improvements, as observed in Chapter 7, on the mechanical properties of composites, such as tensile and flexural performances, and physical properties, i.e.

systematic and accurate assessment of the moisture resistance of H+S treated straw composites.

5) Smart selection of anatomical sections based on their characterisation for the development of high performance products. For instance inner to inner surface bonding scenario was found to have the best bonding quality (see Chapter 7), and on the other hand outer surface would be suitable for moisture resistance. Therefore, it would be a further research to investigate if the arrangement of internode inner and outer surface could be mechanised for production of bio-composites. As the outcomes of this research have shown, the all-important ability to tailor physical and mechanical properties through material selection and modification represents a great future research.

References

1. FAOSTAT. http://faostat.fao.org/site/567/DesktopDefault.aspx?PageID=567#ancor. 2014;Accessed 16/3/2016(2016).

2. Zhang Y, Ghaly A, Li B. Physical properties of wheat straw varieties cultivated under different climatic and soil conditions in three continents. American Journal of Engineering and Applied Sciences 2012;5(2):98-106.

3. Bhattarai S, Bottenus D, Ivory CF, Gao AH, Bule M, Garcia-Perez M, Chen S. Simulation of the ozone pretreatment of wheat straw. Bioresour Technol 2015;196:78-87.

4. Motte J-, Escudié R, Beaufils N, Steyer J-, Bernet N, Delgenès J-, Dumas C. Morphological structures of wheat straw strongly impacts its anaerobic digestion. Industrial Crops and Products 2014;52(0):695-701.

5. Harper SHT, Lynch JM. The chemical components and decomposition of wheat straw leaves, internodes and nodes. J Sci Food Agric 1981;32(11):1057-1062.

6. Lawther JM, Sun R, Banks WB. Extraction, fractionation, and characterization of structural polysaccharides from wheat straw. J Agric Food Chem 1995;43(3):667-675.

7. Schmidt AS, Mallon S, Thomsen AB, Hvilsted S, Lawther JM. Comparison of the chemical properties of wheat straw and beech fibers following alkaline wet oxidation and laccase treatments J Wood Chem Technol 2002;22(1):39-53.

8. Himmel ME, Ding SY, Johnson DK, Adney WS, Nimlos MR, Brady JW, Foust TD. Biomass recalcitrance: engineering plants and enzymes for biofuels production. Science 2007;315(5813):804-807.

9. Lawrence M. Reducing the Environmental Impact of Construction by Using Renewable Materials. Journal of Renewable Materials 2015;3(3):163-174.

10. Chang AJ, Fan J, Wen X. Screening of fungi capable of highly selective degradation of lignin in rice straw. Int Biodeterior Biodegrad 2012;72(0):26-30.

11. Arora DS, Chander M, Gill PK. Involvement of lignin peroxidase, manganese peroxidase and laccase in degradation and selective ligninolysis of wheat straw. Int Biodeterior Biodegrad 2002;50(2):115-120.

12. Arora D. Biodelignification of wheat straw by different fungal associations. Biodegradation 1995;6(1):57-60.

13. Taniguchi M, Suzuki H, Watanabe D, Sakai K, Hoshino K, Tanaka T. Evaluation of pretreatment with Pleurotus ostreatus for enzymatic hydrolysis of rice straw. Journal of Bioscience and Bioengineering 2005;100(6):637-643.

14. Shi J, Chinn MS, Sharma-Shivappa RR. Microbial pretreatment of cotton stalks by solid state cultivation of Phanerochaete chrysosporium. Bioresour Technol 2008;99(14):6556-6564.

15. Zhang X, Yu H, Huang H, Liu Y. Evaluation of biological pretreatment with white rot fungi for the enzymatic hydrolysis of bamboo culms. Int Biodeterior Biodegrad 2007;60(3):159-164.

16. Agbor VB, Cicek N, Sparling R, Berlin A, Levin DB. Biomass pretreatment: Fundamentals toward application. Biotechnol Adv 2011;29(6):675-685.

17. Singh D, Zeng J, Laskar DD, Deobald L, Hiscox WC, Chen S. Investigation of wheat straw biodegradation by Phanerochaete chrysosporium. Biomass Bioenergy 2011;35(3):1030-1040.

18. Chen L, Hong F, Yang X, Han S. Biotransformation of wheat straw to bacterial cellulose and its mechanism. Bioresour Technol 2013;135(0):464-468.

19. Lopez-Abelairas M, A • lvarez Pallin M, Salvachua D, Lu-Chau T, Martinez MJ, Lema JM. Optimisation of the biological pretreatment of wheat straw with white-rot fungi for ethanol production. Bioprocess and Biosystems Engineering 2013;36(9):1251-1260.

20. Maehara T, Ichinose H, Furukawa T, Ogasawara W, Takabatake K, Kaneko S. Ethanol production from high cellulose concentration by the basidiomycete fungus Flammulina velutipes. Fungal Biol 2013;117(3):220-226.

21. Matsumoto K, Taguchi S. Enzyme and metabolic engineering for the production of novel biopolymers: crossover of biological and chemical processes. Curr Opin Biotechnol 2013.

22. Petrik S, Kádár Z, Márová I. Utilization of hydrothermally pretreated wheat straw for production of bioethanol and carotene-enriched biomass. Bioresour Technol 2013;133(0):370-377.

23. Schilling JS, Ai J, Blanchette RA, Duncan SM, Filley TR, Tschirner UW. Lignocellulose modifications by brown rot fungi and their effects, as pretreatments, on cellulolysis. Bioresour Technol 2012;116(0):147-154.

24. Van Dyk JS, Pletschke BI. A review of lignocellulose bioconversion using enzymatic hydrolysis and synergistic cooperation between enzymes—Factors affecting enzymes, conversion and synergy. Biotechnol Adv 2012;30(6):1458-1480.

25. Kim S, Dale BE. Global potential bioethanol production from wasted crops and crop residues. Biomass Bioenergy 2004;26(4):361-375.

26. Sánchez C. Lignocellulosic residues: Biodegradation and bioconversion by fungi. Biotechnol Adv 2009;27(2):185-194.

27. Banerjee G, Scott-Craig J, Walton J. Improving Enzymes for Biomass Conversion: A Basic Research Perspective. BioEnergy Research 2010;3(1):82-92.

28. Zhang YP, Lynd LR. Toward an aggregated understanding of enzymatic hydrolysis of cellulose: Noncomplexed cellulase systems. Biotechnol Bioeng 2004;88(7):797-824.

29. Talebnia F, Karakashev D, Angelidaki I. Production of bioethanol from wheat straw: An overview on pretreatment, hydrolysis and fermentation. Bioresour Technol 2010;101(13):4744-4753.

30. Alvira P, Tomás-Pejó E, Ballesteros M, Negro MJ. Pretreatment technologies for an efficient bioethanol production process based on enzymatic hydrolysis: A review. Bioresour Technol 2010;101(13):4851-4861.

31. Binod P, Sindhu R, Singhania RR, Vikram S, Devi L, Nagalakshmi S, Kurien N, Sukumaran RK, Pandey A. Bioethanol production from rice straw: An overview. Bioresour Technol 2010;101(13):4767-4774.

32. Cheng C, Lo Y, Lee K, Lee D, Lin C, Chang J. Biohydrogen production from lignocellulosic feedstock. Bioresour Technol 2011;102(18):8514-8523.

33. Kaparaju P, Serrano M, Thomsen AB, Kongjan P, Angelidaki I. Bioethanol, biohydrogen and biogas production from wheat straw in a biorefinery concept. Bioresour Technol 2009;100(9):2562-2568.

34. Sapci Z. The effect of microwave pretreatment on biogas production from agricultural straws. Bioresour Technol 2013;128(0):487-494.

35. Zhong W, Zhang Z, Luo Y, Sun S, Qiao W, Xiao M. Effect of biological pretreatments in enhancing corn straw biogas production. Bioresour Technol 2011;102(24):11177-11182.

36. Ribbons R. Chemicals from lignin. Philos Trans R Soc Lond Ser 1987;321:485-494.

37. Shi J, Sharma-Shivappa RR, Chinn M, Howell N. Effect of microbial pretreatment on enzymatic hydrolysis and fermentation of cotton stalks for ethanol production. Biomass Bioenergy 2009;33(1):88-96.

38. Chandra RP, Bura R, Mabee WE, Berlin A, Pan X, Saddler JN. Substrate Pretreatment: The Key to Effective Enzymatic Hydrolysis of Lignocellulosics? In: Olsson L, editor. , vol. 108: Springer Berlin Heidelberg, 2007.

39. Wan C, Li Y. Effect of hot water extraction and liquid hot water pretreatment on the fungal degradation of biomass feedstocks. Bioresour Technol 2011;102(20):9788-9793.

40. Yu H, Du W, Zhang J, Ma F, Zhang X, Zhong W. Fungal treatment of cornstalks enhances the delignification and xylan loss during mild alkaline pretreatment and enzymatic digestibility of glucan. Bioresour Technol 2010;101(17):6728-6734.

41. Salvachúa D, Prieto A, López-Abelairas M, Lu-Chau T, Martínez ÁT, Martínez MJ. Fungal pretreatment: An alternative in second-generation ethanol from wheat straw. Bioresour Technol 2011;102(16):7500-7506.

42. Zhong W, Yu H, Song L, Zhang X. Combined pretreatment with white-rot fungus and alkali at near room-temperature for improving saccharification of corn stalks. BioResources 2011;6:3440-3451.

43. Hatakka A. Pretreatment of wheat straw by white-rot fungi for enzymic saccharification of cellulose. Eur J Appl Microb Biotechnol 1983;18(6):350-357.

44. Yu J, Zhang J, He J, Liu Z, Yu Z. Combinations of mild physical or chemical pretreatment with biological pretreatment for enzymatic hydrolysis of rice hull. Bioresour Technol 2009;100(2):903-908.

45. Wan C, Li Y. Fungal pretreatment of lignocellulosic biomass. Biotechnol Adv 2012;30(6):1447-1457.

46. Blanchette R. Delignification by wood-decay fungi. Annu Rev Phytopathol 1991;29:381-389.

47. Blanchette R, W. Krueger EH,JE., Masood A.Akin D. Cell wall alterations in loblolly pine wood decayed by the white-rot fungus, Ceriporiopsis subvermispora. J Biotechnol 1997;53(2–3):203-213.

48. Daniel G. Use of electron microscopy for aiding our understanding of wood biodegradation. FEMS Microbiol Rev 1994;13(2-3):199-233.

49. Eriksson K, Blanchette R, Ander P. Microbial and enzymatic degradation of wood and wood components. New York: Springer-Verlag, 1990.

50. Martínez AT. Molecular biology and structure-function of lignin-degrading heme peroxidases. Enzyme Microb Technol 2002;30(4):425-444.

51. Guerra A, Mendonca R, Ferraz A. Characterization of the residual lignins in Pinus taeda biodegraded by Ceriporiopsis subvermispora by using in situ CuO oxidation and DFRC methods. Holzforschung 2002;56:157-160.

52. Hatakka A. Lignin-modifying enzymes from selected white-rot fungi: production and role from in lignin degradation. FEMS Microbiol Rev 1994;13(2–3):125-135.

53. Piscitelli A, Del Vecchio C, Faraco V, Giardina P, Macellaro G, Miele A, Pezzella C, Sannia G. Fungal laccases: Versatile tools for lignocellulose transformation. Comptes Rendus Biologies 2011;334(11):789-794.

54. Kirk T. effects of a brown-rot fungus, Lenzites trabea, on lignin in spruce wood. Holzforschung 1975;29:99-107.

55. Enoki A, Tanaka H, Fuse G. Degradation of lignin-related compounds, pure cellulose and wood components by white-rot and brown-rot fingi. Holzforschung 1988;42:85-93.

56. Goodell B. Brown-rot fungal degradation of wood: our evolving view. ACS Sym Ser 2003;845:97-118.

57. Jin L, Schultz T, Nicholas D. Structural characterization of brown-rot lignin. Holzforschung 1990;44:133-138.

58. Lee KH, Wi SG, Singh AP, Kim YS. Micromorphological characteristics of decayed wood and laccase produced by the brown-rot fungus Coniophora puteana. Journal of Wood Science 2004;50(3):281-284.

59. Yelle D, Kaparaju P, Hunt C, Hirth K, Kim H, Ralph J, Felby C. Two-dimensional NMR evidence for cleavage of lignin and xylan substituents in wheat straw through hydrothermal pretreatment and enzymatic hydrolysis. Bioenerg Res 2013;6:211-221.

60. Lu F, Ralph J. Non-degradative dissolution and acetylation of ball-milled plant cell walls: high-resolution solution-state NMR. The Plant Journal 2003;35(4):535-544.

61. Zakzeski J, Bruijnincx PCA, Jongerius AL, Weckhuysen BM. The Catalytic Valorization of Lignin for the Production of Renewable Chemicals. Chem Rev 2010;110(6):3552-3599.

62. Lange H, Decina S, Crestini C. Oxidative upgrade of lignin – Recent routes reviewed. European Polymer Journal 2013;49(6):1151-1173.

63. Jalč D. Straw Enrichment for Fodder Production by Fungi. In: Kempken F, editor. , vol. 11: Springer Berlin Heidelberg, 2002.

64. Dinis MJ, Bezerra RMF, Nunes F, Dias AA, Guedes CV, Ferreira LMM, Cone JW, Marques GSM, Barros ARN, Rodrigues MAM. Modification of wheat straw lignin by solid state fermentation with white-rot fungi. Bioresour Technol 2009;100(20):4829-4835.

65. Kuhad R, Singh A, Eriksson K. Microorganisms and enzymes involved in the degradation of plant fiber cell walls. In: Eriksson K-L, Babel W, Blanch HW, Cooney CL, Enfors S-, Eriksson K-L, Fiechter A, Klibanov AM, Mattiasson B, Primrose SB, Rehm HJ, Rogers PL, Sahm H, Schagerl K, Tsao GT, Venkat K, Villadsen J, Stockar U, Wandrey C, editors. , vol. 57: Springer Berlin Heidelberg, 1997.

66. Borneman W, Hartley R, Morrison WH, Akin D, Ljungdahl L. Feruloyl and p-coumaroyl esterase from anaerobic fungi in relation to plant cell wall degradation. Appl Microbiol Biotechnol 1990;33(3):345-351.

67. Datta A, Bettermann A, Kirk T. Identification of a specific manganese peroxidase among ligninolytic enzymes secreted by Phanerochaete chrysosporium during wood decay. Appl Environ Microbiol 1991;57(5):1453-1460.

68. Reid ID. Optimization of solid-state fermentation for selective delignification of aspen wood with Phlebia tremellosa. Enzyme Microb Technol 1989;11(12):804-809.

69. Hou X, Smith TJ, Li N, Zong M. Novel renewable ionic liquids as highly effective solvents for pretreatment of rice straw biomass by selective removal of lignin. Biotechnol Bioeng 2012;109(10):2484-2493.

70. Bugg TD, Ahmad M, Hardiman EM, Singh R. The emerging role for bacteria in lignin degradation and bio-product formation. Curr Opin Biotechnol 2011;22(3):394-400.

71. Vicuña R. Bacterial degradation of lignin. Enzyme Microb Technol 1988;10(11):646-655.

72. Gupta V, Minocha A, Jain N. Batch and continuous studies on treatment of pulp mill wastewater by Aeromonas formicans. J Chem Technol Biotechnol 2001;76(6):547-552.

73. Raj A, Krishna Reddy MM, Chandra R. Identification of low molecular weight aromatic compounds by gas chromatography–mass spectrometry (GC–MS) from kraft lignin degradation by three Bacillus sp. Int Biodeterior Biodegrad 2007;59(4):292-296.

74. Breen A, Singleton FL. Fungi in lignocellulose breakdown and biopulping. Curr Opin Biotechnol 1999;10(3):252-258.

75. Wang Y, Liu Q, Yan L, Gao Y, Wang Y, Wang W. A novel lignin degradation bacterial consortium for efficient pulping. Bioresour Technol 2013;139(0):113-119.

76. Ragauskas AJ, Beckham GT, Biddy MJ, Chandra R, Chen F, Davis MF, Davison BH, Dixon RA, Gilna P, Keller M, Langan P, Naskar AK, Saddler JN, Tschaplinski TJ, Tuskan GA, Wyman CE. Lignin valorization: improving lignin processing in the biorefinery. Science 2014;344(6185):1246843.

77. Mayer AM, Staples RC. Laccase: new functions for an old enzyme. Phytochemistry 2002;60(6):551-565.

78. Janusz G, Kucharzyk KH, Pawlik A, Staszczak M, Paszczynski AJ. Fungal laccase, manganese peroxidase and lignin peroxidase: Gene expression and regulation. Enzyme Microb Technol 2013;52(1):1-12.

79. Riva S. Laccases: blue enzymes for green chemistry. Trends Biotechnol 2006;24(5):219-226.

80. Rodríguez Couto S, Toca Herrera JL. Industrial and biotechnological applications of laccases: A review. Biotechnol Adv 2006;24(5):500-513.

81. Bourbonnais R, Paice MG. Oxidation of non-phenolic substrates: An expanded role for laccase in lignin biodegradation. FEBS Lett 1990;267(1):99-102.

82. Du X, Li J, Gellerstedt G, Rencoret J, Del Río JC, Martínez AT, Gutiérrez A. Understanding Pulp Delignification by Laccase-Mediator Systems through Isolation and Characterization of Lignin-Carbohydrate Complexes. Biomacromolecules 2013;14(9):3073-3080.

83. Li K, Xu F, Eriksson K-L. Comparison of Fungal Laccases and Redox Mediators in Oxidation of a Nonphenolic Lignin Model Compound. Appl Environ Microbiol 1999:2654-2660.

84. Crestini C, Jurasek L, Argyropoulos DS. On the Mechanism of the Laccase?Mediator System in the Oxidation of Lignin. Chemistry ? A European Journal 2003;9(21):5371-5378.

85. Mattinen ML, Suortti T, Gosselink RJA, Argyropoulos DS, Evtuguin D, Suurnäkki A, Jong E, Tamminen T. Polymerization of different lignins by laccase. BioResources 2008;3(2):549-565.

86. Youn H, Hah YC, Kang S. Role of laccase in lignin degradation by white-rot fungi. FEMS Microbiol Lett 1995;132(3):183-188.

87. Widsten P, Kandelbauer A. Laccase applications in the forest products industry: A review. Enzyme Microb Technol 2008;42(4):293-307.

88. Leonowicz A, Cho N, Luterek J, Wilkolazka A, Wojtas-Wasilewska M, Matuszewska A, Hofrichter M, Wesenberg D, Rogalski J. Fungal laccase: properties and activity on lignin. J Basic Microbiol 2001;41(3-4):185-227.

89. Batog J, Kozlowski R, Przepiera A. Lignocellulosic Composites Bonded by Enzymatic Oxidation of Lignin. Molecular Crystals and Liquid Crystals 2008;484(1):35/-42/408].

90. Barsberg S. Modification phenomena of solid-state lignin caused by electron-abstracting oxidative systems. Arch Biochem Biophys 2002;404(1):62-70.

91. Barsberg S, Thygesen LG. Spectroscopic properties of oxidation species generated in the lignin of wood fibers by a laccase catalyzed treatment: electronic hole state migration and stabilization in the lignin matrix. Biochimica et Biophysica Acta (BBA) - General Subjects 1999;1472(3):625-642.

92. Hüttermann A, Mai C, Kharazipour A. Modification of lignin for the production of new compounded materials. Appl Microbiol Biotechnol 2001;55(4):387-394.

93. Kharazipour A, Bergmann K, Nonninger K, Hüttermann A. Properties of fibre boards obtained by activation of the middle lamella lignin of wood fibres with peroxidase and H2O2 before conventional pressing. J Adhes Sci Technol 1998;12(10):1045-1053.

94. Sain M, Panthapulakkal S. Bioprocess preparation of wheat straw fibers and their characterization. Industrial Crops and Products 2006;23(1):1-8.

95. Kumar R, Singh S, Singh O. Bioconversion of lignocellulosic biomass: biochemical and molecular perspectives. J Ind Microbiol Biotechnol 2008;35(5):377-391.

96. Saha BC. Hemicellulose bioconversion. Journal of Industrial Microbiology and Biotechnology 2003;30(5):279-291.

97. Xu J, Du W, Zhao X, Zhang G, Liu D. Microbial oil production from various carbon sources and its use for biodiesel preparation. Biofuels, Bioproducts and Biorefining 2013;7(1):65-77.

98. Henstra AM, Sipma J, Rinzema A, Stams AJ. Microbiology of synthesis gas fermentation for biofuel production. Curr Opin Biotechnol 2007;18(3):200-206.

99. Zeng X, Ma Y, Ma L. Utilization of straw in biomass energy in China. Renewable and Sustainable Energy Reviews 2007;11(5):976-987.

100. Ibrahim HA. Pretreatment of straw for bioethanol production. Energy Procedia 2012;14(0):542-551.

101. Saha BC, Cotta MA. Comparison of pretreatment strategies for enzymatic saccharification and fermentation of barley straw to ethanol. New Biotechnology 2010;27(1):10-16.

102. Xu C, Ma F, Zhang X, Chen S. Biological Pretreatment of Corn Stover by Irpex lacteus for Enzymatic Hydrolysis. J Agric Food Chem 2010;58(20):10893-10898.

103. Yu X, Zheng Y, Dorgan KM, Chen S. Oil production by oleaginous yeasts using the hydrolysate from pretreatment of wheat straw with dilute sulfuric acid. Bioresour Technol 2011;102(10):6134-6140.

104. Hui L, Wan C, Hai-tao D, Xue-jiao C, Qi-fa Z, Yu-hua Z. Direct microbial conversion of wheat straw into lipid by a cellulolytic fungus of Aspergillus oryzae A-4 in solid-state fermentation. Bioresour Technol 2010;101(19):7556-7562.

105. Huang C, Zong M, Wu H, Liu Q. Microbial oil production from rice straw hydrolysate by Trichosporon fermentans. Bioresour Technol 2009;100(19):4535-4538.

106. Economou CN, Aggelis G, Pavlou S, Vayenas DV. Single cell oil production from rice hulls hydrolysate. Bioresour Technol 2011;102(20):9737-9742.

107. Huang X, Wang Y, Liu W, Bao J. Biological removal of inhibitors leads to the improved lipid production in the lipid fermentation of corn stover hydrolysate by Trichosporon cutaneum. Bioresour Technol 2011;102(20):9705-9709.

108. Babu BV. Biomass pyrolysis: a state-of-the-art review. Biofuels, Bioproducts and Biorefining 2008;2(5):393-414.

109. Cherubini F. The biorefinery concept: Using biomass instead of oil for producing energy and chemicals. Energy Conversion and Management 2010;51(7):1412-1421.

110. Widsten P, Kandelbauer A. Adhesion improvement of lignocellulosic products by enzymatic pre-treatment. Biotechnol Adv 2008;26(4):379-386.

111. Felby C, Hassingboe J, Lund M. Pilot-scale production of fiberboards made by laccase oxidized wood fibers: board properties and evidence for cross-linking of lignin. Enzyme Microb Technol 2002;31(6):736-741.

112. Felby C, Thygesen LG, Sanadi A, Barsberg S. Native lignin for bonding of fiber boards—evaluation of bonding mechanisms in boards made from laccase-treated fibers of beech (Fagus sylvatica). Industrial Crops and Products 2004;20(2):181-189.

113. Lund M, Hassingboe J, Felby C. Oxidoreductase catalyzed bonding of wood fibres. , 2000. p. 113-116.

114. Felby C, Pedersen L, Nielsen B. Enhanced auto-adhesion of wood fibres using phenol oxidases. Holzforschung 1997;51:281-286.

115. Kharazipour A, Huettermann A, Luedemann HD. Enzymatic activation of wood fibres as a means for the production of wood composites. J Adhes Sci Technol 1997;11(3):419-427.

116. Widsten P, Laine JE, Tuominen S, Qvintus-Leino P. Effect of high defibration temperature on the properties of medium-density fiberboard (MDF) made from laccase-treated hardwood fibers. J Adhes Sci Technol 2003;17(1):67-78.

117. BS EN 622-5:2009. Fibreboards. Specifications. Requirements for dry process boards (MDF).

118. BS EN 622-2:2004. Fibreboards. Specifications. Requirements for hardboards.

119. Kharazipour A, Hüttermann A, Kühne G, Rong M. Process for gluing wood chips and articles produced by this process. Eur Pat Appl 1993;EP0565109.

120. Qvintus-Leino P, Widsten P, Tuominen S, Laine J, Kunnas J. Method of producing compressed layered structures such as fiberboard or similar wood-based products. Int Pat Appl 2003;WO03047826.

121. Halvarsson S, Edlund H, Norgren M. Manufacture of non-resin wheat straw fibreboards. Industrial Crops and Products 2009;29(2–3):437-445.

122. Kharazipour A, Huettermann A, Luedemann HD. Enzymatic activation of wood fibres as a means for the production of wood composites. J Adhes Sci Technol 1997;11(3):419-427.

123. Unbehaun H, Dittler B, Kühne G, Wagenführ A. Investigation into the biotechnological modification of wood and its application in the wood-based material industry. Acta Biotechnol 2000;20(3-4):305-312.

124. Petri W, Alfred H, Carol H, Andreas K. A preliminary study of green production of fiberboard bonded with tannin and laccase in a wet process. Holzforschung 2009;63:545.

125. Sarkanen K, Ludwig C. Lignins: Occurrence, formation, structure and reactions, vol. 10. New York: Wiley, 1971.

126. Sjöström E. Wood chemistry: fundamental and applications. New York: Academic press, Inc, 1993.

127. Wen J, Sun S, Xue B, Sun R. Recent Advances in Characterization of Lignin Polymer by Solution-State Nuclear Magnetic Resonance (NMR) Methodology. Materials 2013;6:259-391.

128. Crestini C, Argyropoulos D. Structural Analysis of Wheat Straw Lignin by Quantitative 31P and 2D NMR Spectroscopy. The Occurrence of Ester Bonds and α O-4 Substructures. J Agric Food Chem 1997;45:1212-1219.

129. Derkacheva O, Sukhov D. Investigation of Lignins by FTIR Spectroscopy. Macromol Symp 2008;265:61-68.

130. Xiao B, Sun XF, Sun R. Chemical, structural, and thermal characterizations of alkali-soluble lignins and hemicelluloses, and cellulose from maize stems, rye straw, and rice straw. Polym Degrad Stab 2001;74(2):307-319.

131. Xu F, Sun J, Sun R, Fowler P, Baird MS. Comparative study of organosolv lignins from wheat straw. Ind Crop Prod 2006;23(2):180-193.

132. Sun R. Lignin. In: Lu F, Ralph J, editors. Cereal Straw as a Resource for Sustainable Biomaterials and Biofuels. Amsterdam, the Neitherland: Elsevier, 2010.

133. Ralph J, Lundquist K, Brunow G, Lu F, Kim H, Schatz P, et al. Lignins: natural polymers from oxidative coupling of 4-hydroxyphenyl propanoids, Phytochem Rev 2004;3:29-60.

134. Akin DE. B, R. Degradation of polysaccharides and lignin by ruminal bacteria and fungi. Appl Environ Microbiol 1988;54:1117-1125.

135. Baurhoo B, Ruiz-Feria CA, Zhao X. Purified lignin: Nutritional and health impacts on farm animals—A review. Anim Feed Sci Technol 2008;144(3–4):175-184.

136. Kirk T. Effects of microorganisms on lignin. Annu Rev Phytopathol 1971;9:185-210.

137. Doherty WOS, Mousavioun P, Fellows CM. Value-adding to cellulosic ethanol: Lignin polymers. Ind Crop Prod 2011;33(2):259-276.

138. Smook G,. Handbook for Pulp and Paper Technologies. Vancouver, BC: Angus Wilde Publications Inc., 2002.

139. Azuma J. Analysis of Lignin-Carbohydrate Complexes of Plant Cell Walls. In: Linskens H, Jackson J, editors. , vol. 10: Springer Berlin Heidelberg, 1989.

140. Granata A, Argyropoulos D. 2-Chloro-4, 4, 5, 5-tetramethyl- 1, 3, 2- dioxaphospholane, a reagent for the accurate determination of the uncondensed and condensed phenolic moieties in lignins. J Agric Food Chem 1995;43:1538-1544.

141. Jiang Z, Argyropoulos D, Granata A. Correlation analysis of 31P-NMR chemical shifts with substituent effect of phenols. Magn Reson Chem 1995;43:1538-1544.

142. Zhai H, Lee Z. - Ultrastructure and topochemistry of delignification in alkaline pulping of wheat straw. J Wood Chem Technol 1989;9(- 3):387-406.

143. Yu H, Liu R, Shen D, Wu Z, Huang Y. Arrangement of cellulose microfibrils in the wheat straw cell wall. Carbohydr Polym 2008;72(1):122-127.

144. Reddy N, Yang Y. - Properties of High-Quality Long Natural Cellulose Fibers from Rice Straw. - J Agric Food Chem 2006;54(- 21):- 8077-8081.

145. Lapierre C, Monties B, Rolando C. Thioacidolysis of lignin: Comparison with acidolysis. J Wood Chem Technol 1985;5:277-292.

146. Freudenberg K, Lautsch W, Engler K. Die Bildung von Vanillin aus Fichtenlignin. Berichte der deutschen chemischen Gesellschaft (A and B Series) 1940;73(3):167-171.

147. Lu F, Ralph J,. Derivatization followed by reductive cleavage (DFRC Method), a new method for lignin analysis: Protocol for analysis of DFRC monomers. J Agr Food Chem 1997;45:2590-2592.

148. Kelley SS, Rowell RM, Davis M, Jurich CK, Ibach R. Rapid analysis of the chemical composition of agricultural fibers using near infrared spectroscopy and pyrolysis molecular beam mass spectrometry. Biomass Bioenergy 2004;27(1):77-88.

149. Sanderson MA, Agblevor F, Collins M, Johnson DK. Compositional analysis of biomass feedstocks by near infrared reflectance spectroscopy. Biomass Bioenergy 1996;11(5):365-370.

150. Freudenberg K, Sohns F, Dürr W, Niemann C. Über Lignin, Coniferylalkohol und Saligenin. Cellulosechemie 1931;12:263-275.

151. Martínez ÁT, Rencoret J, Marques G, Gutiérrez A, Ibarra D, Jiménez-Barbero J, del Río JC. Monolignol acylation and lignin structure in some nonwoody plants: A 2D NMR study. Phytochemistry 2008;69(16):2831-2843.

152. Zhang L, Gellerstedt G. Quantitative 2D HSQC NMR determination of polymer structures by selecting suitable internal standard references. Magn Reson Chem 2007;45(1):37-45.

153. Sette M, Wechselberger R, Crestini C. Elucidation of Lignin Structure by Quantitative 2D NMR. Chemistry ? A European Journal 2011;17(34):9529-9535.

154. Morrison I. A semi-micro method for the determination of lignin and its use inpredicting the digestibility of forages. J Sci Food Agric 1972;23:455-463.

155. Theander O, Aman P. Studies on dietary fibres. Swedish J Agric Res 1979;9:97-106.

156. Van Soest P, Wine R. Determination of lignin and cellulose in acid-detergent fibre with permanganate. J Assoc Off Anal Chem 1968;51:780-785.

157. Fidalgo M, Terron M, Martinez A, Gonzalez A, Gonzalez-vila F, Galletti G. Comparative study of fractions from alkaline extraction of wheat straw through chemical degradation, analytical pyrolysis, and spectroscopic techniques. J Agric Food Chem 1993;41:1621-1626.

158. Hortling B, Tarja T, Kentta E. Determination of carboxyl and non-conjugated carbonyl groups in dissolved and residual lignins by IR spectroscopy. Holzforschung 1997;51:405-410.

159. Gilarranz M, Rodríguez F, Oliet M, García J, Alonso V. Phenolic OH group estimation by FTIP and UV spectroscopy. Application to organosolv lignins, J Wood Chem Technol 2001;21:387-395.

160. Durie R, Lynch B, Sternhell S. Comparative studies of brown coal and lignin. I. Infra-red spectra. Austral J Chem 1960;13:156-168.

161. Bolker HI SN. Infrared Spectroscopy of Lignins. Pulp Paper Mag , Canada 1963;64:187-194.

162. Colthup N, Daly L, Wiberley S. Introduction to Infrared and Raman Spectroscopy. London: Academic Press Limited, 1990.

163. Collier W, Kalasinsky V, Schulz T. Infrared study of lignin:reexamination of ary–alkyl ether C–O stretching peak assignment. Holzforschung 1997;46:523-528.

164. Faix O. Classification of lignins from different botanical origins by FT-IRspectroscopy. Holzforschung 1991;45:21-27.

165. Glasser W. Classification of lignin according to chemical and molecular structure. In: Glasser W, Northey R, Schultz T, editors. Lignin: Historical, Biological, and Materials Perspectives,. Washington, DC: ACS Symposium Series No. 742. American Chemical Society, 2000.

166. Hornsby PR, Hinrichsen E, Tarverdi K. Preparation and properties of polypropylene composites reinforced with wheat and flux straw fibres part 1 fibre characterization. Journal of Materials Science 1997;32:443-449.

167. Nowakowski DJ, Jones JM. Uncatalysed and potassium-catalysed pyrolysis of the cell-wall constituents of biomass and their model compounds. J Anal Appl Pyrolysis 2008;83(1):12-25.

168. Qiang L, Wen-zhi L, Dong Z, Xi-feng Z. Analytical pyrolysis–gas chromatography/mass spectrometry (Py–GC/MS) of sawdust with Al/SBA-15 catalysts. J Anal Appl Pyrolysis 2009;84(2):131-138.

169. Fahmi R, Bridgwater AV, Thain SC, Donnison IS, Morris PM, Yates N. Prediction of Klason lignin and lignin thermal degradation products by Py–GC/MS in a collection of Lolium and Festuca grasses. J Anal Appl Pyrolysis 2007;80(1):16-23.

170. del Río JC, Gutiérrez A, Rodríguez IM, Ibarra D, Martínez ÁT. Composition of non-woody plant lignins and cinnamic acids by Py-GC/MS, Py/TMAH and FT-IR. J Anal Appl Pyrolysis 2007;79(1–2):39-46.

171. Brebu M, Vasile C. Thermal degradation of lignin- A review. Cellulose Chem Technol 2009;44:353-363.

172. Müller-Hagedorn M, Bockhorn H. Pyrolytic behaviour of different biomasses (angiosperms) (maize plants, straws, and wood) in low temperature pyrolysis. J Anal Appl Pyrolysis 2007;79(1–2):136-146.

173. Ghaly AE, Ergüdenler A, Al Taweel AM. Determination of the kinetic parameters of oat straw using thermogravimetric analysis. Biomass Bioenergy 1993;5(6):457-465.

174. yang Q, Wu S, Lou R, Lv G. Analysis of wheat straw lignin by thermogravimetry and pyrolysis–gas chromatography/mass spectrometry. J Anal Appl Pyrolysis 2010;87(1):65-69.

175. Carrier M, Loppinet-Serani A, Denux D, Lasnier J, Ham-Pichavant F, Cansell F, Aymonier C. Thermogravimetric analysis as a new method to determine the lignocellulosic composition of biomass. Biomass Bioenergy 2011;35(1):298-307.

176. Ludwig C. Magnetic resonance spectra. In: Sarkanen K, Ludwig C, editors. Lignin, Occorance, Formation, Structure and reactions. New York: Wiler-Interscience, 1971.

177. Lundquist K. NMR-studies of lignins. 4. Investigation of spruce lignin by H-1- NMR spectroscopy. Acta Chem Scand B 1980;34:21-26.

178. Lundquist K. NMR-Studies of Lignins. 5. Investigation of non-derivatized spruce and birch lignin by H-1-NMR spectroscopy. Acta Chem Scand B 1981;35:497-501.

179. Lundquist K,. Proton (1H) NMR spectroscopy. In: Lin S, Dence C, editors. *Methods in Lignin Chemistry*. New York, NY, USA: Springer-Verlag, 1992.

180. Gellerstedt G, Robert D. Quantitative 13C NMR analysis of kraft lignins. Acta Chem Scand B, 1987;41:541-546.

181. Pan D, Tai D, Chen C,. Comparative studies on chemical composition of wood components in recent and ancient woods of Bischofia polycarpa. Holzforschung 1990;44:- 7-16.

182. Robert D. Carbon-13 nuclear magnetic resonance spectrometry. In: - Lin S, - Dence C, editors. - Methods in Lignin Chemistry. New York, NY,USA.: - Springer Berlin Heidelberg, 1992.

183. Hawkes G, Smith C, Utley J, Vargas R. Viertler, H. A comparison of solutionand solid state 13C-NMR spectra of lignins and lignin model compounds. Holzforschung 1993;47:302-312.

184. Ralph J, Landucci L. NMR of lignins. In: Heitner C, Dimmel D, Schmidt J, editors. In *Lignin and Lignans: Advances in Chemistry*. Boca Raton,FL, USA: CRC Press, 2010.

185. Xia Z, Akim L, Argyropulos D. Quantitative 13C NMR analysis of ligninswith internal standards. J Agric Food Chem 2001;49:3573-3578.

186. Capanema E, Balakshin M, Kadla J. A Comprehensive Approach for Quantitative Lignin Characterization by NMR Spectroscopy. J Agric Food Chem 2004;52(- 7):1850-1860.

187. Capanema E, Balakshin M, Kadla J. Quantitative Characterization of a Hardwood Milled Wood Lignin by Nuclear Magnetic Resonance Spectroscopy. J Agric Food Chem 2005;53(- 25):9639-9649.

188. Terashima N, Atalla R, Vanderhart D. Solid state NMR spectroscopy of specifically C-13-enriched lignin in wheat straw from coniferin, Phytochemistry 1997;46:863-870.

189. Gu R, Xie Y, Zeng S, Wu H, Yasuda S. Carbon-13enrichment of rice stalk lignin traced by solid state C-13 NMR spectroscopy. Chem, J, Chinese U 2002;23:1073-1076.

190. Landucci L. Quantitative C-13 NMR Characterization of Lignin. 1. A methodology for high-precision. Holzforschung 1985;39:355-359.

191. Landucci L. Application of modern liquid-state NMR to lignin characterization.2. C-13 signal resolution and useful techniques. Holzforschung 1991;45:425-432.

192. Yelle D, Ralph J, Frihart C. Characterization of nonderivatized plant cell walls using high-resolution solution-state NMR spectroscopy. Magn Reson Chem 2008;46(9):508-517.

193. Kim H, Ralph J, Akiyama T. Solution-state 2D NMR of ball-milled plant cell wall gels in DMSO-*d*6. Bioenerg Res 2008;1:56-66.

194. Kim H, Ralph J. Solution-state 2D NMR of ball-milled plant cell wall gels in DMSO-*d*(6)/pyridine-*d*(5). Org Biomol Chem 2010;8:576-591.

195. Koskela H. Quantitative 2D NMR studies. Ann Rep NMR Spectrosc 2009;66:1-31.

196. Ede R, Brunow G. Application of 2-dimensional homonuclear and heteronuclear correlation NMR-spectroscopy to wood lignin structure determination, J Org Chem 1992;57:1477-1480.

197. Ede R, Kilapelainen I. Homo-Nuclear and Hetero-Nuclear 2d NMR techniques-umambiguous structural probes for noncyclic benzyl aryl ethers in soluble lignin samples, Res Chem Intermediat 1995;21:313-328.

198. Ralph J, Marita J, Ralph S, Hatfield R, Lu F, Ede R, Peng J, Landucci L. Solution-state NMR of lignins. In: Argyropoulos D, editor. *Advances in Lignocellulosics Characterization*. Atlanta, GA, USA: TAPPI Press, 1999.

199. Liitia T, Maunu S, Hortling B, Toikka M, Kilpelainen I. Analysis of technical lignins by two- and three-dimensional NMR spectroscopy. J Agr Food Chem 2003;51:2136-2143.

200. Del Río J, Rencoret J, Marques G, Li J, Gellerstedt G, Jiménez-Barbero J, Martínez Á, Gutiérrez A. Structural characterization of the lignin from jute (*Corchorus capsularis*) fibers. J Agric Food Chem 2009;57:10271-10281.

201. Del Río J, Rencoret J, Prinsen P, Martínez A, Ralph J, Gutiérrez A. Structural characterization of wheat straw lignin as revealed by analytical pyrolysis, 2D-NMR, and reductive cleavage methods. J Agric Food Chem 2012;60:5922-5935.

202. Wen J, Sun Z, Sun Y, Sun S, Xu F, Sun R. Structural characterization of alkali-extractable lignin fractions from bamboo. J Biobased Mater Bioenerg 2010;4:408-425.

203. Wen J, Xue B, Xu F, Sun R, Pinkert A. Unmasking the structural features and property of lignin from bamboo. Ind Crop Prod 2013;42(0):332-343.

204. Li M, Sun SN, Xu F, Sun R. Formic acid based organosolv pulping of bamboo (*Phyllostachys acuta*): Comparative characterization of the dissolved lignins with milled wood lignin. Chem Eng J 2012;179:80-89.

205. Shi Z, Xiao L, Jia-Deng, Xu F, Sun R. Physicochemical characterization of lignin fractions sequentially isolated from bamboo (Dendrocalamus brandisii) with hot water and alkaline ethanol solution. J Appl Polym Sci 2012;125(4):3290-3301.

206. Yuan T, Sun S, Xu F, Sun R. Isolation and physico-chemical characterization of lignins from ultrasound irradiated fast-growing poplar wood. BioResources, 2011;6:414-433.

207. Yuan T, Sun S, Xu F, Sun R. - Characterization of Lignin Structures and Lignin–Carbohydrate Complex (LCC) Linkages by Quantitative 13C and 2D HSQC NMR Spectroscopy. - J Agric Food Chem 2011;59(- 19):- 10604-10614.

208. Yuan T, Sun S, Xu F, Sun R. - Structural Characterization of Lignin from Triploid of Populus tomentosa Carr. - J Agric Food Chem 2011;59(- 12):- 6605-6615.

209. Karhunen P, Rummakko P, Sipilä J, Brunow G, Kilpelainen I. The formation of dibenzodioxocin structures by oxidative coupling. A model reaction for lignin biosynthesis. Tetrahedron Lett 1995;36:4501-4504.

210. Zhang A, Lu F, Sun R, Ralph J. - Isolation of Cellulolytic Enzyme Lignin from Wood Preswollen/Dissolved in Dimethyl Sulfoxide/N-Methylimidazole. - J Agric Food Chem 2010;58(- 6):- 3446-3450.

211. Gutiérrez A, Rencoret J, Cadena EM, Rico A, Barth D, del Río JC, Martínez ÁT. Demonstration of laccase-based removal of lignin from wood and non-wood plant feedstocks. Bioresour Technol 2012;119(0):114-122.

212. Wen J, Xue B, Xu F, Sun R. Unveiling the structural heterogeneity ofbamboo lignin by *in situ* HSQC NMR technique. Bioenergy Res 2012;5(- 4):886-903.

213. Robert D, Ammalahti E, Bardet M, Brunow G, Kilpelainen I, Lundquist K, Neirinck V, Terashima N. Improvement in NMR Structural Studies of Lignin Through Two- and Three-Dimensional NMR Detection and Isotopic Enrichment. In: Anonymous , vol. 697: American Chemical Society, 1998.

214. Ralph J, Grabber JH, Hatfield RD. Lignin-ferulate cross-links in grasses: active incorporation of ferulate polysaccharide esters into ryegrass lignins. Carbohydr Res 1995;275(1):167-178.

215. Ãmmalahti E, Brunow G, Bardet M, Robert D, Kilpelainen I. Identification of Side-Chain Structures in a Poplar Lignin Using Three-Dimensional HMQC-HOHAHA NMR Spectroscopy. J Agric Food Chem 1998;46(12):5113-5117.

216. Balakshin MY, Capanema EA, Chen, Gracz HS. Elucidation of the Structures of Residual and Dissolved Pine Kraft Lignins Using an HMQC NMR Technique. J Agric Food Chem 2003;51(21):6116-6127.

217. Lu F, Ralph J. DFRC method for lignin analysis. 1. New method for beta aryl ether cleavage: lignin model studies, J Agr Food Chem 1997;45:4655-4660.

218. Hu Z, Yeh T, Chang H, Matsumoto Y, Kadla J. Elucidation of thestructure of cellulolytic enzyme lignin, Holzforschung 2006;60:389-397.

219. Lu F, Ralph J. The DFRC method for lignin analysis. 2. Monomers from isolatedlignins, J Agr Foord Chem 1998;46:547-552.

220. Yelle DJ, Ralph J, Lu F, Hammel KE. Evidence for cleavage of lignin by a brown rot basidiomycete. Environ Microbiol 2008;10(7):1844-1849.

221. Tohmura S, Argyropoulos D. Determination of arylglycerol-beta-aryl ethers and other linkages in lignins using DFRC/(31)P NMR. J Agr Food Chem 2001;49:536-542.

222. Guerra A, Norambuena M, Freer J, Argyropoulos D. Determination of arylglycerol-beta-aryl ether linkages in enzymatic mild acidolysis lignins (EMAL): Comparison of DFRC/P-31 NMR with thioacidolysis. J Nat Prod 2008;71:836-841.

223. Lu F, Ralph J. Efficient ether cleavage in lignins: athe “DFRC” method as abasis for new analytical methods, In: Lewis N, Sarkanen S, editors. Lignin and Lignin Biosynthesis . Washington, DC.: American Chemical Society, 1998.

224. Lu F, Ralph J. Detection and determination of p-coumaroylated units in lignins, J Agr Food Chem 1999;47:1988-1992.

225. Del Río J, Marques G, Rencoret J, Martinez A, Gutierrez A. Occurrence of naturally acetylated lignin units. J Agr Food Chem 2007;55:5461-5468.

226. Samuel R, Pu Y, Raman B, Ragauskas A. Structural Characterization and Comparison of Switchgrass Ball-milled Lignin Before and After Dilute Acid Pretreatment. Appl Biochem Biotechnol 2010;162(1):62-74.

227. Mansfield SD, Kim H, Lu F, Ralph J. Whole plant cell wall characterization using solution-state 2D NMR. Nat Protocols 2012;7(9):1579-1589.

228. Grabber J, Quideau S, Ralph J. P-coumaroylated syringyl units in maizelignin: implications for beta-ether cleavage by thioacidolysis. Phytochemistry 1996;43:1189-1194.

229. Durot N, Gaudard F, Kurek B. The unmasking of lignin structures in wheat straw by alkali. Phytochemistry 2003;63(5):617-623.

230. Buranov AU, Mazza G. Lignin in straw of herbaceous crops. Ind Crop Prod 2008;28(3):237-259.

231. Sun RC, Fang JM, Tomkinson J. Delignification of rye straw using hydrogen peroxide. Industrial Crops and Products 2000;12(2):71-83.

232. del Río JC, Gutiérrez A, Martínez ÁT. Identifying acetylated lignin units in non-wood fibers using pyrolysis-gas chromatography/mass spectrometry. Rapid Communications in Mass Spectrometry 2004;18(11):1181-1185.

233. Koo B, Min B, Gwak K, Lee S, Choi J, Yeo H, Choi I. Structural changes in lignin during organosolv pretreatment of Liriodendron tulipifera and the effect on enzymatic hydrolysis. Biomass Bioenergy 2012;42(0):24-32.

234. Ma JF, Yang GH, Mao JZ, Xu F. Characterization of anatomy, ultrastructure and lignin microdistribution in Forsythia suspensa. Ind Crop Prod 2011;33(2):358-363.

235. Sun R. Structure, Ultrastructure, and Chemical Composition. In: Xu F, editor. *Cereal Straw as a Resource for Sustainable Biomaterials and Biofuels*. Amsterdam, the Netherlands: Elsevier, 2010.

236. Sun R, Lawther JM, Banks WB. A tentative chemical structure of wheat straw lignin. Industrial Crops and Products 1997;6(1):1-8.

237. Dence C, Lin S. Introduction. In: Lin S, Dence C, editors. Methods in Lignin Chemistry. Berlin: Springer-Verlag, 1992.

238. Sjöström E. *Wood Chemistry Fundamentals and Applications,*. San Diego.: Academic Press, Inc., 1993.

239. Lora J. Characteristics, industrial sources, and utilization of lignins fromnonwood plants. In: Hu T, editor. Chemical, Modification, Properties, and Usage of Lignin. New York: Kluwer Academic/Plenum Publishers, 2002.

240. Boerjan W, Ralph J, Baucher M. Lignin biosynthesis. Annu Rev Plant Biol 2003;54:519-546.

241. Ralph J. Perturbing lignification. In: Entwistle K, Harris P, Walker J, editors. The Compromised Wood Workshop. Canterbury, New Zealand: University of Canterbury, 2007.

242. Del Río J, Martínez A, Gutiérrez A. Presence of 5-hydroxyguaiacyl units as native lignin constituents in plants as seen by Py-GC/MS. J Anal Appl Pyrolysis 2007;79:33-38.

243. Balakshin MY, Capanema EA, Barry G, John F, Kadla JF. NMR studies on Fraser fir Abies fraseri (Pursh) Poir. lignins. Holzforschung 2005;59:488.

244. Zhang L, Henriksson G, Gellerstedt G. The formation of b–b structures in lignin biosynthesis – are there two different pathways? Org Biomol Chem 2003;1:3621-3624.

245. Shimada M, Fukuzuka T, Higuchi T. Ester linkages of p-coumaric acid in bamboo and grass lignins. TAPPI 1971;54:72-78.

246. Himmelsbach DS. Structure of forage cell walls. In: Jung H, Buxton D, Hartfield R, Ralph J, editors. Forage cell wall structure and digestibility. Madison: American society of agronomy, 1993.

247. Brownell H. Stability of lignin-carbohydrate complexes. TAPPI 1971;54:66-71.

248. Ford C. Comparative structural studies of lignin carbohydrate complexes from Digitaria-Decumbens (Pangola Grass) before and after chlorite delignification, Carbohyd Res 1986;147:101-117.

249. Lundquist K, Simonson R, Tingsvik K. On the occurrence of carbohydrates in milled wood lignin preparations. Sven Papperstidn 1979;82:272-275.

250. Lora J, Glasser W. Recent industrial applications of lignin: A sustainablealternative to nonrenewable materials. J Polym Environ 2002;10:39-48.

251. Muller P, Glasser W. Engineering plastics from lignin. VIII. Phenolic resin prepolymer synthesis and analysis. J Adhes 1984;17:157-173.

252. Milne TA, Chum HL, Agblevor F, Johnson DK. Standardized analytical methods. Biomass Bioenergy 1992;2(1–6):341-366.

253. Cathala B, Saake B, Faix O, Monties B. Association behaviour of lignins and lignin model compounds studied by multidetector size-exclusion chromatography. Journal of Chromatography A 2003;1020(2):229-239.

254. Gargulak J, Lebo S. Commercial use of lignin-based materials. ACS Symp Ser 2000;742:304-320.

255. Timell T. Studies on opposite wood in conifers part III: distribution of lignin, Wood Sci Technol 1973;12:1-15.

256. Lange P. The distribution of lignin in the cell wall of normal and reaction wood from spruce and a few hardwoods. Sven Papperstidn 1954;57:525-532.

257. Wood J, Goring D. The distribution of lignin in stem wood and branch wood of Douglas fir, Pulp Pap Mag Can 1971;72:61-68.

258. Lange P, Kjaer A. Quantitative chemical analysis of the different parts of the cell wall in wood and cellulose fibres by interference microscopy, Norsk Skogind 1957;11:425-432.

259. Donaldson L, Ryan K. A comparison of relative lignin concentration asdetermined by interference microscopy and bromination/EDXA, Wood Sci Technol 1987;21:303-309.

260. Saka S, Goring D. Distribution of lignin in white birch wood as determinedby bromination with TEM-EDXA. Holzforschung 1988;42:149-153.

261. Donaldson L. Determination of lignin distribution in agricultural fibres. Wood Processing Division, New Zealand Forest Research Institute 1996;4418:1-25.

262. Donaldson L, Hague J, Snell R. Lignin distribution in coppice poplar, linseed and wheat straw. Holzforschung 2001;55:379-385.

263. El Mansouri N, Salvadó J. Analytical methods for determining functional groups in various technical lignins. Ind Crop Prod 2007;26(2):116-124.

264. Faix O, Andersons B, Zakis G. Determination of carbonyl groups of six round robin lignins by modified oximation and FTIR spectroscopy. Holzforschung 1998;52:268-274.

265. Lai Y-. Determination of Phenolic Hydroxyl Groups. In: Lin S, Dence C, editors. : Springer Berlin Heidelberg, 1992.

266. Aulin-Erdtman G,. Studies on ultraviolet absorption changes caused by modifications of chromophores with special reference to Lignin chemistry. Stockholm, 1958.

267. Aberu H, Freire M. Methoxyl content determination of lignins by 1H NMR. An Bras Ci 1995;67:379382.

268. Gosselink RJA, Abächerli A, Semke H, Malherbe R, Käuper P, Nadif A, van Dam JEG. Analytical protocols for characterisation of sulphur-free lignin. Ind Crop Prod 2004;19(3):271-281.

269. Sahoo S, Seydibeyoğlu MÖ, Mohanty AK, Misra M. Characterization of industrial lignins for their utilization in future value added applications. Biomass Bioenergy 2011;35(10):4230-4237.

270. Sun R, Tomkinson T. Essential guides for isolation/purification of polysaccharides. In: Woilson I, Adlard T, Poole C, Cook M, editors. EncyclopediaofSeparationScience. London: Academic Press, 2000.

271. McCarthy JL, Islam A. Lignin Chemistry, Technology, and Utilization: A Brief History. In: Anonymous , vol. 742: American Chemical Society, 1999.

272. LIN SY. Lignin utilization: potential and challenge. Progress in biomass conversion 1983;4:31-78.

273. Chen F, Li J. Aqueous Gel Permeation Chromatographic Methods for Technical Lignins. J Wood Chem Technol 2000;20(3):265-276.

274. Kuo M, Hse C, Huang D. Alkali-treated kraft lignin as a component in flakeboard resins. Holzforschung 2009;45:47-54.

275. Lora J, Glasser W. Recent Industrial Applications of Lignin: A Sustainable Alternative to Nonrenewable Materials. Journal of Polymers and the Environment 2002;10(1-2):39-48.

276. Tapin S, Sigoillot J, Asther M, Petit-Conil M. Feruloyl Esterase Utilization for Simultaneous Processing of Nonwood Plants into Phenolic Compounds and Pulp Fibers. J Agric Food Chem 2006;54(10):3697-3703.

277. Pecina R, Burtscher P, Bonn G, Bobleter O. GC-MS and HPLC analyses of lignin degradation products in biomass hydrolyzates. Fresenius' Zeitschrift fÃ¼r analytische Chemie 1986;325(5):461-465.

278. Bobleter O. Hydrothermal degradation of polymers derived from plants. Prog Polym Sci 1994;19(5):797-841.

279. Yoshida T, Matsumura Y. Gasification of Cellulose, Xylan, and Lignin Mixtures in Supercritical Water. Ind Eng Chem Res 2001;40(23):5469-5474.

280. Okuda K, Man X, Umetsu M, Takami S, Adschiri T. Efficient conversion of lignin into single chemical species by solvothermal reaction in water–*p*-cresol solvent. J Phys Condens Matter 2004;16:1325-1330.

281. Piskorz J, Majerski P, Radlein D, Scott DS. Conversion of lignins to hydrocarbon fuels. Energy Fuels 1989;3(6):723-726.

282. Gellerstedt G, Li J, Eide I, Kleinert M, Barth T. Chemical Structures Present in Biofuel Obtained from Lignin. Energy Fuels 2008;22(6):4240-4244.

283. Shabtai J, Zmierczak W, Chornet E. Process for conversion of lignin to reformulated hydrocarbon gasoline. US patent 1998;5,959,167.

284. Klass D. Biomass for renewable energy, fuels and chemicals. New York: Academic press, 1988.

285. Lynd LR. Overview and evaluation of fuel ethanol from cellulosic biomass: Technology, Economics, the Environment, and Policy. Annu Rev Energy Environ 1996;21(1):403-465.

286. Ma F, Hanna MA. Biodiesel production: a review. Bioresour Technol 1999;70(1):1-15.

287. Wool R, Sun X. Polymers and Composites. In: Wool R, editor. Bio-based polymers and composites. California: Elsevier, 2005.

288. Lapierre C, Pollet B, Rolando C. New insights into the molecular architecture of hardwood lignins by chemical degradative methods. Research on Chemical Intermediates 1995;21(3-5):397-412.

289. Lapierre C. Application of new methods for the investigation of lignin structure. In: Jung H, Buxton D, Hatfield R, Ralph J, editors. Forage cell wall structure and digestibility. Madison: American society of agronomy, 1993.

290. Zilliox C, Debeire P. Hydrolysis of wheat straw by a thermostable endoxylanase: Adsorption and kinetic studies. Enzyme Microb Technol 1998;22(1):58-63.

291. Beckman E, Liesche O. Qualitative und quantitative unterschiede der lignine einiger holz-undstroharten. Biochem Z 1923;139:491-508.

292. Scalbert A, Monties B, Rolando C, Sierra-Escudero A. Formation of ether linkage between phenolic acids and graminear lignin: a possible mechanism involving unique methods. Holzforschung 1986;40:191-195.

293. Azuma J, Tetsuo K. Lignin-carbohydrate complexes from various sources. In: Anonymous Methods in Enzymology, vol. Volume 161: Academic Press, 1988.

294. Billa E, Koukios EG, Monties B. Investigation of lignins structure in cereal crops by chemical degradation methods. Polym Degrad Stab 1998;59(1–3):71-75.

295. Nimz H. Lignin-based wood adhesives. In: Pizzi A, editor. Wood Adhesive: Chemistry and Technology. New York: Marcel Dekker, 1983.

296. Smith D. The generation and utilization of residuals from composite panel products. Forest Prod J 2004;25:8-17.

297. Lin Q, Chen N, Bian L, Fan M. Development and mechanism characterization of high performance soy-based bio-adhesives. Int J Adhes Adhes 2012;34(0):11-16.

298. Pizzi A. Recent developments in eco-efficient bio-based adhesives for wood bonding: opportunities and issues. J Adhes Sci Technol 2006;20(8):829-846.

299. Liu Y, Li K. Development and characterization of adhesives from soy protein for bonding wood. Int J Adhes Adhes 2007;27(1):59-67.

300. Despres A, Pizzi A, Vu C, Pasch H. Formaldehyde-free amino resin wood adhesive based on dimethoxyethanal. J Appl Polym Sci 2008;110:3980-3916.

301. Widsten P, Laine J, Qvintus-Leino P, Tuominen S. Effect of high temperature fibrization on the chemical structure of hardwood. Holzforschung 2002;56:51-59.

302. Widsten P, Laine J, Qvintus-Leino P, Tuominen S. Effect of high temperature fibrization on the chemical structure of softwood. J Wood Chem Technol 2001;21:227-245.

303. Ysbrandy R, Sanderson R, Gerischer G. Adhesives from Autohydrolysis Bagasse Lignin, a Renewable Resource - Part II. DSC Thermal Analysis of Novolac Resins. Holzforschung 1992;46:253-256.

304. Gupta R, Singh S, Jolly S. Phenol-lignin-formaldehyde adhesives for plywood. Holzforschung Und Holzverwertung 1978;30:109-112.

305. Peng W, Barry AO, Riedl B. Characterization of Methylolated Lignin by H-Nmr and 13C-Nmr. J Wood Chem Technol 1992;12(3):299-312.

306. Alonso MV, Oliet M, Rodríguez F, García J, Gilarranz MA, Rodríguez JJ. Modification of ammonium lignosulfonate by phenolation for use in phenolic resins. Bioresour Technol 2005;96(9):1013-1018.

307. Olivares M, Guzman JA, Natho A, Saavedra A. Kraft lignin utilization in adhesives. Wood Sci Technol 1988;22(2):157-165.

308. Yang S, Liu Q. Effect of lignin modification on synthetis properties. , 2002. p. 782.

309. Hayashi A, Namura Y, Urkita T. Demethylation of lignosulphonate during the gelling reaction with dichromate. Mokuzai Gakkaishi 1967;13:194-197.

310. Jolly S, Singh S, Singh S, Gupta R. Kinetics and mechanisms of lignin formaldehyde resinification reaction. Cellul Chem Techn 1982;16:511-522.

311. Marton A. Lignin Structure and Reactions, Advances in Chemistry Series. In: Gould Robert F., editor. , vol. 59: AMERICAN CHEMICAL SOCIETY, 1966.

312. Vázquez G, González J, Freire S, Antorrena G. Effect of chemical modification of lignin on the gluebond performance of lignin-phenolic resins. Bioresour Technol 1997;60(3):191-198.

313. Liu G, Qiu X, Xing D, Yang D. Phenolation modification of wheat straw soda lignin and its utilization in lignin-based formaldehyde resins. In: He B, Fu S, Chen F, editors. 3rd International symposium on emerging technologies of pulping and papermaking. Guangzhou: South Chinal University Technology Press, 2006.

314. Ma Y, Zhao X, Chen X, Wang Z. An approach to improve the application of acid-insoluble lignin from rice hull in phenol–formaldehyde resin. Colloids Surf Physicochem Eng Aspects 2011;377(1–3):284-289.

315. Forss K, Fuhrmann A. Finnish plywood, particleboard, and fibreboard made with a lignin-base adhesive. Forest Prod J 1979;29:25-29.

316. Kirkman A, Gratzl J, Edwards L. Kraft lignin recovery by ultrafiltration: economic feasibility and impact on the kraft recovery system. Tappi J 1986;69:110-114.

317. Shen K, Calve L. Improving by fractionation-ammonium-based spent sulphite liquor for waferboard binder. Adhes Age 1980;23:25-29.

318. Jönsson A, Wallberg O. Cost estimates of kraft lignin recovery by ultrafiltration. Desalination 2009;237(1–3):254-267.

319. Doherty WOS, Mousavioun P, Fellows CM. Value-adding to cellulosic ethanol: Lignin polymers. Industrial Crops and Products 2011;33(2):259-276.

320. Feldman D. Lignin and Its Polyblends - A Review. In: Hu T, editor. : Springer US, 2002.

321. Nada A, Abou- • Youssef H, El- • Gohary S. Phenol Formaldehyde Resin Modification with Lignin. Polym Plast Technol Eng 2003;42(4):689-699.

322. Wang Y, Peng W, Chai L, Peng B, Min X, He D. Preparation of adhesive for bamboo plywood using concentrated papermaking black liquor directly. Journal of Central South University of Technology 2006;13(1):53-57.

323. Akhtar T, Lutfullah G, Zahoorullah . Lignosulfonate-phenolformaldehyrde adhesive: a potential binder for wood panel industries. J Chem Soc Pak 2011;33:535-538.

324. Peng W, Riedl B. The chemorheology of phenol-formaldehyde thermoset resin and mixtures of the resin with lignin fillers. Polymer 1994;35(6):1280-1286.

325. Khan MA, Ashraf SM, Malhotra VP. Development and characterization of a wood adhesive using bagasse lignin. Int J Adhes Adhes 2004;24(6):485-493.

326. Kulshreshtha AK, Vasile C. Handbook of Polymer Blends and Composites, Volumes 1-4.

327. Vázquez G, Rodríguez-Bona C, Freire S, González-Álvarez J, Antorrena G. Acetosolv pine lignin as copolymer in resins for manufacture of exterior grade plywoods. Bioresour Technol 1999;70(2):209-214.

328. Çetin NS, Özmen N. Use of organosolv lignin in phenol–formaldehyde resins for particleboard production: I. Organosolv lignin modified resins. Int J Adhes Adhes 2002;22(6):477-480.

329. Çetin NS, Özmen N. Use of organosolv lignin in phenol-formaldehyde resins for particleboard production: II. Particleboard production and properties. Int J Adhes Adhes 2002;22(6):481-486.

330. Zhang W, Ma Y, Xu Y, Wang C, Chu F. Lignocellulosic ethanol residue-based lignin–phenol–formaldehyde resin adhesive. Int J Adhes Adhes 2013;40(0):11-18.

331. Liu G, Qiu X, Yang D. Properties of wheat straw soda lignin of different molecular weights and its influence on properties of LPF adhesive. Huagong Xuebao (Chin Ed) 2008;59:1590-1594.

332. Jin Y, Cheng X, Zheng Z. Preparation and characterization of phenol–formaldehyde adhesives modified with enzymatic hydrolysis lignin. Bioresour Technol 2010;101(6):2046-2048.

333. Hiro-kuni O, Kenichi S. Chapter 25. Wood adhesives from phenolysis lignin. In: Glasser W, Sarkanen S, editors. Lignin: properties and materials. Washington, DC: ACS, 1989.

334. Nieh W, Glasser W. Lignin derivatives with epoxy functionality. In: Glasser W, Sarkanen S, editors. Lignin: Properties and Materials. Washington, DC: ACS, 1989.

335. Hofmann K, Glasser WG. Engineering Plastics from Lignin. 22. Cure of Lignin Based Epoxy Resins. The Journal of Adhesion 1993;40(2-4):229-241.

336. Hofmann K, Glasser W. Engineering plastics from lignin, 23. Network formation of lignin-based epoxy resins. Macromolecular Chemistry and Physics 1994;195(1):65-80.

337. Stewart D. Lignin as a base material for materials applications: Chemistry, application and economics. Industrial Crops and Products 2008;27(2):202-207.

338. Feldman D, Banu D, Luchian C, Wang J. Epoxy lignin polyblends: Correlation between polymer interaction and curing temperature. J Appl Polym Sci 1991;42(5):1307-1318.

339. Feldman D, Banu D, Natansohn A, Wang J. Structure properties relations of thermally cured epoxy lignin polyblends. J Appl Polym Sci 1991;42(6):1537-1550.

340. Nonaka Y, Tomita B, Hatano Y. Synthesis of lignin/epoxy resins in aqueous systems and their properties. Holzforschung 1997;51:183-187.

341. Simionescu C, Rusan V, Turta K, Bobcova S, Macoveanu M, Cazacu G, Stoleriu A. Synthesis and characterization of some iron lignosulfonate-based lignin-epoxy resins. Cellul Chem Techn 1993;27:627-644.

342. Malutan T, Nicu R, Popa V. Lignin modification by epoxidation. BioResources 2008;3:1371-1379.

343. Simionescu CI, Rusan V, Macoveanu MM, Cazacu G, Lipsa R, Vasile C, Stoleriu A, Ioanid A. Lignin/epoxy composites. Composites Sci Technol 1993;48(1–4):317-323.

344. Cazacu G, Popa VI. Lignin-based blends. In: Vasile C, Kulshreshtha A, editors. Hanbook of Polymer Blends and Composites Vol.4B. Shawbury, UK: Rapra Technology Ltd., 2003.

345. Muller PC, Glassert WG. Engineering Plastics from Lignin. VIII. Phenolic Resin Prepolymer Synthesis and Analysis. The Journal of Adhesion 1984;17(2):157-173.

346. Ismail TNMT, Hassan HA, Hirose S, Taguchi Y, Hatakeyama T, Hatakeyama H. Synthesis and thermal properties of ester-type crosslinked epoxy resins derived from lignosulfonate and glycerol. Polym Int 2010;59(2):181-186.

347. Kosbar LL, Gelorme JD, Japp RM, Fotorny WT. Introducing biobased materials into the electronics industry: Developing a lignin-based resin for printed wiring boards. J Ind Ecol 2000;4(3):93-106.

348. O'Dogherty MJ, Huber JA, Dyson J, Marshall CJ. A Study of the Physical and Mechanical Properties of Wheat Straw. J Agric Eng Res 1995;62(2):133-142.

349. Ghaffar SH, Fan M. Structural analysis for lignin characteristics in biomass straw. Biomass Bioenergy 2013;57(0):264-279.

350. Hansen MAT, Jørgensen H, Laursen KH, Schjoerring JK, Felby C. Structural and chemical analysis of process residue from biochemical conversion of wheat straw (Triticum aestivum L.) to ethanol. Biomass Bioenergy 2013;56(0):572-581.

351. Shalini S, Dharm D, CH T. Complete characterization of wheat straw (triticum aestivum PBW-343 L. emend. fiori & paol.) – A renewable source of fibres for pulp and paper making. BioResources 2011;6:154-177.

352. Stelte W, Clemons C, Holm JK, Ahrenfeldt J, Henriksen UB, Sanadi AR. Thermal transitions of the amorphous polymers in wheat straw. Industrial Crops and Products 2011;34(1):1053-1056.

353. Wiśniewska SK, Nalaskowski J, Witka-Jeżewska E, Hupka J, Miller JD. Surface properties of barley straw. Colloids and Surfaces B: Biointerfaces 2003;29(2–3):131-142.

354. Hansen MAT, Kristensen JB, Felby C, Jørgensen H. Pretreatment and enzymatic hydrolysis of wheat straw (Triticum aestivum L.) – The impact of lignin relocation and plant tissues on enzymatic accessibility. Bioresour Technol 2011;102(3):2804-2811.

355. Liu R, Yu H, Huang Y. Structure and morphology of cellulose in wheat straw. Cellulose 2005;12(1):25-34.

356. Yu H, Liu R, Shen D, Jiang Y, Huang Y. Study on morphology and orientation of cellulose in the vascular bundle of wheat straw. Polymer 2005;46(15):5689-5694.

357. Linxin Z, Shiyu F, Feng L, Huaiyu Z. Chlorine dioxide treatment of sisal fibre: surface lignin and its influences on fibre surface characteristics and interfacial behaviour of sisal fibre/phenolic resin composites. BioResources 2010;5:2431-2446.

358. Zhao L, Boluk Y. XPS and IGC characterization of steam treated triticale straw. Appl Surf Sci 2010;257(1):180-185.

359. Jiang H, Zhang Y, Wang X. Effect of lipases on the surface properties of wheat straw. Industrial Crops and Products 2009;30(2):304-310.

360. Das G, Bettotti P, Ferraioli L, Raj R, Mariotto G, Pavesi L, Sorarù GD. Study of the pyrolysis process of an hybrid CH3SiO1.5 gel into a SiCO glass. Vibrational Spectroscopy 2007;45(1):61-68.

361. Frost RL, Mendelovici E. Modification of fibrous silicates surfaces with organic derivatives: An infrared spectroscopic study. J Colloid Interface Sci 2006;294(1):47-52.

362. Fang JM, Fowler P, Tomkinson J, Hill CAS. Preparation and characterisation of methylated hemicelluloses from wheat straw. Carbohydr Polym 2002;47(3):285-293.

363. Jahan MS, Chowdhury DAN, Islam MK, Moeiz SMI. Characterization of lignin isolated from some nonwood available in Bangladesh. Bioresour Technol 2007;98(2):465-469.

364. Sun XF, Xu F, Sun RC, Fowler P, Baird MS. Characteristics of degraded cellulose obtained from steam-exploded wheat straw. Carbohydr Res 2005;340(1):97-106.

365. Le Troëdec M, Peyratout CS, Smith A, Chotard T. Influence of various chemical treatments on the interactions between hemp fibres and a lime matrix. Journal of the European Ceramic Society 2009;29(10):1861-1868.

366. Kristensen J, Thygesen L, Felby C, Jorgensen H, Elder T. Cell-wall structural changes in wheat straw pretreated for bioethanol production. Biotechnology for Biofuels 2008;1(1):5.

367. Himmelsbach DS, Khalili S, Akin DE. The use of FT-IR microspectroscopic mapping to study the effects of enzymatic retting of flax (Linum usitatissimum L) stems. J Sci Food Agric 2002;82(7):685-696.

368. Alemdar A, Sain M. Isolation and characterization of nanofibers from agricultural residues – Wheat straw and soy hulls. Bioresour Technol 2008;99(6):1664-1671.

369. Inglesby MK, Gray GM, Wood DF, Gregorski KS, Robertson RG, Sabellano GP. Surface characterization of untreated and solvent-extracted rice straw. Colloids and Surfaces B: Biointerfaces 2005;43(2):83-94.

370. Merk S, Blume A, Riederer M. Phase behaviour and crystallinity of plant cuticular waxes studied by Fourier transform infrared spectroscopy. Planta 1997;204(1):44-53.

371. Sun RC, Sun XF, Fowler P, Tomkinson J. Structural and physico-chemical characterization of lignins solubilized during alkaline peroxide treatment of barley straw. European Polymer Journal 2002;38(7):1399-1407.

372. Liang CY, Marchessault RH. Infrared spectra of crystalline polysaccharides. II. Native celluloses in the region from 640 to 1700 cm.?1. Journal of Polymer Science 1959;39(135):269-278.

373. Shang L, Ahrenfeldt J, Holm JK, Sanadi AR, Barsberg S, Thomsen T, Stelte W, Henriksen UB. Changes of chemical and mechanical behavior of torrefied wheat straw. Biomass Bioenergy 2012;40(0):63-70.

374. Zhong C, Wang C, Huang F, Jia H, Wei P. Wheat straw cellulose dissolution and isolation by tetra-n-butylammonium hydroxide. Carbohydr Polym 2013;94(1):38-45.

375. She D, Xu F, Geng Z, Sun R, Jones GL, Baird MS. Physicochemical characterization of extracted lignin from sweet sorghum stem. Industrial Crops and Products 2010;32(1):21-28.

376. Sari G, Ammalahti E, Kilpelainen I, Brunow G, Annele H. Characterisation of Milled Wood Lignin from Reed Canary Grass (Phalaris arundinacea). Holzforschung - International Journal of the Biology, Chemistry, Physics and Technology of Wood 2009;51:130.

377. Iskalieva A, Yimmou BM, Gogate PR, Horvath M, Horvath PG, Csoka L. Cavitation assisted delignification of wheat straw: A review. Ultrason Sonochem 2012;19(5):984-993.

378. Günter. M, Christian. S, Hubert. V, Alireza. K, Andrea. P. FTIR-ATR spectroscopic analyses of changes in wood properties during particle- and fibreboard production of hard- and softwood trees. BioResources 2009;4:49-71.

379. Dai D, Fan M. Investigation of the dislocation of natural fibres by Fourier-transform infrared spectroscopy. Vibrational Spectroscopy 2011;55(2):300-306.

380. Dubis EN, Dubis AT, Morzycki JW. Comparative analysis of plant cuticular waxes using HATR FT-IR reflection technique. J Mol Struct 1999;511–512(0):173-179.

381. Singthong J, Cui SW, Ningsanond S, Douglas Goff H. Structural characterization, degree of esterification and some gelling properties of Krueo Ma Noy (Cissampelos pareira) pectin. Carbohydr Polym 2004;58(4):391-400.

382. Sun R, Tomkinson J. Comparative study of lignins isolated by alkali and ultrasound-assisted alkali extractions from wheat straw. Ultrason Sonochem 2002;9(2):85-93.

383. Love GD, Snape CE, Jarvis MC. Comparison of leaf and stem cell-wall components in barley straw by solid-state 13C NMR. Phytochemistry 1998;49(5):1191-1194.

384. Akin DE, Robinson EL, Barton FE, Himmelsbach DS. Changes with maturity in anatomy, histochemistry, chemistry, and tissue digestibility of bermudagrass plant parts. J Agric Food Chem 1977;25(1):179-186.

385. Westermark U. The occurrence of p-hydroxyphenylpropane units in the middle-lamella lignin of spruce (Picea abies). Wood Sci Technol 1985;19(3):223-232.

386. Segal L, Creely JJ, Martin AE, Conrad CM. An Empirical Method for Estimating the Degree of Crystallinity of Native Cellulose Using the X-Ray Diffractometer. Textile Research Journal 1959;29(10):786-794.

387. Helbert W, Sugiyama J, Ishihara M, Yamanaka S. Characterization of native crystalline cellulose in the cell walls of Oomycota. J Biotechnol 1997;57(1–3):29-37.

388. Alemdar A, Sain M. Biocomposites from wheat straw nanofibers: Morphology, thermal and mechanical properties. Composites Sci Technol 2008;68(2):557-565.

389. Panthapulakkal S, Zereshkian A, Sain M. Preparation and characterization of wheat straw fibers for reinforcing application in injection molded thermoplastic composites. Bioresour Technol 2006;97(2):265-272.

390. Le Digabel F, Boquillon N, Dole P, Monties B, Averous L. Properties of thermoplastic composites based on wheat-straw lignocellulosic fillers. J Appl Polym Sci 2004;93(1):428-436.

391. Avella M, Bozzi C, dell'Erba R, Focher B, Marzetti A, Martuscelli E. Steam-exploded wheat straw fibers as reinforcing material for polypropylene-based composites. Characterization and properties. Die Angewandte Makromolekulare Chemie 1995;233(1):149-166.

392. Halvarsson S, Edlund H, Norgren M. Properties of medium-density fibreboard (MDF) based on wheat straw and melamine modified urea formaldehyde (UMF) resin. Industrial Crops and Products 2008;28(1):37-46.

393. Sun R. Extractives. In: peng P, Bian J, Sun R, editors. Cereal Straw as a Resource for Sustainable Biomaterials and Biofuels. United Kingdom: Elsevier, 2010.

394. Deswarte FEI, Clark JH, Hardy JJE, Rose PM. The fractionation of valuable wax products from wheat straw using CO2. Green Chem 2006;8(1):39-42.

395. Han G, Umemura K, Kawai S, Kajita H. Improvement mechanism of bondability in UF-bonded reed and wheat straw boards by silane coupling agent and extraction treatments. Journal of Wood Science 1999;45(4):299-305.

396. Han G, Deng J, Zhang S, Bicho P, Wu Q. Effect of steam explosion treatment on characteristics of wheat straw. Industrial Crops and Products 2010;31(1):28-33.

397. Li X, Cai Z, Winandy JE, Basta AH. Effect of oxalic acid and steam pretreatment on the primary properties of UF-bonded rice straw particleboards. Industrial Crops and Products 2011;33(3):665-669.

398. Mo X, Hu J, Sun XS, Ratto JA. Compression and tensile strength of low-density straw-protein particleboard. Industrial Crops and Products 2001;14(1):1-9.

399. Zheng Y, Pan Z, Zhang R, Jenkins BM, Blunk S. Particleboard quality characteristics of saline jose tall wheatgrass and chemical treatment effect. Bioresour Technol 2007;98(6):1304-1310.

400. Han G, Umemura K, Wong E, Zhang M, Kawai S. Effects of silane coupling agent level and extraction treatment on the properties of UF-bonded reed and wheat straw particleboards. Journal of Wood Science 2001;47(1):18-23.

401. Zhang Y, Lu X, Pizzi A, Delmotte L. Wheat straw particleboard bonding improvements by enzyme pretreatment. Holz als Roh- und Werkstoff 2003;61(1):49-54.

402. Mwaikambo LY, Ansell MP. Chemical modification of hemp, sisal, jute, and kapok fibers by alkalization. J Appl Polym Sci 2002;84(12):2222-2234.

403. Reiniati I, Osman N, Mc Donald A, Laborie M. Linear viscoelasticity of hot-pressed hybrid poplar relates to densification and to the in situ molecular parameters of cellulose. Ann For Sci 2015;72(6):693-703.

404. Nelson ML, O'Connor RT. Relation of certain infrared bands to cellulose crystallinity and crystal latticed type. Part I. Spectra of lattice types I, II, III and of amorphous cellulose. J Appl Polym Sci 1964;8(3):1311-1324.

405. Åkerholm M, Hinterstoisser B, Salmén L. Characterization of the crystalline structure of cellulose using static and dynamic FT-IR spectroscopy. Carbohydr Res 2004;339(3):569-578.

406. Ninomiya K, Kamide K, Takahashi K, Shimizu N. Enhanced enzymatic saccharification of kenaf powder after ultrasonic pretreatment in ionic liquids at room temperature. Bioresour Technol 2012;103(1):259-265.

407. Cao S, Aita GM. Enzymatic hydrolysis and ethanol yields of combined surfactant and dilute ammonia treated sugarcane bagasse. Bioresour Technol 2013;131:357-364.

408. Xiao L, Lin Z, Peng W, Yuan T, Xu F, Li N, Tao Q, Xiang H, Sun R. Unraveling the structural characteristics of lignin in hydrothermal pretreated fibers and manufactured binderless boards from Eucalyptus grandis. Sustainable Chemical Processes 2014;2(1):1-12.

409. Kaparaju P, Felby C. Characterization of lignin during oxidative and hydrothermal pre-treatment processes of wheat straw and corn stover. Bioresour Technol 2010;101(9):3175-3181.

410. Li J, Henriksson G, Gellerstedt G. Lignin depolymerization/repolymerization and its critical role for delignification of aspen wood by steam explosion. Bioresour Technol 2007;98(16):3061-3068.

411. Sun RC, Salisbury D, Tomkinson J. Chemical composition of lipophilic extractives released during the hot water treatment of wheat straw. Bioresour Technol 2003;88(2):95-101.

412. Sun R, Lawther JM, Banks WB. Influence of alkaline pre-treatments on the cell wall components of wheat straw. Industrial Crops and Products 1995;4(2):127-145.

413. Grethlein HE. The Effect of Pore Size Distribution on the Rate of Enzymatic Hydrolysis of Cellulosic Substrates. Nat Biotech 1985;3(2):155-160.

414. Mosier N, Hendrickson R, Brewer M, Ho N, Sedlak M, Dreshel R, Welch G, Dien B, Aden A, Ladisch M. Industrial scale-up of pH-controlled liquid hot water pretreatment of corn fiber for fuel ethanol production. Appl Biochem Biotechnol 2005;125(2):77-97.

415. Kronbergs E. Mechanical strength testing of stalk materials and compacting energy evaluation. Industrial Crops and Products 2000;11(2–3):211-216.

416. Han G, Cheng W, Deng J, Dai C, Zhang S, Wu Q. Effect of pressurized steam treatment on selected properties of wheat straws. Industrial Crops and Products 2009;30(1):48-53.

417. Ouajai S, Shanks RA. Composition, structure and thermal degradation of hemp cellulose after chemical treatments. Polym Degrad Stab 2005;89(2):327-335.

418. Sun FF, Wang L, Hong J, Ren J, Du F, Hu J, Zhang Z, Zhou B. The impact of glycerol organosolv pretreatment on the chemistry and enzymatic hydrolyzability of wheat straw. Bioresour Technol 2015;187:354-361.

419. Sauter SL.Developing composites from wheat straw , 1996. p. 197-214.

420. Shen J, Liu Z, Li J, Niu J. Wettability changes of wheat straw treated with chemicals and enzymes. Journal of Forestry Research 2011;22(1):107-110.

421. Stelte W, Clemons C, Holm J, Ahrenfeldt J, Henriksen U, Sanadi A. Fuel Pellets from Wheat Straw: The Effect of Lignin Glass Transition and Surface Waxes on Pelletizing Properties. BioEnergy Research 2012;5(2):450-458.

422. Kaushik A, Singh M. Isolation and characterization of cellulose nanofibrils from wheat straw using steam explosion coupled with high shear homogenization. Carbohydr Res 2011;346(1):76-85.

423. Ghaffar SH, Fan M. Revealing the morphology and chemical distribution of nodes in wheat straw. Biomass Bioenergy 2015;77(0):123-134.

424. Ghaffar SH, Fan M. Differential behaviour of nodes and internodes of wheat straw with various pre-treatments. Biomass Bioenergy 2015;83:373-382.

425. Ghaffar SH, Fan M, McVicar B. Bioengineering for utilisation and bioconversion of straw biomass into bio-products. Industrial Crops and Products 2015;77:262-274.

426. Ghaffar SH, Fan M. Lignin in straw and its applications as an adhesive. Int J Adhes Adhes 2014;48(0):92-101.

427. Harper SHT, Lynch JM. The chemical components and decomposition of wheat straw leaves, internodes and nodes. J Sci Food Agric 1981;32(11):1057-1062.

428. Hess JR, Thompson DN, Hoskinson RL, Shaw PG, Grant DR. Physical separation of straw stem components to reduce silica. In: Anonymous Biotechnology for Fuels and Chemicals: Springer, 2003.

429. Hames B, Ruiz R, Scarlata C, Sluiter A, Sluiter J, Templeton D. Preparation of samples for compositional analysis. Laboratory Analytical Procedure (LAP).National Renewable Energy Laboratory 2008.

430. Sluiter A, Ruiz R, Scarlata C, Sluiter J, Templeton D. Determination of extractives in biomass. Laboratory Analytical Procedure (LAP) 2005;1617.

431. Sluiter A, Hames B, Ruiz R, Scarlata C, Sluiter J, Templeton D, Crocker D. Determination of structural carbohydrates and lignin in biomass. Golden, Colorado: National Renewable Energy Laboratory; 2010 Jul. Report N.TP-510-42618 2011:17.

432. Sluiter A, Hames B, Ruiz R, Scarlata C, Sluiter J, Templeton D. Determination of ash in biomass (NREL/TP-510-42622). National Renewable Energy Laboratory, Golden 2005.

433. Dodson J. Wheat straw ash and its use as a silica source. 2011.

434. Stelte W, Nielsen NPK, Hansen HO, Dahl J, Shang L, Sanadi AR. Reprint of: Pelletizing properties of torrefied wheat straw. Biomass Bioenergy 2013;53(0):105-112.

435. Monlau F, Sambusiti C, Barakat A, Guo XM, Latrille E, Trably E, Steyer J, Carrere H. Predictive models of biohydrogen and biomethane production based on the compositional and structural features of lignocellulosic materials. Environ Sci Technol 2012;46(21):12217-12225.

436. Sun RC, Tompkinson J. Comparative study of organic solvent and water-soluble lipophilic extractives from wheat straw I: yield and chemical composition. Journal of wood science 2003;49(1):0047-0052.

437. Sluiter JB, Ruiz RO, Scarlata CJ, Sluiter AD, Templeton DW. Compositional analysis of lignocellulosic feedstocks. 1. Review and description of methods. J Agric Food Chem 2010;58(16):9043-9053.

438. Pothula AK, Igathinathane C, Kronberg S, Hendrickson J. Digital image processing based identification of nodes and internodes of chopped biomass stems. Comput Electron Agric 2014;105:54-65.

439. Mckean W, Jacobs R. Wheat straw as a paper fiber source. Washington, USA: Clean Washington Center 1997.

440. Sun R, Tomkinson J. Comparative study of organic solvent-soluble and water-soluble lipophilic extractives from wheat straw 2: spectroscopic and thermal analysis. Journal of Wood Science 2002;48(3):222-226.

441. Merk S, Blume A, Riederer M. Phase behaviour and crystallinity of plant cuticular waxes studied by Fourier transform infrared spectroscopy. Planta 1997;204(1):44-53.

442. Donohoe BS, Tucker MP, Davis M, Decker SR, Himmel ME, Vinzant TB. Tracking lignin coalescence and migration through plant cell walls during pretreatment. 29th Symposium on Biotechnology for Fuels and Chemicals, 2007. p. 67.

443. Li M, Si S, Hao B, Zha Y, Wan C, Hong S, Kang Y, Jia J, Zhang J, Li M. Mild alkali-pretreatment effectively extracts guaiacyl-rich lignin for high lignocellulose digestibility coupled with largely diminishing yeast fermentation inhibitors in Miscanthus. Bioresour Technol 2014;169:447-454.

444. Xu N, Zhang W, Ren S, Liu F, Zhao C, Liao H, Xu Z, Huang J, Li Q, Tu Y. Hemicelluloses negatively affect lignocellulose crystallinity for high biomass digestibility under NaOH and H 2 SO 4 pretreatments in Miscanthus. Biotechnology for biofuels 2012;5(1):1.

445. Wu Z, Zhang M, Wang L, Tu Y, Zhang J, Xie G, Zou W, Li F, Guo K, Li Q. Biomass digestibility is predominantly affected by three factors of wall polymer features distinctive in wheat accessions and rice mutants. Biotechnology for biofuels 2013;6(1):1.

446. Studer MH, DeMartini JD, Davis MF, Sykes RW, Davison B, Keller M, Tuskan GA, Wyman CE. Lignin content in natural Populus variants affects sugar release. Proc Natl Acad Sci U S A 2011;108(15):6300-6305.

447. Brienzo M, Abud Y, Ferreira S, Corrales RCNR, Ferreira-Leitão VS, Souza Wd, Sant'Anna C. Characterization of anatomy, lignin distribution, and response to pretreatments of sugarcane culm node and internode. Industrial Crops and Products 2016;84:305-313.

448. Carpita NC. Structure and biogenesis of the cell walls of grasses. Annual review of plant biology 1996;47(1):445-476.

449. Desaeger M, Verpoest I. On the use of the micro-indentation test technique to measure the interfacial shear strength of fibre-reinforced polymer composites. Composites Sci Technol 1993;48(1–4):215-226.

450. Fuentes CA, Brughmans G, Tran LQN, Dupont-Gillain C, Verpoest I, Van Vuure AW. Mechanical behaviour and practical adhesion at a bamboo composite interface: Physical adhesion and mechanical interlocking. Composites Sci Technol 2015;109:40-47.

451. Pocius AV. Adhesion and adhesives technology: an introduction: Carl Hanser Verlag GmbH Co KG, 2012.

452. Gardner DJ, Blumentritt M, Wang L, Yildirim N. Adhesion Theories in Wood Adhesive Bonding. Reviews of Adhesion and Adhesives 2014;2(2):127-172.

453. GardnerT DJ. Dynamic adhesive wettability of wood. Wood Fiber Sci 2001;330:58-68.

454. Li Y, Mai Y, Ye L. Sisal fibre and its composites: a review of recent developments. Composites Sci Technol 2000;60(11):2037-2055.

455. Stelte W, Holm JK, Sanadi AR, Barsberg S, Ahrenfeldt J, Henriksen UB. A study of bonding and failure mechanisms in fuel pellets from different biomass resources. Biomass Bioenergy 2011;35(2):910-918.

456. Quaresimin M, Ricotta M. Fatigue behaviour and damage evolution of single lap bonded joints in composite material. Composites Sci Technol 2006;66(2):176-187.

457. Quaresimin M, Ricotta M. Stress intensity factors and strain energy release rates in single lap bonded joints in composite materials. Composites Sci Technol 2006;66(5):647-656.

458. Quaresimin M, Schulte K, Zappalorto M, Chandrasekaran S. Toughening mechanisms in polymer nanocomposites: From experiments to modelling. Composites Sci Technol 2016;123:187-204.